The role of human pentraxins for the *Leishmania*-vector interaction

Eve Christina Doran

Thesis submitted in accordance with the requirements for the degree of
Doctor of Philosophy

University of London
January 2024

Department of Disease Control

Faculty of Infectious and Tropical Diseases

London School of Hygiene & Tropical Medicine

Research group affiliations: Matthew Rogers (First supervisor)
John Raynes (Second supervisor)

Declaration of Own Work

I, Eve Doran, confirm that the work presented in this thesis is my own. Where information has been derived from other sources, I confirm that this has been indicated in the thesis.

Abstract

Survival and transmission of the protozoan *Leishmania* is dependent on attachment by the parasite to the sand fly midgut. Without this, *Leishmania* parasites are lost when the sand fly defecates the bloodmeal remnants. Previous work found human pentraxin C-reactive protein (CRP) was able to bind *Leishmania* lipophosphoglycan (LPG), and activate complement. Only one published study has investigated human pentraxin Serum Amyloid P (SAP) with *Leishmania*, finding no interaction. However, preliminary experiments by both the Rogers and Raynes labs have suggested otherwise.

Here, we hypothesise SAP acts as a cross-linker between *Leishmania* and the vector midgut, allowing attachment. We expand on CRP binding with *Leishmania*, specifically with the promastigote secretory gel (PSG). The methods and results of *in vivo* fly infections and *ex vivo* midgut binding assays are assessed through a systematic review and meta-analysis.

From comparing previous *in vivo* fly infection experiments, we propose there is a cap in the number of parasites a sand fly can sustain. Though SAP binds both *Leishmania mexicana* and *Lutzomyia longipalpis* midgut extract, it is not a cross-linker between the two, with anti-SAP antibodies and drug unable to block *Leishmania*-midgut attachment. An inverse correlation was seen between PSG repeating disaccharide side chain substitutions and the strength of CRP binding. We have not observed SAP binding to midgut extract from midge *Culicoides sonorensis* in preliminary experiments, however N-acetylgalactosamine (GalNAc) may be displayed on midge midguts as previously found for permissive sand flies.

Together, this work shows pentraxins likely have a role in the *Leishmania* lifecycle within the sand fly midgut, with the extent of pentraxin interaction likely differing between species due to differing surface molecule composition. Future models of *Leishmania*-vector interaction should include the roles of bloodmeal components, providing a fuller picture of the *Leishmania* lifecycle for development of transmission-blocking strategies.

Table of contents

List of Figures

Chapter 4

Chapter 5

Chapter 6

List of Tables

Abbreviations

AB	Add back
AF	Alexa Fluor
AP	Alkaline phosphatase
aPPG	Amastigote proteophosphoglycan
BCIP	Bromo-4-chloro-3-indolyl phosphate
BF	Bright Field
BSA	Bovine serum albumin
CDC	Centers for Disease Control and Prevention
CPHPC	(R-1-[6-[R-2-carboxy-pyrrolidin-1-y1]-6-oxohexanoyl]pyrrolidine-2-carboxylic acid)
CRP	C-Reactive Protein
DMF	Dimethylformamide
DTT	Dithiothreitol
EAH	2-Ethylhexanoic acid
EDC	1-Ethyl-3-(3-dimethylaminopropyl) carbodiimide
EDTA	Ethylenediaminetetraacetic acid
EGTA	Ethyleneglycol-bis(β-aminoethyl)-N,N,N',N'-tetraacetic acid
ELISA	Enzyme-linked Immunosorbent Assay
FACS	Fluorescence-activated cell sorting
fPPG	Filamentous Proteophosphoglycan
FCS	Fetal calf serum
Gal	Galactose
GalNAc	N-acetylgalactosamine
gGAPDH	glycosomal Glyceraldehyde-3-Phosphate Dehydrogenase
GIPL	Glycoinsositolphospholipid
GlcN	Glucosamine
GPI	Glycophosphatidylinositol
GVBS	Veronal buffered saline with gelatin
HBS	HEPEs buffered saline
HBSC	HEPEs buffered saline with calcium
HFP	Hamster Female Protein
HIV	Human Immunodeficiency Virus
HPA	*Helix pomatia* aggluntinin
HPS	Haptomonad Parasite Sphere
HRP	Horseradish peroxidase

HSP70	Heat shock Protein 70
kDa	Kilodaltons
kDNA	Kinetoplast Deoxyribonucleic acid
LC	Long chain
LPG	Lipophosphoglycan
Man	Mannose
mPPG	Membrane proteophosphoglycan
NBT	4-Nitrotetrazolium blue chloride
NHS	N-hydroxysuccinimide
OD	Optical density
PBM	Post Blood Meal
PBS	Phosphate buffered saline
PBST	Phosphate buffered saline with Tween
PCh	Phosphorylcholine
PEth	Phosphorylethanolamine or phosphoethanolamine
PFA	Paraformaldehyde
PG	Phosphoglycan
PPG	Proteophosphoyglycan
PI	Phosphatidylinositol
PKDL	Post-Kala-azar Dermal Leishmaniasis
PM	Peritrophic Matrix
PMSF	Phenylmethanesulfonyl fluoride
PNA	Peanut agglutinin
PSG	Promastigote Secretory Gel
PVDF	Polyvinylidene fluoride
RIPA	Radioimmunoprecipitation assay buffer
rRNA	Ribosomal Ribonucleic acid
SAP	Serum Amyloid P
ScAP or sAP	Secreted Acid Phosphatase
SDS-PAGE	Sodium dodecyl sulfate-polyacrylamide gel electrophoresis
SPR	Surface Plasmon Resonance
TBS	Tris buffered saline
TBST	Tris buffered saline with Tween
TLC	Thin layer chromatography
TMB	Tetramethylbenzidine
VBS	Veronal buffered saline

VSG	Variant Surface Glycoprotein
WHO	World Health Organisation
WT	Wild-type

1. **Introduction**

1.1 *Leishmania*

The leishmaniases are a group of neglected tropical diseases, caused by the protozoan parasite genus *Leishmania* (WHO, 2023a). Figures 1.1 and 1.2 show the endemic regions for cutaneous and visceral leishmaniasis, respectively, in 2021.

Status of endemicity of cutaneous leishmaniasis (CL) worldwide, 2021
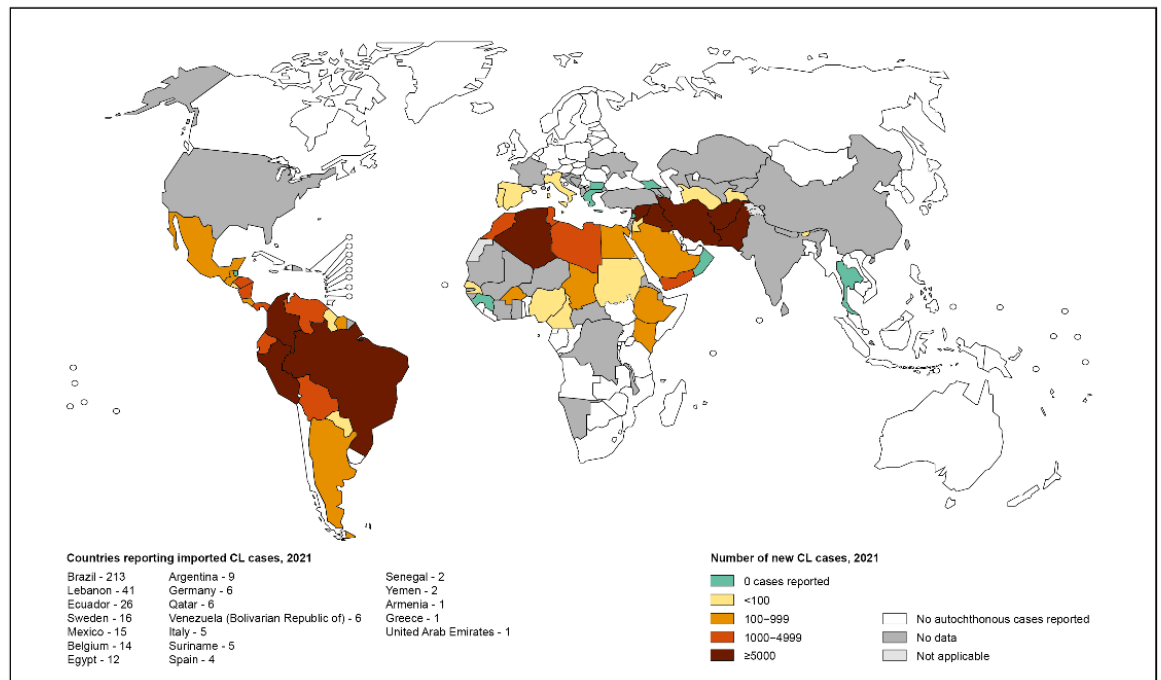
Figure 1.1. Prevalence and location of reported new cutaneous leishmaniasis cases in 2021. More than 5000 cases were reported in Brazil, Colombia, Peru, Algeria, Syria, Iraq, Iran, Afghanistan and Pakistan (WHO, 2023b).

Status of endemicity of visceral leishmaniasis (VL) worldwide, 2021
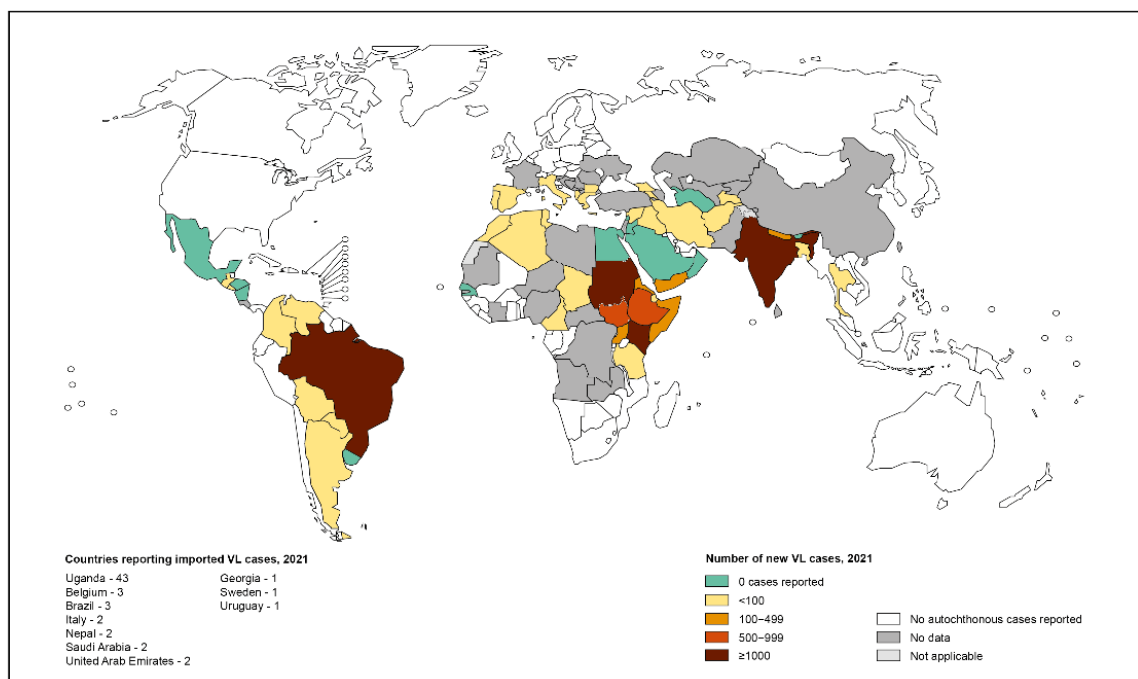
Data Source: World Health Organization
Map Production: Control of Neglected
Tropical Diseases (NTD)
World Health Organization

Figure 1.2. Prevalence and location of reported new visceral leishmaniasis cases in 2021. More than 1000 cases were reported in Brazil, Sudan, Kenya and India (WHO, 2023b).

Leishmania are kinetoplastids (Order: kinetoplastida), meaning they have the kinetoplast organelle which holds mitochondrial kinetoplast DNA (kDNA). They are flagellated with a cell membrane invagination at the flagella base called the flagellar pocket which is the only region of the parasite where endo- or exocytosis can occur (reviewed in Field and Carrington, 2004; Sunter and Gull, 2017). The parasite's form changes throughout its lifecycle, with differences in flagella length and positioning of the kinetoplast and the nucleus (Sunter and Gull, 2017).

The lifecycle of *Leishmania* is digenetic, with a stage in mammalian hosts, and a stage within the insect vector (Sunter and Gull, 2017). This lifecycle is commonly zoonotic, with only *Leishmania donovani* thought to have an anthroponotic cycle (with this now being debated) (Cecílio et al., 2022). Zoonotic hosts include dogs, rodents, hyraxes, rabbits, hares, horses, marsupials and opossums (Cecílio et al., 2022). The lifecycle, showing humans as the host, is shown in Figure 1.3 (CDC, 2020). When discussing both *Leishmania* and sand fly species, they are divided into Old World (Asia, Middle East, Africa, Southern Europe) and New World (Central and South America) (CDC, 2020).
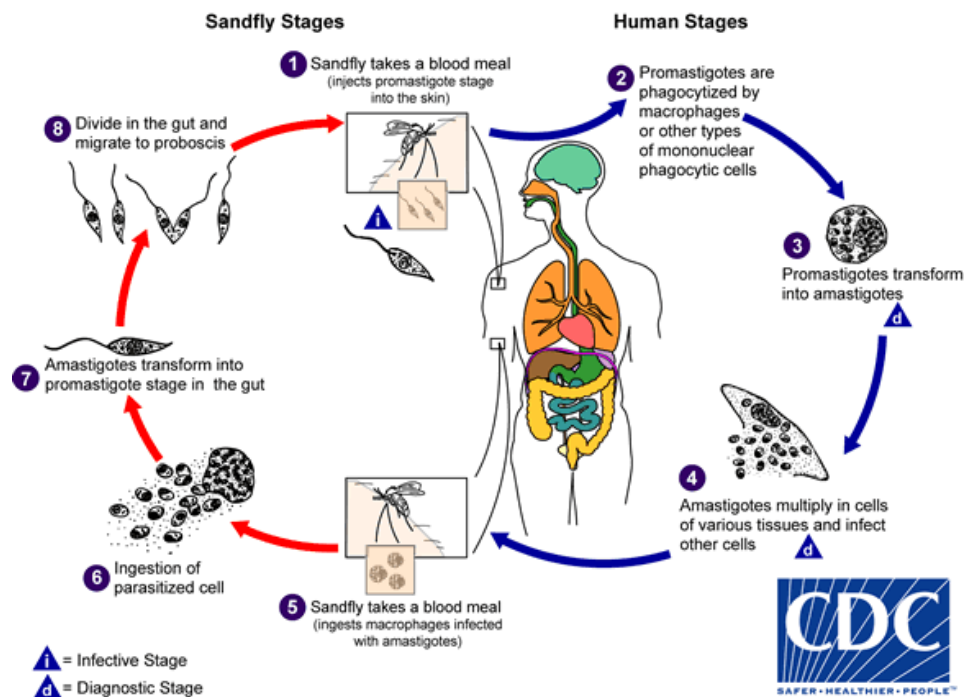
Figure 1.3. The lifecycle of the *Leishmania* parasite goes through two stages: one in the mammalian host (depicted here as a human) and one in the insect vector. When an infected vector takes a bloodmeal on a mammalian host, parasites are transferred to the skin (1) and taken up by phagocytic cells (2). Within these cells, the infectious metacyclic promastigote stage transforms into amastigotes (3). The amastigote stage multiples in these cells, bursting and infecting nearby cells or infected cells can disseminate in the case of visceral leishmaniasis causing disease in other organs (Meira and Gedamu, 2019) (4). When a sand fly bites an infected host, amastigotes will be taken up as part of the bloodmeal (5, 6) and within the sand fly gut will transform into promastigote forms (7). The promastigotes will divide and migrate to the proboscis of the sand fly, ready for transmission when the sand fly takes another bloodmeal (8). Image from CDC, 2020.

1.1.1   Disease

There are three forms of leishmaniasis, and these vary in their disease severity. The most deadly form is visceral (or kala-azar), where *Leishmania* spreads and infects macrophages within organs such as the spleen and liver, leading to their enlargement (Kumar and Nylén, 2012). This form is also characterised by weight loss, anemia and fever (WHO, 2023a). The World Health Organisation (WHO, 2023a) estimates there are 50,000 to 90,000 new cases annually found mainly in Brazil, India and East Africa. The most common form is cutaneous

leishmaniasis where disease is only observed on the skin, which can be slow to heal (Kaye and Scott, 2011) but also self-limiting (Rogers, 2012). The WHO predicts 600,000 to one million new cases of this form each year which is found over a wider geographical range. Though milder in disease, the ulcers formed can cause disability and stigma (WHO, 2023a). The third form is mucocutaneous leishmaniasis, where *Leishmania* spread through the blood or lymphatic system to mucosal tissue (Mann et al., 2021) with the majority of cases found in Bolivia, Peru, Brazil and Ethiopia (WHO, 2023a). This form is associated with a hyperinflammatory immune response leading to the destruction of mucus membranes (Ives et al., 2011). This can result in severe disfigurement due to collapse and destruction of the nose and mouth (Mann et al., 2021).

Patients with visceral leishmaniasis caused by *L. donovani* can sometimes develop post-kala-azar dermal leishmaniasis (PKDL), usually six months to one year after recovery from the visceral form but it can be up to 10 years (WHO, 2023a; Mukhopadhyay et al., 2014). PKDL is usually only found in Sudan (and surrounding areas) and on the Indian subcontinent (WHO, 2023a; Ganguly et al., 2010). This form of leishmaniasis displays as a rash made up of small lesions, which can be macules, papules or nodules, commonly found on the face and torso. These lesions are parasite-rich, and so PKDL patients are thought to be a source of *Leishmania* parasites, playing a role in disease transmission (WHO, 2023a; Mukhopadhyay et al., 2014).

1.1.2   Risk factors

There are a range of risk factors that can increase the likelihood of an individual becoming infected with *Leishmania* and developing disease. Leishmaniasis is described as an opportunistic infection when infecting individuals with HIV due to high coinfection rates in endemic areas (Kantzanou et al., 2023). Poverty is a major risk for leishmaniasis and the interaction of the two has become a vicious cycle (Alvar et al., 2006). These individuals tend to be more exposed to sand flies, either for work or housing location/conditions and once infected, have barriers to healthcare (such as cost of treatment) meaning delayed treatment and increase morbidity and mortality. Increased morbidity will decrease productivity due to school or work absences, and with potential debts from treatment cost, individuals are more likely to stay in poverty (Alvar et al., 2006). Furthermore, these individuals may also be malnourished, a factor that increases the likelihood of disease progression (WHO, 2023a; Alvar et al., 2006). Displacement of people in endemic areas can lead to outbreaks of leishmaniasis, which has been seen due to the conflict in Syria (Du et al., 2016). These outbreaks can be

caused by a lack of healthcare, poor living conditions and disease introduction to new areas or individuals exposed to the disease for the first time (Du et al., 2016).

1.1.3 Subgenus

Three *Leishmania* subgenera have been described since the 1980s, but with some outlier species (Lainson and Shaw, 1987). These subgenera are *Leishmania (Viannia), Leishmania (Leishmania)* and *Leishmania (Sauroleishmania). Leishmania (Sauroleishmania)* is the subgenus given to *Leishmania* which infect reptiles. *Leishmania (Viannia)* contains *Leishmania* species who have peripylarian development within the sand fly – the promastigotes attach to the wall of the hindgut or have a proportion of their lifecycle in the hindgut. *Leishmania (Leishmania)* contains species with suprapylarian development, where development only takes place within the midgut and foregut (Lainson and Shaw, 1987). More recently, the subgenus *Leishmania (Mundinia)* has been added, with species assigned to this group through phylogenetic analysis of V7V8 SSU rRNA, heat shock protein 70 (HSP70) and glycosomal glyceraldehyde-3-phosphate dehydrogenase (gGAPDH) sequencing. It is also thought the vector of species in this subgenus may be midges (Espinosa et al., 2016). *Leishmania (Viannia)* and *Leishmania (Leishmania)* are the main subgenus causing human disease, but human infections with *Leishmania (Mundinia)* have also been seen (Kwakye-Nuako et al., 2023).

1.1.4 Treatment, prevention and control

The most recent WHO report for control of leishmaniasis discusses the treatment and control options available for this disease (WHO, 2010). Drugs and the combinations they are used in is dependent on the drug policy in a particular country, the presentation of the disease and potentially the species of *Leishmania* causing the infection. For cutaneous leishmaniasis, thermo- and cryo-therapy and ointments can be used. Many drugs need to be given intravenously and can have severe side effects, including hepato- and cardiotoxicity and in some cases, death. Furthermore, these drugs have increased toxicity in HIV positive patients, who as mentioned earlier, are one of the groups most likely to progress to severe disease. Using drugs in combination does reduce side effects and helps to prevent resistance. At the time of this report, there was no vaccine against leishmaniasis (WHO, 2010). A review in 2022 reported there was still no vaccine, with the complexity of the immune response to *Leishmania* and range of species causing disease stated as the main challenges (Abdellahi et al., 2022).

As previously mentioned, there are animal and human (PKDL patients) reservoirs of *Leishmania*. For PKDL patients, it is encouraged for them to sleep under an insecticide treated bed net while receiving treatment to eliminate the parasite (WHO, 2010). The main method of controlling infected stray and feral dogs is for them to be culled, whereas domestic dogs are usually treated for their infection. Topical insecticides and collars can also be used to prevent infection. Vaccines are available for canine leishmaniasis but their impact is yet to be seen. Leishmune which consists of the fucose-mannose ligand (FML) from *L. donovani* (Borja-Cabrera et al., 2002) was withdrawn in Brazil due to lack of effectiveness (Velez and Gállego, 2020), with Leish-Tec, a vaccine constructed using *L. donovani* amastigote A2 cysteine proteinase (Grimaldi et al., 2017), now administered in this region instead. In Europe, the vaccines are produced against *Leishmania infantum*. CaniLeish is a vaccine developed using excreted-secreted proteins (ESP) (Moreno et al., 2012; Velez and Gállego, 2020) and LetiFend is a vaccine composed of a recombinant chimeric protein made from five antigenic fragments (Fernández Cotrina et al., 2018; Velez and Gállego, 2020). For wild animal reservoirs, culling is the main method suggested for control but environmental management such as clearing forest around villages may also be useful. For vector control, the behaviour of the sand fly in question needs to be taken into account. For example, indoor residual spraying can be used for endophilic species and other species can be targeted by spraying outdoor resting places (WHO, 2010). Transmission blocking sugar baits are also a potential vector control method offering an environmentally-friendly alternative (Ferreira et al., 2018). The poor flying ability of some sand flies species may mean populations would be easily targeted by this vector control method.

Climate change is predicted to change the distribution of leishmaniasis, as discussed by Ready (2008). Temperature changes will directly affect *Leishmania* development within the sand fly and the number of gonotrophic cycles of the sand fly. Along with temperature, rainfall will determine sand fly numbers. There will also be indirect effects such as changes in the abundance and species of sand flies which are vectors. Climate change will inevitably lead to migration and malnutrition which will indirectly increase and enhance disease (Ready, 2008).

1.2 Vectors of *Leishmania*

1.2.1   Vector incrimination

Criteria have been developed to allow clear identification of the vectors that can transmit human leishmaniasis (Killick-Kendrick, 1990; Cecílio et al., 2022). The vector must:

1. Feed on humans
2. Feed on relevant reservoir hosts (for species with zoonotic lifecycle)
3. Be found in the same geographical region as the *Leishmania* species
4. Support the development of the entire *Leishmania* lifecycle, including post bloodmeal remnant defecation
5. Transmit parasites when taking a bloodmeal from a susceptible host

Since these criteria were reported, modifications have been raised by other researchers (discussed in Ready, 2013). In a review by Bates (2007), *Leishmania* attachment to and damage of the cuticle-lined stomodeal valve which divides the midgut and foregut was raised as potentially being needed for transmission. The percentage of metacyclics at late stages of sand fly infection are now regularly reported as indicators of vector competence and parasite transmission (Giraud et al., 2019; Louradour et al., 2019; Bongiorno et al., 2019; Stamper et al., 2011). Shaw (2007), Ready (2013) and Bates et al., (2015) also discussed whether ecological criteria should be added, such as seasonality and other environmental factors which might impact *Leishmania*-vector interactions. This has been incorporated into the criteria of some researchers, such as in Seblova et al. (2015). Ready (2013) suggested two criteria involving mathematical modelling to show the vector of interest can maintain *Leishmania* transmission independently of other vectors and to show disease cases drop with decreasing biting density of the vector when control programs are used.

1.2.2 Sand flies

Sand flies are small, dipteran insects all within the family Psychodidae, usually only 3 mm in length (Killick-Kendrick, 1999). Killick-Kendrick (1999) previously described the key characteristics of these flies, as covered in hairs (setae), wings held angled to the body when at rest and a hopping behaviour before biting a host. Killick-Kendrick (1999) discussed that this hopping behaviour has been suggested to mean flies bite very close to breeding sites. Killick-Kendrick et al. (1986) reported a flight speed for *Phlebotomus ariasi* of 2.3 to 2.5 km per hour, around half of the speed of *Anopheles*. Sand fly flight is likely largely affected by wind speed, for both propelling the fly (Killick-Kendrick et al., 1986) and potentially knocking the flies off course (Colaciccio-Mayhugh et al., 2011). Flying behaviour varies between sand fly species, with *Nyssomyia intermedia* and *Evandromyia lenti* reported to fly 90 m continuously (Tonelli et al., 2021) and *Phlebotomus argentipes* found to have more sustained flights compared to *Sergentomyia* spp. which hopped (Poché et al., 2012).

Female sand flies feed on blood for egg production (Ready, 1979) and tend to be opportunistic feeders, biting a range of mammalian and avian species, depending on the sand fly species (Rossi et al., 2008; González et al., 2021; Cecílio et al., 2022). They feed in a range of environments including peridomestic, silvatic, savannas and highlands, with biting of humans usually being in rural communities (Ready, 2013). Sand flies use their sharp mouthparts to saw into the skin of their host until they reach the capillaries which are lacerated forming a pool of blood from which they can feed (and therefore are named pool feeders) (Kamhawi, 2000; Rogers, 2012). Biting behaviour can be endo- or exo-phagic and occurs mainly between dusk and dawn (Killick-Kendrick, 1999; Cecílio et al., 2022).

Sand flies are present on all continents except Antarctica but are absent above 50°N, below 40°S, in New Zealand and the Pacific islands (Lane, 1993; Killick-Kendrick, 1999). This is due to the lifecycle requiring temperatures over 10-15°C, with female flies unable to survive below this (Koch et al., 2017). The eggs also require high humidity (Modi and Tesh, 1983; Volf and Volfova, 2011; Koch et al., 2017) along with organic matter for laying of eggs and larval feeding (Modi and Tesh, 1983; Cecílio et al., 2022). For these reasons, sand flies are usually most active in the months of April to November (ECDC, 2020).

There are over 800 species of sand fly, within six genus: *Phlebotomus, Sergentomyia, Lutzomyia, Brumptomyia*, *Warileya* and *Chinius* (Akhoundi et al., 2016; Cecílio et al., 2022). Only 98 of these species have been incriminated as or are suspected vectors of human *Leishmania* (Sadlova et al., 2018), with these all within the genus of *Phlebotomus* or *Lutzomyia* (Bates, 2008). The genus *Sergentomyia* is thought to be a vector for some *Sauroleishmania* (Maroli et al., 1988; Tiche et al., 2022), with this species suggested as a vector for human leishmaniasis (Senghor et al., 2016), but so far no species has met the incrimination criteria (Sadlova et al., 2013; 2018).

1.2.3   Midges and *Mundinia*

Similarly to sand flies, biting midges are found nearly worldwide, only absent in Antarctica and New Zealand (Mellor et al., 2000). They are smaller in size, usually 1-2.5 mm in length (Service, 2012). Biting midges commonly lay eggs on wet soil (Service, 2012) and organically rich material (Mullen, 2009), and are therefore found near swaps, marshes or on matter partially submerged in water. However, some species are known to lay in tree-holes or in decomposing vegetation, with the latter the main food source for larvae (Service, 2012). This being said, the larvae are reported to be omnivorous, feeding opportunistically on a range of available food

(Mullen, 2009). Adult midges usually stay within a few hundred metres of larval habitats, though some species can fly 2-3 km, with this largely affected by wind velocity (Mullen, 2009; Service, 2012). Most biting midge species are multivoltine, meaning they have multiple broods in one season. This can lead to multiple overlapping generations and so there can be an extended peak in adult numbers over warmer months (Mullen, 2009). Depending on the species of biting midge, these insects can survive from one to seven weeks in the field (Mullen, 2009; Service, 2012).

Like sand flies, female biting midges require blood for egg production. They are pool feeders and are unable to bite through clothing, meaning exposed areas of the skin such as arms, legs and the face are where blood feeding occurs (Mullen, 2009; Service, 2012). Biting occurs mainly outdoors and at night time, with activity dependent on temperature and light intensity (Mullen, 2009; Service, 2012). Different species of biting midge show different host preferences, with females feeding on mammals, birds, reptiles or amphibians (Mullen, 2009).

Until recently, sand flies were thought to be the only vectors to transmit *Leishmania* parasites. This was until cutaneous leishmaniasis cases were found in red kangaroos in Australia – a country previously considered free from this disease (Rose et al., 2004). Cases were later reported in wallaroos and wallabies, with the *Leishmania* sequence matching that found in kangaroos (Dougall et al., 2009). Dougall et al. (2011) screened over 1500 *Sergentomyia queenslandi*, but all were negative for *Leishmania* using qPCR. However, a *Leishmania* prevalence of 5.8% in the day-feeding midge *Forcipomyia (Lasiohelea)* sp. was found. These midges had been observed feeding on the kangaroos, and sequence analysis found the flies and infected kangaroo samples had *Leishmania* with the same RNA polymerase subunit II gene sequence. A gel-like plug was seen in one dissection along with metacyclic-like forms (the vertebrate-infective stage, discussed further in section 1.3). Though transmission could not be demonstrated, it seemed likely midges were the vector for *Leishmania* in this lifecycle. The *Leishmania* species was later named *Leishmania macropodum* (Barratt, Kaufer and Ellis, 2017, described in Barratt et al., 2017).

L. macropodum, along with similar species isolated were classified together in the new *Mundinia* complex of *Leishmania* (Shaw, Camargo and Teixeira, 2016, described in Espinosa et al., 2016). Classification into this complex was done using phylogenetic analysis of gGAPDH and HSP70 sequences (Espinosa et al., 2016). Another species in this complex is *Leishmania enriettii*, which was isolated from a domestic guinea pig in Brazil, first in 1946 and then again in 1988 (Machado et al., 1994). *Leishmania martiniquensis* (Desbois, Pratlong and Dedet, 2014;

described in Desbois et al., 2014) was isolated from human patients on the island of Martinique (Boisseau-Garsaud et al., 2000). Isolates have also been obtained from a cow in Switzerland (Lobsiger et al., 2010), a horse in Florida (Reuss et al., 2012) and horses in Germany and Switzerland (Müller et al., 2009) (referenced as this species in Butenko et al., 2019). This species was isolated from human patients in Thailand (Jariyapan et al., 2018), along with another species *Leishmania orientalis* (Bates and Jariyapan, 2018, described in Jariyapan et al., 2018). This year, two more *Mundinia* species have been named and described: *Leishmania chancei* and *Leishmania procaviensis* (Kwakye-Nuako et al., 2023). *L. chancei* was previously isolated in Ghana from cutaneous lesions on human patients (Kwakye-Nuako et al., 2015). *L. procaviensis* was identified from a cryopreserved sample, taken from the tip of the nose of a rock hyrax (*Procavia capensi*) in Namibia (Kwakye-Nuako et al., 2023).

This complex has a wide geographical range, which suggests it may have originated before the break up of Gondwana (Jariyapan et al., 2018; Kwakye-Nuako et al., 2023), and phylogenetically is the earliest branching *Leishmania* subgenus (Butenko et al., 2019). Interestingly, midges can sustain development of species in this complex. Seblova et al. (2015) found *L. enrietti* and *L. macropodum* could survive in the midge *Culicoides sonorensis* up to 10 days post infection, with vertebrate-infectious forms present and parasites colonising the stomodeal valve. *C. sonorensis* flies fed on infected guinea pigs led to infected flies. Chanmol et al. (2019) compared *L. orientalis* development in *Lutzomyia longipalpis* and *C. sonorensis*, finding infection only established in the midge. Becvar et al. (2021) compared the late-stage infection intensities of all *Mundinia* species except for *L. procaviensis* in *C. sonorensis* and sand flies. They found *L. martiniquensis, L. orientalis* and *L. chancei* had significantly heavier infection in the midge compared to the sand fly. Only in a low percentage of flies had *L. macropodum* and *L. enrietti* colonised the stomodeal valve, but it was suggested this may be due to the genus of midge. Currently, there are only a few midge colonies available for experimental infection.

1.3   *Leishmania*-sand fly interactions

1.3.1   *Leishmania* lifecycle within the sand fly

The *Leishmania* lifecycle within the sand fly vector is complex, with a variety of morphological forms. Most studies have focused on the subgenus *Leishmania (Leishmania)* and suprapylarian development (Dostálová and Volf, 2012), with the lifecycle seen in Figure 1.4 (Cecílio et al., 2022). A summary of the lifecycle stages can be seen in Table 1.1. When amastigote parasites first enter the sand fly as part of the bloodmeal, a type I peritrophic matrix (PM) is formed

separating the blood from the midgut (Kamhawi, 2006; discussed further in section 1.3.3). Due to the change in pH and temperature from the mammalian host to the sand fly (Dostálová and Volf, 2012), amastigotes quickly transform into procyclic promastigotes (Figure 1.4, 1), and then into nectomonad promastigotes which will escape the PM (Figure 1.4, 2) and attach to the midgut lining to resist expulsion with the digested bloodmeal (Kamhawi, 2006; Dostálová and Volf, 2012; discussed further in sections 1.3.5 and 1.3.6). This binding appears to occur flagellum first (Figure 1.4, 3a) (Killick-Kendrick et al., 1974). Following bloodmeal digestion and defecation, attached nectomonad promastigotes detach from the midgut epithelium and start moving from the abdominal to the thoracic midgut as well as transforming to leptomonad promastigotes, the stage that produces the promastigotes secretory gel (PSG) (Figure 1.4, 3a) (Rogers et al., 2002; discussed in section 1.3.7). A small population of parasites called haptomonads attach to the stomodeal valve, but the role of this form is not fully understood (Figure 1.4, 3b). Haptomonad attachment may lead to damage of the valve, improving transmission of parasites when the sand fly takes another bloodmeal (Volf et al., 2004; Kamhawi, 2006). Large populations of haptomonad promastigotes were recently found to form a haptomonad parasite sphere (HPS) that can block the stomodeal valve (Serafim et al., 2018). It has also been suggested that this promastigote stage may be able to divide and even fuse allowing sexual recombination (Yanase et al., 2023). The infective metacyclic stage transforms from the leptomonad stage and is found between the stomodeal valve and the thoracic midgut, ready to be transmitted when the sand fly next bites [4,5] (Rogers et al., 2002; Kamhawi, 2006; Serafim et al., 2018).

Recently, another lifecycle stage has been proposed called the retroleptomonad (Serafim et al., 2018), where upon exposure to a second bloodmeal, metacyclic stages can transform back to a leptomonad-like stage – the retroleptomonad promastigote (Figure 1.4, 4). This stage can replicate further, then transform to metacyclics, increasing the infection intensity within the sand fly. Although not defined, the cue for leptomonad transformation into metacyclics is thought to be the depletion of a nutrient, but upon a second bloodmeal, the increase in this nutrient allows for a reversion to the leptomonad-like stage (Serafim et al., 2018).
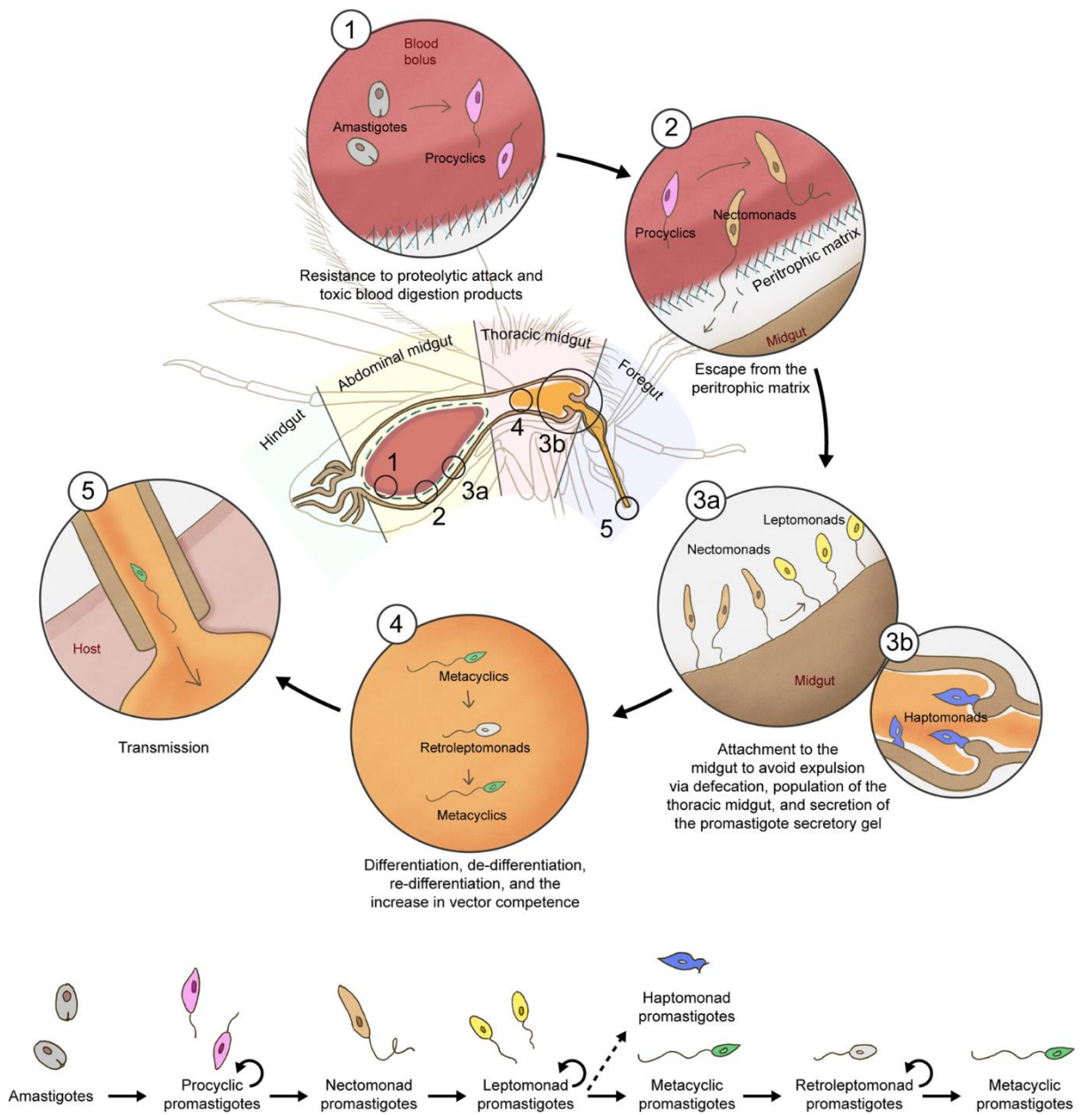
Figure 1.4. This figure shows the lifecycle stages of *Leishmania* and where they are located within the fly as well as highlighting the barriers the parasite must overcome to survive (Cecílio et al., 2022).

Table 1.1. An overview of the various *Leishmania* lifecycle forms within the insect vector (Rogers et al., 2002; Kamhawi, 2006; Pruzinova et al., 2015; Serafim et al., 2018; Cecílio et al., 2022).

Stage	Shape/size	Location	Stage significance
Procyclic	Short body and flagella	Confined to bloodmeal in abdominal midgut	• Nutrient rich environment for replication • Must survive midgut digestive enzymes/toxic blood digestion products
Nectomonad	Long and slender	Abdominal and thoracic midgut	• Escape peritrophic matrix • Bind midgut preventing defecation along with bloodmeal remnants • Migrates towards stomodeal valve
Leptomonad	Shorter body but long flagella	Thoracic midgut	• Produces promastigote secretory gel (PSG) • Migrates towards stomodeal valve • Conditions midgut for efficient metacyclogenesis
Haptomonad	Very short flagella	Stomodeal valve	• Attach to stomodeal valve and form plug (haptomonad parasite sphere (HPS)) • Non-motile minor population
Metacyclic	Small, narrow bodied with long flagella	Thoracic midgut	• Infective to mammalian host • Motile
Retroleptomonad	Leptomonad-like, large body, shorter flagella	Thoracic midgut	• Replication upon second bloodmeal, increasing parasite numbers and extending the period of vector infectiousness • Low motility

1.3.2   Restrictive and permissive vectors

In 2007, a clear division in sand flies was described by Volf and Myskova. Sand flies that are only able to support the development of one *Leishmania* species were described as specific (or restrictive) vectors. This included *Phlebotomus papatasi*, known to only support *Leishmania major*. Most sand fly species fall into the other category named permissive, which are capable of supporting the development of multiple *Leishmania* species. This group includes Old World species like *Phlebotomus arabicus* and New World species like *Lu. longipalpis* (Volf and Myskova, 2007).

1.3.3 Barriers to *Leishmania* development within the sand fly

There are a few barriers to *Leishmania* development within the initial days of sand fly infection. One of these barriers is proteolytic enzymes, mainly trypsin and chymotrypsin (Dostálová and Volf, 2012; Pruzinova et al., 2015), which has been discussed previously (Kamhawi, 2006; Dostálová and Volf, 2012). A few studies have been highlighted here to show the different discussions that have taken place regarding the role of proteases in sand flies. Protease activity is low for unfed or sugar fed flies, with activity being triggered by a bloodmeal (Schlein and Romano, 1986; Dostálová and Volf, 2012). Early transitional stage *L. major* parasites were found to be susceptible to killing by *P. papatasi* trypsin (Pimenta et al., 1997), suggesting killing could be stage-specific. Another study found *L. major* but not *L. donovani* could reduce *P. papatasi* gut enzyme activity (Schlein and Romano, 1986), suggesting protease activity may contribute to vector competence. However, trypsin inhibitors have been found to increase the survival of *Leishmania* species in competent sand flies, highlighting that trypsin activity kills both 'compatible' and 'non-compatible' *Leishmania* species (Borovsky and Schlein, 1987; Dostálová and Volf, 2012). The timing of proteolytic activity differs between sand fly species, which may also affect vector competence, with 18-48 hours post bloodmeal (PBM) previously reported depending on the sand fly species (Dostálová and Volf, 2012). Pruzinova et al. (2015) found that proteolytic activity peaked at 24-36 hours PBM for *P. argentipes* and 48-72 hours for *Phlebotomus orientalis*. However, both of these sand flies are able to support development of *L. donovani*, and clearly have very different protease timing. Therefore, the role of protease activity as a barrier to development of *Leishmania* is still up for debate with other factors playing a more prominent role.

Another barrier to *Leishmania* development within the sand fly is the peritrophic matrix (PM). The PM is a barrier made of proteins and chitinous microfibrils that forms around the bloodmeal, separating it from, and protecting the sand fly midgut epithelium (Kamhawi, 2006). Initially it was thought the PM surrounds the bloodmeal within four hours of feeding (Kamhawi, 2006), but for some sand flies, it is thought to be much later with up to 12 hours observed for *P. argentipes* (Pruzinova et al., 2015). The PM acts as a barrier to *Leishmania*, preventing the crucial binding of nectomonad stage parasites to the midgut epithelium (Dostálová and Volf, 2012). It has been suggested the PM can protect the susceptible parasite forms from proteolytic attack (Pimenta et al., 1997). Pruzinova et al. (2015) proposed the timing between PM breakdown and bloodmeal remnant defecation may be important for *Leishmania* survival in the sand fly, with enough time needed for transformation to the nectomonad stage and attachment to the midgut. It was previously thought *Leishmania* escape

the PM by producing chitinases (Schlein et al., 1991; Rogers et al., 2008), but through RNA interference experiments it is now thought sand fly chitinases are the cause of the PM breakdown (Coutinho-Abreu et al., 2010).

The impact of sand fly innate immunity on the *Leishmania* parasite is under researched. A role for *Phlebotomus duboscqi* (Boulanger et al., 2004) but not *Lu. longipalpis* (Telleria et al., 2013) defensin against *L. major* and *Leishmania mexicana* infection, respectively, has been proposed with this suggested to potentially be a difference between restrictive and permissive vectors (Telleria et al., 2018). *L. infantum* survival in *Lu. longipalpis* was found to be reduced by depletion of Caspar, a negative regulator of the IMD signaling pathway. This suggests effectors of this signaling pathway may be important in parasite killing in *Lu. longipalpis* (Telleria et al., 2012). Understanding the immunity of the sand fly to *Leishmania* is made difficult as the response to midgut microbiota may complicate results (Telleria et al., 2018).

1.3.4   Role of lipophosphoglycan in sand fly attachment

Lipophosphoglycan (LPG) is a molecule covering the entire surface of the *Leishmania* parasite, including the flagella (Pimenta et al., 1994). Promastigotes have approximately 6×10^6 LPG molecules per cell (McConville and Blackwell, 1991) forming a densely packed glycocalyx (Sacks and Kamhawi, 2001). This is reduced in amastigote stages with only 100 molecules per cell (McConville and Blackwell, 1991).

LPG molecules have four domains: phosphatidylinositol lipid anchor; hexasaccharide glycan core; $[-6\text{Gal}\beta1,4\text{Man}\alpha1\text{-PO}_4\text{-}]_x$ repeats and an oligosaccharide cap (Turco and Descoteaux, 1992; Sacks and Kamhawi, 2001), seen in Figure 1.5. However, the side chains off the $[-6\text{Gal}\beta1,4\text{Man}\alpha1\text{-PO}_4\text{-}]_x$ repeats differ between and within species, with these differences for *L. infantum* classed into three groups. Type I LPG are *Leishmania* strains which are devoid of side chains, type II LPG have one β-glucose and type III can have side chains of up to three glucose (Coelho-Finamore et al., 2011). Similar groupings of LPG can be seen for other *Leishmania* species, however the sugars can vary, such as *L. amazonensis* which has β-galactose residues (Nogueira et al., 2017). Substitutions can be on the C-2 or C-3 position and this varies between species (Forestier et al., 2015).

The structure of LPG changes during metacyclogenesis, and was first described for *L. major*, finding metacyclic LPG differed in the number and make-up of the repeat units (Sacks et al., 1990). This was further studied by McConville et al. (1992), finding an increase in side chains

displaying arabinose and a decrease in those displaying galactose, suggesting this allows metacyclic detachment from the midgut and continuation of the lifecycle. For an *L. donovani* strain (1S, Sudan), the same increase in size was seen for metacyclic LPG, but they also proposed folding of the terminal sugars making them inaccessible (Sacks et al., 1995). The inability of metacyclics to bind the midgut has now been shown (Wilson et al., 2010) suggesting that rather than this being a method of detachment from the midgut, it prevents already detached metacyclics from binding.

It was proposed that polymorphisms in LPG were the reason for different survival rates of *Leishmania* in different sand flies (Pimenta et al., 1994), meaning LPG side chain structure is another barrier to development within the sand fly. This is discussed further in sections 1.3.5 and 1.3.6.

LPG is also protective against the toxic blood components produced during bloodmeal digestion for some *Leishmania* species but not others (Coutinho-Abreu et al., 2020). This was seen when comparing two *L. infantum* strains lacking LPG, with BH46 *lpg1*^{-/-} parasites surviving and BH262 *lpg1*^{-/-} parasite numbers drastically decreasing when exposed to extracts from blood-engorged *Lu. longipalpis* (Coutinho-Abreu et al., 2020). Pruzinova et al. (2018) observed mortality of parasites of both susceptible and refractory parasite-vector pairs, with promastigotes found to be the most susceptible lifecycle stage (compared to amastigotes or transitional stages) and mortality being highest at the end of bloodmeal digestion.

In the mammalian host, LPG is a virulence factor (Späth et al., 2000). It was initially thought LPG protected *Leishmania* from complement-mediated lysis and so was essential for mammalian infection (Sacks, 1989), however, Ilg (2000) argued there was not strong experimental evidence to claim this. He showed LPG-deficient *L. mexicana* injected into a mouse footpad developed into footpad lesions with parasites also recovered from draining lymph nodes (Ilg, 2000). Ilg and colleagues later found *L. mexicana* deficient in phosphoglycan (PG) repeats, caused similar disease progression to that of wild-type and LPG-deficient parasites (2001). LPG-deficient *L. major* have a delayed disease progression with lesions appearing four times later than seen for wild-type parasites. However, this delay is not seen if a saturating parasite dose is used for infection (Späth et al., 2000).
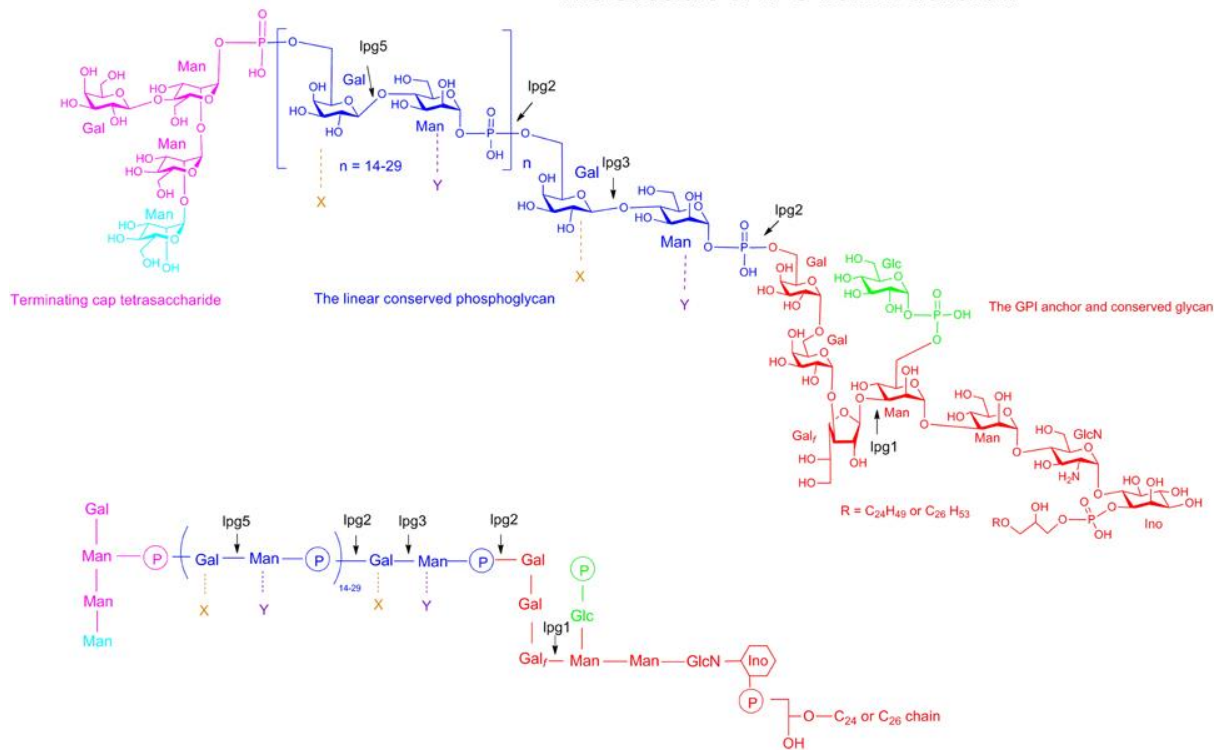
Figure 1.5. The structure of LPG for *L. donovani*, from Forestier et al. (2015), is shown in two different diagrams. The four domains are divided, with the phosphatidylinositol lipid anchor and hexasaccharide glycan core both shown in red. The green structure branching off the glycan core is a glucose phosphate, seen in *L. donovani* and some other species but not all. In dark blue is the [- 6Galβ1,4Manα1-PO₄-]ₓ repeats and in pink is the oligosaccharide cap. In light blue, off the cap structure, is a mannose that is seen in some *Leishmania* species and not others. The X and Y labels represent regions off the [- 6Galβ1,4Manα1-PO₄-]ₓ repeating backbone that can be substituted in different *Leishmania* species. Lpg1, lpg2, lpg3 and lpg5 show the regions of truncation for various mutant lines (Forestier et al., 2015).

1.3.5   *Leishmania major* attachment in *Phlebotomus papatasi*

The most studied sand fly-*Leishmania* pair is the interaction of *L. major* with the restrictive vector *P. papatasi*. Pimenta et al. (1992) found procyclic promastigotes from log stage culture but not metacyclics could attach to the *P. papatasi* midgut. LPG from both stages were purified and hydrolysed into fragments to see if they inhibited binding of promastigotes to midguts. The phosphoglycans from procyclics and fragments containing the Gal(β1,3) side chain of LPG were the most inhibitory. Butcher et al. (1996) generated *L. major* LPG mutants deficient in Gal(β1,3), and found a reduction in midgut binding. *P. papatasi* microvillar proteins were

31

extracted by Dillon and Lane (1999) and binding of LPG to multiple proteins was seen by Western blotting, but no *P. papatasi* proteins were identified. Kamhawi et al. (2004) identified a *P. papatasi* midgut galectin, which was named PpGalec and showed binding of this galectin to the poly-Gal(β1-3) side chains of *L. major* promastigote LPG. Later in 2015, Di-Blasi et al. suggested a flagellar protein called FLAG1/SMP1 could also be involved in the attachment of *L. major* promastigotes to the midgut, finding an anti-FLAG1/SMP antibody lead to a reduction in binding. As this protein is only on the flagellum, it was hypothesised the FLAG1/SMP1 interaction with the midgut allows for initial binding that facilitates LPG binding to the midgut via the galectin receptor.

1.3.6   *Leishmania* attachment in *Lutzomyia longipalpis* and permissive vectors

Progress has been made looking at the binding interaction of *Leishmania* to the permissive vector *Lu. longipalpis*, with suggestions it is LPG-independent. Rogers et al. (2004) found *L. mexicana lpg1*$^{-/-}$ mutants could survive to late-stage development in *Lu. longipalpis* and Svárovská et al. (2010) found the same for *L. major lpg1*$^{-/-}$ mutants in *Phlebotomus perniciosus* and *P. argentipes*. Myskova et al. (2007) reported all midgut lysates from permissive but not restrictive vectors tested bound *Helix pomatia* agglutinin (HPA). HPA also bound the luminal surface of *Phlebotomus halepenis*, suggesting permissive midguts display N-acetylgalactosamine (GalNAc)-containing glycoconjugates. This study also found that *L. major lpg1*$^{-/-}$ mutants could develop to late-stage infections in *Lu. longipalpis* and *P. arabicus*. Myskova et al. (2016) later characterised a glycoconjugate from *Lu. longipalpis* named LuloG, that displayed GalNAc. Recombinant LuloG bound to promastigotes and anti-LuloG antibody stained the midgut epithelium, however anti-LuloG did not alter *L. infantum* late-stage development in *Lu. longipalpis*. It has been suggested that LPG-independent binding seen in these experiments may only be occurring due to the unnatural sand fly and *Leishmania* pairs used (Coutinho-Abreu et al., 2020). This study found *L. infantum lpg1*$^{-/-}$ mutants failed to bind *Lu. longipalpis*. The importance of GalNAc epitopes was supported in work by Hall et al. (2020) using force microscopy to show glycan-glycan interactions occurred between GalNAc epitopes and *L. mexicana* LPG.

1.3.7 Other *Leishmania* surface and excreted products
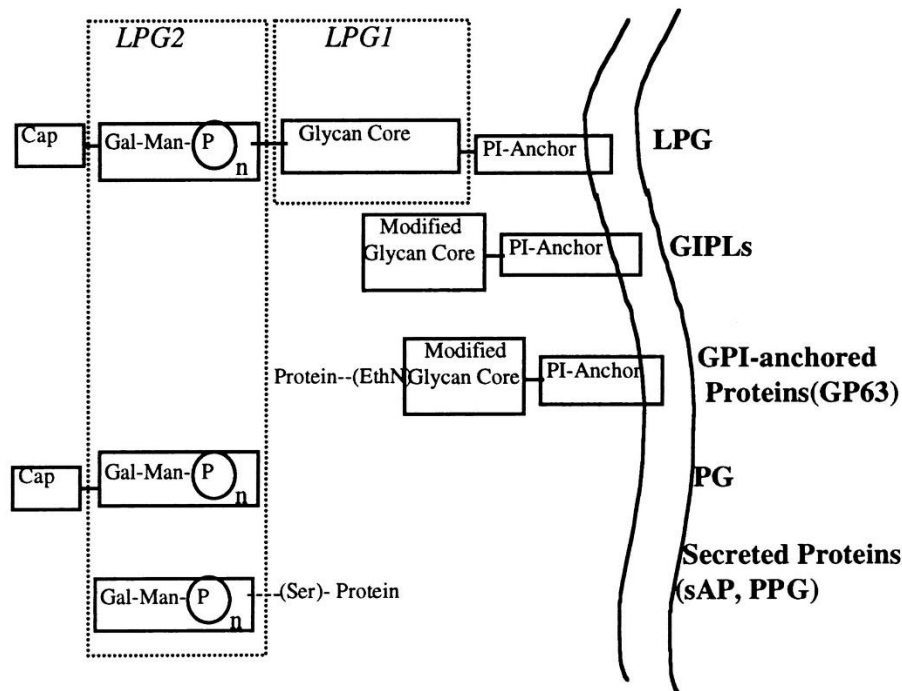
Figure 1.6. This diagram shows the *Leishmania* surface and excreted phosphoglycan containing molecules. It also highlights the structures of these molecules affected in *LPG1* and *LPG2*-deficient mutant parasites, highlighted by the dashed boxes. PI, phosphatidylinositol; GIPL, glycoinositolphospholipid; GPI, glycophosphatidylinositol; sAP (referred to in this report as ScAP), secreted acid phosphatase; PPG, proteophosphoglycan (reproduced from Sacks et al., 2000).

There are other surface and excreted products that are important for the *Leishmania* lifecycle within the sand fly, seen in Figure 1.6. GP63 (also known as leishmanolysin) is a glycosylated, zinc metalloprotease, that ranges from 60 to 66 kDa in size (Isnard et al., 2012). It is thought GP63 may have an additive role in attachment of parasites to the sand fly midgut (Jecna et al., 2013; Soares et al., 2017).

A viscous gel has been observed in the anterior midgut of experimentally-infected and wild-caught infected sand flies (Lawyer et al., 1990; Rogers et al., 2002; Dougall et al., 2011). In 1999, Stierhof and colleagues identified the structural component of the gel as filamentous proteophosphoglycan (fPPG), which was biochemically the same as that extracted from parasite culture supernatant. This was earlier characterised for *L. major* by Ilg et al. (1996) finding fPPG can be up to 6 µm long and is composed of 75.6% carbohydrate, 20% phosphate

and 4.4% amino acids. The majority of the carbohydrate portion of fPPG is composed of mannose, galactose and galactose-6-phosphate with no GalNAc detected. Of the amino acids present in fPPG, more than 50% are serine, with alanine and proline also making up a high proportion, with the serines forming phosphodiester linkages to glycans. Rogers et al. (2002) identified that the main producer of fPPG was the leptomonad stage. The fPPG accumulates and condenses within the sand fly, forming the promastigote secretory gel (PSG) which forces the stomodeal valve open. This allows parasites access to the foregut and pharynx where they will mix with incoming bloodmeals and be regurgitated into the bite site. Due to PSG preventing the sand fly from taking a full bloodmeal, it also causes a change in feeding behaviour (biting more frequently and for longer) which impacts *Leishmania* transmission (Rogers, 2012).

PSG also contains other *Leishmania* proteoglycans, LPG and secreted acid phosphatase (ScAP) (Ilg et al., 1996). ScAP is a large phosphorylated glycoprotein, that comes together to form filaments that are released from the flagellar pocket (Stierhof et al., 1994). ScAP is found in all *Leishmania* species tested except for *L. major* (Fernandes et al., 2013), though there are structural differences between species (Stierhof et al., 1998). For *L. mexicana*, there are two ScAP named ScAP1 (100 kDa) and ScAP2 (200 kDa), which form filaments together that can be up to 2 μm in length (Stierhof et al., 1998).

Glycoinositolphospholipids (GIPLs) are small surface molecules, first characterised by McConville and Bacic (1989). There are $10^7 – 4\times10^7$ molecules per cell, for both promastigotes and amastigotes (McConville and Blackwell, 1991; Yoneyama et al., 2006). Research so far suggests GIPLs have roles in cell signaling (Assis et al., 2012). All GIPLs have an alkylacylglycerol tail, followed by phosphatidylinositol residues, attached to Manα1-4GlcN (Assis et al., 2012). They are structurally diverse (McConville and Bacic, 1989), and can be divided into type-1, type-2 and hybrid GIPLs as seen in Figure 1.7 (Assis et al., 2012) defined by the structure of the alkylacylglycerol tail and the sugars attached to Manα1-4GlcN. Some forms can have ethanolamine residues (Assis et al., 2012) with this found to be the predominant form for *L. mexicana* amastigotes (2×10^7 estimated per cell) (Winter et al., 1994).
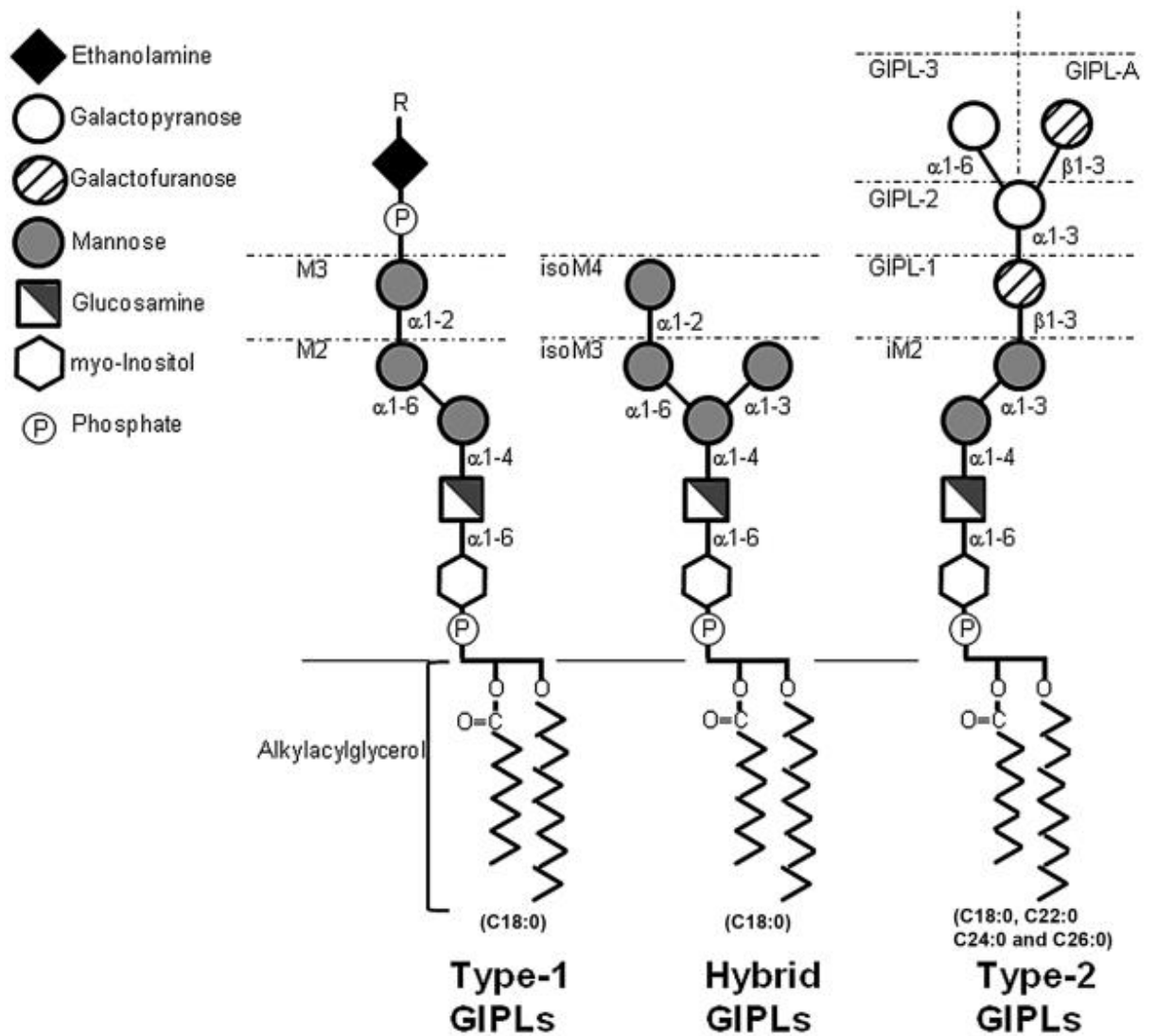
Figure 1.7. Structures of the different types of GIPLs. Type-1 GIPLs have anchors with homogeneous lipid composition, whereas type-2 have heterogeneous lipid composition. Type-2 have α1,3-mannose residues attached to the Manα1-4GlcN core, whereas type-1 have α1,6-mannose. All types vary in their size as shown with the dashed lines dividing different forms. The hybrid GIPLs can have either α1,3-mannose or α1,6-mannose residues (Assis et al., 2012).

1.4   Pentraxins

1.4.1   The pentraxin family

The pentraxin family is an ancient group of pattern recognition proteins found in the serum (Du Clos, 2013). Pentraxins can be divided into the classical short pentraxins which includes C-reactive protein (CRP) and Serum Amyloid P (SAP), and the long pentraxins which includes PTX3, PTX4 and neuronal pentraxins 1 and 2 (nPTX1 and nPTX2) (Oggioni et al., 2021). All contain the pentraxin domain at the C-terminus, but the long pentraxins have an extended and unrelated N-terminal domain (Du Clos, 2013). For the purposes of this work, we will be focusing on CRP and SAP, with a comparison of these two proteins seen in Figure 1.8. They share 51% amino acid sequence similarity and are similar in size around 23 kDa for CRP and 25 kDa for SAP. Both of these pentraxins have calcium-dependent binding and a pentameric structure, with two Ca^{2+} binding sites per subunit (Du Clos, 2013).
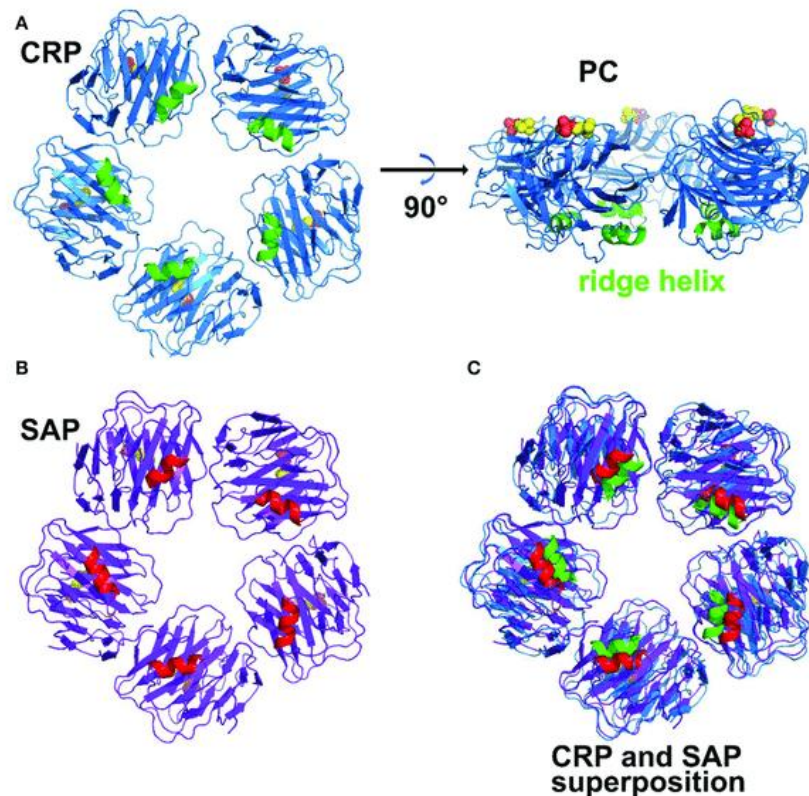
Figure 1.8. The structures of CRP (**A**) and SAP (**B**) can be seen. A different angle of CRP can also be seen with phosphocholine binding shown and the ridge helix, a deep groove with unknown function (Du Clos, 2013), shown in green. Figure from Lu et al. (2018).

1.4.2   C-Reactive Protein (CRP)

CRP was named due to its coprecipitation with C-polysaccharide from Pneumococcus bacteria (Abernethy and Avery, 1941). It is now known CRP is an acute phase protein with baseline levels of less than 1 µg/mL, that can rapidly increase to 10-500 µg/mL upon infection (Li et al., 1994; Du Clos, 2013). Calcium was required for C-polysaccharide precipitation to occur and similar precipitation results were seen for other infections (Abernethy and Avery, 1941). It was later found that phosphorylcholine (PCh) could effectively inhibit this precipitation, with phosphorylethanolamine (PEth) having a much lower inhibitory power (Volanakis and Kaplan, 1971). However, it is now known CRP does bind PEth (Mikolajek et al., 2011). Further study found residues on CRP important for PCh binding (Agrawal et al., 1992). These binding sites are found next to those for calcium on each of the five subunits on the B face of CRP. On the A face, there are binding sites for C1q, allowing the activation of complement (Thompson et al., 1999). CRP undergoes a conformational change when bound to a ligand, and it is only in this form CRP can bind C1q (Ahmed et al., 2016). PCh is found in mammalian cell membranes and is exposed only when they become damaged (Volanakis and Wirtz, 1979), allowing CRP to bind (Du Clos et al., 1981; Li et al., 1994) and target dead or disrupted cells. CRP is also able to bind histones (Du Clos et al., 1998; 2013) and small nuclear ribonucleoproteins (snRNPs) (Du Clos, 1989; 2013). All these traits allow CRP to be a part of host defense mechanisms (Thompson et al., 1999).

The interaction of CRP with parasites has been studied previously, such as for the rodent filarial nematode *Acanthocheilonema viteae* (Ahmed et al., 2016)*. Adult stages secrete ES-62, a glycoprotein containing PCh, which binds CRP, with CRP subsequently binding C1q. Due to PCh attachment via a flexible glycan, there is limited interaction with other components of the complement pathway and inhibition of complement activation, enabling immunomodulation of the host by *A. viteae* (Ahmed et al., 2016).

1.4.3   CRP and *Leishmania*

Previous work has studied the interaction of CRP with *Leishmania* and its products, with regards to the interaction with the human host. Pritchard et al. (1985) found human CRP was able to precipitate *Leishmania tropica* and *L. donovani* excreted factors in a calcium-dependent manner, similar to that observed for pneumococcal C-polysaccharide. In 1993, Raynes et al. used Fluorescence-activated cell sorting (FACS) and radiolabeling to show that CRP bound to a range of *Leishmania* species and strains, but did not bind to others. CRP did not bind to an *L.*

donovani mutant deficient in LPG, suggesting a possible binding site. In 1996, Culley et al. confirmed the ligand for CRP was LPG. They saw an increase in CRP binding as *L. donovani* parasites transitioned from log phase promastigotes to metacyclics, with CRP binding with high avidity. LT6 and LT15 antibodies, both specific for the $[-6Gal\beta1,4Man\alpha1-PO_4-]_x$ repeats of LPG competed with CRP for binding to *L. donovani*. CRP was also found to bind *L. donovani* ScAP which shares epitopes of LPG. As seen in Raynes et al. (1993), CRP was unable to bind *L. major*, with suggestions this could be due to substitutions in the LPG structure or differences in structure during metacyclogenesis (Culley et al., 1996). This was taken further, with Culley et al. (2000) finding CRP bound a synthetic form of the *L. donovani* $[-6Gal\beta1,4Man\alpha1-PO_4-]_x$ repeats. They then tested the binding abilities of CRP to a range of monosaccharides finding CRP had the highest avidity for galactose 6-phosphate, which makes up LPG.

The interaction of CRP and *L. donovani* was also found to increase the uptake of parasites into macrophages (Culley et al., 1996), which was later suggested to be due to increased C3 deposition on promastigotes when CRP was bound (Culley et al., 1997). However, in 2002, it was reported that this increased uptake was due to CRP binding Fcγ receptors or a CRP specific receptor (Bodman-Smith et al., 2002). CRP was found to mediate the transformation of *L. mexicana* metacyclic promastigotes to amastigotes (Bee et al., 2001) with the same found later for *L donovani*, and a suggestion made that CRP may be important within the PSG plug found in sand flies (Mbuchi et al., 2006).

1.4.4   Serum Amyloid P (SAP)

Though SAP and CRP have many structural similarities, such as the ligand binding sites for SAP also being found on the B face (Du Clos, 2013), they differ in ligands. Unlike CRP, SAP is unable to bind PCh, but does bind to PEth (Mikolajek et al., 2011). SAP itself is glycosylated, displaying a single N-linked biantennary oligosaccharide (Pepys et al., 1994). SAP binds to amyloid fibrils in a calcium-dependent manner (Pepys et al., 1977), with this suggested to protect amyloid fibrils against enzyme digestion (Li and McAdam, 1984). Binding of SAP to DNA (Pepys, 2018) can lead to displacement of H1-type histones and subsequent solubilisation of chromatin (Butler et al., 1990). SAP also binds heparin (Du Clos, 2013) and galactose (Hind et al., 1985; Pepys et al., 1994). SAP is not an acute phase protein in humans, usually found at an average serum level of 33 μg/mL in women and 43 μg/mL in men (Pepys et al., 1978; Du Clos, 2013).

SAP is thought not to have an essential function in adults (Pepys, 2018) and the literature is opposing on if SAP acts as an opsonin and if it activates complement. Conclusions drawn from

mouse work, where SAP is an acute phase protein (Pepys et al., 1979), will not necessarily apply to humans. Pepys (2018) argued the only definite function of mouse SAP was in the innate immune response to some bacterial infections based off findings by Noursadeghi et al. (2000). In this study, bacterial species which bound SAP had enhanced virulence, with SAP exhibiting an "anti-opsonin" effect. This is due to SAP being resistant to proteolytic attack (Kinoshita et al., 1992). The classical complement pathway is reported to be blocked by human SAP binding lipopolysaccharide with C1q and C3 deposition inhibited, with SAP also inhibiting phagocytosis (de Haas et al., 2000). However, mice deficient in SAP were found to have increased susceptibility to *Aspergillus fumigatus*. Mouse and human SAP were able to bind condidia spores and act as an opsonin for phagocytosis, leading to complement activation (Doni et al., 2021). A similar sequence of events was found for SAP binding *Streptococcus pneumoniae* (Yuste et al., 2007). Mouse SAP has also been reported to bind IgG on mouse phagocytic cells allowing SAP-mediated phagocytosis (Mold et al., 2001) of apoptotic cells (Mold et al., 2002).

SAP can be difficult to work with and will aggregate in high calcium concentrations (Baltz et al., 1982). Under non-physiological conditions, without calcium, SAP can form decamers, with the B-faces of two SAP molecules binding together (Pepys, 2018).

1.4.5   SAP and *Leishmania*

Less work has been done on the interaction of SAP with *Leishmania*. In 1993, Raynes et al. found no binding of SAP to a range of *Leishmania* species and strains tested when mainly metacyclic parasites were used. SAP was also found not to have an effect on transformation of *L. mexicana* promastigotes to amastigotes (Bee et al., 2001). However, preliminary experiments in the Raynes and Rogers labs since then (unpublished) have suggested interactions of SAP with *Leishmania* products and sand fly midgut proteins.

1.4.6   Treatments available against SAP

A lot of work has been done to study the role of SAP in human amyloidosis, with this leading to the production of a SAP depleting drug, CPHPC (R-1-[6-[R-2-carboxy-pyrrolidin-1-y1]-6-oxohexanoyl]pyrrolidine-2-carboxylic acid) (Pepys et al., 2002). CPHPC acts by blocking the B face binding sites, as well as crosslinking SAP pentamers together to form B-face to B-face decamers, seen in Figure 1.9. Studies in humans found CPHPC cross-linked SAP was removed from circulation by the liver (Pepys et al., 2002). This same group later produced an anti-SAP

antibody capable of producing a complement-dependent reaction that removed amyloid deposits in mice (Bodin et al., 2010). It was suggested that both these treatments would be used together, first CPHPC to deplete circulating SAP and then anti-SAP to act on amyloid deposits (Bodin et al., 2010). In 2017, both of these treatments were given WHO International non-proprietary names, being used in clinical trials by GSK. CPHPC became miridesap and the anti-SAP antibody, dezamizumab (Pepys, 2018), with the clinical trial known as DESPIAD (Depletion of Serum Amyloid P Component in Alzheimer's Disease) (Alzheimer Europe, 2019). The trial continued for three years but was not extended past phase I (Richards et al., 2022).
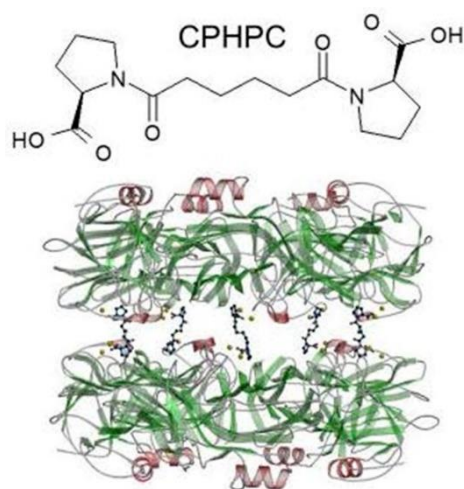
Figure 1.9. Structure of CPHPC and the complex formed between CPHPC and SAP (Pepys, 2018).

2. Research question

2.1 PhD overview and hypotheses

The main hypothesis of this thesis is SAP acts as a cross-linker between the midgut of the permissive sand fly *Lu. longipalpis* and the *Leishmania* logarithmic stage parasite, preventing loss of parasites when bloodmeal remnants are defecated. This requires understanding of the binding interactions of SAP with molecules on the surface of the sand fly midgut lumen and on the *Leishmania* parasite. As there may be alternative roles for SAP and CRP within the lifecycle of *Leishmania*, a variety of binding interactions will be studied. The growing field of research into midges as vectors of *Leishmania* will provide a further system to test our hypotheses. *In vivo* and *ex vivo* sand fly assays are crucial methods for studying *Leishmania*-vector interactions, however limited research has been carried out on the effect of differing methods for their outcome. Therefore, another aim of this thesis is to conduct a systematic review and meta-analysis of data from *in vivo* and *ex vivo* sand fly assays to see if and/or how differences in methods affects the infection intensity outcome.

2.2 Chapter overview

Chapter 3 will report methods I have carried out as part of this project as well as clarifying my contributions to work described in subsequent chapters. It will contain discussion of protocol optimisation and preliminary results to show how the path of the project was influenced.

In Chapter 4, the results of the systematic review and meta-analysis will be reported. The aim of this analysis is to see if differences in infection dose or morphological form used for the infection affects the infection intensity at a range of days post infections, as well as comparing the results of *ex vivo* and *in vivo* studies. This chapter will also allow the collation, assessment and comparison of *in vivo* and *ex vivo* sand fly assay protocols to optimise ones for use in the laboratory.

In Chapter 5, the main hypothesis of this thesis will be investigated. One of the objectives of this work is to identify the binding partner for SAP on the *L. mexicana* surface and on the sand fly midgut lumen surface. We want to compare binding of SAP to different *Leishmania* morphological stages as well as comparing binding to sand flies in different physiological states. As part of this hypothesis, it is important to investigate if SAP can 'survive' the sand fly environment. A further objective is to carry out *in vivo* and *ex vivo* sand fly assays to see if the addition of SAP or anti-SAP molecules affects the parasite infection intensity within the sand fly, or parasite attachment to dissected midguts.

In Chapter 6, the pentraxin CRP and its interactions with *Leishmania* secreted material will be the focus. The hypothesis of this chapter is CRP binds *Leishmania* promastigote secretory gel (PSG) and activates complement. The objectives are to identify the binding interaction between CRP and PSG, to see if the binding capacities of CRP for PSG differ between *Leishmania* species and to use complement assays to see if complement is activated by this complex and if so, by which pathway.

Chapter 7 will report and discuss the preliminary results of experiments using colony midge species *Culicoides sonorensis* and *Culicoides nubeculosus* and parasite *L. (M.) chancei*. The main objectives of this chapter are to find the binding partner of SAP on both *L. (M.) chancei* and on the midge lumen surface. Another aim is to look at the interaction of the midge midguts with GalNAc, which as previously mentioned has been found to be important for *Leishmania (Leishmania)* attachment to sand fly midguts.

Chapter 8 will consist of an overview discussion of results from Chapters 4, 5, 6 and 7. This will allow the results of this thesis to be put into context of previous research as well as giving an opportunity to discuss future work that will expand our knowledge of this field.

3. Methods, optimisation and preliminary results

This chapter will go through the methods I carried out as part of this project in detail, discussing challenges that were faced and how methods were optimised. It will include preliminary results that influenced future work, with some discussion of their relevance to the project and the field.

The parasites used throughout, unless otherwise stated are *Leishmania (Leishmania) mexicana* (MNYC/BZ/62/M379). When parasites were needed, cryopreserved mid-logarithmic (log) growth phase promastigotes were thawed and grown in supplemented M199 + 20% FCS (described further in Chapter 5). The sand fly colony*, Lutzomyia longipalpis* (Jacobina), was maintained by Dr Matthew Rogers at LSHTM. Some experiments used sugar fed flies, where flies had access to 50% sucrose *ad libitum*. For some experiments, flies were blood fed with more details of this found in section 3.9.

3.1   Pentraxin purification

3.1.1   Overview of process
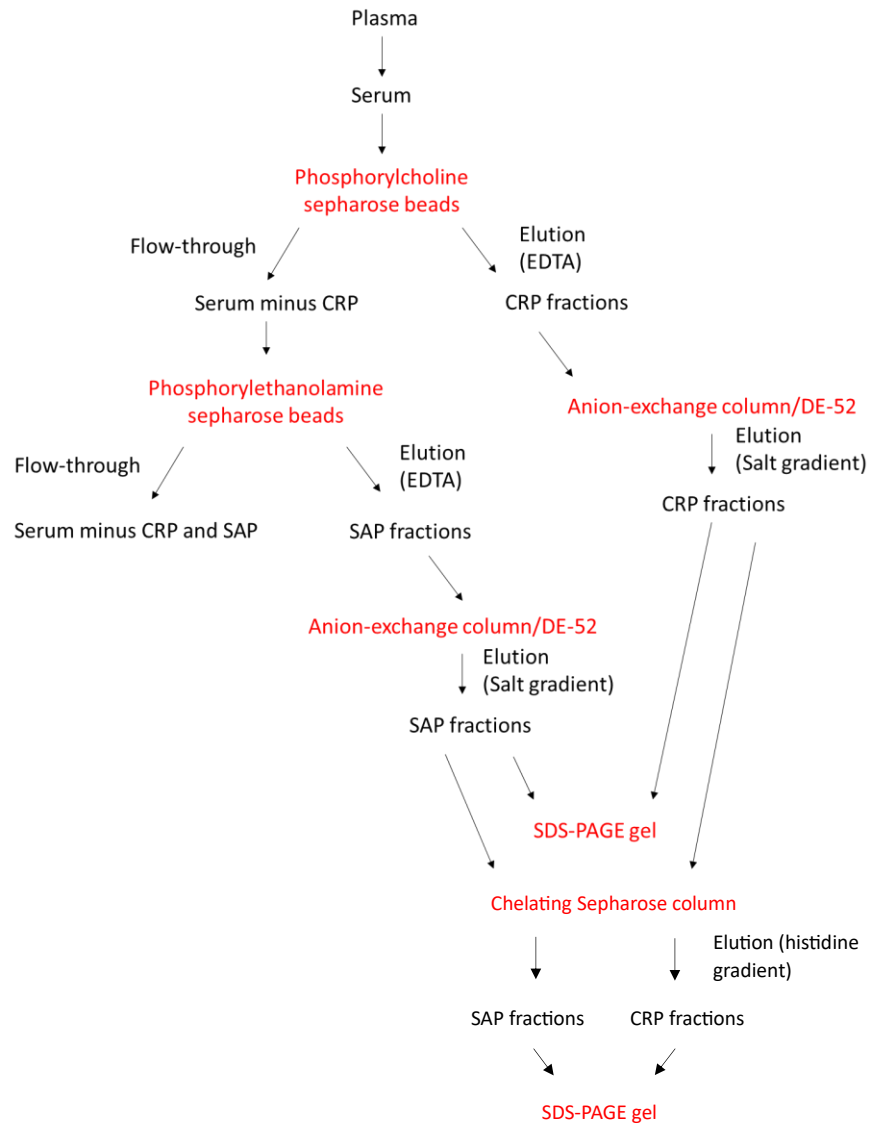
Figure 3.1. An overview of the pentraxin purification process.

3.1.2   Preparation of serum from plasma

The protocol for pentraxin extraction was kindly provided by Dr John Raynes. Human plasma was obtained from Dr M Bramham (The Binding Site, Birmingham, UK).

Serum was first prepared from plasma using 40 mg/mL protamine sulphate in 0.33 M $CaCl_2$, with 40 mL added per 1 L of plasma. This was left in a water bath at 37°C until the plasma become "jelly"-like and then spun down at 2000 g (JLA-9.1000 rotor, Beckman-Coulter) for 1 hour at 10°C. The serum could then be collected, and the pellet discarded.

3.1.3   Phosphorylcholine and phosphorylethanolamine Sepharose bead columns

Phosphorylcholine (PCh) beads (generated by the Raynes Laboratory from ρ-amino phenylphosphorylcholine linked to NHS activated Sepharose) were added to a column. This was the first step as only CRP binds efficiently to PCh. Elution buffer (10 mM Tris pH 8, 10 mM EDTA) was first run through the column to remove any protein that may be attached to the beads. The beads were then equilibrated using equilibration buffer (10 mM Tris pH 8, 0.15 M NaCl, 1 mM $CaCl_2$). Normally, the serum would then be passed over the beads within the column, however due to the large amount of serum available, it was more time efficient and therefore better for the protein quality, to add the equilibrated beads to the serum. The beads and serum were left for 30 minutes, with the bottle mixed every 5 minutes. Again, due to the amount of serum, it was then passed through a filter (grade 3) using a vacuum pump, allowing the separation of the beads and the flow through serum. The flow through was stored at 4°C ready for purification using phosphorylethanolamine (PEth) beads.

The beads collected from on top of the filter were then transferred back to the column. Equilibration buffer was then again run through the column, removing contaminants and non-specific binding. Flow-through from the column was set up to be collected in 6 mL fractions using a fraction collector (Redirac). Elution buffer was then run through the column. The protein concentration of collected fractions was determined using a quartz cuvette and spectrophotometer set at 280 nm, with elution buffer used as the reference sample. Once plotted, a clear peak of CPR elution could be seen (Figure 3.2). Fractions with high protein content (ODs) were combined and stored for use in the anion-exchange column.

The same process took place for the PEth column, using the flow through serum from the PC column, with the protein concentration of the fractions seen in Figure 3.3. PEth Sepharose 4B

was generated by the Raynes Laboratory by coupling phosphorylethanolamine to EAH Sepharose 4B using EDC.
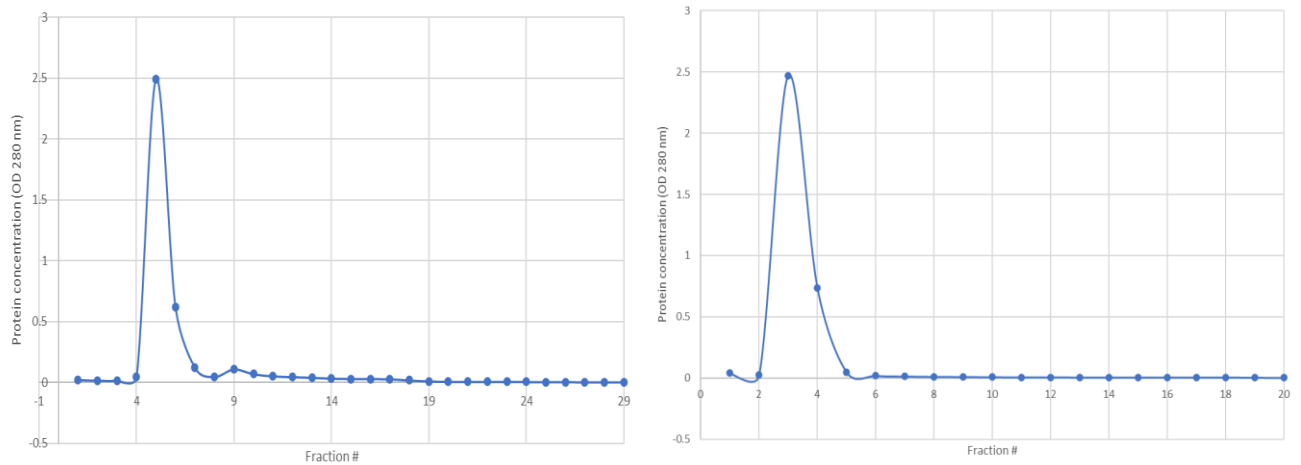
Figure 3.2. Protein concentration of each fraction collected off phosphorylcholine beads incubated with serum. The concentration of each fraction was determined using a spectrophotometer set at 280 nm, with the optical density of each fraction shown. Clear peaks can be seen of purified protein. Two serum samples were used, with the fractions of both shown.
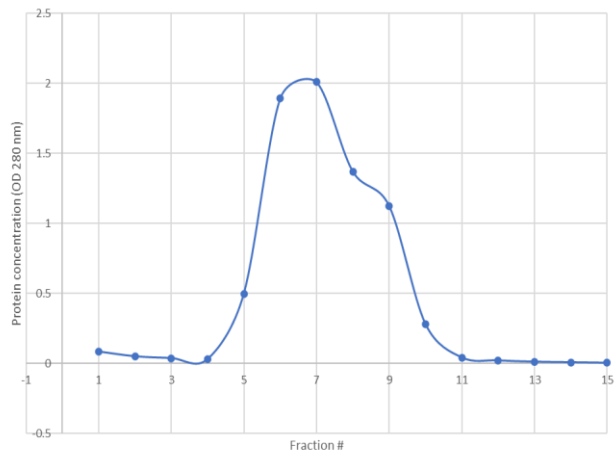
Figure 3.3. Protein concentration of each fraction collected off phosphorylethanolamine beads incubated with serum. The concentration of each fraction was determined using a spectrophotometer set at 280 nm, with the optical density of each fraction shown. The peak shows purified protein.

3.1.4 Anion-exchange column

The purified SAP and CRP samples were diluted by 0.5 using distilled water before addition to the anion-exchange column. DE-52 anion exchange resin (12 g) (Merck) was prepared by mixing with 100 mL 100 mM Tris pH 8, 1.5 M NaCl, three times. DE-52 was allowed to settle, with the remaining liquid removed, and the DE-52 transferred to a column. Then, 100 mM Tris pH 8, 1.5 M NaCl was then run through the column, followed by 7.5 mM Tris, 0.1 M NaCl until the pH of the flow through was 8. The combined, diluted CRP fractions from the PCh column were added to the column, and the fraction collector set up to collect new fractions. A salt gradient was set up with a low salt buffer (7.5 mM Tris pH 8, 0.1 M NaCl) and a high salt buffer (10 mM Tris pH 8, 1 M NaCl). As previously, protein concentrations of fractions were determined using a spectrophotometer. The same was done using fresh DE-52 and the SAP samples. The protein concentrations for CRP and SAP can be seen in Figure 3.4.

A

B
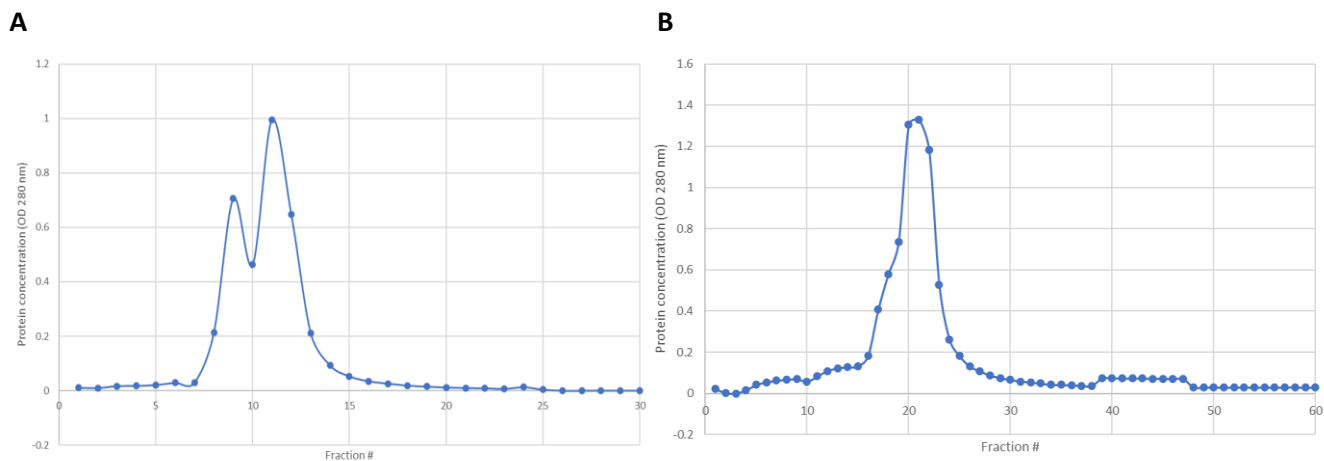
Figure 3.4. **A** shows the protein concentration of the CRP fractions collected off the anion-exchange column. **B** shows the same but for the SAP fractions.

It is clear in Figure 3.4A that there are two protein peaks for the supposedly CRP only fractions eluted from the DE-52 column. To confirm multiple proteins were present, 15 μL of these fractions were run on an SDS-PAGE gel, under reducing conditions and stained with Coomassie (section 3.6), seen in Figure 3.5. SAP was found to contaminate the CRP fractions, and the reverse seen for the SAP fractions. However, Fraction 9 of the CRP fractions collected off the anion-exchange column gave a clear SAP band (Figure 3.5A and B).
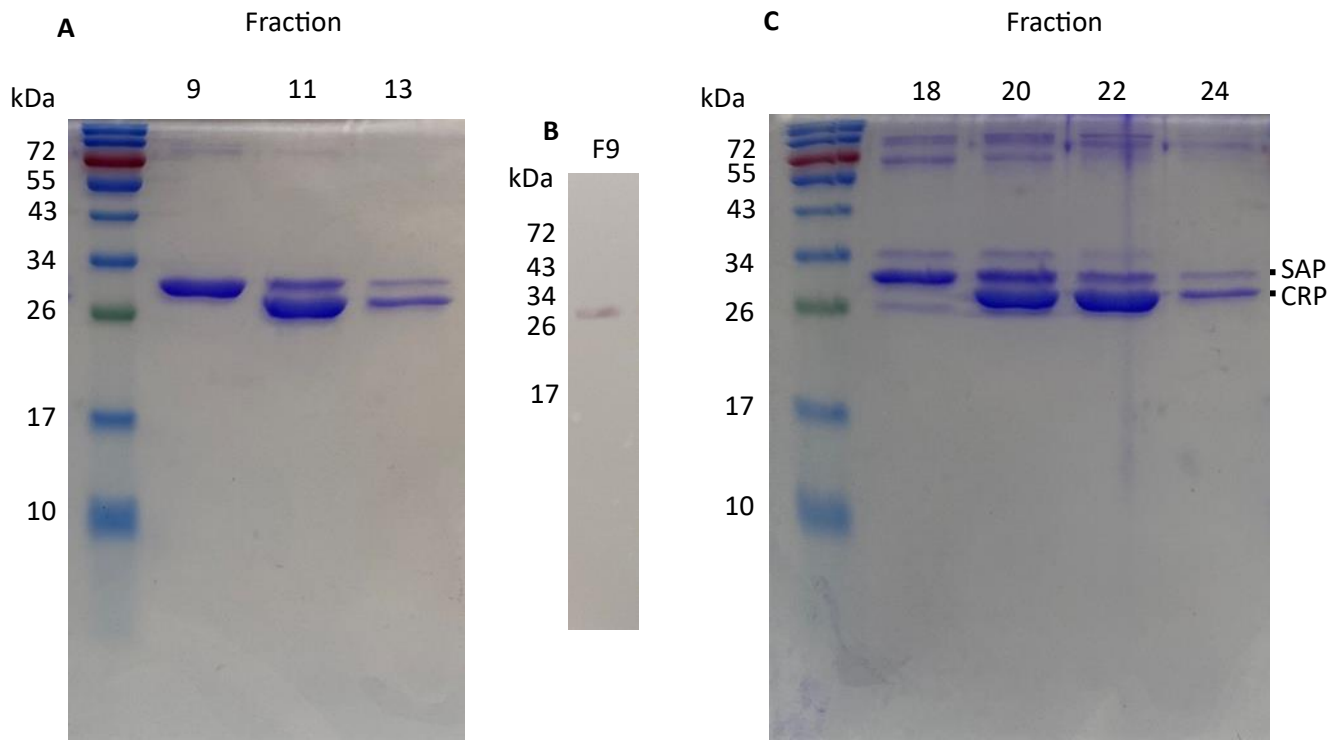
Figure 3.5. Fractions off the anion exchange column had reciprocal contamination of the pentraxins. Fraction 9 showed a Coomassie stained band correlating to SAP only. **A** Fractions 9, 11 and 13 from the anion exchange column that had the CRP sample passed over it. **B** Western blot of Fraction 9 seen in A, probed with 5.4D-biotin (anti-SAP antibody) and streptavidin-alkaline phosphatase. **C** Fractions 18, 20, 22 and 24 from the anion exchange column that had the SAP sample passed over it. In **A** and **C**, there is reciprocal contamination of the pentraxins with the other.

3.1.5   Chelating Sepharose column

Due to reciprocal contamination of the CRP and SAP fractions with the other pentraxin, a chelating Sepharose column was used to further separate these proteins from each other. This final stage of purification was similar to that described by Loveless et al. (1992). This takes advantage of the slightly different binding affinities of these pentraxins to Zn^{2+}. 'CRP' fractions 10-13 and 'SAP' fractions 17-24 were combined and dialysed (using VISKING dialysis tubing 12-14 kDa cut off) into 20 mM Tris pH 8, 0.15 M NaCl. The chelating beads (Fast flow 17-0575-01, Pharmacia) were added to the column, washed with distilled water and equilibrated with 20 mM Tris pH 8, 0.15 M NaCl. The column was loaded with zinc using three column volumes of 5 mM $ZnCl_2$ and the column connected to the fraction collector. The sample was added, then washed with 20 mM Tris pH 8, 0.15 M NaCl and then protein eluted using 20 mM Tris pH 8, 0.15 M NaCl, with a gradient of 0 - 30 mM histidine. Protein concentration was recorded as previously described, with the fractions seen in Figure 3.6. Fractions with high ODs were run on an SDS-PAGE gel (15 µL sample) under reducing conditions and stained using Coomassie, which can be seen in Figure 3.7, clearly showing CRP was in the first peak, and SAP in the second.
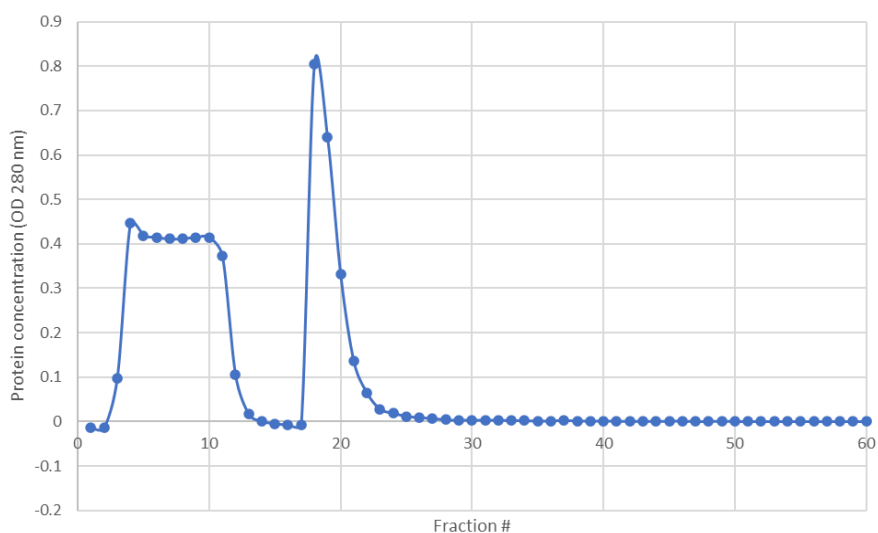
Figure 3.6. The protein concentrations of the fractions collected off the chelating Sepharose column are shown, with two clear peaks of CRP followed by SAP.
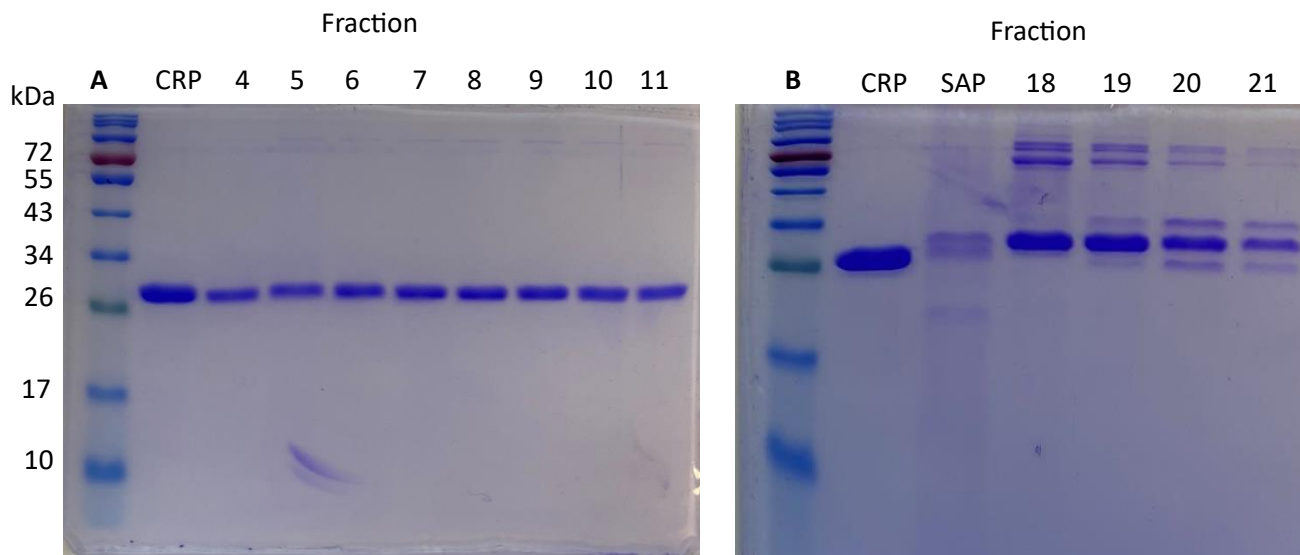
Figure 3.7. Fractions with only a CRP Coomassie stained band were collected off the chelating Sepharose column. **A** Fractions from the first peak off the chelating Sepharose column (Figure 3.6) are shown, alongside a control CRP sample. **B** Fractions from the second peak off the chelating Sepharose column are shown, alongside a control CRP and SAP sample.

Though the chelating Sepharose column provided purer fractions of CRP, the purest SAP fraction was Fraction 9 of the CRP samples ran over the anion exchange column (seen in Figure 3.5A and B). This fraction was used for all experiments. CRP Fractions 4-11 (Figure 3.7A) were combined and used for experiments.

3.2   *Leishmania* material purification
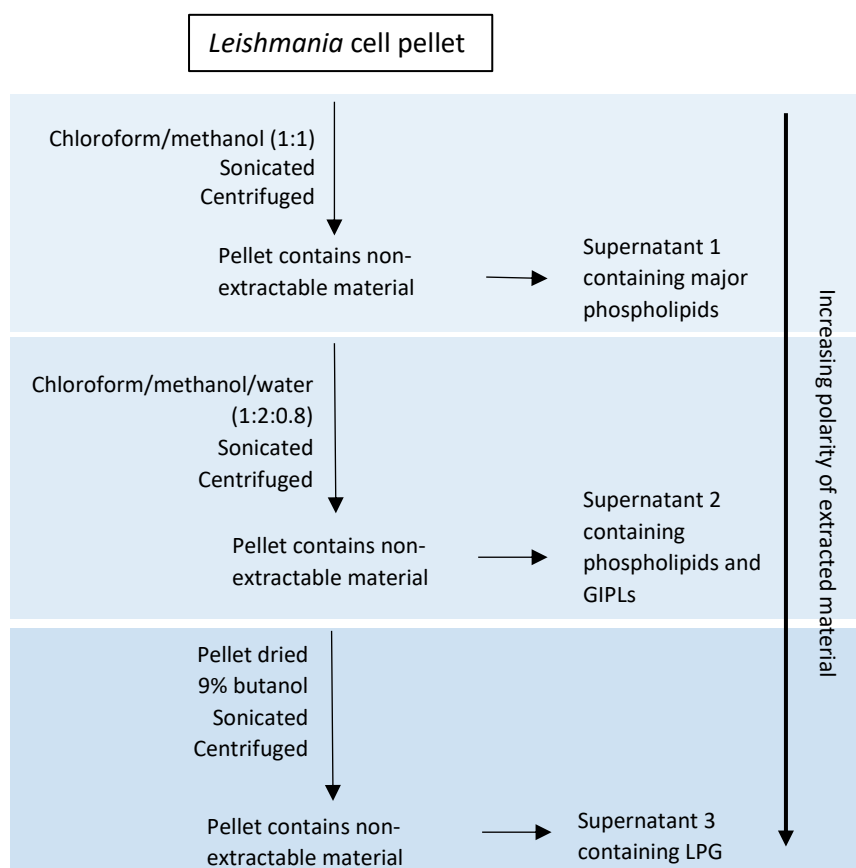
Figure 3.8. A summary of the methods used to extract GIPLs and LPG from whole *Leishmania* parasites.

3.2.1   LPG and GIPL purification

The protocol for LPG and GIPL purification was kindly provided by Dr Alvaro Acosta-Serrano, and is shown in Figure 3.8. Depending on the number of parasites used, this protocol was scaled appropriately. For 10^9 parasites, 5 mL 1:1 chloroform:methanol (v/v) was added to the pellet and bath-sonicated (50-60 Hz) until the pellet was homogenised (5 to 15 minutes). The sample was spun down at 2246 g (3500 rpm) (ALC PK 130R), with the supernatant separated. This was repeated twice. The same steps were used when 1:2:0.8 chloroform:methanol:water was added to the pellet, but with an increase in centrifuge speed to 2934 g (4000 rpm) and the extraction being repeated three times. The supernatant from this extraction contains GIPLs. The pellet was then dried using a speed vacuum with nitrogen flow (Reacti-Therm III, Pierce) and resuspended in 0.5 mL 9% butanol in distilled water. The sample was sonicated until the pellet was homogenised, and spun down at 16060 g (maximum speed) (Biofuge fresco Heraeus) for 15 minutes. This extraction was repeated twice more, with the supernatant

containing LPG. The LPG supernatants were combined, and speed vacuumed with nitrogen flow, before resuspending in distilled water.

Two separate LPG extractions were carried out during this project, the first time, only log phase and metacyclic stage *Leishmania (Leishmania) mexicana* (MNYC/BZ/1962/M379) parasites were used and only LPG was extracted. To enrich the culture for metacyclics, stationary phase parasites were centrifuged over a Ficoll gradient (Späth and Beverley, 2011; Giraud et al., 2019), with this carried out by Dr Matthew Rogers. The protocol was slightly different to described above with the chloroform:methanol:water extractions only carried out twice, and the butanol extraction only carried out once with the final spin lasting 40 minutes. Supernatants from earlier stages were not collected. The second time, log phase and metacyclic stage *L. mexicana* and *Leishmania (Mundinia) chancei* (MHOM/GH/2012/GH5;LV757) were used, with LPG and GIPLs being extracted.

Further GIPL purification was attempted, following a protocol described in Assis et al. (2012). The combined GIPL supernatants were dried using a speed vacuum with nitrogen flow. The pellet was resuspended in 0.1 M ammonium acetate pH 6.5 containing 5% propan-1-ol. An octyl Sepharose column (Amersham Biosciences) was equilibrated in the same buffer with 25% (100 µL) of the *L. mexicana* GIPL sample added, diluted in a total of 2 mL buffer. The column was washed again with the buffer, connected to a fraction collector and a propan-1-ol buffer gradient set up, using 0.1 M ammonium acetate pH 6.5, 5% propan-1-ol and 0.1 M ammonium acetate pH 6.5, 60% propan-1-ol. However, the full gradient could not be run due to slow movement and pullback of liquid through the column system. At the end of the run, 0.1 M ammonium acetate pH 6.5, 60% propan-1-ol was added to elute any GIPLs still bound to the octyl Sepharose. This may have been due to the presence of larger structures that were purified alongside the GIPLs clogging the top of the column and preventing the flow of liquid through the system. Each fraction from this attempt was dotted (3 µL) onto a nitrocellulose membrane (0.45 µm, Amersham), blocked overnight and probed with CA7AE, SAP and CRP (section 3.6) but results were difficult to interpret with the slow flow likely affecting the propanol gradient. With limited sample and time, it was decided not to attempt a new purification, and to use the GIPL sample as it was.

3.2.2 Thin layer chromatography

Part of this project was to identify the binding site on *Leishmania* for SAP. It was thought that SAP may be binding to type I GIPLs which were contaminating the LPG from the first round of extraction. This was due to very low signal being detected in ELISAs of LPG probed with SAP. Thin layer chromatography (TLC) was attempted to try and separate these molecules. A total of 7.65 µg and 15.3 µg of log phase *L. mexicana* LPG was dotted on a silica plate (540088215, Merck) and placed into a glass vessel containing the solvent system. The solvent system was 90 mL chloroform, 70 mL methanol, 4.5 mL 1 M ammonium acetate, 4.5 mL 13 M ammonia and 11.5 mL water. The solvent was roughly 1 cm lower than the dots on the silica plate. The lid on the glass tank was closed, and the system left until the solvent reached near the top of the silica plate. The plate was left to dry before spraying with an orcinol stain diluted in sulphuric acid. Two different staining protocols were tried, based off Culley (1997). One used 0.02 g orcinol in concentration sulphuric acid diluted 1:20 with water. The second used 1 g orcinol diluted in 45 mL 1:2:15 water:concentrated sulphuric acid:ethanol. The silica plate was then incubated at 100°C (Daewoo KOC 8HAFR) until bands appeared, however no bands were seen.

We also tried to transfer the GIPLs to a polyvinylidene fluoride (PVDF) (IPVH00010, Millipore) membrane to see if we could probe for SAP and CRP binding. After being placed in the solvent system, the silica plate was placed briefly in a transfer solution consisting of 40 mL isopropanol, 20 mL 0.2% $CaCl_2$ and 7 mL methanol (Taki et al., 2009). A PVDF membrane was briefly activated in methanol, before being added on top of filter paper, followed by the silica plate and another layer of filter paper. A heat block (Reacti-Therm III, Pierce) was used to apply slight temperature to the transfer stack. The PVDF was then removed, blocked and probed with SAP and CRP as discussed later (see 3.6). Again, no bands were seen, though a circular pattern of non-specific binding was observed. This may suggest that solvents from the solvent system still remained on the plate when dipped into the transfer solution, meaning the transfer solution did not fully soak the plate. The lack of banding may have been due to a lack of sensitivity of the system and not enough material being used to get a signal.

3.2.3 Phenol sulphuric quantitation assay

Quantitation of the first round of LPG extraction was done using a phenol sulphuric quantitation assay. 50 μL of doubling dilutions of 10 mg/mL mannose (M4625, Sigma) down to 0.0006 mg/mL in distilled water were added in triplicate to a NUNC maxisorp plate (3855, Thermo Scientific). 1:10, 1:20, 1:40 and 1:80 dilutions of the LPG samples were made using distilled water, with 50 μL added to the plate. For each LPG sample, six repeats were used. To each well, 150 μL concentrated sulphuric acid was added, followed by 30 μL of 5% phenol. A pipette was used to mix the samples. The plate was covered and placed on a shaker to mix the reagents with the sample. The plate was heated to 90°C using a water bath and left for 30 minutes until a colour change was seen. This was recorded using 340 nm on a plate reader (titertek multiscan). A mean OD was calculated for the LPG samples, with the concentration then interpolated using the mannose standard curve. The log phase *L. mexicana* concentration was 1.53 mg/mL and the metacyclic concentration 1.16 mg/mL.

This method of quantitation was tried for the second round of LPG and GIPL extraction, however no colour change was observed, even for the mannose dilutions. The same protocol and reagents were used as previously, but products may have degraded in the years between the two experiments. Due to the harmful substances and processes used in this method, an alternative method of quantitation was sought.

3.2.4 Dot blots

An alternative quantitation method used for the second round of LPG extracts was dot blots to semi-quantitatively deduce the concentration of new LPG samples compared to the known concentration of the older samples. For each sample, 3 μL was dotted onto a nitrocellulose membrane, left to dry and blocked overnight (see 3.6). The blot was then probed with anti-LPG antibody CA7AE, with the results seen in Figure 3.9. A no CA7AE control showed no binding.
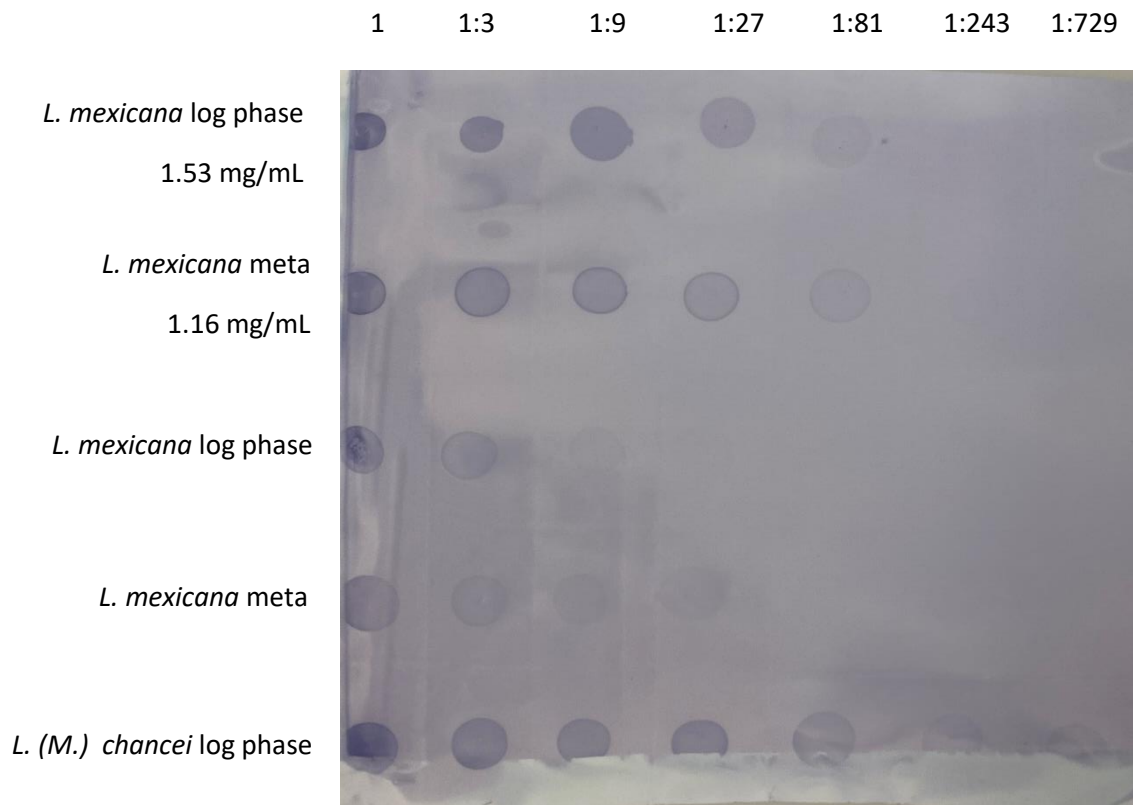
Figure 3.9. A nitrocellulose dot blot of two *L. mexicana* LPG samples of known concentration, with two unknown *L. mexicana* and one unknown *L. (M.) chancei.* The blot was blocked and probed with anti-LPG antibody CA7AE.

A

B

Dilution	Conc log phase (µg/mL)	Integrated Density
1	1530	68070
1:3	510	41916
1:9	*170*	*57922*
1:27	56.7	32093
1:81	*18.9*	*23061*
1:243	6.3	X
1:729	2.1	X
1	510.5	54722
1:3	26.55	27682

C

$Y = 21053*X - 2293$
$R^2 = 0.7375$

Log(Concentration logathrimic phase) (µg/mL)

D

Dilution	Conc meta (µg/mL)	Integrated Density
1	1160	60007
1:3	386.7	42141
1:9	128.9	35362
1:27	43	26883
1:81	14.3	22040
1:243	4.8	X
1:729	1.6	X
1	193.64	40656
1:3	28.56	24756
1:9	11.91	17487
1:27	11.61	16968

E

$Y = 19127*X - 3086$
$R^2 = 0.9406$

Log(Concentration metacyclic LPG) (µg/mL)

Figure 3.10. LPG concentration interpolation using simple linear regression. **A** shows the dot blot inverted in ImageJ and the circular selection used to measure the integrated density of each dot. **B** shows the integrated density values for the log phase *L. mexicana* sample of known concentration, with the integrated density for the unknown new log phase *L. mexicana* samples shown in red. **C** shows the linear regression of the known log phase *L. mexicana* samples and the interpolated new samples are shown in red. **D** shows the same as B but for the metacyclic *L. mexciana* samples. **E** shows the same as C but for the metacyclic *L. mexicana* samples.

Using ImageJ (ImageJ.JS (imjoy.io), the integrated density of each dot of known LPG concentration was calculated (displayed in Figure 3.10A). This was carried out following an ImageJ protocol (ImageJ dot blot). Using GraphPad Prism, the integrated density results were plotted against the log concentration, with a simple linear regression carried out. The results for the log phase *L. mexicana* sample of known concentration can be seen in Figure 3.10B and 3.10C, and in 3.10D and 3.10E for metacyclic *L. mexicana*. The concentration of the unknown samples could then be interpolated (shown by red square points in Figures 3.10C and 3.10E). The log phase results were used to interpolate the new log phase sample concentration, with the metacyclic results used for the new metacyclic sample. For the log phase sample, two varying concentrations were interpolated. As the undiluted sample gave the clearest dot, the concentration of this dot was taken forward (510.5 µg/mL). For the new metacyclic *L. mexicana* sample, a mean of the four interpolated values was used to calculated the concentration of 172 µg/mL. A similar protocol was used by Masters student, William Paine, to calculate the concentration of log phase *L. (M.) chancei* LPG, finding it to be 1.008 mg/mL.

3.3 Vector dissection

Vector dissection (sand flies and midges) has been a large part of this project, and is needed for a range of the methods discussed in this chapter. The vectors are knocked down on ice, and then transferred to a detergent-water mix to remove some of the setae and this also helps with the static charge that can make sand flies hard to move. The vector was then placed into a drop of PBS on a glass slide under a stereo dissecting microscope (SZX9, Olympus), for dissection with fine needles (26 G x 13 mm). The set up can be seen in Figure 3.11 for dissection of a sand fly. Two cuts are made, one removing the head of the vector, and the second removing the last few segments of the abdomen. This allows for the entire digestive system, seen in Figure 3.12, to be pulled out of the vector, from the second cut site. Cuts are then made to remove the hindgut, malpighian tubules and the foregut (leaving the stomodeal valve). In some experiments, the midgut was carefully opened or 'unzipped' using fine needles, to reveal the inner lumen.
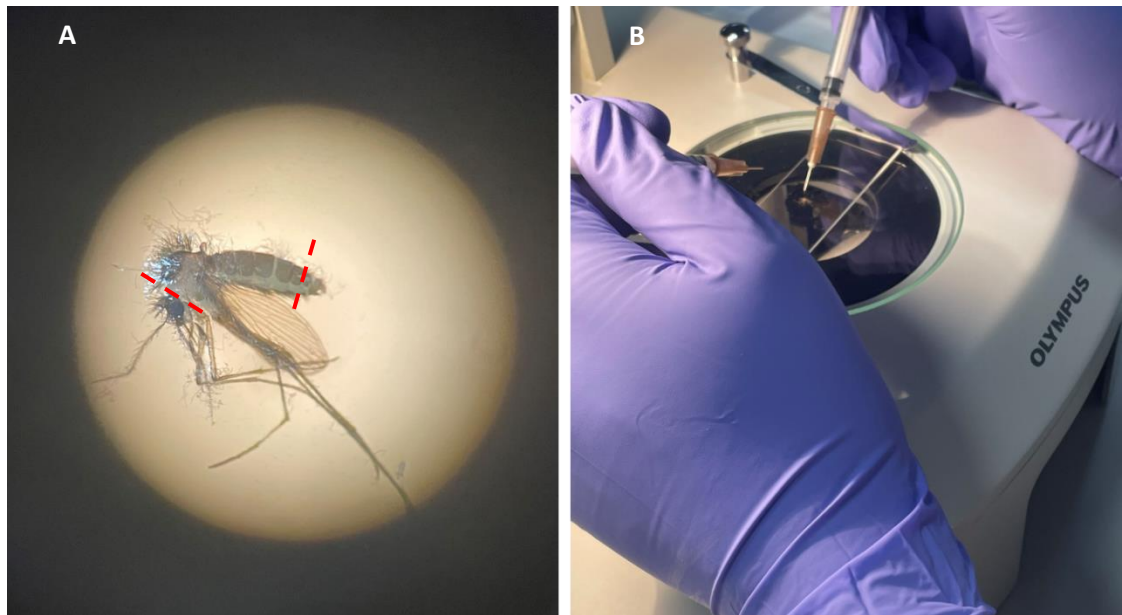
Figure 3.11. A shows a sand fly under a dissecting microscope with red dashed lines marking the cut points during dissection. The first cut removes the head and the second removes the last few segments of the abdomen. **B** shows the set-up of the dissection and the fine needles used. Images from Alsford, 2022 with edits made.
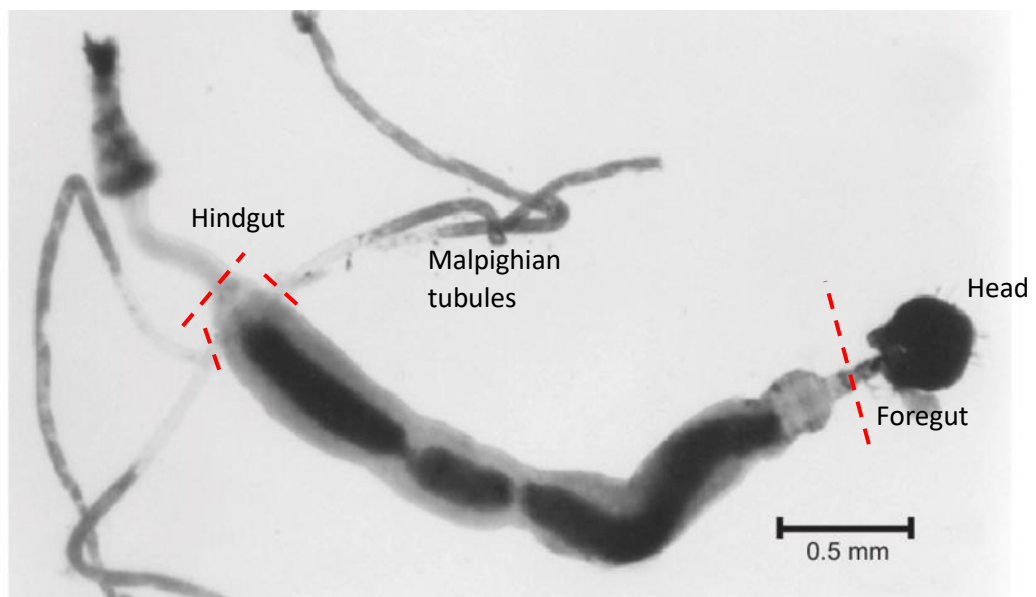
Figure 3.12. The full digestive tract of the sand fly is shown. This image contains the head which is removed before the digestive tract is removed from the sand fly in our protocol. Red dashed lines mark the cut sites to remove the hindgut, malpighian tubules and the foregut. Image from do Vale et al. (2007) with edits made.

3.4   Vector protein purification

For some experiments, such as Western blots, midgut material enriched for microvillar proteins was used. Though this protocol is enriching for microvillar proteins, samples may also contain other non-protein microvillar material. Extraction of proteins from midguts was carried out following the protocol from Dillon and Lane (1999). Once an intact midgut was dissected, it was placed in 200 μL ice cold isolation buffer (300 mM mannitol, 100 mM Tris-HCl pH 7.2, 1 mM phenylmethylsulphonyl fluoride (PMSF)). In each round, 50-100 midguts were dissected at a time. The buffer and midguts were then transferred to a glass homogeniser and homogenised on ice for 5 minutes. Isolation buffer with 10 mM $CaCl_2$ (300 μL) was used to 'clean' the pestle of the homogeniser, collecting any protein and buffer that was still present. The 500 μL of buffer with the homogenised midgut protein was then transferred to a 1.5 mL microcentrifuge tube and incubated on ice for 15 minutes. The sample was spun down at 6000 g, for 15 minutes at 4°C. The supernatant was stored on ice, and 500 μL fresh isolation buffer with 10 mM $CaCl_2$ added and the sample incubated on ice for 15 minutes. The spin was then repeated. The two supernatants were combined and centrifuged at 18213 g for 30 minutes. The supernatant was discarded and the pellet resuspended in distilled water and stored at -20°C until required. The protein concentration of the sample was determined using a nanodrop (DS-11, DeNovix).

3.4.1   SAP stability post bloodmeal

Another experiment, looking at the presence of SAP in the sand fly midgut over a range of days post infection also required the purification of proteins from the midgut. A similar experiment was previously carried out by Serafim et al. (2023). This experiment did not require the enrichment of microvillar proteins, instead looking at all of the proteins within the midgut. The Serafim et al. (2023) protocol was followed but using a different RIPA lysis buffer (sc-24948) with product instructions followed. Every day 10 midguts were dissected and placed into 50 μL RIPA lysis buffer containing 0.5 μL PMSF solution, 0.5 μL sodium orthovanadate solution and 0.5 μL protease inhibitor cocktail. The midguts were homogenised in the buffer using a disposable pestle (Fisherbrand), vortexed and spun down at 16260 g (12,000 rpm) for 10 minutes at 4°C as in Serafim et al. (2023). The supernatant was collected and protein concentration determined using nanodrop. Samples were then used in Western blot experiments (see 3.6). This experiment was carried out on days 0 to 4 post bloodmeal, with feeding carried out by Dr Matthew Rogers. A second group of flies were given a bloodmeal, and

then given a second bloodmeal 6 days after the first one, with midguts then collected from these flies over the following days.

3.5   Enzyme-Linked Immunosorbent Assays (ELISAs)

A range of ELISA assays were used and trialled during this project, with the details of those carried out by myself and referenced in the following chapters shown in Table 3.1. A range of plates have been used depending on the immobilised ligand with PVC (2595, Costar) used for LPG and the control materials, PCh-Bovine Serum Albumin (BSA) and PEth-cellulose.

PEth-cellulose was generated by the Raynes lab from PEC overexpressing K-12 non-pathogenic (CL1) vector provided by Dr L. Cegelski (Thongsomboon et al., 2018). Supernatants from homogenised and pelleted bacteria were dialysed in 100 kDa dialysis tubing. PCh-BSA was generated by the Raynes lab using carbodiimide (EDC) coupling of BSA and ρ-amino phenyl phosphorylcholine (Ahmed et al., 2016). These are both controls, with CRP known to bind PCh and SAP known to bind PEth. The larger molecules allow the presentation of PCh and PEth as found on the cell surface as well as improving binding to the plate. Each sample was run in at least triplicate, with a control of either no pentraxin or no LPG included on every plate with this background binding taken away from the other results. Graphs were created using GraphPad Prism.

All ELISAs used the same protocol and reagents. 50 μL of the ligand was immobilised to the plate overnight at 4°C. Plates were then washed three times with 1 x HEPEs buffered saline (HBS) with 0.05% Tween-20 v/v and 0.5 mM Ca^{2+}. This was done by forcefully flicking the contents of the plate out, adding the wash solution, tapping the plate to agitate the solution within the wells, and then expelling the contents again. Wells were blocked for 2 hours at room temperature using 100 μL 1 x PBS with 2% w/v BSA and 0.05% Tween-20 v/v. The wash step was repeated with 50 μL analyte in 1 x HBS, 0.5 mM Ca^{2+} with 1% w/v BSA added to the appropriate wells and incubated at room temperature for 1 hour. The plates were washed again, with the primary antibodies added and incubated under the same conditions. The same occurred for the secondary antibodies, which were all horseradish peroxidase (HRP) conjugated. Then, 100 μL of the HRP substrate tetramethylbenzidine (TMB) was added resulting in a colour change reaction that was stopped with 15 μL 2 M H_2SO_4. The plate was read using a plate reader set to wavelength 450 nm (titertek multiscan).

Table 3.1. The details of the ELISAs carried out myself which are presented in this report are shown.

Assay	Immobilised ligand	Plate type	Analyte	Primary antibody	Secondary antibody
CRP/SAP competition	2 µg/mL metacyclic LPG or log phase LPG or PC-BSA or 1:20 PE-cellulose	PVC	0.5 µg/mL CRP + 0 – 20 µg/mL SAP	Rabbit anti-CRP (235752, Calbiochem) 1:1000	Goat anti-rabbit HRP (170-6515, BioRad) 1:3000
			0.5 µg/mL SAP + 0 – 20 µg/mL CRP	Mouse 5.4D (generated in house) 1:1000	Goat anti-mouse HRP (170-6516, BioRad) 1:3000
LT6 competition	1 µg/mL metacyclic or log phase LPG	PVC	0 - 2 µg/mL CRP +/- 1:10 LT6 antibody	Rabbit anti-CRP 1:1000	Goat anti-rabbit HRP 1:3000
			0 - 2 µg/mL SAP +/- 1:10 LT6 antibody	Rabbit anti-SAP (565191, Sigma-Aldrich) 1:1000	Goat anti-rabbit HRP 1:3000

Initially 1 µg/mL SAP-biotin made in house by the Raynes Lab was used with a secondary streptavidin-HRP (1:15,000) (BioSource). However the signal for this detection system was weak and so was changed to that seen in Table 3.1. 5.4D (anti-SAP antibody) also generated by the Raynes lab was used in these experiments. Previous cell supernatants (low FCS) were purified on an anti-mouse IgG column with standard glycine elution into Tris pH 8.0 buffer, followed by concentration and dialyses into PBS before storage.

3.6   SDS-PAGE and Western blots

SDS-PAGE gels and Western blotting have been used heavily during this project. A summary of the experiments carried out by myself and presented in this thesis are shown in Table 3.2.

All SDS-PAGE gels used in this project are 10% resolving with an extended 4% stacking gel. This is due to samples containing *Leishmania* molecules which are too large to enter the resolving gel. The stacking gel remains attached to the resolving gel for the transfer. Gels are made as seen in Table 3.3, using the Mini-Protean tetra cell casting module from BioRad. Samples were loaded alongside 1-3 µL of the colour prestained protein standard (10-250 kDa) (P7719 NEB). Samples were diluted with 2 x sample buffer (0.125 M Tris-Cl, 4% SDS, 20% v/v glycerol, 0.02% bromophenol blue, pH 6.8). Depending on the experiment, this buffer also contained 0.2 M

dithiothreitol (DTT). Samples were boiled for at least 5 minutes in a water bath. Running buffer for the gels was 25 mM Tris, 192 mM glycine, 0.1% SDS. Gels were run slowly at 30 mA and 80 volts.

For some experiments, gels were immediately incubated in Coomassie stain (1 g Coomassie brilliant blue R-250 per 1 L solution, 50% methanol, 10% glacial acetic acid, 40% distilled water). The gel was left in the stain for at least 1 hour, with 40% destaining solution (40% methanol, 10% acetic acid, 50% distilled water) incubated with the gel overnight. 10% destaining solution (10% methanol, 10% acetic acid, 80% distilled water) was then added, with a mix of incubations and addition of fresh solution until the bands were clear against the background.

For other experiments, the gels were transferred to PVDF, which had been activated in methanol for 30 seconds or nitrocellulose. The transfer was done using a semi-dry transfer system, with filter paper presoaked in transfer buffer (25 mM Tris, 192 mM glycine, 20% methanol). The transfer system ran for at least 1 hour at 11 volts and maximum mA. The membrane blot was then blocked overnight at 4°C in 1 x PBS + 2% BSA + 0.05% Tween-20. The blots were washed three times for 5 minutes in 1 x TBS + 0.05% Tween-20 (with either 0.5 mM Ca^{2+} or 10 mM EDTA). The washes took place after every incubation step. Incubations with probes or antibodies diluted in 1 x TBS + 0.05% Tween-20 + 1% BSA (with either 0.5 mM Ca^{2+} or 10 mM EDTA) took place on a roller for 1 hour at room temperature. The final step was incubation of the blots with BCIP/NBT solution, the substrate for the alkaline phosphatase (AP) conjugated antibodies used, until bands appeared. The solution consists of 32 µL 50 mg/mL 5-Bromo-4-chloro-3-indolyl phosphate (BCIP) in dimethylformamide (DMF), 60 µL 50 mg/mL 4-nitrotetrazolium blue chloride (NBT) in distilled water, in 10 mL 100 mM Tris-HCl, 150 mM NaCl, 1 mM $MgCl_2$, pH 9. For each blot, 5 mL of solution was used.

As part of an immunoprecipitation experiment, discussed later in section 3.10, a previously Coomassie stained gel was silver stained (based off Mortz et al., 2001). The results of this work are not part of the papers in this thesis, however it was a useful step in confirming a range of proteins were extracted as part of the sand fly midgut microvillar protein enrichment extraction (discussed in section 3.4). The results of this staining can be seen in section 3.10, Figure 3.20. The Coomassie stained gel (already fixed) was left in distilled water at least overnight. Following this, the gel was incubated for 1 minute in 100 mL 0.02% sodium thiosulphate in distilled water. The gel was washed three times in distilled water by incubating for 20 seconds. Cold 0.1% silver nitrate solution (0.2 g $AgNO_3$, 200 mL distilled water, 0.02%

formaldehyde) was added and incubated for 20 minutes. The gel was washed again, moved to a new staining tray, and washed in distilled water for 1 minute. Developing solution made of 3% sodium carbonate, 0.05% formaldehyde was added to the gel, with this solution changed four times during the development process. When sufficient staining was seen, developing solution was replaced with distilled water.

During this project, a previously purified sample of 5.4D produced in house by the Raynes lab ran out, and Western blots were carried out to confirm the 5.4D supernatant could be used instead, as well as to confirm the appropriate concentration to be used, with blots seen in Figure 3.13A. The concentration of CA7AE to be used was also tested, seen in Figure 3.13B, with 1:1000 deemed the appropriate dilution, agreeing with previously published work (Guimarães et al., 2018). The details of both of these Western blots can be seen in Table 3.2.
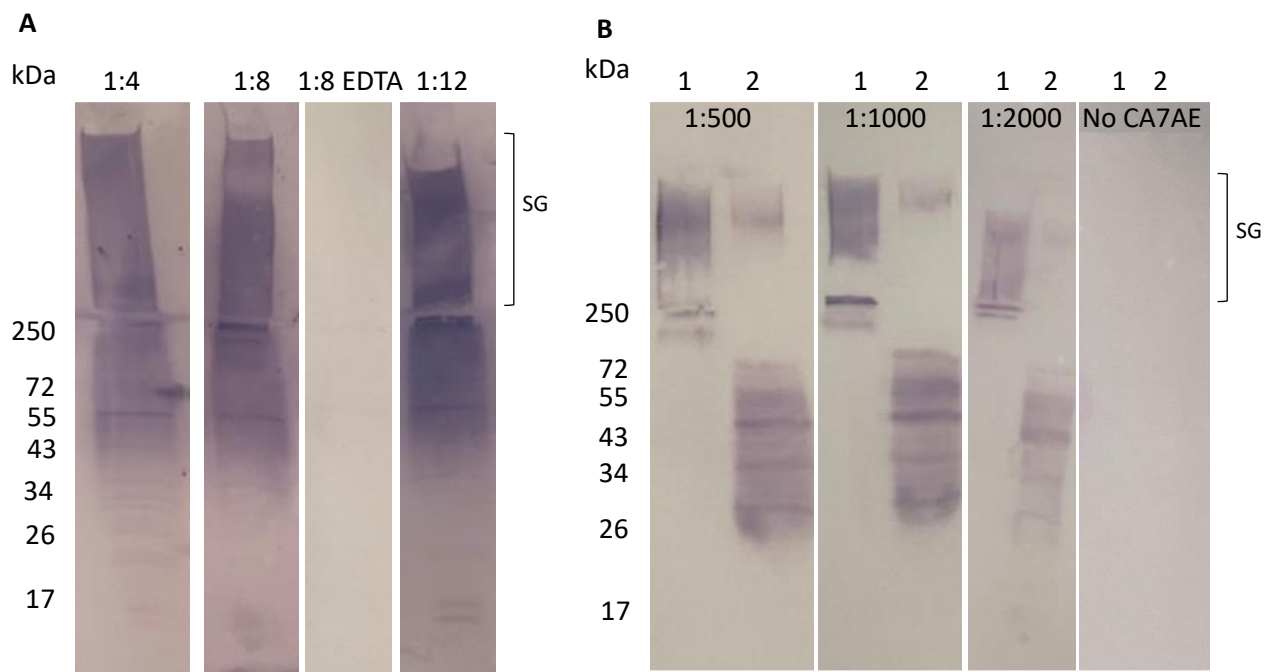
Figure 3.13. A shows the optimisation of 5.4D supernatant dilution for use in Western blotting, with 1 µg *L. mexicana* log phase LPG used as the ligand. A control blot is included for the 1:8 5.4D dilution where SAP was incubated with 10 mM EDTA. **B** shows the optimisation of CA7AE dilution for use in Western blotting, with 3 µg *L. mexicana* fPPG (1) and *L. mexicana* log phase LPG (2) used as the ligand. A control blot is included where blots were only incubated with the secondary antibody (no CA7AE present). SG = stacking gel.

Table 3.2. Summary of the Western blot experiments reported in this thesis

Experiment	Material	Probe	Primary	Secondary	Controls
Chapter 3:					
Figure 3.5B: Probing purified SAP	Fraction 9 off anion exchange column (previously thought to be CRP fractions)	-	1:1000 5.4D-biotin (Raynes Lab)	1:1000 Streptavidin-AP (Vector Laboratories)	-
Figure 3.13A: 5.4D supernatant dilution optimisation	1 µg *L. mexicana* log phase LPG	1 µg/mL SAP	1:4, 1:8 or 1:12 5.4D supernatant	1:3000 anti-mouse-AP (AP124A)	1 µg/mL SAP + 10 mM EDTA
Figure 3.13B: CA7AE dilution optimisation	3 µg *L. mexicana* log phase LPG, 3 µg *L. mexicana* fPPG	-	1:500, 1:1000 or 1:2000 CA7AE (GTX39838 GeneTex)	1:30,000 anti-IgM-AP (A-9688)	No CA7AE
Chapter 5:					
Figure 3: SAP, CRP and LT6 binding to *L. mexicana* material over subsequent days	2x10^5 *L. mexicana* parasites per lane	1 µg/mL CRP	1:10,000 rabbit anti-CRP (calbiochem)	1:5000 anti-rabbit-AP (Serala)	CRP + 10 mM EDTA
		1 µg/mL SAP	1:500 5.4D	1:3000 anti-mouse-AP	SAP + 10 mM EDTA
		-	1:8 LT6	1:3000 anti-mouse-AP	No LT6
Figure 4: Comparison of pentraxin, CA7AE and LT6 binding to LPG and GIPLs	3 µg *L. mexicana* log phase and metacyclic LPG, 1 µL GIPL-enriched material	1 µg/mL CRP	1:10,000 rabbit anti-CRP	1:5000 anti-rabbit-AP	CRP + 10 mM EDTA, No CRP
		1 µg/mL SAP	1:12 5.4D supernatant	1:3000 anti-mouse-AP	SAP + 10 mM EDTA, No SAP
		-	1:1000 CA7AE	1:30,000 anti-IgM-AP	No CA7AE
		-	1:8 LT6	1:3000 anti-mouse-AP	No LT6
Figure 7: SAP survival in sand flies	Protein from the equivalent of 2 *Lu. longipalpis* flies run per lane	-	1:12 5.4D supernatant	1:3000 anti-mouse-AP	No 5.4D supernatant
Figure 8: SAP and CRP binding to *Lu. longipalpis* midgut protein	1 µg *Lu. longipalpis* microvillar-enriched midgut extract from unfed, sugar fed or blood fed flies.	1 µg/mL SAP	1:500 5.4D and 1:12 5.4D supernatant	1:3000 anti-mouse-AP	SAP + 10 mM EDTA
		1 µg/mL CRP	1:10,000 rabbit anti-CRP	1:5000 anti-rabbit-AP	CRP + 10 mM EDTA

Chapter 6:					
Figure 2: CRP binding to culture PPG	3 µg *L. mexicana* WT PPG, Δ*lmScAP*1/2 PPG, Δ*lmScAP*1/2 + *ScAP2* PPG, *L. infantum* WT PPG	1 µg/mL CRP	1:10,000 rabbit anti-CRP	1:5000 anti-rabbit-AP	No CRP, 1 µg/mL CRP + 10 mM EDTA
CRP binding to PSG from sand fly	0.5 µg *L. mexicana* PSG (from fly), 0.5 µg *L. mexicana* PPG (from culture)	1 µg/mL CRP-biotin	-	1:500 Streptavidin-AP (SA-5100, Vector Laboratories)	-
Chapter 7:					
Figure 7.1: CA7AE binding to *L. (M.) chancei* LPG	10 µL log phase and metacyclic LPG from *L. (M.) chancei*	-	1:1000 CA7AE	1:30,000 anti-IgM-AP	No CA7AE
Figure 7.4: *L. mexicana* LPG and SAP binding to *Lu. longipalpis* midgut protein	3 µg microvillar-enriched midgut extract from *Lu. longipalpis*. 1 µg *L. mexicana* log phase LPG.	1 µg/mL SAP followed by 1 µg/mL *L. mexicana* log phase LPG / 1 µg/mL *L. mexicana* log phase LPG	1:1000 CA7AE	1:30,000 anti-IgM-AP	CA7AE and IgM-AP; IgM-AP only
Figure 7.5: *L. (M.) chancei* LPG binding to *C. sonorensis*, *C. nubeculosus* and *Lu. longipalpis* midgut protein	1 µg microvillar-enriched midgut extract from *C. sonorensis*, *C. nubeculosus* and *Lu. longipalpis*. 5 µL *L. (M.) chancei* log phase LPG	1 µg/mL *L. (M.) chancei* log phase LPG	1:1000 CA7AE	1:30,000 anti-IgM-AP	250 mM GalNAc with LPG and no LPG
Figure 7.6: *Helix pomatia* agglutinin (HPA) binding to *C. sonorensis*, *C. nubeculosus* and *Lu. longipalpis* midgut protein	1 µg microvillar-enriched midgut extract from *C. sonorensis*, *C. nubeculosus* and *Lu. longipalpis*	1 µg/mL HPA-biotin	-	1:500 Streptavidin-AP	250 mM GalNAc with HPA or no HPA

Table 3.3. Protocol for making 10% resolving and 4% stacking SDS-PAGE gels

Reagent	Volume for 1 resolving gel	Volume for 1 stacking gel
40% acrylamide (Bis-acrylamide ratio 19:1, Severn Biotech)	2 mL	0.5 mL
0.5 M Tris-HCl pH 6.8	x	1.25 mL
1.5 M Tris-HCl pH 8.8	2 mL	x
10% SDS (VWR chemicals)	80 µL	50 µL
Distilled water	3.8 mL	3.1 mL
Ammonium Persulphate (APS)	< 1 mg	< 1 mg
N, N, N', N'-Tetramethylethylenediamine (TEMED) (Sigma-Aldrich)	8 µL	5 µL

3.7 Immunofluorescence

Immunofluorescence has been used extensively during this project, with multiple methods trialled. The first method used was that of Bee et al. (2001), who had previously shown CRP binding to the surface of *L. mexicana* metacyclic promastigotes. This method incubated 10^6 promastigotes with 10 μg/mL CRP in supplemented M199 + 20% FCS media for 1 hour on ice. Parasites were then washed by centrifugation and resuspension, with incubations with primary and secondary antibodies taking place under the same conditions as that for CRP. Parasites were washed and then imaged. No CRP and CRP + 15 mM EDTA controls were included. This protocol was used, with spins and incubations taking place at 4°C and only resuspensions being at room temperature. Parasites were spun down for 5 minutes at 1500 g and resuspended in M199 + 20% FCS (M5017, Merck, see supplements in Chapter 5) with 10 μg/mL SAP or 1:10 LT6 and incubated for 1 hour on ice. Samples were spun down for 5 minutes at 1500 g with the pellet resuspended in 200 μL M199 + 20% FCS, this step was carried out twice. The SAP sample was then incubated with primary antibody 5.4D (1:100) and the LT6 sample incubated with secondary antibody anti-mouse IgG-TRITC (T-5393 Sigma, 1:500) in M199 + 20% FCS for 1 hour on ice, wash steps repeated and the SAP sample was incubation with the secondary antibody under the same conditions. After two washes, the parasites were resuspended in PBS and airdried to a slide with a drop of Vectashield + DAPI (H-2000-2) and a coverslip added which was sealed with nail varnish.

Images were captured using the Zeiss LSM880 and ZEN Black software. Image analysis was carried out in ZEN Blue lite, with image contrast and brightness improved by using the histogram feature. The histogram displays the "pixel count vs intensity from 0 to the maximum bit depth range" (Zeiss, 2020). The white field was changed to alter the brightness of the image and changing the gamma field allowed an increase in the weight of low level signals (when gamma values < 1.0). For the Bee protocol, a 63x objective was used and a frame time of 3.78 seconds. A 561 nm HeNe laser was used to excite TRITC and a 405 nm laser diode used to excite DAPI.

The results from this experiment were unexpected with LT6 only binding to the parasite in certain regions, seen in Figure 3.14. There were other issues with this experiment, such as using supplemented M199 + 20% FCS which will contain heat inactivated SAP and CRP with unknown binding abilities. It was possible the protocol lead to an unintentional pulse-chase experiment, and suggested there is turnover of the LPG on the surface of the parasite. No binding of SAP to parasites was observed in this experiment.

69
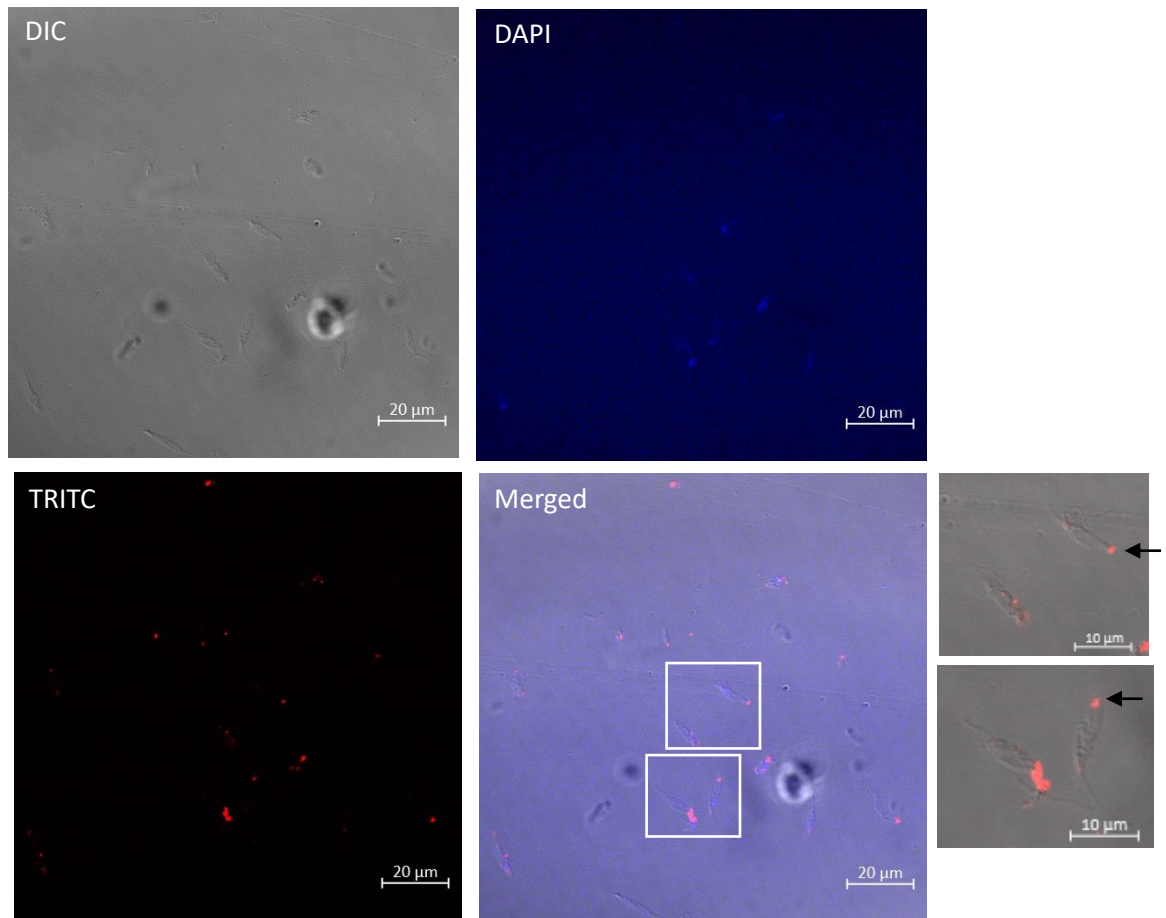
Figure 3.14. Immunofluorescence images of inconsistent LT6 binding *L. mexicana* log phase promastigotes using the Bee et al. (2001) protocol. For enlarged inset images, DAPI has been removed from the merged image to more clearly view the TRITC signal. Black arrows highlight LT6 binding to the posterior of the *Leishmania* body.

After this experiment and discussion with Dr Elizabeth McCarthy (LSHTM), a protocol used for staining trypanosomes was kindly given by Dr Francisco Olmo Arevalo (LSHTM). Parasites were incubated in supplemented M199 (no serum) with or without 10 µg/mL SAP or with 10 µg/mL SAP + 15 mM EDTA at 28°C and then fixed by adding an equal volume of 4% paraformaldehyde (PFA) and leaving at room temperature for 30 minutes. The parasites were washed three times in PBS by centrifugation and resuspension. Then, 25 µL was airdried to the wells of multitest slides (096041805E, MP Biomedicals). Slides were occasionally stored at 4°C before staining. The longest period slides were stored for any experiment was just over two weeks. Slides were rehydrated using a Coplin jar filled with PBS. For SAP and SAP + EDTA samples, 1:100 5.4D in M199 (no serum) was added and incubated with the slide in a humid chamber for 2 hours at 37°C, followed by three washes in PBS. A sample incubated in only supplemented M199 was

also stained using the SAP antibodies (no SAP control). For some parasite samples incubated only in M199, 1:10 LT6 was added and incubated under the same conditions. For all samples, 1:500 anti-mouse TRITC was then added, and incubated in the same conditions for 1 hour and again washed. A no LT6 control was also included, where only the secondary antibody was used. Excess PBS was tapped away and the slide left to airdry. To each well, 3 µL of Vectashield + DAPI was added with a coverslip placed on top and sealed with nail varnish. A 63x objective was used for imaging. For LT6, SAP and SAP + EDTA frame times of 3.78 seconds were used. For no LT6 the frame time was 8.17 seconds. The same lasers as the Bee protocol were used.

Staining was improved for LT6 when fixed parasites were used, as seen in Figure 3.15. Though some SAP staining was seen, it was not over the entire surface of the parasite.

C SAP
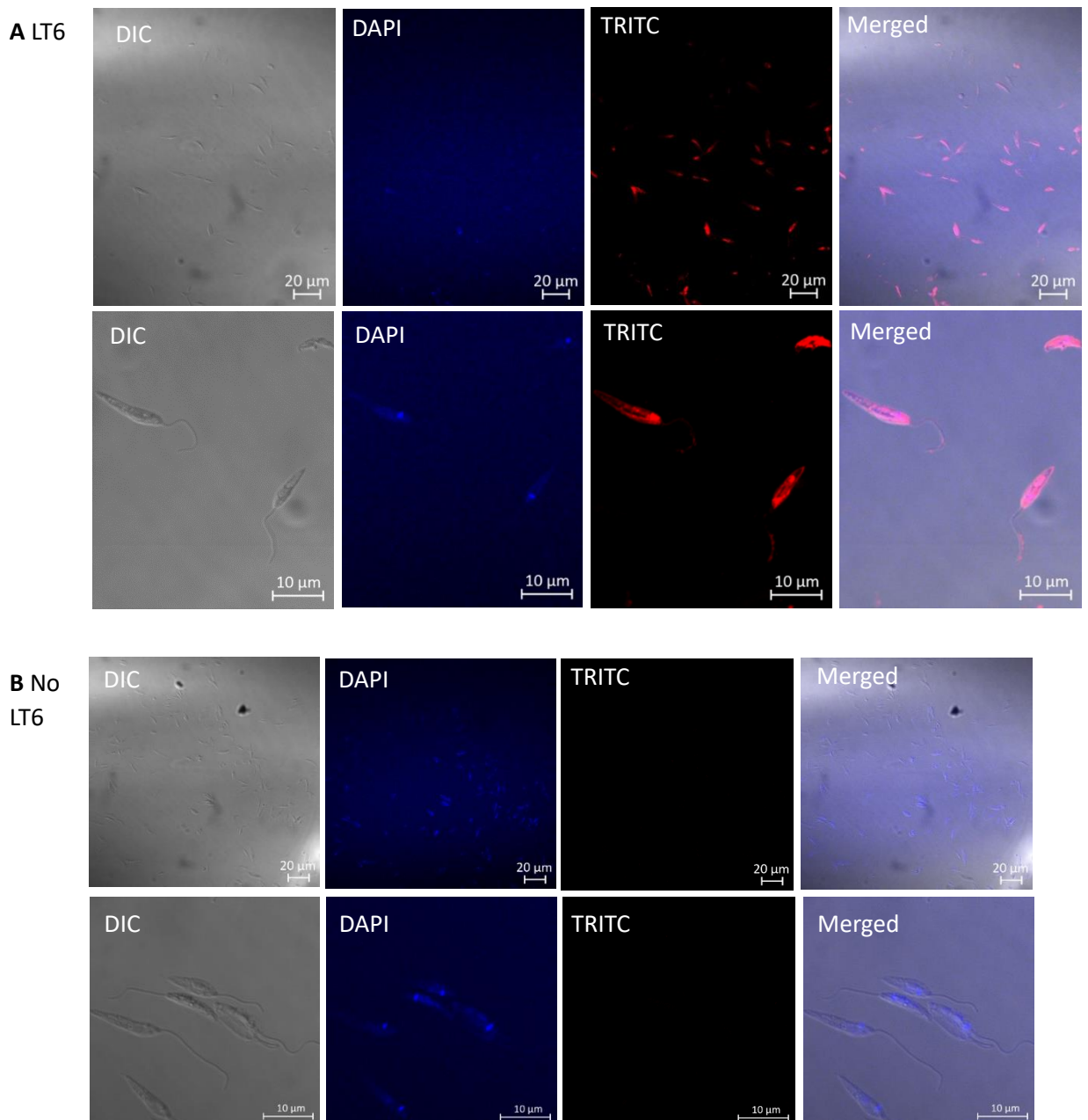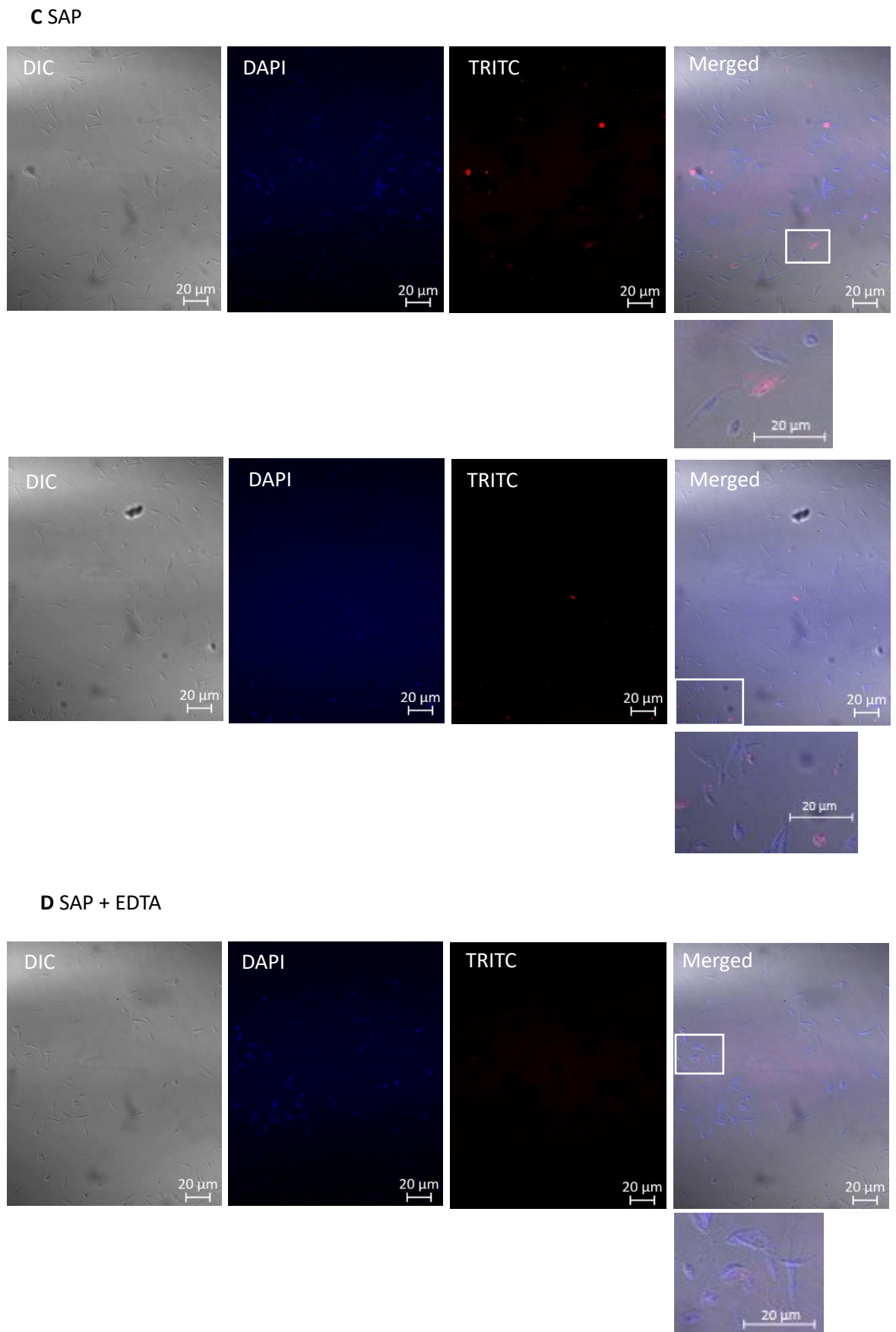
D SAP + EDTA

Figure 3.15. Immunofluorescence images of LT6 (**A**), no LT6 (**B**), SAP (**C**) and SAP + EDTA (**D**) binding *L. mexicana* log phase promastigotes using the protocol from Dr Francisco Olmo Arevalo.

Subsequently, the protocol shown in Figure 3.16 was used, with all steps taking place at room temperature. This protocol changed slightly for different experiments. To begin with 10 µg/mL pentraxins were used (Bee et al., 2001), however, it was decided to reduce this to 5 µg/mL to minimise the risk of pentraxin leading to parasite clumping seen at higher concentrations, an issue previously observed by the Raynes lab. The dilution of the anti-CRP antibody was also increased, to more closely match the concentration of anti-SAP used. LT6 and CRP binding was fairly consistent and seen over the surface of the parasites, whereas SAP binding varied, binding only some parasites, seen in Figure 3.17. Images were collected using a 63x objective. For LT6 and no LT6 a frame time of 1 minute and 52 seconds was used. For SAP, SAP + EDTA, CRP and CRP + EDTA a 56.43 second frame time was used. A 561 nm HeNe laser was used to excite TRITC, a 405 nm laser diode used to excite DAPI and a 488 argon laser to excite FITC.

A live/dead stain was incorporated into an experiment. After the 1.6×10^7 parasites were washed with 10 mM EDTA + PBS, followed by PBS, they were incubated in the dark for 30 minutes with 12 µL live/dead fixable orange (602) viability kit (L34983, Invitrogen), diluted in 12 mL PBS. This stain binds free amines found inside and on the surface of cells, with increased fluorescence seen when binding amines from the cell interior. Parasites were washed by centrifugation and resuspension and then incubated using the described protocol (but with incubations in the dark) with the pentraxins. SAP binding was again seen to some parasites, but these differed to the dead cells, seen in Figure 3.18. This work was imaged using the Nikon Ti E widefield microscope and analysis carried out using NIS-elements (Nikon). A 100x objective was used. Using NIS-elements, auto scale settings were adjusted to low 0.005% and high 0.05%. This edits the number of pixels left outside of the auto scale function (Laboratory Imaging, 2020). LED line 365 nm was used to excite DAPI, 525 nm used for live/dead 602 and 635 nm used for AF660. LED intensities were then adjusted using controls of parasites stained with AF660 or live/dead 602 only, to reduce bleed through between these two fluorophores. Imaging was ordered so the longest wavelength (AF660) was imaged first and the shortest imaged last to prevent red fluorescence being detected in the far-red channel.

	LT6	No LT6	CA7AE	No CA7AE	SAP	SAP + 15 mM EDTA	No SAP	CRP	CRP + 15 mM EDTA	No CRP
					Count parasites, spun down 10^6 parasites per sample					
					wash in PBS x3 OR PBS + 10 mM EDTA x1, PBS x2					
Incubation 1 hour in M199	100 µL M199	100 µL M199	100 µL 1:500 **CA7AE GTX39838 GeneTex**	100 µL M199	5-10 µg/mL, 100 µL **SAP**	5-10 µg/mL, 100 µL **SAP, EDTA**	100 µL M199	5-10 µg/mL, 100 µL **CRP**	5-10 µg/mL, 100 µL **CRP, EDTA**	100 µL M199
					spun 5 mins 2500 g					
					Some protocols: wash 2 x PBS					
Incubation 20-30 mins					RS in 100 µL 4% PFA					
					spun 5 mins 1500 g, 200 µL wash PBS (x3)					
					RS pellet in 100 µL PBS, 25 µL airdried onto slide					
					rehydrate slide by placing in Coplin jar with PBS (few mins)					
Incubation 1 hour in M199	1:10, 25 µL **LT6**		1:100, 25 µL **Anti-IgM-AF488 406522 Biorad**		25 µL **1:10 5.4D supernatant or 1:100 5.4D**			1:100 or 1:2500, 25 µL **calbiochem anti-c-reactive protein rabbit AB 235752**		
					Wash in coplin jar with PBS (5 mins x3)					
Incubation 1 hour in M199	1:500, 25 µL **Anti-mouse IgG TRITC T-5393 Sigma**		M199 only		1:500, 25 µL **Anti-mouse IgG TRITC T-5393 Sigma**			1:500, 25 µL **Anti-rabbit FITC F0205 Dako**		
					1:500, 25 µL **Anti-mouse AF660 A21054, Invitrogen**			1:500, 25 µL **Anti-rabbit AF488 A11008, Invitrogen**		
					Wash in Coplin jar with PBS (5 mins x3)					
					tap slide and wipe back dry, let airdry					
					Add 3uL Vectashield, add coverslip, seal with nail varnish					

Figure 3.16. Immunofluorescence protocol used for most experiments in this project.

A LT6
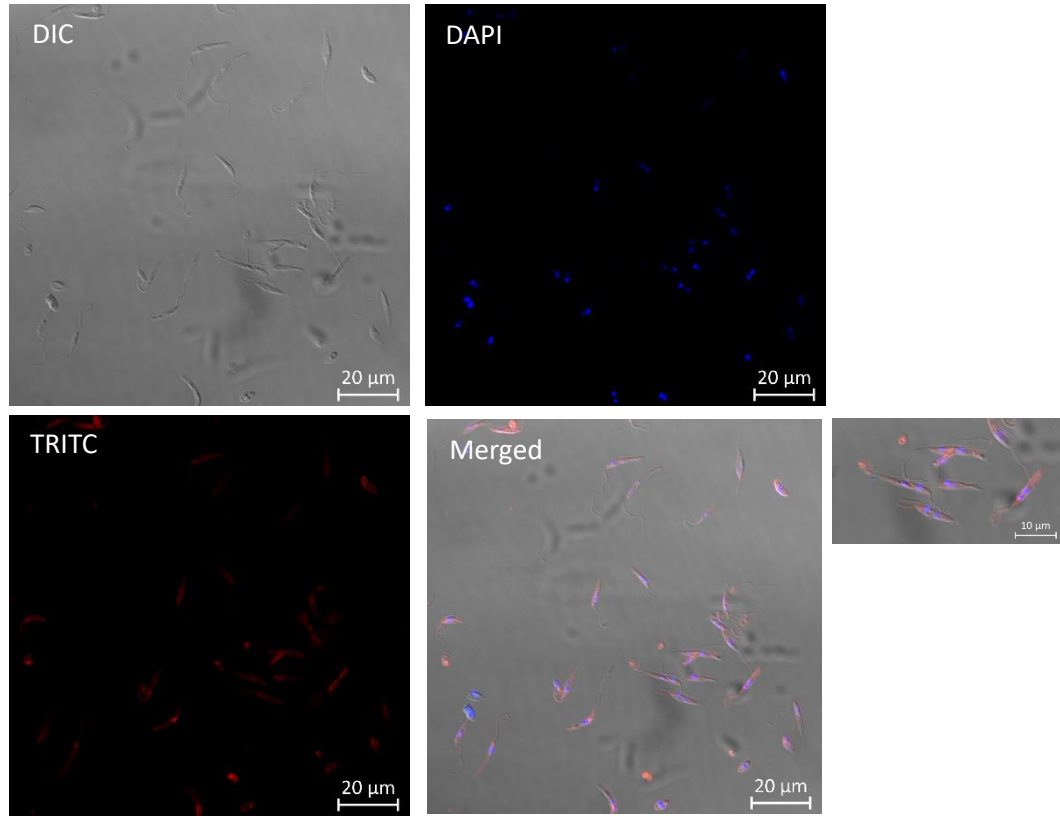
B No LT6

C SAP

D SAP + EDTA

E CRP
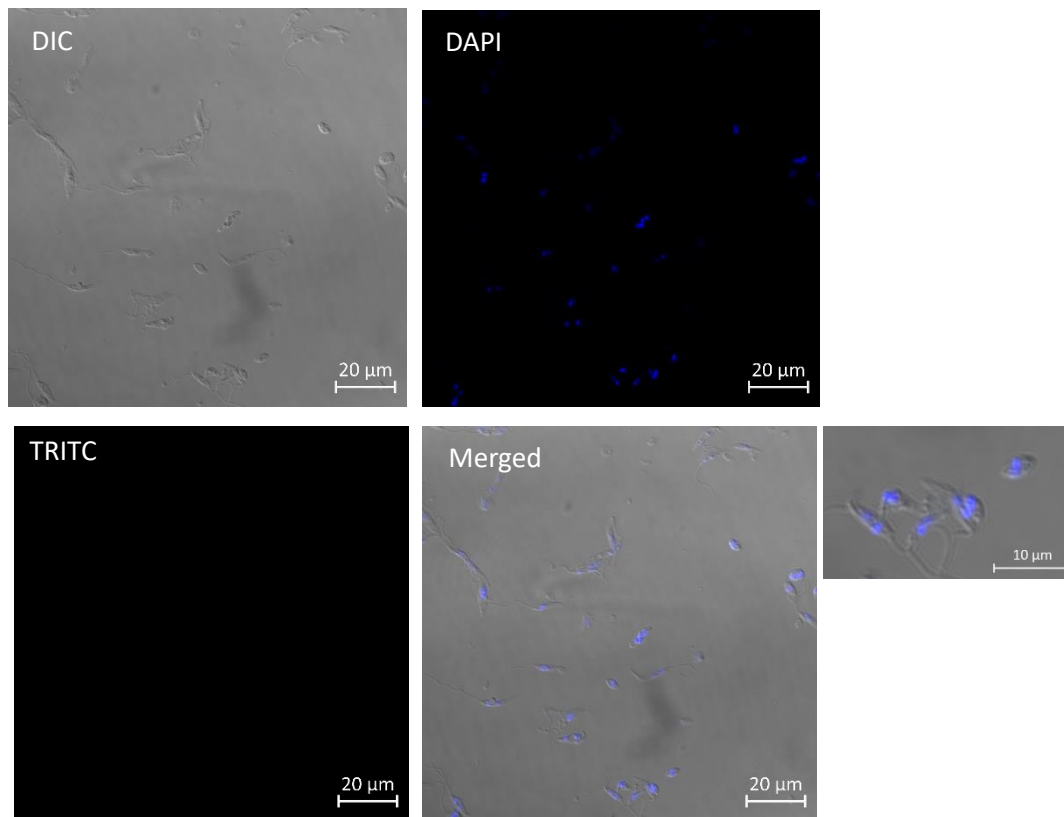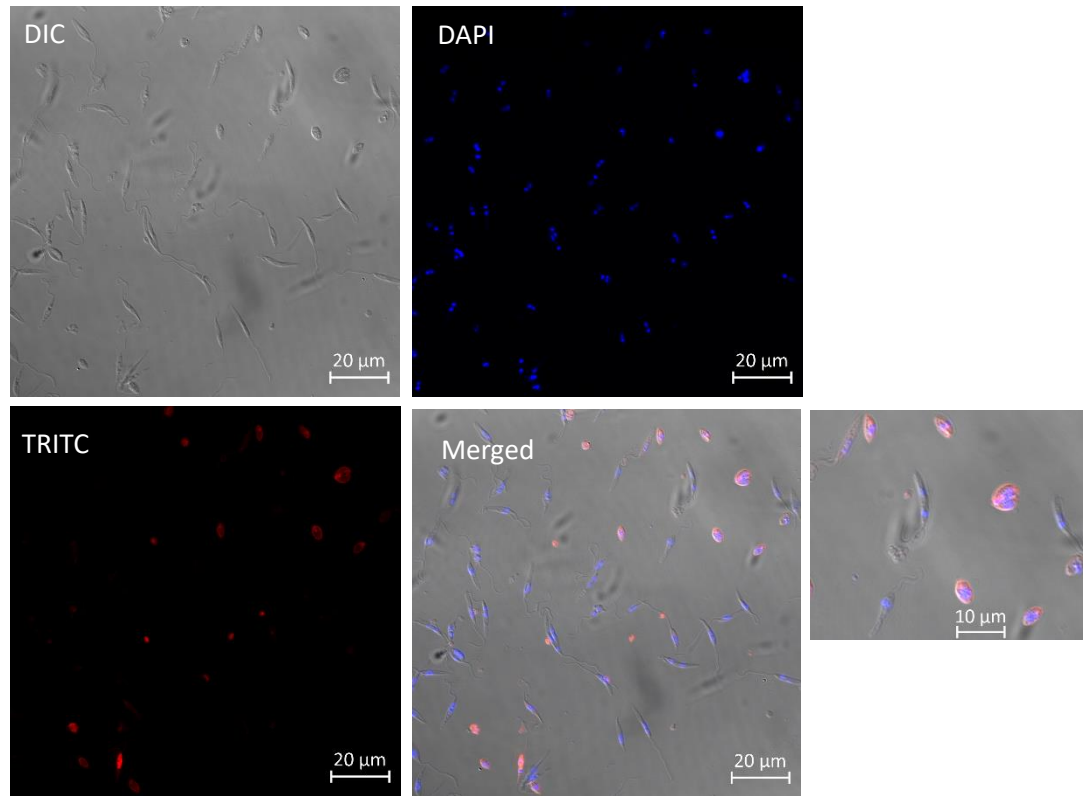
F CRP + EDTA
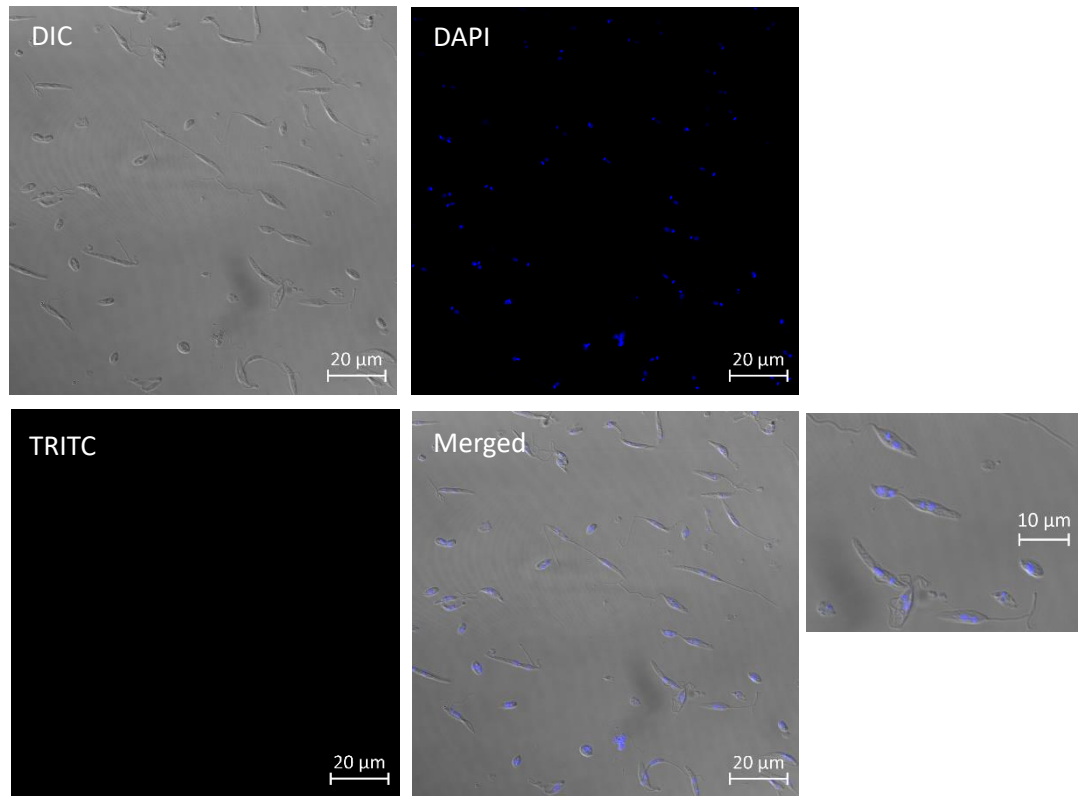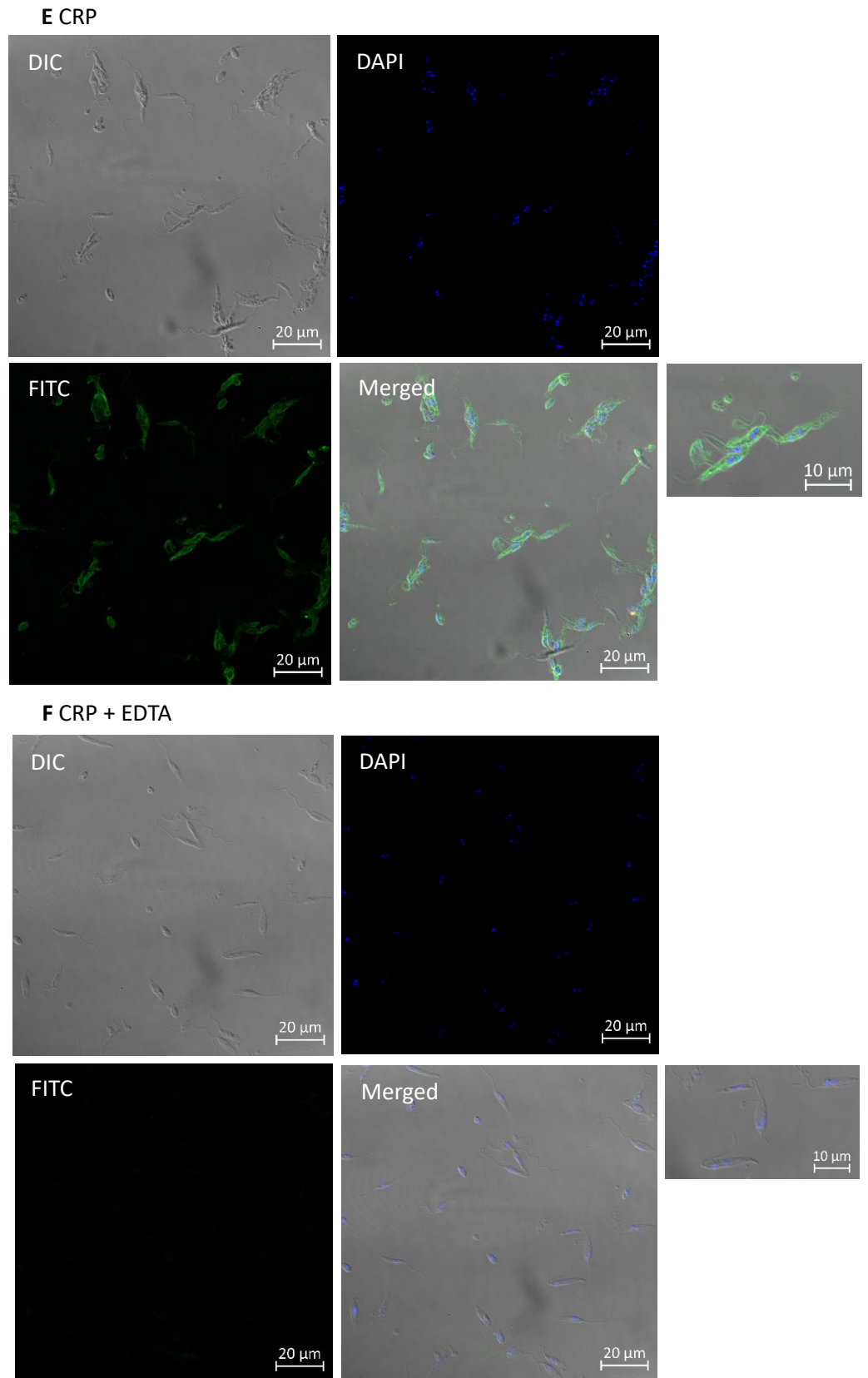
Figure 3.17. Immunofluorescence images of LT6 (**A** and **B**), SAP (**C** and **D**), CRP (**E** and **F**) and controls binding *L. mexicana* promastigotes. Parasites were incubated with pentraxins, followed by fixing and staining. LT6 and CRP bind the entire surface of the parasite, whereas SAP binds to only some parasites.
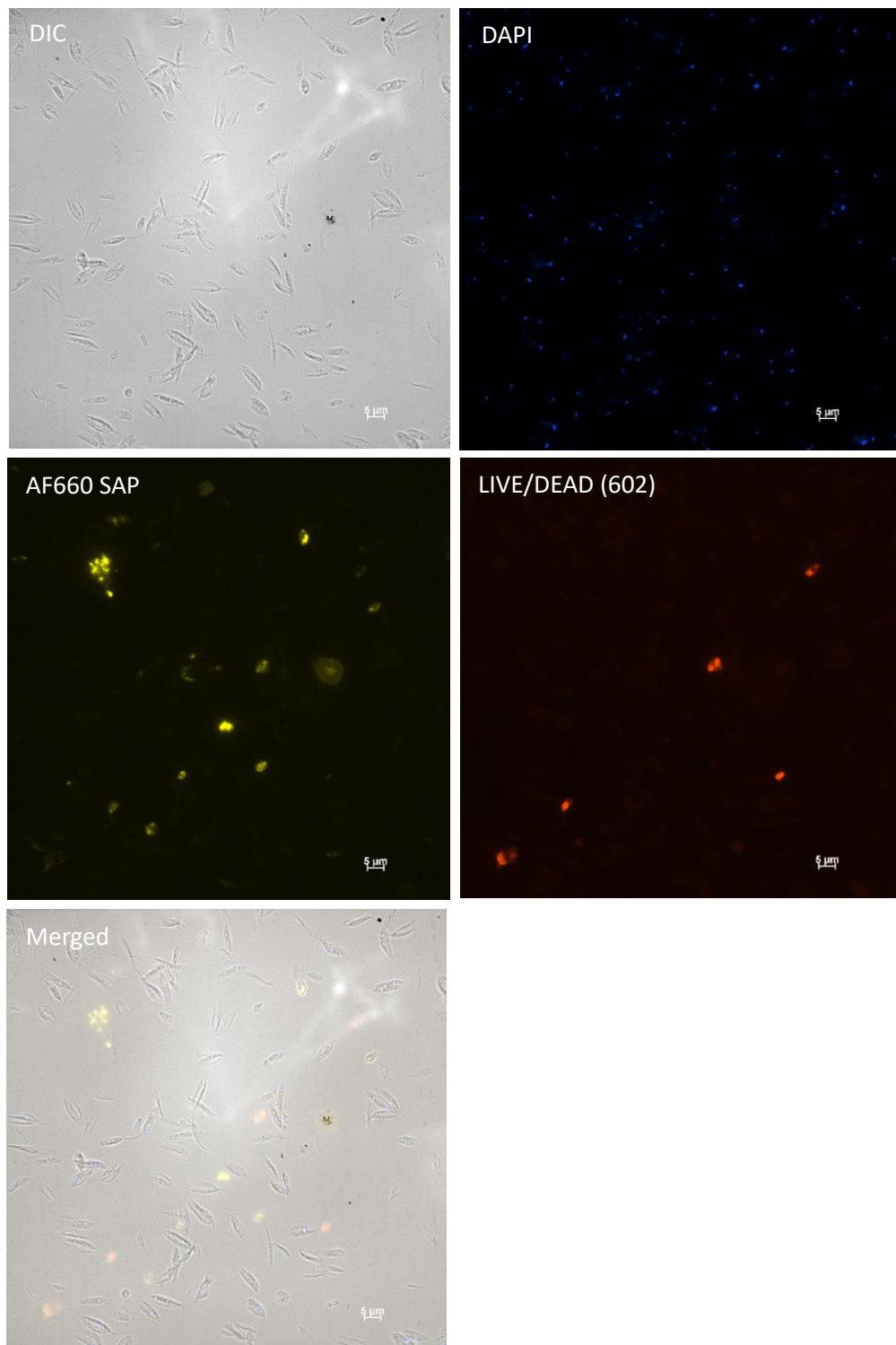
Figure 3.18. Immunofluorescence images of SAP binding *L. mexicana* promastigotes. A live/dead stain has been included to show SAP binding is not occurring due to binding to dead cells. The AF660 has been false coloured while imaging to differentiate from the live/dead stain. White error bars represent 5 μm.

As previously established, SAP is not binding to dead cells, so another possibility for the binding to only some parasites may be it is stage-dependent. Many of the parasites with SAP staining look similar to amastigotes (seen in Figure 3.17) suggesting the binding site may be GIPLs. These parasites were taken from a log phase culture and so there is likely to be a small percentage of amastigotes still present. This reasoning is due to a large reduction in LPG on amastigote stage parasites, with only 100 molecules estimated per cell (McConville and Blackwell, 1991), whereas there are thought to be 2×10^7 PEth containing GIPLs on and within *L. mexicana* amastigotes (Winter et al., 1994). As seen in Chapter 5, immunofluorescence was carried out on *lpg1*$^{-/-}$ *L. mexicana* promastigotes, with binding seen to promastigote stages, which supports binding to GIPLs, as these will be more exposed when LPG is absent.

For the time course experiment seen in Chapter 5, parasites had to be dried to the slide prior to incubation with pentraxins as this was done on a separate day. When this protocol was used, SAP binding was seen to all stages suggesting the different results seen previously were due to the methods used.

As previously mentioned, part of the issue with incubation of live parasites with pentraxins may be the movement of surface structures. Pulse-chase experiments were attempted to try and capture the movement of LPG over the surface of *Leishmania*, with different incubation lengths of the parasite with pentraxins being used, followed by fixing and staining. However, no movement was captured, with incubations likely too long and therefore live cell imaging may need to be used. As this was not the focus of this project, this was not pursued any further.

Hydrodynamic flow-mediated protein sorting as previously suggested for trypanosomes (Engstler et al., 2007) may explain the differing immunofluorescence results seen in this work. Immunoglobulins bound to the variant surface glycoproteins (VSG) of *Trypanosoma brucei* were found to move in the opposite direction of the parasite movement where they were endocytosed by the flagellar pocket. This process was independent of the actin cytoskeleton. Like VSG, many of the *Leishmania* surface molecules have a GPI anchor and may move over the parasite surface in the same way. Therefore, staining of live parasites followed by fixing may be capturing this process. This seems likely due to the loss of LPG staining for live parasites, which is retained in the fixed protocol. If this assumption is true, then pentraxin staining should be seen at the posterior end of the cell, with examples of this seen in Figure 3.14. Unlike trypanosomes, the flagellar pocket is found at the anterior end of the *Leishmania* parasite and so GPI-anchored molecules that gather at the posterior end will not be endocytosed. Accumulation of GPI-anchored molecules in this region may lead to shedding and loss of

pentraxin staining. Furthermore, unlike trypanosomes, the motile forms of *Leishmania* are within the vector. For trypanosomes, directional movement occurred in viscous mediums such as the blood (Engstler et al., 2007). For *Leishmania*, the directional movement will therefore be taking place within the bloodmeal of the sand fly. For trypanosomes, the removal of immunoglobulins prevents complement-mediated lysis and so there may be a similar role occurring to prevent parasite killing in the sand fly midgut. Binding of SAP to amastigotes could be due to the reduced movement of these stages, and therefore less movement of the surface molecules, allowing binding to be observed. The differences in this potential phenomena seen between SAP and CRP may be due to their different binding sites.

For immunofluorescence experiments seen in Chapter 7, both log phase and metacyclic cultures (enriched using a Ficoll gradient as described previously) of *L. (M.) chancei* parasite cultures were provided by Dr Matthew Rogers. Parasites were washed as usual and then fixed. Fixed parasites were washed and dried to a slide. Slides were incubated with CA7AE and anti-IgM-AF488, then prepared for imaging as usual. A 100x objective was used for imaging, with frame times varying from 1.46 seconds to 1 minute 2 seconds. A 405 nm laser diode used to excite DAPI and a 488 argon laser to excite FITC.

3.8   Midgut binding assays

Midgut binding assays are a crucial method in studying the parasite interaction with the vector. An initial hypothesis of this project was that SAP may act as a cross-linker between *Leishmania* log phase stage parasites and the *Lu. longipalpis* midgut, allowing attachment and survival when the sand fly defecates. There are a variety of methods for midgut binding assays as well as a range of parasite intensity quantitation methods, described in Chapter 4. The results of assays carried out as part of this project are seen in Chapter 4 and 5.

The method used in this study evolved to include improvements, but the overall process remained the same. The first step was to check the parasite culture to confirm a large percentage were log phase promastigotes. A sample of the culture was airdried to a multitest slide (096041505, MP Biomedicals) in order for the percentage of different lifecycle stages to be determined at a later date if needed. Parasites were grown in supplemented M199 + 20% FCS and for initial experiments, parasites were not washed, and incubations of parasites with midguts took place in this media. These preliminary experiments were to see if the heat inactivated bovine SAP and CRP in the media may affect the intensity of parasites attaching to the midgut, with 10 mM EDTA added to some incubations as a control. However, with little

change seen between the test and control groups and the binding abilities of these heat inactivated pentraxins unknown, the incubation media was changed. Future experiments used PBS for the wash steps and incubations of parasites with the midgut. Future attempts by Dr John Raynes to purify SAP from heat inactivated human serum revealed an inability of SAP of this form to bind PEth beads, suggesting heat inactivated SAP does not have the same binding abilities as the native form. Initially, the wash step was centrifugation followed by resuspension in 10 mL PBS + 10 mM EDTA, however, as it has been noted that some proteins (such as albumin) bind strongly (King et al., 1987) to the parasite surface, the first wash step of 10 mL PBS + 10 mM EDTA was done on a shaker for 30 minutes as this would increase the chances of removal of media components from the parasite surface. This was followed by two washes in 10 mL PBS. Some later experiments used 20 mM EDTA for both the wash and incubation steps as little difference was seen between the test and control.

Parasites were resuspended in the same buffers as used for the wash steps depending on the experiment. When using PBS, 1 mM $CaCl_2$ was added. A range of parasite concentrations were trialled, from 10^5 to 10^7 parasites per 50 µL. SAP was used at 40 µg/mL to reflect the physiological concentration found in human blood. Once washed, parasites were left in a 26°C incubator in the buffer they would be incubated with the midguts in. This meant the parasites and buffer were incubating for 1 hour or 4 hours before midguts were added. This was due to two rounds of dissections taking place each day to try and increase the number of midguts that could be dissected per day, without leaving any dissected midgut too long causing degradation.

For experiments seen in Chapter 4 and 5, midguts were dissected in PBS as described previously in section 3.3. They were unzipped and left in a drop of PBS within a humid chamber while other dissections were carried out. To the well of a 2-well concave slide (2CS000, Hawksley) 50 µL of parasites were added with midguts added by carefully transferring from the PBS drop using fine forceps under a stereo microscope. The parasites and midguts were incubated for 30 minutes, in a humid chamber at 26°C. Midguts were then removed from the parasites using fine forceps and a stereo microscope. Each midgut was washed by placing into three successive fresh drops of PBS for 10 seconds, with slight agitation being applied. Each midgut was then transferred to a 1.5 mL microcentrifuge tube containing 30 µL PBS. Midguts were homogenised using a disposable pestle and 3 µL, 5 µL and/or 10 µL airdried to wells of a multitest slide (096041505, MP Biomedicals). Slides were fixed with methanol and then Giemsa stained (VWR Chemical). Parasite intensity was quantitated by scanning the entire well using a light microscope (Laborlux K, Leitz), counting the number of parasites seen, and scaling to the number of parasites per midgut. A range of volumes were airdried to the slide in case of low or

high parasite numbers. This quantitation method was extremely time consuming and it was difficult to differentiate parasites from midgut debris. However, it was used to try and increase sensitivity as well as removing the need for large scaling of results as sometimes seen when using a hemocytometer.

There is no way around midguts being treated slightly differently during this protocol. Dissection is technically demanding, with sand fly midguts varying in shape which effects the ease at which they can be 'unzipped'. Some midguts will be left in PBS longer after dissection, or be incubated with the parasites for slightly longer. These issues were managed as much as possible, working with midguts in the same order (first added to the parasites was the first out as well), but variation is inevitable.

Slight differences were made for future midgut binding assays carried out by Masters student William Paine (not shown in this thesis). Incubations of parasites with midguts was done in supplemented M199 media. Parasite quantitation was achieved using a hemocytometer. Midguts were homogenised in 30 µL like previously with 5 µL airdried to a slide for Giemsa staining. The remaining 25 µL was centrifuged at 3000 g (4000 rpm, ALC PK130R) for 5 minutes and resuspended in 10 µL of 4% PFA which was added to the hemocytometer. A full hemocytometer grid (BV5100H, Immune Systems) (160 squares or 10 4x4 grids) was counted and multiplied up to give number of parasites per midgut.

3.9   Fly infections

To confirm whether SAP has a role in attachment of parasites to the sand fly midgut, fly infections followed by parasite intensity quantitation was carried out. Fly infections were carried out as previously described (Rogers et al., 2002), by my supervisor Dr Matthew Rogers. Human blood was donated as part of the blood donate scheme at LSHTM. Typically, 9 mL blood was collected in sodium heparin (17 units/mL) coated Vacutainer tubes (Becton Dickinson) on the day of infection. The blood was centrifuged at 2500 g for 15 minutes at 4°C. The plasma was removed from the cell pellet (taking care to avoid the buffy coat layer of leukocytes and platelets) and heat-inactivated at 56°C for 45 minutes in a water bath. The remaining cells were washed twice in 10 mL PBS + 10 mM EDTA, followed by two washes in PBS with rolling for 10 minutes between changes of wash buffer. The heat-inactivated plasma was cooled to room temperature before recombining with the washed cells. The heat-inactivated blood was pre-incubated for 1 hour at 37°C with 25 µg/mL SAP as well as the anti-SAP treatment being tested. These included 1 mg/mL CPHPC (SML2571, Sigma-Aldrich) diluted in 10 mM Tris, 140 mM NaCl,

2 mM CaCl$_2$ in PBS (as described in Kolstoe et al., 2009). Anti-SAP antibodies dezamizumab (PX-TA1441-1MG, ProteoGenix) and 5.4D.3B (CBL305, Chemicon) were also used, diluted 1:50 in blood, (67 μg/mL and 2 μg/mL, respectively). Axenic first passage amastigotes at 5x10^5 per mL were added to the blood, with 2 mL added to the reservoir of a hemotek feeder. The feeder was covered in chicken skin, heated to 37°C and placed on top of a mesh cage of 5 days-old unfed flies. This was left for at least 30 minutes, or until the majority of flies had fed. Blood fed flies were carefully separated using a mechanical aspirator into a new cage supplied with a cotton wool pad soaked in 50% w/v sucrose and maintained inside a humidified bag at 25-26°C in a locked incubator. This was all carried out by Dr Matthew Rogers.

Flies were sampled on days 3, 5, 7 and 10 post bloodmeal, with midguts dissected. On day 3, results were only included for flies yet to defecate the bloodmeal, as at this stage in the lifecycle for the hypothesis being tested, the test and control should have similar parasite intensities. For days 5, 7, and 10, only female flies which had defecated their bloodmeal and contained eggs were included to study the potential differences in parasite numbers after potential attachment. Midguts were removed as previously described and placed into 30 μL PBS, and homogenised with a disposable pestle. For each sample, 5 μL was airdried to a well of a multitest slide (096041505, MP Biomedicals), to assess the morphology of the parasites and 10 μL added to 2 μL 4% PFA and loaded on to a hemocytometer. A total of 16 squares of the hemocytometer were counted, with a further 16 squares counted if no parasites were seen. The number of parasites counted were then scaled up to calculate the number of parasites per midgut. Results were plotted using GraphPad Prism and the Kolmogorov-Smirnov test used for statistical analysis. This was used as it looks at differences in the distribution of the data as well as the median, and not just rank each value as with the Mann-Whitney test.

3.10   Immunoprecipitation

SAP was found to bind some microvillar-enriched midgut extracts from *Lu. longipalpis*, seen in Chapter 5. To identify the *Lu. longipalpis* proteins, an immunoprecipitation experiment was devised using 5.4D-coupled beads incubated with SAP. The protocol closely followed that recommended for use with the Pierce NHS-activated magnetic beads (88826, Thermo Scientific), however it was carried out on a reduced scale.

During these experiments, dissection stations and equipment were cleaned with 70% ethanol before use. Midgut dissections were carried out wearing a hairnet and gloves that covered the cuffs of a clean lab coat to prevent any contamination of the sample, particularly with keratin.

3.10.1 Preparation of antibody-coupled beads

The anti-SAP antibody prepared in house in the Raynes lab, 5.4D, was used for this experiment. It was dialysed (VISKING) overnight into coupling buffer (50 mM borate pH 8.5). The antibody and the magnetic beads were equilibrated to room temperature, with 100 μL of the well mixed beads added to a 1.5 mL microcentrifuge tube. The tube was placed into a magnetic tube stand (36912, Qiagen), and the supernatant discarded. The beads were washed using 350 μL wash buffer (ice-cold 1 mM hydrochloric acid) and vortexed for 15 seconds. The beads were collected, and the supernatant discarded. The beads were incubated with 50 μg 5.4D in 100 μL coupling buffer for 2 hours at room temperature on a rotator (Blood tube rotator SB1, Stuart Scientific). The sample was vortexed every 5 minutes for 15 seconds during the first 30 minutes, and vortexed every 15 minutes for the remaining time. The beads were collected and the supernatant (SN1) saved. Deviating from the recommended protocol (wash in 0.1 M glycine, pH 2), the beads were then washed in 350 μL PBS + 0.5 M NaCl, pH 7, and vortexed for 15 seconds. The original protocol was changed to avoid potentially inactivating the anti-SAP. The beads were then collected with the wash step repeated. The wash step was also carried out using 350 μL distilled water. The beads were collected and the supernatant discarded, with 350 μL quenching buffer (3 M ethanolamine, pH 9) then added, vortexed for 30 seconds and then incubated on a rotator at room temperature for 2 hours. The beads were collected and washed with 350 μL distilled water. The collected beads were then washed three times with 350 μL storage buffer (50 mM borate, pH 8.5 + 0.5% sodium azide), followed by resuspension of the beads in 100 μL of the buffer and stored at 4°C until needed. The concentration of the magnetic beads was 10 mg/mL.

3.10.2 Preparing SAP + antibody-coupled beads

In a 1.5 mL centrifuge tube, 20 μL of antibody-coupled beads were placed, the beads collected and the supernatant discarded. Then, 400 μL binding/wash buffer (TBS + 0.5 mM calcium + 0.05% tween) was added, the tube mixed well and the beads collected. It is recommended to use three times the mass of protein to antibody. To 100 μL of beads, 50 μg of antibody was added, so the antibody concentration can be estimated as 500 μg/mL, with 10 μg antibody for 20 μL beads. In test experiments, 30 μg of SAP was added to the 20 μL beads but a lot of excess SAP was seen in the incubation supernatant. Therefore, the amount was reduced by 1:10, to 3 μg per 20 μL beads. SAP diluted in binding/wash buffer to a total of 20 μL was incubated with the antibody-coupled beads for 2 hours at room temperature on a rotator. The sample was vortexed for 15 seconds every 5 minutes for the first 30 minutes, after that the sample was

vortexed every 15 minutes. The beads were collected and the supernatant saved (SN2). The beads were washed twice again in 400 µL binding/wash buffer, and resuspended in 20 µL of the same buffer. The immunoprecipitation was then carried out.

3.10.3   Preclearing

Prior to the immunoprecipitation, any components of the protein sample that may bind to the antibody-coupled beads were removed by preclearing. To a 1.5 mL microcentrifuge tube, 7.5 µL antibody-coupled beads were added, with the beads collected and the supernatant discarded. Then, 200 µL binding/wash buffer was added, vortexed and the beads collected. The 200 µL microvillar midgut protein sample from 1195 *Lu. longipalpis* (~150 µg protein) was dialysed overnight into TBS + 0.5 mM Ca^{2+} + 0.05% Tween. The protein was added to the beads and incubated for 30 minutes at room temperature. The sample was vortexed for 15 seconds every 5 minutes. The beads were collected and later run on a gel checking the individual steps of the experiment. The midgut protein supernatant was used in the immunoprecipitation experiment.

3.10.4   Immunoprecipitation

A volume of 7.5 µL antibody-coupled beads + SAP was added to a 1.5 mL microcentrifuge tube, the beads collected and the supernatant discarded. The precleared microvillar midgut protein in binding/wash buffer was added to the beads and incubated overnight on a rotator at 4°C. The beads were collected and the supernatant saved (SN3). The beads were washed with 200 µL binding/wash buffer and mixed, the beads collected and the supernatant discarded. This wash step was repeated. The beads were resuspended in sample buffer, boiled (section 3.6) and run on an SDS-PAGE gel with results seen in Figures 3.19 and 3.20.

Care was taken during the running and staining of the gel containing the proteins to be sent for sequencing to prevent contamination with keratin. The gel was placed into a new large plastic weighing boat and covered while staining, with the bands cut with sterile blades. Bands were sent to the University of York Centre of Excellence in Mass Spectrometry. Here they were sequenced using LCMS, with the following description of methods provided: "following in-gel digestion, peptides were analysed over 10 min acquisitions with elution from a 50cm Micro Pillar C18 column (Pharma Fluidics) onto a Bruker maXis qTOF operated in a data dependent acquisition mode." The peptides returned were searched against Uniprot and SwissProt protein databases. The results of which are discussed in Chapter 5.

An SDS-PAGE gel was also run on the supernatants of bead-antibody and bead-antibody-SAP incubations to check each step had worked correctly (seen in Figures 3.19 and 3.20). A total midgut protein sample was also run to show the outcome of the microvillar-enrichment process.
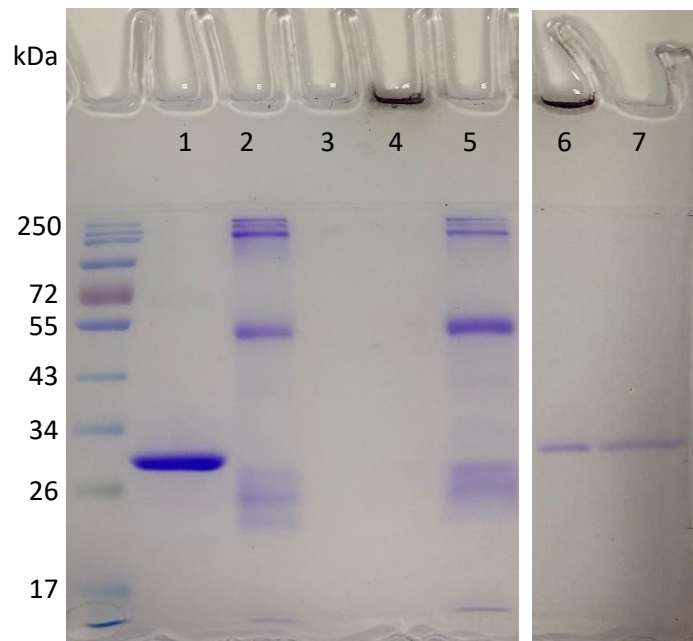
Figure 3.19. Coomassie stained SDS-PAGE gel of stages within the immunoprecipitation protocol. 1: 5 µg SAP; 2: 5 µg 5.4D; 3: blank; 4: 5.4D-coupled beads; 5: supernatant from 5.4D and beads incubation (SN1); 6: SAP + 5.4D-coupled beads; 7: supernatant from SAP and 5.4D-coupled beads incubation (SN2)
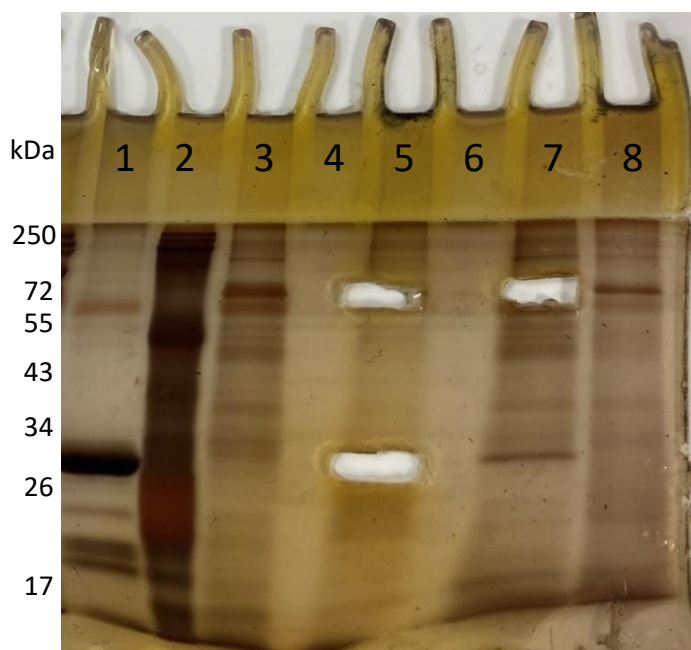
Figure 3.20. Silver staining of a previously Coomassie stained gel. The gel shows the results of the immunoprecipitation experiment where 5.4D-coupled beads + SAP were incubated with midgut proteins. Lane 1: 5 ug SAP; 2: 5 ug 5.4D; 3: 10 ug total midgut protein; 4: blank; 5: midgut protein + SAP + 5.4D-coupled beads; 6: blank; 7: Supernatant of midgut proteins + SAP + 5.4D-coupled beads; 8: preclearing beads.

3.11   Surface Plasmon Resonance (SPR)

Surface Plasmon Resonance allows for a more detailed study of molecular interactions, providing information of binding kinetics and affinity. I have only used this method on occasion, however it was used extensively by previous PhD student Eu Shen Seow with the results of these experiments seen in Chapter 6. This method was also used by Masters student Laura Stennett, with results of her work seen in Chapter 5. The methods of both experiments are described in the respective chapters.

4. Understanding experimental *Leishmania* infection intensities within the sand fly midgut: a systematic review and meta-analysis

RESEARCH PAPER COVER SHEET

Please note that a cover sheet must be completed <u>for each</u> research paper included within a thesis.

SECTION A – Student Details

Student ID Number	1601303	**Title**	Miss
First Name(s)	Eve Christina		
Surname/Family Name	Doran		
Thesis Title	The role of human pentraxins for the *Leishmania*-vector interaction		
Primary Supervisor	Dr Matthew Rogers		

If the Research Paper has previously been published please complete Section B, if not please move to Section C.

SECTION B – Paper already published

Where was the work published?			
When was the work published?			
If the work was published prior to registration for your research degree, give a brief rationale for its inclusion			
Have you retained the copyright for the work?*	Choose an item.	Was the work subject to academic peer review?	Choose an item.

*If yes, please attach evidence of retention. If no, or if the work is being included in its published format, please attach evidence of permission from the copyright holder (publisher or other author) to include this work.

SECTION C – Prepared for publication, but not yet published

Where is the work intended to be published?	Parasites & Vectors
Please list the paper's authors in the intended authorship order:	Doran, Eve C., Hair, Molly., Raynes, John G., Rogers, Matthew E.
Stage of publication	**Not yet submitted**

SECTION D – Multi-authored work

For multi-authored work, give full details of your role in the research included in the paper and in the preparation of the paper. (Attach a further sheet if necessary)	I designed the search and inclusion/exclusion criteria for the systematic review. Along with Molly Hair, I read the abstracts of the papers retrieved as part of the search to decide their relevance. I then read papers in full, along with Molly, to confirm relevance and extract data. Preliminary data analysis was carried out by myself and Molly. However, the analysis shown here was carried out by myself. I also carried out a second search at a later date to include new published studies. I carried out the *ex vivo* midgut binding assays. Matthew Rogers carried out the *in vivo* fly infections. I wrote the first draft of the manuscript, and updated the revisions given by my supervisors John Raynes and Matthew Rogers.

SECTION E

Student Signature	EVE DORAN
Date	20/06/2023

Supervisor Signature	MATTHEW ROGERS
Date	04/07/2023

Understanding experimental *Leishmania* infection intensities within the sand fly midgut: a systematic review and meta-analysis

Doran, Eve C.*, Hair, Molly., Raynes, John G., Rogers, Matthew E.

Dept. of Infection Biology, Faculty of Infectious and Tropical Diseases, London School of Hygiene and Tropical Medicine, Keppel St., London. WC1E 7HT.

*Corresponding author eve.doran@lshtm.ac.uk

Abstract

In vivo fly infections and *ex vivo* midgut binding assays are commonly used to research the interaction of *Leishmania* with the sand fly vector. Both methods involve the quantitation of *Leishmania* infection or attachment intensities, with previous work studying how differences in methods can affect this outcome. However, no study has conducted a systematic review and meta-analysis to answer this question. Through this meta-analysis we address an unanswered research question of is there a maximum number of parasites a sand fly can sustain. The majority of relevant papers retrieved in this systematic review collected and presented data categorically and we were unable to include them in our analysis. Using data from studies quantitating infections using hemocytometers and experimental work presented here, we suggest that *in vivo* infection concentrations over 10^6 parasites/mL are superfluous and do not affect infection intensities. This conclusion is supported by *ex vivo* midgut binding assays carried out as part of this study incubating midguts with increasing numbers of parasites and *in vivo* studies of flies infected with varying numbers of amastigotes. Our results support previous findings that no difference in infection intensities is seen when using promastigotes or amastigotes for initial infections. Future research is needed to understand the maximum number of parasites a sand fly can sustain and the limiting factor(s) that contribute to this. In future, following individual sand flies until defecation and using this as a comparison time point between flies and studies may allow for clearer conclusions and may improve comparisons of numbers of parasites attached to the midgut between *ex vivo* and *in vivo* studies.

Introduction

Phlebotomine sand flies are vectors of a range of diseases, including leishmaniasis caused by the protozoan parasite genus, *Leishmania* (Cecílio et al., 2022). Female sand flies require bloodmeals for egg production (Ready, 1979), and when feeding on an infected host, will also take up the *Leishmania* parasite. Within the gut of the sand fly, *Leishmania* parasites cycle through a range of morphological forms allowing survival, colonisation and transmission of the parasite when the sand fly takes subsequent bloodmeals (Rogers et al., 2002; Kamhawi, 2006).

Research is ongoing to understand multiple aspects of *Leishmania* interaction within the sand fly gut at a range of lifecycle stages. This can be achieved by two similar methods, one of which is *in vivo,* and the other is *ex vivo*, also known as *in vitro,* both first described by Pimenta et al. (1992; 1994). The *in vivo* method involves sand flies being experimentally infected and the guts dissected, followed by quantitation of the *Leishmania* infection intensity. This occurs over a range of days to follow colonisation of the sand fly and to study the occurrence of promastigote forms, to determine the infection intensity and its infectiousness. The *ex vivo* method requires the sand fly to be dissected and the midgut incubated with parasites, before it is washed (to remove unattached or weakly attached parasites) and the attached parasite population quantitated. This measures the number of parasites capable of attaching to the sand fly midgut as part of the assessment of its vectorial competency.

Initially, these types of study used hemocytometers for quantitation (Pimenta et al., 1992;1994), where infected midguts would be homogenised before counting. However, another method was developed called *in situ* grading, first described by Killick-Kendrick et al. (1994; 1995, as cited in Myskova et al., 2008). For this method, whole midguts are opened to expose the inner lumen, they are viewed under a microscope and then the number of parasites in a field of view estimated with this being recorded categorically. Myšková et al. (2008) experimentally compared the use of these methods for quantitation along with a third method of qPCR.

The three commonly used methods of infection intensity quantitation offer different advantages and disadvantages. Hemocytometers provide a cheap and fully quantitative method, however it can be time consuming and relies on consistent homogenisation of the midgut (Myšková et al., 2008). It also lacks sensitivity with low intensity infections likely leading to false negatives (Myšková et al., 2008). *In situ* grading is also cheap, as well as being quick and allows further information such as parasite location and morphology to be learned, however it is only semi-quantitative and when bloodmeals are present, parasites can be hard to distinguish (Myšková et al., 2008). It requires skill and experience to correctly categorise the

number of parasites present and is therefore subject to experimenter bias. It has also been noted that identifying morphological forms relies on parasites lying flat in the plane of focus (Wilson et al., 2010). qPCR provides a highly sensitive and fully quantitative option, as well as being the only method where operator counting errors and bias can be excluded. However, it is comparatively expensive and relies on accurate standard curves and reproducible DNA extraction methods. The most common target for detection of *Leishmania* currently is the kDNA minicircles whose numbers can vary (Galluzzi et al., 2018).

An important biological question for sand fly infection and transmission is to understand if there is a limit to the number of parasites a sand fly can sustain. This knowledge will help inform vector and transmission-blocking control strategies. Previous studies have compared the effect of parasite concentrations used for infection on the infection intensity of sand flies on a variety of days post infection. However, though significant differences have been found between infection concentrations, the doses that gave statistically significant different infection intensities have varied between studies (Myšková et al., 2008; Stamper et al., 2011; Seblova et al., 2013; Pruzinova et al., 2015). There has also been work to see if infection intensity is affected by infecting flies with amastigotes (reflecting natural infections) or promastigotes (Freitas et al., 2012; Sadlova et al., 2017; Vaselek et al., 2020). Conclusions varied between studies and these experiments have still only been done for a handful of *Leishmania*-sand fly pairs.

To our knowledge, a systematic review of papers using these methods and a meta-analysis of their results has not been carried out. The aim of this study was to collate papers that quantitate parasite infection intensity after sand fly infection. The aim of the meta-analysis was to understand the changes in parasite intensity within the sand fly when infected with different forms and concentrations of parasites. The study also aimed to see how comparable *ex vivo* and *in vivo* methods are. The data presented here suggests there may be a limit to parasite density which is supported by *ex vivo* and *in vivo* experimental midgut binding assays.

Methods

Literature criteria and analysis

The PRISMA checklist was used to guide this work. The search strategy used to identify relevant papers for this review and meta-analysis is seen in Table 1. The initial inclusion and exclusion criteria decided is seen in Table 2, however further criteria was needed once the analysis of relevant papers started which is discussed later. The search was carried out using Ovid MEDLINE and EMBASE, with duplications removed using the Ovid database tool. Papers that are not in English have been excluded. Papers deemed as relevant from their abstract were read in full and relevance decided using the inclusion and exclusion criteria. From relevant papers, details of the methods used were recorded, such as: infection method, sand fly age and previous feeding history, infecting parasite density and form (amastigote or promastigote). For data retrieval, *Leishmania* infection intensity was sometimes noted in text or clearly in figures, but if this was not the case, data was retrieved from graphs using ImageJ software. If sets of data had unclear or overlapping data points, then they had to be excluded from the analysis. Two-tailed Mann Whitney tests were carried out using GraphPad Prism. A Levene's test for homogeneity of variance using the median was carried out for comparing the parasites per midgut recorded for fly infections and midgut binding assays (Figure 6). This was carried out in Excel using guidance from GraphPad (2023). A *P*-value of <0.05 was deemed statistically significant (*$P < 0.05$, **$P<0.01$, ***$P<0.001$).

Experimental midgut binding assay and fly infections

Ex vivo midgut binding assays were carried out using a range of logarithmic phase *Leishmania mexicana* (MNYC/BZ/62/M379) parasite numbers. *Lutzomyia longipalpis* (Jacobina colony) reared at the London School of Hygiene and Tropical Medicine were fed 50% sucrose *ad libitum* prior to dissection. Midguts were dissected in a drop of PBS, with hindgut, foregut and malpighian tubules removed and then opened longitudinally. Uncut midguts (not opened longitudinally) were also used as a control to show specificity of attachment to the midgut epithelium as previously seen (Coutinho-Abreu et al., 2020b). A volume of 50 µL parasites in M199 supplemented parasite culture media + 20% (v/v) FCS, 1 x Basal Medium Eagle vitamins (v/v), 1% (v/v) human urine, 1% (v/v) penicillin streptomycin solution, 20 mM (v/v) sodium bicarbonate, pH 7.2 was added to individual midguts each within a well of a multi-test slide and incubated for 30 minutes in a humidified chamber at 26°C. Midguts were washed by transferring between 3 successive drops of PBS and gently agitated in each drop for 30 seconds to remove non-adherent parasites. Using fine forceps, midguts were transferred to 30 µL PBS in a 1.5 mL Eppendorf and homogenised using a disposable pestle. A range of homogenate volumes (3-10 µL) were dried to wells of a multi-test slide, fixed with methanol and stained

with 10% (v/v) Giemsa in dH$_2$O then counted using a light microscope (Leitz) at x1000 magnification under oil-immersion. Parasite counts were then multiplied to give the number in 30 µL, equivalent to the whole midgut.

For *in vivo* infections, unfed flies (3-5 days old) were fed through a chicken skin membrane on heat-inactivated (h.i.) human blood in an artificial feeder (Hemotek) containing *L. mexicana* axenic amastigotes. The blood contained either 5x10^4, 1x10^5, 5x10^5, 1x10^6 or 5x10^6 amastigotes per mL. Assuming the fly will take a 1 µL volume bloodmeal, concentrations were equivalent to 50, 100, 500, 1000 or 5000 amastigotes per fly. Midguts were dissected (as previously described) on day 5 post infection and were added to 30 µL PBS followed by homogenisation with a disposable pestle. For each midgut sample, 10 µL with 2 µL 4% PFA was added to a disposable hemocytometer (BVS100H, Immune Systems) and 16 squares counted. If no parasites were observed, another 16 squares were counted. The number of parasites per midgut was then calculated by multiplying the number of parasites counted in 16 squares by 10^4 and the dilution factor of 1.2 to get the number of parasites per mL. As the midgut was homogenised into 30 µL, the result was multiplied by 0.03.

Results

The majority of studies retrieved had to be excluded from the analysis

A total of 1731 potentially relevant papers were identified during this search, with 150 full texts assessed for eligibility. Of these, 68 matched inclusion criteria and could potentially be included in the meta-analysis of this review. When assessing full texts, it became apparent that small differences in methods made some data incomparable and therefore, further exclusion criteria were needed, which is seen in Figure 1. Furthermore, we had to exclude studies we had previously hoped to include as we only retrieved a few papers on the topic, for example those using sand fly cell lines. The majority of studies used *in situ* grading for parasite quantitation (Table S1, S2 and S3), however, results are reported as categorical, relative frequency data which makes a meta-analysis of previous studies difficult to achieve. A range of studies used qPCR (Table S4), but few used the same *Leishmania*-sand fly pairs or protocols. We therefore limited the meta-analysis to studies that used a hemocytometer or similar for *Leishmania* intensity quantitation. We also limited the papers to those working on *Leishmania (Leishmania)* only, focussing on two parasite-vector combinations of public health importance that represent restrictive and permissive vectoral relationships. Out of these studies, only *Phlebotomus papatasi* infected with *Leishmania major* (restrictive vector; zoonotic cutaneous leishmaniasis) and *Lu. longipalpis* infected with *Leishmania infantum* (permissive vector; zoonotic visceral leishmaniasis) had multiple papers for the same days post fly infection. Studies looking at *Lu. longipalpis* infected with *L. mexicana* were also included, as a commonly used experimental infection model, but data are from different days. Studies not using these *Leishmania*-sand fly combinations were excluded. For the studies included in this analysis, drawing conclusions has been difficult due to the range of concentrations, strains and days used between different studies.

A summary of data from studies using *in vivo* fly infections and quantitating *Leishmania* infection intensities using a hemocytometer are seen in Figure 2A for *P. papatasi* infected with *L. major* and Figure 3 for *Lu. longipalpis* infected with *L. infantum*. For Figure 3, Coutinho-Abreu et al. (2020b), did look at day 3, 9 and 15 comparing infection concentrations of $2x10^6$ and $5x10^6$ *L. infantum* parasites/mL in *Lu. longipalpis* but we found no other relevant papers in the search to compare it to.

Infection with amastigotes or promastigotes does not affect infection intensity

In contrast to other studies, Saraiva et al. (1995) used amastigotes to infect *P. papatasi*. The median *L. major* FV1 (MHOM/IL/80/Friedlin) parasites per midgut was lower on day 2 (Figure 2B) than the other infections using promastigotes, mirroring the delay in replication due to

transformation from amastigotes to promastigotes needing to occur. However, no significant difference in parasite numbers per midgut was seen for day 2 when comparing 10^6 amastigotes per mL to 10^6 amastigotes/promastigotes per mL. Statistically significant differences were seen when comparing to other promastigote per mL concentrations. For day 5, no statistically significant difference was seen when comparing flies infected with 10^6 promastigotes or 10^6 amastigotes per mL (Figure 2B).

Higher parasite infection concentrations do not always lead to higher infection intensities and vice versa

For *P. paptasi* infected with *L. major* FV1, there were significant differences found between the infection concentration used and the number of parasites per midgut. However, high infection concentrations did lead to lower median parasites per midgut and vice versa (Figures 2B). The same analysis was not carried out for *Lu. longipalpis* and *L. infantum* as there was not enough data of the same *L. infantum* strain on the same day from different studies.

The percentage of flies infected for each study per day was also recorded. For *P. papatasi* infected with *L. major*, 100% of flies were infected on day 2. Over the following days, like seen with infection intensity, higher infection concentrations were seen with lower percentages of infected flies and vice versa. The same pattern was seen for *Lu. longipalpis* infected with *L. infantum*. However, these conclusions are hard to draw with a range of *Leishmania* strains being compared.

High parasite infection concentrations are superfluous and lead to large ranges in binding

For both sand flies, a large range in parasites per midgut was observed (Figure 2A and 3), however no individual sand fly infection reached over 128,000 parasites/midgut post-defecation for *P. papatasi* infected with *L. major* (Day 5) or over 210,000 parasites/midgut (Day 12) for *Lu. longipalpis* infected with *L. infantum*. This was true for studies using up to 10^7 promastigotes per mL for fly infections, equivalent to a sand fly ingesting 6600 – 10,000 parasites (bloodmeal size 0.66 μL – 1 μL depending on sand fly (Pruzinova et al., 2015; Rogers et al., 2002)). This may suggest parasites do reach saturation, with many infections at least 10-fold lower. There was one exception with Moraes et al. (2018) finding *Lu. longipalpis* infected with over 2.3×10^7 *L. mexicana* parasites on day 3 and 2.7×10^7 parasites on day 6 (Figure 4).

Further work is needed to determine if parasite attachment numbers from ex vivo *and* in vivo *methods are comparable*

Ex vivo midgut binding assays are also used to study *Leishmania* attachment to the sand fly midgut. However, it is unknown if the number of parasites that attach to the midgut using this

method is comparable to the numbers seen attached in *in vivo* infections. In Table S5, a summary of the *ex vivo* methods can be seen. Only details of incubations with parasites (rather than parasite material) have been noted. In Figure 5, the median and range of parasites per midgut recorded by studies using *ex vivo* midgut binding assays can be seen. For *P. papatasi* incubated with *L. major*, the overall median of all studies included was just over 14,500 parasites/midgut. However, for *Lu. longipalpis* incubated with *L. infantum*, this was a lot lower at just over 5000 parasites/midgut. Coutinho-Abreu et al. (2020b) compared cultures from days 3 and 4, with percentage of infected flies lower for day 3. When data using day 3 cultures was removed, the overall median only increased to just over 7000 parasites/midgut.

When comparing *ex vivo* to *in vivo* data, *in vivo* data was taken from the day post bloodmeal (PBM) which best matches the timing of parasite attachment before bloodmeal remnant defecation in the sand fly. For *P. papatasi* and *L. major* experiments, this was day 5 PBM (Pruzinova et al., 2015) and for *Lu. longipalpis* infected with *L. infantum*, this was day 4 PBM (Rogers et al., 2002). When comparing all study data points for *P. papatasi* infected with *L. major* from *in vivo* day 5 to *ex vivo*, a statistically significant difference was found (Two-tailed Mann-Whitney U = 846.5, *P* = 0.0072). For *Lu. longipalpis* and *L. infantum*, only one *in vivo* study fit our criteria (Coutinho-Abreu et al., 2020a). When comparing all study data points from *in vivo* day 4 to *ex vivo*, no significant difference was found (Two-tailed Mann-Whitney U = 1224, *P* = 0.6353).

Experimental* ex vivo *and* in vivo *data also demonstrates saturation of parasite numbers when high parasite infection concentrations are used

For *ex vivo* midgut binding assays, an increase in range of parasites per midgut was seen, with increasing parasite concentrations (Figure 6). *Lu. longipalpis* midguts were incubated with 10^4 – 10^7 parasites per 50 µL with the number of parasites attached recorded. The number of parasites bound increased with increasing parasite numbers, with statistically significant differences seen between all concentrations except for 10^6 and 2×10^6. However at 10^7 parasites per 50 µL, the number of parasites bound ranged from 3 to over 16,000, suggesting non-specific binding was occurring. Significant differences in variance were found when comparing 10^7 to 2×10^6 ($F(1,39) = 7.7$, $p = 0.0084$) and 10^6 parasites per 50 µL ($F(1,42) = 9.44$, $p = 0.0037$). Uncut midguts had similar levels of binding to cut midguts at all concentrations tested.

For *in vivo* fly infections, increasing the number of amastigotes used for the infection increased the number of promastigotes per midgut. However no significant difference was seen when comparing the promastigotes per sand fly number when 50 or 100 amastigotes (Mann Whitney *U* = 563, *p* = 0.61) or for when 1000 or 5000 amastigotes (Mann Whitney *U* = 623, *p* =

0.78) were used for the infection. Unlike seen for the *ex vivo* assays, there was not a significant increase in variance at the higher concentrations (1000 and 5000, (F(1,70) = 0.076, p = 0.78)).

<u>Discussion</u>

Quantitation of *Leishmania* infection intensities within sand flies is crucial to understanding the lifecycle progression of this parasite and its transmission. The methods used to study this can be either *in vivo* or *ex vivo* with a range of techniques used to quantitate the infection intensities. The majority of studies retrieved as part of this systematic review used *in situ* grading. Though this method offers many advantages as discussed previously, it is clear when comparing to hemocytometer results, that the most commonly used grades (<100, 100-1000, >1000) miss variation at the higher parasites/midgut counts. It also makes comparisons between studies more difficult. Very few studies currently have taken advantage of the qPCR methods developed for *Leishmania* quantitation (Figure S4).

A meta-analysis of sand fly gut *Leishmania* infection intensities quantitated using a hemocytometer was carried out. One of the aims of this analysis was to see if infections with amastigotes or promastigotes differ in their intensity. Our data supports previous findings that no difference in infection intensity is seen during late-stage infections when amastigotes or promastigotes are used for fly infections. A statistically significant difference was seen when comparing *P. papatasi* infected with *L. major* amastigotes compared to promastigotes for day 2. This has previously been seen by Sadlova et al. (2017) who observed lower intensity and different morphological forms for *L. infantum* amastigote infections of *Phlebotomus argentipes* day 1 and 2 PBM. However, for the meta-analysis, these studies also differed in parasite concentration, with this likely contributing to the results. On day 5, there was no significant difference in infection intensity for flies infected with 10^6 amastigotes or promastigotes/mL. This is consistent with previous studies at time points post-defecation and later stages of infections (Freitas et al., 2012; Sadlova et al., 2017). This differs to Vaselek et al. (2020) who found statistically significant differences at late-stage infections for *Phlebotomus perniciosus* infected with amastigote or promastigotes of *L. infantum*. These differences may be *Leishmania*-sand fly pair specific.

Another aim of this analysis was to add to and hopefully provide clarity to previous work seeing if higher infection concentrations lead to an increase in the percentage of infected flies and higher fly infection intensities. Previous work has found statistically significant differences between infection loads, but flies still had heavy infections. Stamper et al. (2011) studied *L. major* infections of *Phlebotomus dubosqci*, finding significant differences in parasite intensities between flies infected with 10^4 or $2x10^5$ and $4x10^6$ promastigotes per mL. For Seblova et al. (2013) significant differences were only seen for *Phlebotomus orientalis* infected with $2x10^3$ *L. infantum* promastigotes per mL compared to $2x10^4$, 10^5 and $5x10^5$ promastigotes per mL. Pruzinova et al. (2015) found statistically significant differences between $2x10^3$ or $2x10^4$

Leishmania donovani promastigotes per mL compared to 5×10^5 promastigotes per mL for infections of *P. argentipes*.

In this study, a meta-analysis of data using *P. papatasi* infected with *L. major* found no clear pattern between infection concentration and sand fly infection intensity or percentage of flies infected. However, the lowest infection concentration used for *in vivo* fly infections in the meta-analysis was 10^6 parasites/mL, whereas previous studies found differences when much lower concentrations were used for infections ($2 \times 10^3 - 2 \times 10^5$ promastigotes per mL). This may suggest there is a maximum concentration needed for consistent infection with higher concentrations superfluous, meaning we saw no pattern in infection intensity with different infection concentrations as the maximum concentration of below 10^6 parasites/mL had already been achieved. Experimental *in vivo* infections carried out in our study showed no significant difference in promastigotes per sand fly at day 5 when 1×10^6 or 5×10^6 amastigotes per mL were used for infections. This would further suggest there is a cap in the number of parasites a sand fly can sustain. In this study the majority of flies did not reach an infection intensity higher than 2×10^5 parasites per midgut. What this cap is may vary between *Leishmania*-sand fly pairs, explaining the differences in the infection concentration that gave statistically significant parasite intensities in previous studies.

Ex vivo midgut binding assays carried out in this study also revealed a large range of parasites per midgut when 10^7 parasites per 50 µL were used, suggesting non-specific binding increases dramatically with high infection concentrations. The statistically significant differences in variance seen between 10^7 parasites per 50 µL compared to 2×10^6 and 10^6 parasites per 50 µL supports this theory. Lower parasite concentrations should be used in the future to remove variation in infection intensities. This will also mean *in vivo* infections more closely match natural infections where fewer parasites are ingested (Serafim et al., 2018). Furthermore, the use of uncut midguts in this study seem to show binding was not specific to the midgut epithelium and could bind the outer surface of the midgut as well, unlike previously reported by Coutinho-Abreu et al. (2020b).

If there is a cap in the number of parasites a sand fly can sustain, this opens up many interesting questions about what causes this limit and if the number of parasites sustained differs between species or permissive and restrictive vectors. Though sand flies are thought to take up less than 100 parasites when feeding on an infected host in nature (Serafim et al., 2018), there have also been naturally infected sand flies found with higher parasite loads. Parasite loads of *L. infantum* in *P. perniciosus* ranged from 1 to over 100,000 (González et al., 2017), with over 1 million *L. infantum* recorded in naturally infected *Lu. longipalpis* (Rodrigues et al., 2016). It may be a bottleneck in the number of parasites that can attach the midgut,

and/or it may be caused by something later in the lifecycle, such as the accumulation of filamentous proteophosphoglycan (fPPG) (Rogers and Bates, 2007) with space being the limiting factor.

To fully understand the maximum number of *Leishmania* parasites a sand fly can sustain, it is crucial to include the impact of retroleptomonads, the form thought to replicate after an infected fly takes a second bloodmeal (Serafim et al., 2018). It has been suggested that the increase in nutrients that comes with a second bloodmeal leads to the reversion of metacyclics to retroleptomonads and the increase in parasite replication (Serafim et al., 2018). Nutrients may be the limiting factor for lower parasite numbers even when infection concentrations are high, with nutrients available for only a certain number of parasites to survive. There are limited studies to carry out a meta-analysis of parasite numbers following second bloodmeals at present, with our search retrieving four papers referring to second or sequential bloodmeals (Elnaiem et al., 1994; Vivenes et al., 2001; Moraes et al., 2018; Serafim et al., 2018).

Ex vivo midgut binding assays are used less frequently and only allow information to be learned about *Leishmania* attachment to the midgut. However, one advantage is they avoid the use of infected sand flies. Previous studies have used both *ex vivo* and *in vivo* methods but have not directly compared the number of parasites attached to the midgut between them (Pimenta et al., 1994; Kamhawi et al., 2004; Di-Blasi et al., 2015). When comparing *ex vivo* to *in vivo* data, there was a significant difference found for *P. papatasi* with *L. major* but not for *Lu. longipalpis* with *L. infantum*. A range of strains for both *Leishmania* species as well as parasite concentrations and incubation conditions have been used in this analysis, which may lead to these differing results. Learning if *ex vivo* and *in vivo* methods are comparable will give us the opportunity to study if the number of attachment sites on the midgut is a limiting factor to *Leishmania* numbers within the sand fly.

The difficulty in comparing *ex vivo* studies highlights the variation in methods used, and the need for standardisation. Different infection concentrations and incubation times were used across the studies included in this meta-analysis. All studies also only used sugarfed flies noted by Wilson et al. (2010) to be inappropriate with blood fed flies exhibiting physiological midgut changes that may affect binding. Many studies also used PBS as the incubation media, in which midguts have been reported to deteriorate (Kamhawi et al., 2000). In future, stating the percentage of each morphological form in the parasite culture used may provide more consistent results between studies.

Such large ranges in *in vivo* parasites per midgut at the same day post infection may suggest more specific timings are need for comparison of flies. Variation in sand fly infections is

unavoidable, however, tracking individual sand flies to capture defecation and using this as a marker for comparison of flies may be more suitable allowing clear conclusions to be drawn between sand flies. This would also allow for more confident comparisons between *ex vivo* and *in vivo* experiments, with *in vivo* time points accurately reflecting the timing of parasite attachment.

Conclusion

This systematic review and meta-analysis has highlighted the need for changes to current reporting of the results of *Leishmania* infection intensities. Though advantageous in other areas, the use of *in situ* grading prevents comparison between studies as well as masking variation in parasite infection intensities over 1000 parasites. Further steps need to be taken to reduce controllable heterogeneity of *in vivo* assays by tracking sand fly defecation timing more closely and recording the percentage of morphological forms used for infections of flies. This will also allow for improved comparison in the numbers of parasites attached to the midgut in *ex vivo* and *in vivo* studies. The results of the meta-analysis and experimental work suggest infection concentrations over 10^6 parasites/mL are superfluous and do not affect infection intensities, with excess parasites also increasing non-specific binding in *ex vivo* midgut binding assays. It is likely there is a cap in the number of parasites a sand fly can sustain, with further work needed to deduce the limiting factor(s) for this interaction.

References

Cecílio P, Cordeiro-da-Silva A, Oliveira F. Sand flies: basic information on the vectors of leishmaniasis and their interactions with *Leishmania* parasites. Commun Biol. 2022;5:305.

Ready PD. Factors affecting egg production of laboratory-bred *Lutzomyia longipalpis* (Diptera: Psychodidae). J Med Entomol. 1979;16(5):413-423.

Rogers ME, Chance ML, Bates PA. The role of promastigote secretory gel in the origin and transmission of the infective stage of *Leishmania mexicana* by the sandfly *Lutzomyia longipalpis*. Parasitology. 2002;124:495–507.

Kamhawi S. Phlebotomine sand flies and *Leishmania* parasites: friends or foes? Trends Parasitol. 2006;22(9):439-445.

Pimenta PFP, Turco SJ, McConville MJ, Lawyer PG, Perkins PV, Sacks DL. Stage-specific adhesions of *Leishmania* promastigotes to the sandfly midgut. Science. 1992;256:1812-1815.

Pimenta PFP, Saraiva EMB, Rowton E, Modi GB, Garraway LA, Beverley SM, Turco SJ, Sacks DL. Evidence that the vectorial competence of phlebotomine sand flies for different species of *Leishmania* is controlled by structural polymorphisms in the surface lipophosphoglycan. Proc Natl Acad Sci USA. 1994; 91:9155-9159.

Killick-Kendrick R, Killick-Kendrick M, Tang Y. Anthroponotic cutaneous leishmanaiasis in Kabul, Afghanistan: the low susceptibility of *Phlebotomus papatasi* to *Leishmania tropica*. Trans R Soc Trop Med Hyg. 1994;88(2):252-253.

Killick-Kendrick R, Killick-Kendrick M, Tang Y. Anthroponotic cutaneous leishmanaiasis in Kabul, Afghanistan: the high susceptibility of *Phlebotomus sergenti* to *Leishmania tropica*. Trans R Soc Trop Med Hyg. 1995;89(5):477.

Myšková J, Votypka J, Volf P. *Leishmania* in sand flies: comparison of quantitative polymerase chain reaction with other techniques to determine the intensity of infection. J Med Entomol. 2008;45(1):133–8.

Wilson R, Bates MD, Dostalova A, Jecna L, Dillon RJ, Volf P, Bates PA. Stage-specific adhesion of *Leishmania* promastigotes to sand fly midguts assessed using an improved comparative binding assay. PLoS Negl Trop Dis. 2010;4(9):e816.

Galluzzi L, Ceccarelli M, Diotallevi A, Menotta M, Magnani M. Real-time PCR applications for diagnosis of leishmaniasis. Parasit Vectors. 2018;11:273.

Stamper LW, Patrick RL, Fay MP, Lawyer PG, Elnaiem DEA, Secundino N, Debrabant A, Sacks DL, Peters NC. Infection parameters in the sand fly vector that predict transmission of *Leishmania major*. PLoS Negl Trop Dis. 2011;5(8):e1288.

Seblova V, Volfova V, Dvorak V, Pruzinova K, Votypka J, Kassahun A, Gebre-Michael T, Hailu A, Warburg A, Volf P. *Phlebotomus orientalis* sand flies from two geographically distant Ethiopian localities: biology, genetic analyses and susceptibility to *Leishmania donovani*. PLoS Negl Trop Dis. 2013;7(4): e2187.

Pruzinova K, Sadlova J, Seblova V, Homola M, Votypka J, Volf P. Comparison of bloodmeal digestion and the peritrophic matrix in four sand fly species differing in susceptibility to *Leishmania donovani*. PLoS ONE. 2015;10(6):e0128203.

Freitas VC, Parreiras KP, Duarte APM, Secundino NFC, Pimenta PFP. Development of *Leishmania (Leishmania) infantum chagasi* in its natural sandfly vector *Lutzomyia longipalpis*. Am J Trop Med Hyg. 2012;86(4):606-612.

Sadlova J, Myšková J, Lestinova T, Votypka J, Yeo M, Volf P. *Leishmania donovani* development in *Phlebotomus argentipes*: comparison of promastigote- and amastigote-initiated infections. Parasitology. 2017;144:403-410.

Vaselek S, Prudhomme J, Myšková J, Lestinova T, Spitzova T, Bañuls AL, Volf P. Comparative study of promastigote- and amastigote-initiated infection of *Leishmania infantum* (Kinetoplastida: Trypanosomatidae) in *Phlebotomus perniciosus* (Diptera: Psychodidae) conducted in different biosafety level laboratories. J Med Entomol. 2020;57(2):601-607.

GraphPad | What to do when data fail tests for homogeneity of variance (part of one-way ANOVA)? 2023 [cited 2023 November 3] Available from: https://www.graphpad.com/support/faq/what-to-do-when-data-fail-tests-for-homogeneity-of-variance/

Coutinho-Abreu IV, Oristian J, de Castro W, Wilson TR, Meneses C, Soares RP, Borges VM, Descoteaux A, Kamhawi S, Valenzuela JG. Binding of *Leishmania infantum* lipophosphoglycan to the midgut is not sufficient to define vector competence in *Lutzomyia longipalpis* sand flies. mSphere. 2020b;5:e00594-20.

Saraiva EMB, Pimenta PFP, Brodin TN, Rowton E, Modi GB, Sacks DL. Changes in lipophosphoglycan and gene expression associated with the development of *Leishmania major* in *Phlebotomus papatasi*. Parasitology. 1995;111:275-287.

Moraes CS, Aguiar-Martins K, Costa SG, Bates PA, Dillon RJ, Genta FA. Second blood meal by female *Lutzomyia longipalpis*: enhancement by oviposition and its effects on digestion, longevity, and *Leishmania* infection. Hindawi. 2018:2472508.

Coutinho-Abreu IV, Serafim TD, Meneses C, Kamhawi S, Oliveira F, Valenzuela JG. Distinct gene expression patterns in vector-residing *Leishmania infantum* identify parasite stage-enriched markers. PLoS Negl Trop Dis. 2020a;14(3):e0008014.

Serafim TD, Coutinho-Abreu IV, Oliveira F, Meneses C, Kamhawi S, Valenzuela JG. Sequential blood meals promote *Leishmania* replication and reverse metacyclogenesis augmenting vector infectivity. Nat Microbiol. 2018;3:548-555.

González E, Álvarez A, Ruiz S, Molina R, Jiménez M. Detection of high *Leishmania infantum* loads in *Phlebotomus perniciosus* captured in the leishmaniasis focus of southwestern Madrid region (Spain) by real time PCR. Acta Trop. 2017:68-73.

Rodrigues ACM, Melo LM, Magalhães RD, de Moraes NB, de Souza Júnior AD, Bevilaqua CML. Molecular identification of *Lutzomyia migonei* (Diptera: Psychodidae) as a potential vector for *Leishmania infantum* (Kinetoplastida: Trypanosomatidae). Vet Parasitol. 2016:28-32.

Rogers ME, Bates PA. *Leishmania* manipulation of sand fly feeding behavior results in enhanced transmission. PLoS Pathog. 2007;3(6):e91.

Elnaiem DA, Ward RD, Young PE. Development of *Leishmania chagasi* (Kinetoplastida: Trypanosomatidae) in the second blood-meal of its vector *Lutzomyia longipalpis* (Diptera: Psychodidae). Parasitol Res. 1994;80(5):414-419.

Vivenes A, Oviedo M, Márquez JC, Montoya-Lerma J. Effect of second bloodmeal on the oesophagus colonisation by *Leishmania mexicana* complex in *Lutzomyia evansi* (Diptera: Psychodidae). Mem Inst Oswaldo Cruz. 2001;96(3):281-283.

Kamhawi S, Ramalho-Ortigao M, Pham VM, Kumar S, Lawyer PG, Turco SJ, Barillas-Mury C, Sacks DL, Valenzuela JG. A role for insect galectins in parasite survival. Cell. 2004;119:329-341.

Di-Blasi T, Lobo AR, Nascimento LM, Córdova-Rojas JL, Pestana K, Marín-Villa M, Tempone AJ, Telleria EL, Ramalho-Ortigão M, McMahon-Pratt D, Traub-Csekö YM. The flagellar protein FLAG1/SMP1 is a candidate for *Leishmania*-sand fly interaction. Vector Borne Zoonotic Dis. 2015;15(3): 202-209.

Kamhawi S, Modi GB, Pimenta PFP, Rowton E, Sacks DL. The vectorial competence of *Phlebotomus sergenti* is specific for *Leishmania tropica* and is controlled by species-specific, lipophosphoglycan-mediated midgut attachment. Parasitology. 2000;121:25-33.

Dobson DE, Kamhawi S, Lawyer P, Turco SJ, Beverley SM, Sacks DL. *Leishmania major* survival in selective *Phlebotomus papatasi* sand fly vector requires a specific SCG-encoded lipophosphoglycan galactosylation pattern. PLoS Pathog. 2010;6(11):e1001185.

Butcher BA, Turco SJ, Hilty BA, Pimenta PF, Panunzio M, Sacks DL. Deficiency in β1,3-galactosyltransferase of a *Leishmania major* lipophosphoglycan mutant adversely influences the *Leishmania*-sand fly interaction. J Biol Chem. 1996;271(34):20573-20579.

Aslan H, Dey R, Meneses C, Castrovinci P, Jeronimo SMB, Oliva G, Fischer L, Duncan RC, Nakhasi HL, Valenzuela JG, Kamhawi S. A new model of progressive visceral leishmaniasis in hamsters by natural transmission via bites of vector sand flies. J Infect Dis. 2013;207:1328-1338.

Diaz-Albiter H, Sant'Anna MRV, Genta FA, Dillon RJ. Reactive oxygen species-mediated immunity against *Leishmania mexicana* and *Serratia marcescens* in the Phlebotomine sand fly *Lutzomyia longipalpis*. J Biol Chem. 2021;287(28):23995-24003.

Telleria EL, Sant'Anna MRV, Ortigão-Farias JR, Pitaluga AN, Dillon VM, Bates PA, Traub-Csekö YM, Dillon RJ. Caspar-like gene depletion reduces *Leishmania* infection in sand fly host *Lutzomyia longipalpis*. J Biol Chem. 2012;287(16):12985-12993.

Soares RPP, Macedo ME, Ropert C, Gontijo NF, Almeida IC, Gazzinelli RT, Pimenta PFP, Turco SJ. *Leishmania chagasi*: lipophosphoglycan characterisation and binding to the midgut of the sand fly vector *Lutzomyia longipalpis* . Mol Biochem Parasitol. 2002;121(2):213-224.

Table 1 shows the search strategy used for the systematic review. Each block was searched with OR with the three blocks then being combined with AND.

Leishmania/ or Leishmania.mp.	Searched Leishmania as a MeSH term and as keyword		
(sandfl* OR sand fl*).mp.	Searched sand fly in two different forms as keywords	OR	
exp Psychodidae/	Exploded search term Psychodidae		
Lutzomyia.mp.	Searched as keyword		
Phlebotomus.mp.	Searched as keyword		
Cell Adhesion/	Searched as MeSH term		AND
Host-Parasite Interaction/	Searched as MeSH term		
Defecat*	Searched as keyword		
Bind*.mp.	Searched as keyword	OR	
Attach*.mp.	Searched as keyword		
Interact*.mp.	Searched as keyword		
Bloodmeal.mp.	Searched as keyword		
Blood meal.mp.	Searched as keyword		
Vector* competence.mp.	Searched as keyword		
Adhesion.mp.	Searched as keyword		
Midgut*.mp.	Searched as keyword		

Table 2 shows the inclusion and exclusion criteria used for the systematic review.

Inclusion criteria	Exclusion criteria
Studies where sand flies have been artificially infected with parasites with midguts then dissected and parasite binding quantified	Studies were sand flies or cell lines have been infected or incubated with an unknown concentration of parasites
Studies where sand fly midguts have been dissected and incubated with parasites with binding then quantified	Studies where sand flies have acquired their infection naturally
Studies where sand fly cell lines have been incubated with parasites and binding has been quantified	Studies where flies have been fed off an infected animal (and therefore studies quantifying midgut infections for the purpose of xenodiagnoses)
	Studies where parasite interactions with the midgut have only been reported through imaging
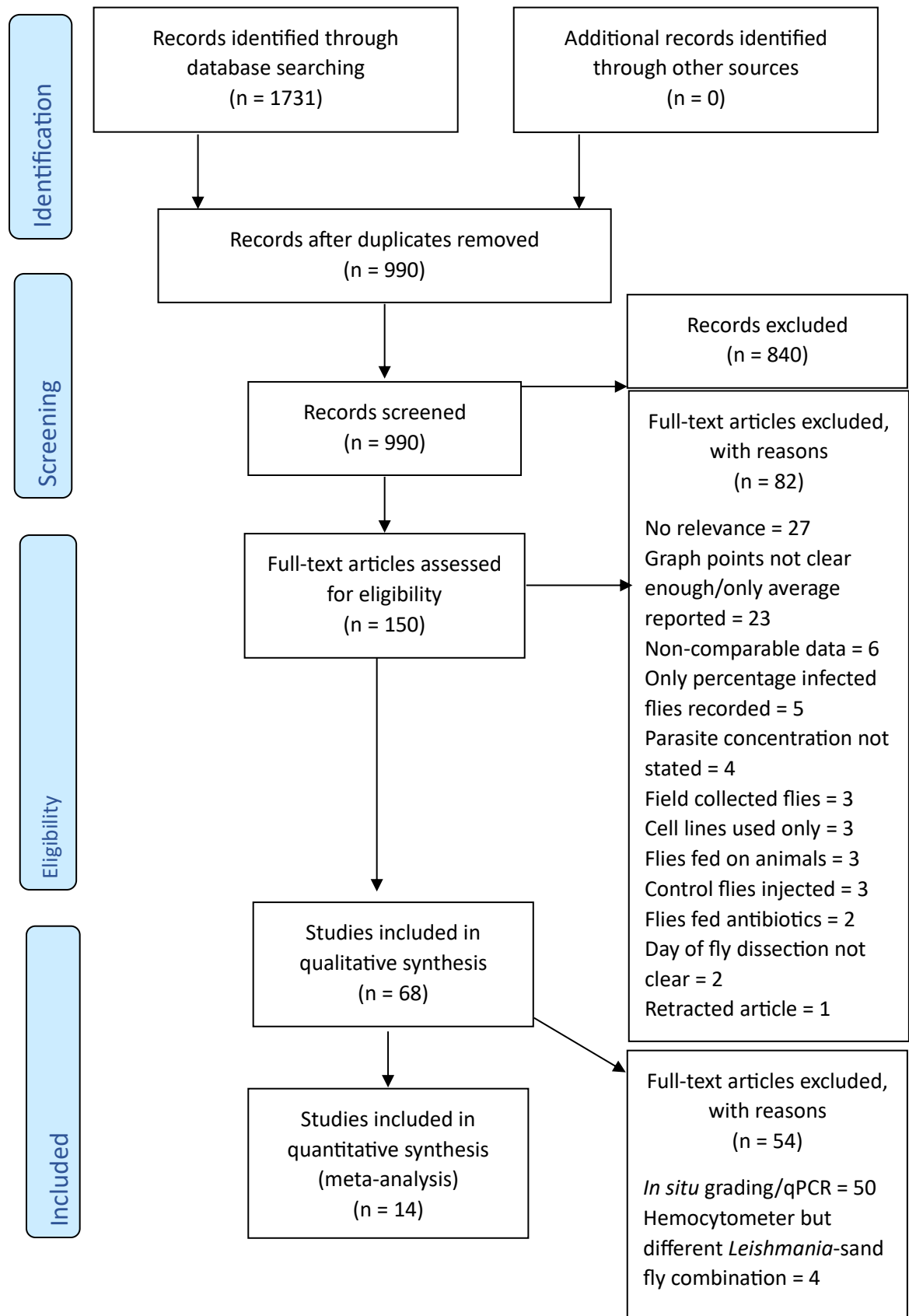
Figure 1. PRISMA flow diagram showing the number of papers included and excluded at each stage of the review process.

A

Parasites/midgut

10⁻² 10⁻¹ 10⁰ 10¹ 10² 10³ 10⁴ 10⁵ 10⁶ 10⁷

Overall Day 2
Overall Day 3
Overall Day 4
Overall Day 5
Saraiva et al., 1995 10⁶ama/mL FV1
Pimenta et al., 1994 10⁶ama or pros/mL Neal
Pimenta et al., 1994 10⁶ama or pros/mL LRC-137
Pimenta et al.,1994 10⁶ama or pros/mL L199
Pimenta et al., 1994 10⁶ama or pros/mL FV1
Dobson et al., 2010 4x10⁶pros/mL SD 75.1
Dobson et al., 2010 4x10⁶pros/mL FV1
Dobson et al., 2010 4x10⁶pros/mL LV39c5
Dobson et al., 2010 5x10⁶pros/mL FV1
Dobson et al., 2010 8x10⁶pros/mL FV1
Dobson et al., 2010 8x10⁶pros/mL LV39c5
Dobson et al., 2010 10⁷pros/mL FV1
Saraiva et al., 1995 10⁶ama/mL FV1
Di-Blasi et al., 2015 5x10⁶ pros/mL ASKH — 86%
Saraiva et al., 1995 10⁶ama/mL FV1
Dobson et al., 2010 8x10⁶pros/mL FV1 — 94%
Dobson et al., 2010 8x10⁶pros/mL LV39c5 — 69%
Saraiva et al., 1995 10⁶ama/mL FV1
Butcher et al., 1996 10⁶pros/mL FV1
Dobson et al., 2010 4x10⁶pros/mL FV1 — 82%
Dobson et al., 2010 4x10⁶pros/mL LV39c5 — 58%
Dobson et al., 2010 5x10⁶pros/mL FV1
Dobson et al., 2010 10⁷pros/mL FV1

Day 2
Day 3
Day 4
Day 5

Figure 2. *Leishmania major* concentrations used for *Phlebotomus papatasi in vivo* infection and the resulting range of infection intensities reported vary (A). Higher infection concentrations do not necessarily lead to higher infection intensities, and infection with amastigotes or promastigotes lead to similar late-stage infection intensities (B). Statistical differences (Mann Whitney U test) are seen between the infection intensities (parasites/midgut) when different concentrations of *L. major* FV1 parasites are used for an infection (B). The box plot shows the median, 25th and 75th percentiles along with the range of *L. major* infection intensities of individual *P. papatasi* midguts. FV1 – MHOM/IL/80/Friedlin V1; Neal – MRHO/SU/59/P; LRC-137 – clone V121 (MHOM/IL/67/Jericho-II); L199 – MTAT/KE/00/T4; LV39c5 – clone derivative of NIH/SD line; SD 75.1 – clonal derivative of NIH/Sd line (MHOM/SN/74/SD); ASKH – MHOM/SU/1973-ASKH. If 100% flies were not infected, the percentage of flies infected per condition are shown. Zero results have been plotted as 0.1 so that a log scale could be used. *$P < 0.05$, **$P < 0.01$, ***$P < 0.001$.
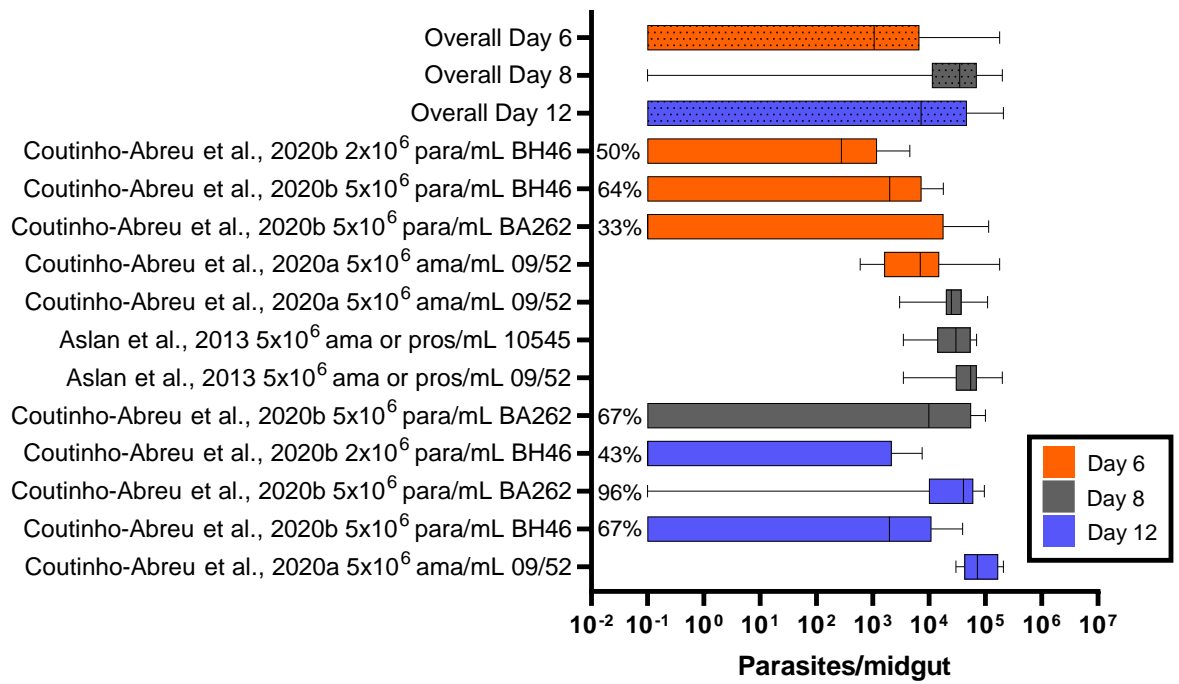
Figure 3. Infection intensities (parasites/midgut) of *in vivo Lutzomyia longipalpis* infections with *Leishmania infantum* vary. The box plot shows the median, 25th and 75th percentiles along with the range of *L. infantum* infection intensities of individual *Lu. longipalpis* midguts. If 100% flies were not infected, the percentage of flies infected per condition are shown. Zero results have been plotted as 0.1 so that a log scale could be used. BH46 – MCAN/BR/89/BH46; BA262 – MCAN/BR/89/BA262; 10545 – MCAN/IT/11/10545; 09/52 – MCAN/BR/09/52.
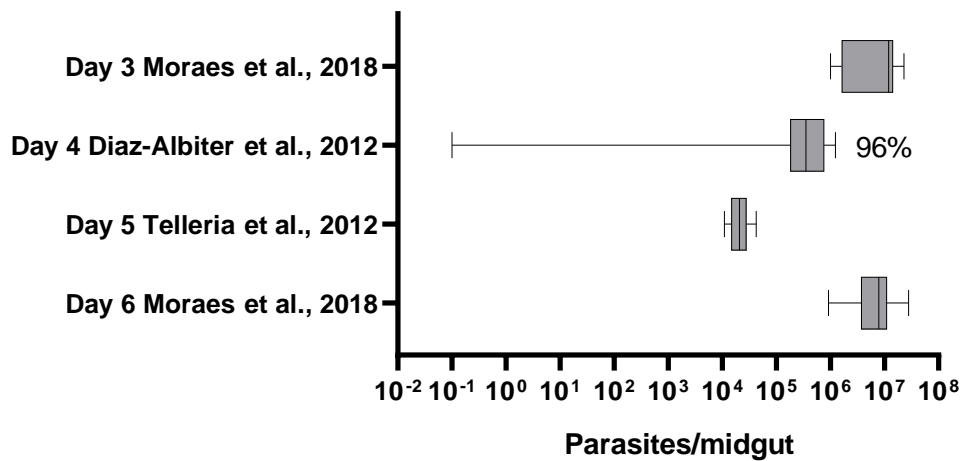
Figure 4. **Moraes et al. (2018) reported high parasite/midgut numbers for *Leishmania mexicana in vivo* infections of *Lutzomyia longipalpis* compared to other studies. Only one study per day using *L. mexicana - Lu. longipalpis* fit the criteria to be included in this meta-analysis.** The box plot shows the median, 25th and 75th percentiles along with the range of *L. mexicana* (MNYC/BZ/62/M379) infection intensities of individual *Lu. longipalpis* midguts. The concentration used for all fly infections was $2x10^6$ amastigotes/mL. If 100% flies were not infected, the percentage of flies infected per condition are shown. Zero results have been plotted as 0.1 so that a log scale could be used.

A

P. papatasi x L. major

Coutinho-Abreu et al., 2020b $2x10^6$ D3 culture 2885

Di-Blasi et al., 2015 $5x10^6$ pros ASKH

Kamhawi et al., 2004 $2x10^6$ parasites FV1

10^{-2} 10^{-1} 10^0 10^1 10^2 10^3 10^4 10^5 10^6 10^7

Parasites/midgut

B

Lu. longipalpis x *L. infantum*

Soares et al., 2002 $6x10^5$ pros PP75

Coutinho-Abreu et al., 2020b $2x10^6$ D3 culture BA262 — 92%

Coutinho-Abreu et al., 2020b $2x10^6$ D3 culture 09/52

Coutinho-Abreu et al., 2020b $2x10^6$ D3 culture 320 — 90%

Coutinho-Abreu et al., 2020b $2x10^6$ D4 culture 09/52

Coutinho-Abreu et al., 2020b $2x10^6$ D4 culture BH46

Di-Blasi et al., 2015 $5x10^6$ pros UCM-1

10^{-2} 10^{-1} 10^0 10^1 10^2 10^3 10^4 10^5 10^6 10^7

Parasites/midgut

Figure 5. The number of parasites attached to midguts in *ex vivo* midgut binding assays differ between *Leishmania* – sand fly pairs. *Ex vivo* midgut binding assays using *Phlebotomus papatasi* and *Leishmania major* (overall parasites/midgut median: 14596) (**A**) and *Lutzomyia longipalpis* and *Leishmania infantum* (overall parasites/midgut median: 5127) (**B**) are shown. The box plot shows the median, 25th and 75th percentiles along with the range of parasites bound per midgut. Zero results have been plotted as 0.1 so that a log scale could be used. The total number of parasites the midgut was incubated with is shown. If not all midguts had parasite attachment, the percentage of midguts with attachment is shown. 2885 – WR 2885 (RFP expressing); ASKH – MHOM/SU/1973-ASKH; FV1 – MHOM/IL/80/FN; PP75 – MHOM/BR/74/PP75; BA262 – MCAN/BR/89/BA262; 09/52 – MCAN/BR/09/52; 320 – MHOM/ES/92/LLM-320; BH46 – MCAN/BR/89/BH46; UCM-1 – MHOM/ES/00/UCM-1; D3 – Day 3; D4 – Day 4.
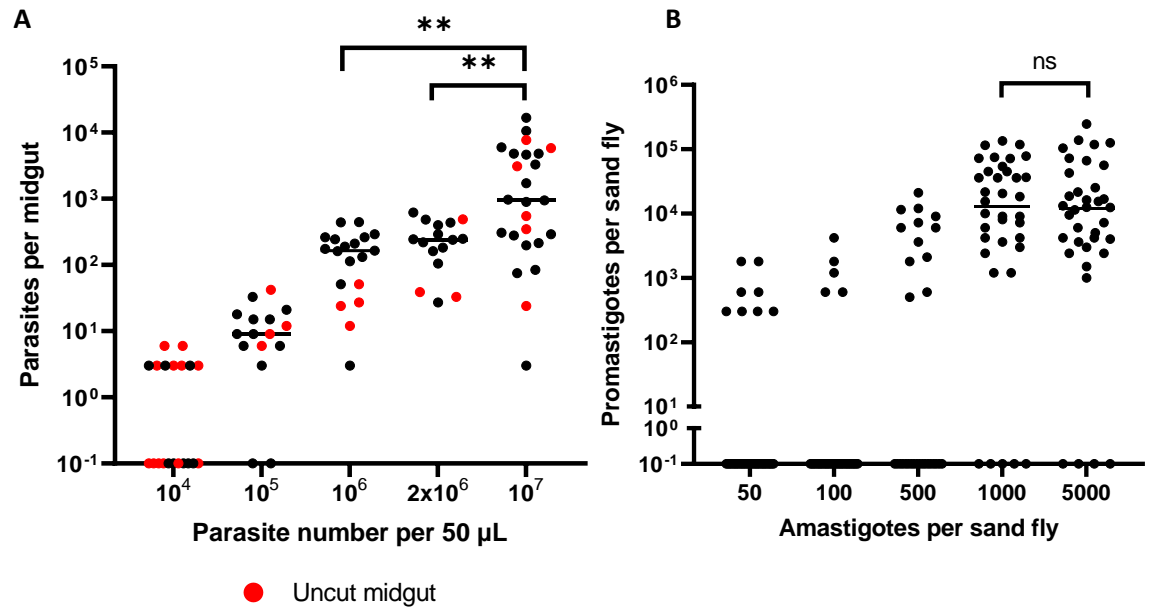
Figure 6. Midgut binding assays where midguts are incubated with 10^7 parasites per 50 μL show an increased variance in the number of parasite bound, suggesting increased non-specific binding. *In vivo* **fly infections plateau when higher parasite numbers are used for infections, suggesting a limit in the parasite numbers a fly can sustain. A** Binding of *L. mexicana* to *Lu. longipalpis* midguts when incubated with various parasite concentrations. Uncut midguts were tested as a control as done by Coutinho-Abreu et al. (2020b). A statistically significant difference (Mann Whitney U test) was seen between all concentrations except for 10^6 and 2×10^6 parasites per 50 μL. Analysis included both cut and uncut midguts. A statistically significant difference in variance was seen (shown on graph) when 10^7 parasites per 50 μL was used compared to 2×10^6 ($F_{(1,39)}$ = 7.7, *p* = 0.0084) or 10^6 ($F_{(1,42)}$ = 9.44, *p* = 0.0037). For 10^4 parasites per 50 μL, 11 midguts were recorded with no parasites attached. **B** *Lu. longipalpis* infections with various concentrations of *L. mexicana*. Sand flies were dissected 5 days post infection and parasite load assessed. A statistically significant difference (Mann Whitney U test) was seen between all concentrations except for 50/100 and 1000/5000. No significant difference in variance was seen between 1000 and 5000 infection concentrations ($F_{(1,70)}$ = 0.076, *p* = 0.78) (shown on graph). The numbers of uninfected flies per group are: 50 - 28; 100 - 28; 500 - 18. For both graphs, zero results have been plotted as 0.1 so that a log scale could be used. The lines shows the median.

Table S1. Studies using <100, 100-1000, >1000 Myšková et al. (2008) *in situ* grading systems for *Leishmania (Leishmania)* intensity quantitation in Old World sand fly species.

Sand fly species	*Leishmania* species	Reference
Phlebotomus arabicus	*L. infantum* (MHOM/TR/2000/OG-VL)	Myšková et al., 2007; Myšková et al., 2008
	L. major LV39 (MRHO/SU/1959/Neal P)	Myšková et al., 2007
	L. turanica (MRHO/MN/08/BZ18(GFP+)	Chajbullinova et al., 2012
Phlebotomus argentipes	*L. donovani* (MHOM/NP/03/BPK282)	Seblova et al., 2019
	L. donovani (MHOM/NP/03/BPK275)	Seblova et al., 2019
	L. donovani (MHOM/NP/02/BPK026)	Seblova et al., 2019
	L. donovani RFP (MHOM/ET/2009/AM459)	Pruzinova et al., 2018
	L. donovani GR374 (MHOM/ET/2010/DM-1033)	Pruzinova et al., 2015
	L. donovani/L. infantum hybrid (ITOB/TR/2005/TOB2)	Becvar et al., 2021
Phlebotomus duboscqi	*L. major* LV561 (MHOM/IL/67/LRC-L137 Jericho-II)	Myšková et al., 2008; Sadlova and Volf, 2009; Pruzinova et al., 2013; Boulanger et al., 2004
	L. major (MHOM/IL/81/Friedlin/VI;FVI)	Sadlova et al., 2013
	L. major CC1 (MHOM/IR/83/LT252)	Diniz et al., 2021
	L. major (MARV/SN/XX/RV24)	Becvar et al., 2021
	L. major (LV39 clone 5, MRHO/SU/59/P)	Boulanger et al., 2004
Phlebotomus orientalis	*L. donovani* (MHOM/ET/2010/DM-1033)	Seblova et al., 2013; Pruzinova et al., 2015

	L. donovani RFP (MHOM/ET/2009/AM 459)	Pruzinova et al., 2018
Phlebotomus papatasi	*L. amazonensis* (IFLA/BR/1967/PH8)	Nogueira et al., 2017
	L. amazonensis (MHOM/BR/1975/Josefa)	Nogueira et al., 2017
	L. donovani RFP (MHOM/ET/2009/AM 459)	Pruzinova et al., 2018
	L. donovani (MHOM/NP/02/BPK026)	Seblova et al., 2019;
	L. infantum OG-VL (MHOM/TR/2000/OG-VL)	Volf et al., 2007
	L. major LV561 (MHOM/IL/67/LRC-L137 Jericho II)	Volf et al., 2007
	L. major LV39 (MRHO/SU/1959/Neal P)	Myšková et al., 2007
	L. major (MHOM/IL/81/Friedlin /VI; FVI)	Sadlova et al., 2010
	L. major (WHOM/IR/-/13-DsRED(RFP+)	Chajbullinova et al., 2012
Phlebotomus papatasi	*L. major* (MHOM/IL/1980/Friedlin)	Guimaraes et al., 2018
	L. major-like BH49 (MHOM/BR/1971/BH49)	Guimaraes et al., 2018
	L. major-like BH1221 (MHOM/BR/1971/BH121)	Guimaraes et al., 2018
	L. turanica (MRHO/MN/08/BZ18(GFP+)	Chajbullinova et al., 2012
	L. major- *L. infantum* MHOM/PT/94/IMT208	Volf et al., 2007
	L. major- *L. infantum* MHOM/PT/2004/IMT367	Volf et al., 2007
Phlebotomus perniciosus	*L. infantum* (MHOM/MA/67/ITMAP-263)	Gazanion et al., 2012
	L. infantum (MCAN/PT/2005/IMT373)	Hlavacova et al., 2013

	L. infantum (MHOM/BR/76/M4192)	Jecna et al., 2013
Phlebotomus sergenti	L. killicki (MHOM/DZ/2005/LIPA 11)	Boubidi et al., 2011
	L. tropica SU23 (MHOM/TR/98/HM)	Jancarova et al., 2015
	L. tropica SU23 (MHOM/TR/98/HM)	Jancarova et al., 2016; Jancarova et al., 2015
	L. turanica (MRHO/MN/08/BZ18(GFP+)	Chajbullinova et al., 2012
Sergentomyia schwetzi	L. donovani (MHOM/ET/2010/GR374)	Sadlova et al., 2013; Sadlova et al., 2018
	L. donovani RFP (MHOM/ET/2009/AM459)	Pruzinova et al., 2018
	L. infantum (ITOB/TR/2005/CUK3)	Sadlova et al., 2013
	L. major (MHOM/IL/81/Friedlin/VI;FVI)	Sadlova et al., 2013
	L. major LV561 (LRC-L137; MHOM/IL/1967/Jericho-II)	Sadlova et al., 2018

Table S2. Studies using <100, 100-1000, >1000 Myšková et al. (2008) *in situ* grading systems for *Leishmania (Leishmania)* intensity quantitation in New World sand fly species.

Sand fly species	*Leishmania* species	Reference
Lutzomyia longipalpis	*L. amazonensis* (IFLA/BR/1967/PH8)	Nogueira et al., 2017
	L. amazonensis (MHOM/BR/1975/Josefa)	Nogueira et al., 2017
	L. donovani (MHOM/ET/2010/GR374)	Sadlova et al., 2013
	L. enriettii LV90 (MCAV/BR/45/LV90)	Seblova et al., 2015a
	L. infantum (MHOM/BR/76/M4192)	Myšková et al., 2016; Guimaraes et al., 2016
	L. infantum (MCAN/PT/2005/IMT373)	Hlavacova et al., 2013
	L. infantum (ITOB/TR/2005/CUK3)	Sadlova et al., 2013
	L. infantum OG-VL (MHOM/TR/2000/OG-VL)	Volf et al., 2007; Sadlova et al., 2022
	L. infantum (OGVL marked with mCherry)	Alexandre et al., 2020
	L. major LV561 (MHOM/IL/67/LRC-L137 Jericho II)	Volf et al., 2007
	L. major LV39 (MRHO/SU/1959/Neal P)	Myšková et al., 2007
	L. major (MHOM/IL/1980/Friedlin)	Guimaraes et al., 2018
	L. major-like BH49 (MHOM/BR/1971/BH49)	Guimaraes et al., 2018
	L. major-like BH1221 (MHOM/BR/1971/BH121)	Guimaraes et al., 2018
	L. mexicana (MNYC/BZ/62/M379)	Ishemgulova et al., 2017; Jecna et al., 2009; Beneke et al., 2019; Sunter et al., 2019; Halliday et al., 2020
	L. mexicana Cas9 T7 strain (derived MNYC/BZ/62/M379)	Corrales et al., 2021
	L. major-L. infantum hybrid (MHOM/PT/94/IMT208)	Volf et al., 2007
	L. major-L. infantum hybrid (MHOM/PT/2004/IMT367)	Volf et al., 2007
Lutzomyia migonei	*L. amazonensis* (IFLA/BR/1967/PH8)	Nogueira et al., 2017
	L. amazonensis (MHOM/BR/1975/Josefa)	Nogueira et al., 2017
	L. infantum (MHOM/BR/76/M4192)	Guimaraes et al., 2016
	L. infantum (ITOB/TR/2005/CUK3)	Guimaraes et al., 2016
	L. infantum (OGVL marked with mCherry)	Alexandre et al., 2020

Table S3. Studies using *in situ* grading systems which differ from Myšková et al. (2008) for *Leishmania (Leishmania)* intensity quantitation in sand flies.

Grading	Sand fly species	*Leishmania* species	Reference
0 1-10 10-100 >100-1000 >1000	*Phlebotomus papatasi*	L. donovani (MHOM/SD/??/Khartoum)	Schlein and Jacobson, 1998
Weak < 100 parasites/gut Moderate 100-500 parasites/gut Heavy 500-1000 parasites/gut Very heavy > 1000	*Phlebotomus (adlerius) halepensis*	L. major LV561 (MHOM/IL/67/LRC-L137 Jericho II)	Sadlova et al., 2003
	Phlebotomus (adlerius) halepensis	L. tropica (MHOM/TR/99/Vedha)	
	Lutzomyia longipalpis	L. major LV561 (MHOM/IL/67/LRC-L137 Jericho II)	
	Phlebotomus duboscqi	L. major LV561 (MHOM/IL/67/LRC-L137 Jericho II)	
	Phlebotomus (paraphlebotomus) sergenti	L. tropica (MHOM/TR/99/Vedha)	
Weak < 100 parasites/gut Moderate 100-1000 parasites/gut Heavy > 1000 parasites/gut Very heavy > 10,000 parasites/gut	*Phlebotomus perniciosus*	L. infantum MON-1 (MHOM/TN/2003/23S)	Remadi et al., 2018
		L. infantum MON-24 (MHOM/TN/2005/SFC51)	
		L. infantum MON-80 (MHOM/TN/2006/PLC8)	
Weak < 100 parasites/gut Moderate 100-1000 parasites/gut Heavy > 1000 parasites/gut Very heavy >> 1000 parasites/gut	*Phlebotomus papatasi*	L. major Friedlin V1 (MHOM.IL/81/Friedlin/V1; FV1)	Doehl et al., 2017
	Phlebotomus duboscqi	L. major Friedlin V1 (MHOM.IL/81/Friedlin/V1; FV1)	
Weak < 100 parasites/gut Moderate 100-500 parasites/gut Heavy > 500 parasites/gut	*Phlebotomus argentipes*	L. donovani (MHOM/ET/2010/GR374) GFP	Sadlova et al., 2017
Weak < 500 parasites/gut	*Phlebotomus tobbi*	L. major LV561 (MHOM/IL/67/LRC-L137 Jericho-II)	Seblova et al., 2015b

Moderate 500-1000 parasites/gut Heavy > 1000 parasites/gut		*L. infantum/donovani* CUK3 (CUK3: ITOB/TR/2005/CUK3)	
	Lutzomyia longipalpis	*L. infantum/donovani* CUK3 (CUK3: ITOB/TR/2005/CUK3)	
		L. donovani (CYPR: MHOM/CY/2011/592/11)	
		L. infantum (OG-VL: MHOM/TR/2000/OG-VL)	
		L. infantum (IMT373: MCAN/PT/2005/IMT373)	
		L. donovani (GEBRE: MHOM/ET/72/GEBRE1)	
	Phlebotomus perniciosus	*L. infantum/donovani* CUK3 (CUK3: ITOB/TR/2005/CUK3)	
		L. donovani (CYPR: MHOM/CY/2011/592/11)	
		L. infantum (OG-VL: MHOM/TR/2000/OG-VL)	
		L. infantum (IMT373: MCAN/PT/2005/IMT373)	
		L. donovani (GEBRE: MHOM/ET/72/GEBRE1)	
Weak 1-1000 parasites/gut Moderate 1001-10000 parasites/gut Heavy > 10000 parasites/gut	*Phlebotomus papatasi*	*L. major* V1 strain	Coutinho-Abreu et al., 2010
Weak < 100 parasites/gut Moderate 100-500 parasites/gut Heavy > 500 parasites/gut	*Phlebotomus duboscqi*	*L. major* LV561 AV (MHOM/IL/67/LRC-L 137 Jericho-II)	Volf et al., 1998; Volf et al., 2001
		L. major Neal-P (MRHO/SU/59/P)	Volf et al., 1998
Light Moderate Heavy	*Phlebotomus papatasi*	*L. donovani* (MHOM/ET/2010/GR374)	Sloan et al., 2021
		L. major (LRC-L137; MHOM/IL/1967/Jericho-II)	

| Light <50 promastigotes/gut Moderate 50-500 promastigotes/gut Heavy > 500 promastigotes/gut | *Phlebotomus sergenti* | *L. tropica* (IARA/IL/2001/L810) | Svobodova et al., 2006 |
| | *Phlebotomus arabicus* | *L. tropica* (MHOM/IL/2001/L-836) | |

Table S4. Studies using qPCR for *Leishmania (Leishmania)* intensity quantitation in sand flies.

Sand fly species	*Leishmania* strain	*Leishmania* concentration and stage used for infection	Details of sample	Days post infection studied	Methods	Reference
Phlebotomous duboscqi	*L. major* (MHOM/IL/67/LRC-L137 Jericho II)	5×10^4 or 5×10^5 promastigotes per mL	30 per group Used individual females midguts	Day 2 and 8	DNA tissue isolation kit (Roche); SYBR green (iQ SYBR Green Supermix, Bio-Rad); Kinetoplastid DNA target (Mary et al., 2004)	Myšková et al., 2008
Phlebotomous arabicus	*L. infantum* (MHOM/TR/2000/OG-VL)	10^6 promastigotes per mL				
Phlebotomus perniciosus	*L. tropica* (MHOM/IT/2016/ISS3183)	10^7 or 2×10^5 promastigote per mL or *in vivo* amastigotes	Looked at parasite load per sand fly gut	Days 2-10, 12, 14, 16	Mary et al., 2004; Seblova et al., 2015	Bongiorno et al., 2019
Phlebotomus orientalis	*L. donovani* GR 374 (MHOM/ET/2010/DM-1033)	2×10^3, 2×10^4, 10^5 or 5×10^5 promastigotes per mL	For colony comparison: 50 engored females For infective dose comparison: 20 females per group Used individual female midguts	Day 10	High pure PCR template preparation kit (Roche); SYBR green (iQ SYBR Green Supermix, Bio-Rad); Kinetoplastid DNA target (Mary et al., 2004)	Seblova et al., 2013
Lutzomyia longipalpis	*L. mexicana* (MNYC/BZ/62/M379)	10^6 promastigotes per mL	Used individual females guts	Day 1 and 7	High Pure PCR Template Preparation Kit (Roche); Myšková et al., 2008	Ishemgulova et al., 2017
Phlebotomus papatasi *Phlebotomus duboscqi*	*L. major* (MHOM/IL/81/Friedlin/V1 ;FVI)	10^6 parasites per mL	30 sand flies per group Used individual midguts	Day 12	Sadlova et al., 2010	Doehl et al., 2017
Lutzomyia longipalpis	*L. infantum/donovani* hybrid (CUK3: ITOB/TR/2005/CUK3)	10^6 promastigotes per mL	30-60 sand flies per line Used individual midguts	Day 8	SYBR green (BioRad); Mary et al., 2004	Seblova et al., 2015

	L. donovani (CYPR: MHOM/CY/2011/592/11)					
	L. infantum ((OG-VL: MHOM/ET/72/GEBRE1)					
	L. infantum (IMT373:MCAN/PT/2005/IMT373)					
	L. donovani (GEBRE: MHOM/ET/72/GENRE1)					
Phlebotomus perniciosus	*L. infantum/donovani* hybrid (CUK3: ITOB/TR/2005/CUK3)					
	L. donovani (CYPR: MHOM/CY/2011/592/11)					
	L. infantum ((OG-VL: MHOM/ET/72/GEBRE1)					
	L. infantum (IMT373:MCAN/PT/2005/IMT373)					
	L. donovani (GEBRE: MHOM/ET/72/GENRE1)					
Phlebotomus argentipes	*L. donovani* (GR374: MHOM/ET/2010/DM-1033)	2×10^3, 2×10^4 or 5×10^5 promastigotes per mL	20 females per group Used Individual females	Day 8	High pure PCR template preparation kit (Roche); SYBR green (iQ SYBER Green Supermix, Bio-Rad); Mary et al., 2004	Pruzinova et al., 2015
Phlebotomus orientalis		2×10^3 promastigotes/mL				
Lutzomyia longipalpis	*L. infantum* (MCAN/PT/2005/IMT373)	10^6 promastigotes per mL	Used individual females	Day 2 and 8	High pure PCR template preparation kit (Roche); SYBER green (iQ SYBER Green Supermix, Bio-Rad); Mary et al., 2004	Hlavacova et al., 2013
Phlebotomus perniciosus						

Phlebotomus duboscqi	*L. major* (LRC-L137: MHOM/IL/1967/Jericho-II)	10^6 promastigotes per mL	50 females per group Used individual females	Day 6	High pure PCR template preparation kit (Roche); SYBER green (iQ SYBER Green Supermix, Bio-Rad); Mary et al., 2004	Pruzinova et al., 2013
Phlebotomus perniciosus	*L. infantum* (MHOM/MA/67/ITMAP-263)	10^6 promastigotes per mL	20 per line Used individual female midguts	Day 12	High Pure PCR Template Preparation Kit (Roche); Myšková et al., 2008; Mary et al., 2004	Gazanion et al., 2012
Phlebotomus papatasi	*L. major* (MHOM/IL/81/Friedlin/V1;FVI)	10^6 promastigotes per mL	30-40 midguts per line Used individual female midguts	Days 10-12	SYBR green (iQ SYBR Green Supermix, Bio-Rad); DNA tissue isolation kit (Roche); Mary et al., 2004; Myšková et al., 2008	Sadlova et al., 2010
Lutzomyia longipalpis	*L. mexicana* (MNYC/BZ/62/M379)	10^6 promastigotes per mL	50 ng sand fly DNA from 12 pools of 5 insects	Day 6	Nicolas et al., 2002	Sant'Anna et al., 2014

Table S5. Studies using *Leishmania (Leishmania)* in *ex vivo* midgut binding assays.

Sand fly species	Previous feeding of sand flies	*Leishmania* strain	Dissection and incubation media	*Leishmania* concentration and stage used for incubation	Incubation length	Wash step	Counting and reporting method	Reference
Phlebotomus papatasi	Unfed	*L. major* (WR 2885 RFP expressing)	PBS used for dissection, Parasites in PBS	2×10^6 parasites in 40 µL PBS. Early and late stage parasites used, sorted using Ficoll gradient	45 minutes, room temperature	Passed through PBS twice	Homogenised in 30 µL PBS, counted using neubauer improved chambers. Reported as number of parasites per midgut	Coutinho-Abreu et al., 2020
Lutzomyia longipalpis	Unfed and 5 days post blood feeding used	*L. infantum* (MCAN/BR/09/52)						
		L. infantum RFP-strain (MHOM/ES/92/LLM-320)						
		L. infantum (MCAN/BR/89/BH46)						
		L. infantum (MCAN/BR/89/BA262)						
		Mutants and addbacks of some strains also used						
Lutzoymia longipalpis Field-collected *Lutzomyia intermedia*	30% sucrose	*L. infantum* (MHOM/BR/2002/LPC-RPV)	PBS for dissection Incubation media not stated	2×10^7 cells/mL procyclic promastigotes, volume of 50 µL	20 minutes	Drops of PBS	Neubauer-counting chamber. Reported as average attached parasites/mL	Soares et al., 2017
Lutzomyia longipalpis *Phlebotomus papatasi*	Non-blood fed	*L. infantum* (MHOM/ES/00/UCM-1) *L. major* (MHOM/SU/1973-ASKH)	PBS for dissection and incubation	5×10^6 promastigotes	1 hour, room temperature	Washed three times with cold PBS	Homogenised in 30 µL PBS, counted using hemocytometer. Reported as	Di-Blasi et al., 2015

							parasites bound per midgut	
Lutzomyia longipalpis	Non-blood fed	*L. amazonensis* (WHOM/BR/75/Josefa) *L. chagasi* (MHOM/BR/00/1669) *L. donovani* (MHOM/IN/83/Mongi-142) *L. donovani* (MHOM/SD/00/1S) *L. major* (MHOM/IL/80/Friedlin, clone V1)	As Pimenta et al., 1992	As Pimenta et al., 1992. Procyclics (1-2 days of culture)	As Pimenta et al., 1992		Reported as mean number of promastigotes bound per gut + standard error of the mean	Pinto-da-Silva et al., 2005
Phlebotomus papatasi	50% sucrose	*L. major* clone V1 (NIH/V1) (MHOM/IL/80/FN)	Midguts dissected in PBS, fixed in 2% paraformaldehyde (20 minutes, 4°C), washed twice in PBS	2×10^6 parasites (procyclic promastigotes harvested from 1-2 day logarithmic phase cultures)	1 hour, room temperature	Four times in PBS	Homogenised in 30 µL 1% BSA/PBS, parasite counted using hemocytometer, reported as parasites bound per midgut	Kamhawi et al., 2004
Field-collected *Lutzomyia longipalpis*	30% sucrose	*L. chagasi* (MHOM/BR/74/PP75)	PBS for dissection Incubation media not stated	2×10^7 cells/mL (PNA+ or PNA- culture), volume of 30 µL	30 minutes	In PBS	Number of attached parasites counted, reported as promastigotes bound per midgut	Soares et al., 2002
				2×10^7 procyclic promastigotes/ mL	20 minutes	Successive drops of PBS	Guts homogenised, released promastigotes	

126

							counted, reported as parasites bound per midgut	
Phlebotomus papatasi	30% sucrose	*L. major* (MHOM/IL80/Friedlin, clone V1)	PBS for dissection Incubation media not stated	2.5×10^7 promastigotes, in 40 μL	45 minutes	Successive drops of PBS	Homogenised in 30 μL PBS, released promastigotes counted using hemocytometer. Reported as average promastigotes/midgut	Butcher et al., 1996
Phlebotomus argentipes	30% sucrose	*L. donovani* (MHOM/SD/00/1S-2D)	PBS for dissection Incubation media not stated	4×10^7 promastigotes/ mL, in 50 μL (used procyclic and metacyclic)	45 minutes, room temperature	Successive drops of PBS	Homogenised in 30 μL PBS, released promastigotes counted using hemocytometer. Reported as mean number of promastigotes bound per midgut	Sacks et al., 1995
Phlebotomus papatasi	30% sucrose	*L. major* clone V1 (MHOM/IL/80/Friedlin) *L. major* LRC-137, clone V121 (MHOM/IL/67/Jericho-II) *L. major* Neal (MRHO/SU/59/P) *L. major* L119 (MTAT/KE/00/T4)	PBS for dissection Incubation media not stated	2.5×10^7 promastigotes, in 40 μL	45 minutes, room temperature	Successive drops of PBS	Homogenised in 30 μL PBS, released promastigotes counted using hemocytometer. Reported as mean promastigotes bound per midgut	Pimenta et al., 1994

		L. donovani (MHOM/SD/00/1S-2D)						
		L. donovani (MHOM/IN/83/Mongi-142)						
		L. tropica (MHOM/AF/83/Azad)						
		L. amazonensis (MHOM/BR/00/Josefa)						
		L. major Friedlin mutant KIRK						
Phlebotomus argentipes		*L. major* clone V1 (MHOM/IL/80/Friedlin)						
		L. donovani (MHOM/SD/00/1S-2D)						
		L. donovani (MHOM/IN/83/Mongi-142)						
		L. tropica (MHOM/AF/83/Azad)						
		L. amazonensis (MHOM/BR/00/Josefa)						
		L. donovani 1S mutant R2D2						
Phlebotomus papatasi	30% fructose	*L. major* (MHOM/IL80/Friedlin, clone V1)	PBS for dissection, parasites in HBSS^{2+} + 1% BSA	10^6 in 40 µL ^{125}I-labelled procyclic or PNA-promastigotes	45 minutes, room temperature	Four or five washes in successive drops of PBS	Counted using LKB gamma counter. Mean promastigotes bound per midgut	Pimenta et al., 1992

References for supplementary figures

Alexandre J, Sadlova J, Lestinova T, Vojtkova B, Jancarova M, Podesvova L, Yurchenko V, Dantas-Torres F, Brandão-Filho SP, Volf P. Experimental infections and co-infections with *Leishmania braziliensis* and *Leishmania infantum* in two sand fly species, *Lutzomyia migonei* and *Lutzomyia longipalpis*. Sci Rep. 2020;10(1):3566.

Becvar T, Vojtkova B, Siriyasatien P, Votypka J, Modry D, Jahn P, Bates P, Carpenter S, Volf P, Sadlova J. Experimental transmission of *Leishmania (Mundinia)* parasites by biting midges (Diptera: Ceratopogonidae). PLoS Pathog. 2021;17(6):e1009654.

Beneke T, Demay F, Hookway E, Ashman N, Jeffery H, Smith J, Valli J, Becvar T, Myšková J, Lestinova T, Shafiq S, Sadlova J, Volf P, Wheeler RJ, Gluenz E. Genetic dissection of a *Leishmania* flagellar proteome demonstrates requirement for directional motility in sand fly infections. PLoS Pathog. 2019;15(6):e1007828.

Bongiorno G, Di Muccio T, Bianchi R, Gramiccia M, Gradoni L. Laboratory transmission of an Asian strain of *Leishmania tropica* by the bite of the southern European sand fly *Phlebotomus perniciosus*. Int J Parasitol. 2019;49(6):417-421.

Boubidi SC, Benallal K, Boudrissa A, Bouiba L, Bouchareb B, Garni R, Bouratbine A, Ravel C, Dvorak V, Votypka J, Volf P, Harrat Z. *Phlebotomus sergenti* (Parrot, 1917) identified as *Leishmania killicki* host in Ghardaia, south Algeria. Microbes Infect. 2011;13(7):691-696.

Boulanger N, Lowenberger C, Volf P, Ursic R, Sigutova L, Sabatier L, Svobodova M, Beverley SM, Späth G, Brun R, Pesson B, Bulet P. Characterisation of a defensin from the sand fly *Phlebotomus duboscqi* induced by challenge with bacteria or the protozoan parasite *Leishmania major*. Infect Immun. 2004;72(12):7140-7146.

Butcher BA, Turco SJ, Hilty BA, Pimenta PF, Panunzio M, Sacks DL. Deficiency in β1,3-galactosyltransferase of a *Leishmania major* lipophosphoglycan mutant adversely influences the *Leishmania*-sand fly interaction. J Biol Chem. 1996;271(34):20573-20579.

Chajbullinova A, Votypka J, Sadlova J, Kvapilova K, Seblova V, Kreisinger J, Jirku M, Sanjoba C, Gantuya S, Matsumoto Y, Volf P. The development of *Leishmania turanica* in sand flies and competition with *L. major*. Parasit Vectors. 2012;5:219.

Corrales RM, Vaselek S, Neish R, Berry L, Brunet CD, Crobu L, Kuk N, Mateos-Langerak J, Robinson DR, Volf P, Mottram JC, Sterkers Y, Bastien P. The kinesin of the flagellum attachment zone in *Leishmania* is required for cell morphogenesis, cell division and virulence in the mammalian host. PLoS Pathog. 2021;17(6):e1009666.

Coutinho-Abreu IV, Sharma NK, Robles-Murguia M, Ramalho-Ortigao M. Targeting the midgut secreted PhChit1 reduces *Leishmania major* development in its natural vector, the sand fly *Phlebotomus papatasi*. PLoS Negl Trop Dis. 2010;4(11):e901.

Coutinho-Abreu IV, Oristian J, de Castro W, Wilson TR, Meneses C, Soares RP, Borges VM, Descoteaux A, Kamhawi S, Valenzuela JG. Binding of *Leishmania infantum* lipophosphoglycan to the midgut is not sufficient to define vector competence in *Lutzomyia longipalpis* sand flies. mSphere. 2020;5:e00594-20.

Di-Blasi T, Lobo AR, Nascimento LM, Córdova-Rojas JL, Pestana K, Marín-Villa M, Tempone AJ, Telleria EL, Ramalho-Ortigão M, McMahon-Pratt D, Traub-Csekö YM. The flagellar protein FLAG1/SMP1 is a candidate for *Leishmania*-sand fly interaction. Vector Borne Zoonotic Dis. 2015;15(3): 202-209.

Diniz JA, Chaves MM, Vaselek S, Magalhães RDM, Ricci-Azevedo R, Carvalho RVH. Lorenzon LB, Ferreira TR, Zamboni D, Walrad PB, Volf P, Sacks DL, Cruz AK. Protein methyltransferase 7 deficiency in *Leishmania major* increases neutrophil associated pathology in murine model. PLoS Negl Trop Dis. 2021;15(3):e0009230.

Doehl JSP, Sádlová J, Aslan H, Pružinová K, Metangmo S, Votýpka J, Kamhawi S, Volf P, Smith DF. *Leishmania* HASP and SHERP genes are required for *in vivo* differentiation, parasite transmission and virulence attenuation in the host. PLoS Pathog. 2017;13(1):e1006130.

Gazanion E, Seblova V, Votypka J, Vergnes B, Garcia D, Volf P, Sereno D. *Leishmania infantum* nicotinamidase is required for late-stage development in its natural sand fly vector, *Phlebotomus perniciosus*. Int J Parasitol. 2012;42(4):323-327.

Guimarães VCFV, Pruzinova K, Sadlova J, Volfova V, Myšková J, Filho SPB, Volf P. *Lutzomyia migonei* is a permissive vector competent for *Leishmania infantum*. Parasit Vectors. 2016;9:159.

Guimarães AC, Nogueira PM, Silva SdO, Sadlova J, Pruzinova K, Hlavacova J, Melo MN, Soares RP. Lower galactosylation levels of the lipophosphoglycan from *Leishmania (Leishmania) major*-like strains affect interaction with *Phlebotomus papatasi* and *Lutzomyia longipalpis.* Mem Inst Oswaldo Cruz. 2018;113(5):e170333.

Halliday C, Yanase R, Catta-Preta CMC, Moreira-Leite F, Myšková J, Pruzinova K, Volf P, Mottram JC, Sunter JD. Role for the flagellum attachment zone in *Leishmania* anterior cell tip morphogenesis. PLoS Pathog. 2020;16(10):e1008494.

Hlavacova J, Votypka J, Volf P. The effect of temperature on *Leishmania* (Kinetoplastida: Trypanosomatidae) development in sand flies. J Med Entomol. 2013;50(5):955-958.

Ishemgulova A, Kraeva N, Hlaváčová J, Zimmer SL, Butenko A, Podešvová L, Leštinová T, Lukeš J, Kostygov A, Votýpka J, Volf P, Yurchenko V. A putative ATP/GTP binding protein affects *Leishmania mexicana* growth in insect vectors and vertebrate hosts. PLoS Negl Trop Dis. 2017;11(7):e0005782.

Jancarova M, Hlavacova J, Volf P. The development of *Leishmania tropica* in sand flies (Diptera: Psychodidae): a comparison of colonies differing in geographical origin and a gregarine coinfection. J Med Entomol. 2015; 52(6):1378-1380.

Jancarova M, Hlavacova J, Votypka J, Volf P. An increase of larval rearing temperature does not affect the susceptibility of *Phlebotomus sergenti* to *Leishmania tropica* but effectively eliminates the gregarine *Psychodiella sergenti*. Parasit Vectors. 2016;9:553.

Jecná L, Svárovská A, Besteiro S, Mottram J, Coombs GH, Volf P. Inhibitor of cysteine peptidase does not influence the development of *Leishmania mexicana* in *Lutzomyia longipalpis*. J Med Entomol. 2009;46(3):605-609.

Jecna L, Dostalova A, Wilson R, Seblova V, Chang KP, Bates PA, Volf P. The role of surface glycoconjugates in *Leishmania* midgut attachment examined by competitive binding assays and experimental development in sand flies. Parasitology. 2013;140:1026-1032.

Kamhawi S, Ramalho-Ortigao M, Pham VM, Kumar S, Lawyer PG, Turco SJ, Barillas-Mury C, Sacks DL, Valenzuela JG. A role for insect galectins in parasite survival. Cell. 2004;119:329-341.

Myšková J, Svobodova M, Beverley SM, Volf P. A lipophosphoglycan-independent development of *Leishmania* in permissive sand flies. Microbes Infect. 2007;9(3):317-324.

Myšková J, Votypka J, Volf P. *Leishmania* in sand flies: comparison of quantitative polymerase chain reaction with other techniques to determine the intensity of infection. J Med Entomol. 2008;45(1):133–8.

Myšková J, Dostálová A, Pěničková L, Halada P, Bates PA, Volf P. Characterization of a midgut mucin-like glycoconjugate of *Lutzomyia longipalpis* with a potential role in *Leishmania* attachment. Parasit Vectors. 2016;9:413.

Nogueira PM, Guimarães AC, Assis RR, Sadlova J, Myšková J, Pruzinova K, Hlavackova J, Turco SJ, Torrecilhas AC, Volf P, Soares RP. Lipophosphoglycan polymorphisms do not affect *Leishmania amazonensis* development in the permissive vectors *Lutzomyia migonei* and *Lutzomyia longipalpis.* Parasit Vectors. 2017;10:608.

Pimenta PFP, Turco SJ, McConville MJ, Lawyer PG, Perkins PV, Sacks DL. Stage-specific adhesions of *Leishmania* promastigotes to the sandfly midgut. Science. 1992;256:1812-1815.

Pimenta PFP, Saraiva EMB, Rowton E, Modi GB, Garraway LA, Beverley SM, Turco SJ, Sacks DL. Evidence that the vectorial competence of phlebotomine sand flies for different species of *Leishmania* is controlled by structural polymorphisms in the surface lipophosphoglycan. Proc. Natl. Acad. Sci. 1994; 91:9155-9159.

Pinto-da-Silva LH, Fampa P, Soares DC, Oliveira SMP, Souto-Padron T, Saraiva EM. The 3A1-La monoclonal antibody reveals key features of *Leishmania (L) amazonenesis* metacyclic promastigotes and inhibits procyclics attachment to the sand fly midgut. Int J Parasitol. 2005;35(7):757-764.

Pruzinova K, Votypka J, Volf P. The effect of avian blood on *Leishmania* development in *Phlebotomus duboscqi*. Parasit Vectors. 2013;6:254.

Pruzinova K, Sadlova J, Seblova V, Homola M, Votypka J, Volf P. Comparison of bloodmeal digestion and the peritrophic matrix in four sand fly species differing in susceptibility to *Leishmania donovani*. PLoS ONE. 2015:10(6):e0128203.

Pruzinova K, Sadlova J, Myšková J, Lestinova T, Janda J, Volf P. *Leishmania* mortality in sand fly blood meal is not species-specific and does not result from direct effect of proteinases. Parasit Vectors. 2018;11:37.

Remadi L, Jiménez M, Chargui N, Haouas N, Babba H, Molina R. The vector competence of *Phlebotomus perniciosus* for *Leishmania infantum* zymodemes of Tunisia. Parasitol Res. 2018;117(8):2499-2506.

Sacks DL, Pimenta PFP, McConville MJ, Schneider P, Turco SJ. Stage-specific binding of *Leishmania donovani* to the sand fly vector midgut is regulated by conformational changes in the abundant surface lipophosphoglycan. J Exp Med. 1995;181(2):685-697.

Sádlová J, Hajmová M, Volf P. *Phlebotomus (Adlerius) halepensis* vector competence for *Leishmania major* and *Le. Tropica*. Med Vet Entomol. 2003;17(3):244-250.

Sádlová J, Volf P. Peritrophic matrix of *Phlebotomus duboscqi* and its kinetics during *Leishmania major* development. Cell Tissue Res. 2009;337(2):313-325.

Sádlová J, Price HP, Smith BA, Votýpka J, Volf P, Smith DF. The stage-regulated HASPB and SHERP proteins are essential for differentiation of the protozoan parasite *Leishmania major* in its sand fly vector, *Phlebotomus papatasi*. Cell Microbiol. 2010;12(12):1765-1779.

Sadlova J, Dvorak V, Seblova V, Warburg A, Votypka J, Volf P. *Sergentomyia schwetzi* is not a competent vector for *Leishmania donovani* and other *Leishmania* species pathogenic to humans. Parasit Vectors. 2013;6:186.

Sadlova J, Myšková J, Lestinova T, Votypka J, Yeo M, Volf P. *Leishmania donovani* development in *Phlebotomus argentipes*: comparison of promastigote- and amastigote-initiated infections. Parasitology. 2017;144(4):403-410.

Sadlova J, Homola M, Myšková J, Jancarova M, Volf P. Refractoriness of *Sergentomyia schwetzi* to *Leishmania* spp. is mediated by the peritrophic matrix. PLoS Negl Trop Dis. 2018;12(4):e0006382.

Sadlova J, Bacikova D, Becvar T, Vojtkova B, England M, Shaw J, Volf P. *Porcisia* transmission by prediuresis of sand flies. Front Cell Infect Microbiol. 2022;12:981071.

Sant'Anna MRV, Diaz-Albiter H, Aguiar-Martins K, Al Salem WS, Cavalcante RR, Dillon VM, Bates PA, Genta FA, Dillon RJ. Colonisation resistance in the sand fly gut: *Leishmania* protects *Lutzomyia longipalpis* from bacterial infection. Parasit Vectors. 2014;7:329.

Schlein Y, Jacobson RL. Resistance of *Phlebotomus papatasi* to infection with *Leishmania donovani* is modulated by components of the infective bloodmeal. Parasitology. 1998;117(5):467-473.

Seblova V, Volfova V, Dvorak V, Pruzinova K, Votypka J, Kassahun A, Gebre-Michael T, Hailu A, Warburg A, Volf P. *Phlebotomus orientalis* sand flies from two geographically distant Ethiopian localities: biology, genetic analyses and susceptibility to *Leishmania donovani.* PLoS Negl Trop Dis. 2013;7(4):e2187.

Seblova V, Sadlova J, Vojtkova B, Votypka J, Carpenter S, Bates PA, Volf P. The biting midge *Culicoides sonorensis* (Diptera: Ceratopogonidae) is capable of developing late stage infections of *Leishmania enriettii*. PLoS Negl Trop Dis. 2015a;9(9):e0004060.

Seblova V, Myšková J, Hlavacova J, Votypka J, Antoniou M, Volf P. Natural hybrid of *Leishmania infantum/L. donovani*: development in *Phlebotomus tobbi*, *P. perniciosus* and *Lutzomyia longipalpis* and comparison with non-hybrid strains differing in tissue tropism. Parasit Vectors. 2015b;8:605.

Seblova V, Dujardin JC, Rijal S, Domagalska MA, Volf P. ISC1, a new *Leishmania donovani* population emerging in the Indian sub-continent: vector competence of *Phlebotomus argentipes*. Infect Genet Evol. 2019;76:104073.

Sloan MA, Sadlova J, Lestinova T, Sanders MJ, Cotton JA, Volf P, Ligoxygakis P. The *Phlebotomus papatasi* systemic transcriptional response to trypanosomatid-contaminated blood does not differ from the non-infected blood meal. Parasit Vectors. 2021;14:15.

Soares RPP, Macedo ME, Ropert C, Gontijo NF, Almeida IC, Gazzinelli RT, Pimenta PFP, Turco SJ. *Leishmania chagasi*: lipophosphoglycan characterisation and binding to the midgut of the sand fly vector *Lutzomyia longipalpis*. Mol Biochem Parasitol. 2002;121(2):213-224.

Soares RP, Altoé ECF, Ennes-Vidal V, da Costa SM, Rangel EF, de Souza NA, da Silva VC, Volf P, d'Avila-Levy CM. *In vitro* inhibition of *Leishmania* attachment to sandfly midguts and LL-5 cells by divalent metal chelators, anti-gp63 and phosphoglycans. Protist. 2017;168(3):326-334.

Sunter JD, Yanase R, Wang Z, Catta-Preta CMC, Moreira-Leite F, Myšková J, Pruzinova K, Volf P, Mottram JC, Gull K. *Leishmania* flagellum attachment zone is critical for flagellar pocket shape,

development in the sand fly, and pathogenicity in the host. Proc Natl Acad Sci USA. 2019;116(13):6351-6360.

Svobodova M, Votypka J, Peckova J, Dvorak V, Nasereddin A, Baneth G, Sztern J, Kravchenko V, Meir AOD, Schnur LF, Volf P, Warburg A. Distinct transmission cycles of *Leishmania tropica* in 2 adjacent foci, Northern Israel. Emerg Infect Dis. 2006;12(12):1860-1868.

Volf P, Kiewegová A, Svobodová M. Sandfly midgut lectin: effect of galactosamine on *Leishmania major* infections. Med Vet Entomol. 1998;12(2):151-154.

Volf P, Svobodová M, Dvoráková E. Bloodmeal digestion and *Leishmania major* infections in *Phlebotomus duboscqi*: effect of carbohydrates inhibiting midgut lectin activity. Med Vet Entomol. 2001;15(3):281-286.

Volf P, Benkova I, Myšková J, Sadlova J, Campino L, Ravel C. Increased transmission potential of *Leishmania major/Leishmania infantum* hybrids. Int J Parasitol. 2007;37(6):589-593.

Papers using different *Leishmania* subgenus:

Chanmol W, Jariyapan N, Somboon P, Bates MD, Bates PA. Development of *Leishmania orientalis* in the sand fly *Lutzomyia longipalpis* (Diptera: Psychodidae) and the biting midge *Culicoides sonorensis* (Diptera: Ceratopogonidae). Acta Trop. 2019;199:105157.

Ticha L, Kykalova B, Sadlova J, Grammiccia M, Gradoni L, Vof P. Development of various *Leishmania (Sauroleishmania) tarentolae* strains in three Phlebotomus species. Microorganisms. 2021;9(11):2256.

Ticha L, Sadlova J, Bates P, Volf P. Experimental infections of sand flies and geckos with *Leishmania (Sauroleishmania) adleri* and *Leishmania (S.) hoogstraali*. Parasit Vectors. 2022;15(1):289.

Zauli RC, Yokoyama-Yasunaka JK, Miguel DC, Moura AS, Pereira LL, da Silva Jr IA, Lemes LG, Dorta ML, de Oliveira MP, Pitaluga AN, Ishikawa EA, Rodrigues JC, Traub-Cseko YM, Bijovsky AT, Ribeiro-Dias F, Uliana SR. A dysflagellar mutant of *Leishmania (Viannia) braziliensis* isolated from a cutaneous leishmaniasis patient. Parasit Vectors. 2012;5:11.

Cited by qPCR studies:

Mary C, Faraut F, Lascombe L, Dumon H. Quantification of *Leishmania infantum* DNA by a real-time PCR assay with high sensitivity. J Clin Microbiol. 2004;42(11):5249-5255.

5. The role of human serum pentraxins in attachment of *Leishmania mexicana* promastigotes to the midgut of the permissive sand fly vector *Lutzomyia longipalpis*

RESEARCH PAPER COVER SHEET

Please note that a cover sheet must be completed <u>for each</u> research paper included within a thesis.

SECTION A – Student Details

Student ID Number	1601303	**Title**	Miss
First Name(s)	Eve Christina		
Surname/Family Name	Doran		
Thesis Title	The role of human pentraxins for the *Leishmania*-vector interaction		
Primary Supervisor	Dr Matthew Rogers		

If the Research Paper has previously been published please complete Section B, if not please move to Section C.

SECTION B – Paper already published

Where was the work published?			
When was the work published?			
If the work was published prior to registration for your research degree, give a brief rationale for its inclusion			
Have you retained the copyright for the work?*	Choose an item.	Was the work subject to academic peer review?	Choose an item.

*If yes, please attach evidence of retention. If no, or if the work is being included in its published format, please attach evidence of permission from the copyright holder (publisher or other author) to include this work.

SECTION C – Prepared for publication, but not yet published

Where is the work intended to be published?	Parasites & Vectors
Please list the paper's authors in the intended authorship order:	Doran, Eve C., Seow, Eu Shen., Stennet, Laura., Raynes, John G., Rogers, Matthew E.
Stage of publication	**Not yet submitted**

SECTION D – Multi-authored work

For multi-authored work, give full details of your role in the research included in the paper and in the preparation of the paper. (Attach a further sheet if necessary)	Most experiments were designed by myself and my supervisors John Raynes and Matthew Rogers. All experimental work was carried out, at least in part, by myself, except the SPR work which was carried out by Laura Stennet and John Raynes. ELISAs were designed and carried out with Eu Shen Seow. Sand fly infections, mouse work and parasite culture was carried out by Matthew Rogers. Pentraxin purification and LPG/GIPL fractionation was carried out with John Raynes. The manuscript first draft and data analysis was carried out by myself, with guidance, advice and comments provided by John Raynes and Matthew Rogers.

SECTION E

Student Signature	EVE DORAN
Date	20/06/2023

Supervisor Signature	MATTHEW ROGERS
Date	04/07/2023

The role of human serum pentraxins in attachment of *Leishmania mexicana* promastigotes to the midgut of the permissive sand fly vector *Lutzomyia longipalpis*

Doran, Eve C., Seow, Eu Shen., Stennet, Laura., Raynes, John G., Rogers, Matthew E.*

Dept. of Infection Biology, Faculty of Infectious and Tropical Diseases, London School of Hygiene and Tropical Medicine, Keppel St., London. WC1E 7HT.

*Corresponding author matthew.rogers@lshtm.ac.uk

Abstract

The human pentraxin, Serum amyloid P (SAP), enters the sand fly during a bloodmeal alongside *Leishmania* parasites. This project hypothesised SAP may be involved in attachment of parasites to permissive sand fly midguts, a lifecycle stage essential for preventing parasite loss during bloodmeal remnant defecation. Both SAP and another human pentraxin C-reactive protein (CRP) were found to bind every *Leishmania mexicana* morphological stage. However, unlike the closely related pentraxin CRP, SAP did not bind *Leishmania* lipophosphoglycan (LPG), with phosphoethanolamine (PEth) found on glycoinositolphospholipids (GIPLs) suggested as the SAP ligand. SAP but not CRP bound *Lutzomyia longipalpis* midgut microvillar extract shown by Western blot and Surface Plasmon Resonance (SPR), with a preliminary immunoprecipitation experiment suggesting an interacting protein may be α-glucosidase. However, *ex vivo* midgut binding assays showed no increase in *L. mexicana* binding in the presence of SAP compared to an EDTA control. *Lu. longipalpis* infections with *L. mexicana* and SAP-chelating drug, CPHPC, or anti-SAP antibodies failed to reduce promastigote numbers over a range of days post infection.

Introduction

Leishmaniasis is a spectrum of disease caused by the protozoan parasite *Leishmania*. Annually there are estimated to be 600,000 to one million new cases of the cutaneous form and 50,000 to 90,000 new cases of the visceral form (WHO, 2023).

A crucial part of the *Leishmania* lifecycle is within the phlebotomine sand fly vector. Here, nectomonad-stage *Leishmania* must attach to the sand fly midgut in order to prevent defecation along with the bloodmeal remnants. For the restrictive vector *Phlebotomus papatasi*, that only supports the development of *Leishmania major* (Volf and Myšková, 2007), the *Leishmania* surface molecule lipophosphoglycan (LPG) is implicated in binding. LPG consists of a glycosylphosphatidylinositol (GPI) anchor, glycan core, repeating [-6Galβ1,4Manα1-PO$_4$-]$_x$ and terminates in an oligosaccharide cap (Turco, 1990; McConville et al., 1990; Forestier et al., 2015). The Gal(β1-4) side chains off the repeating region of *L. major* LPG were identified as the ligand for midgut attachment (Pimenta et al., 1992; 1994), binding to *P. papatasi* galectin, PpGalec (Kamhawi et al., 2004). The *L. major* flagella protein FLAG1/SMP1 is also thought to strengthen the attachment of the parasite to the *P. papatasi* midgut (Di-Blasi et al., 2015).

The attachment interaction of *Leishmania* with permissive vectors such as *Lutzomyia longipalpis* which can support the development of many *Leishmania* species is still unknown, but studies have reported that parasites lacking LPG can survive defecation (Rogers et al., 2004; Myšková et al., 2007; Svárovská et al., 2010; Secundino et al., 2010; Jecna et al., 2013). Though these studies have been performed with unnatural *Leishmania*-sand fly pairs, many *Leishmania* species transmitted by permissive vectors have strains which lack or have varying LPG side chains (Dostálová and Volf, 2012) making an LPG-independent attachment mechanism likely. Poor development of LPG-deficient parasites has been reported for some natural combinations (Sacks et al., 2000; Jecna et al., 2013). However, this may be due to LPG providing protection to the hydrolytic environment created during bloodmeal digestion rather than an inability to attach to the midgut, though this may be species-specific (Coutinho-Abreu et al., 2020). Myšková et al. (2007) found all permissive but not restrictive sand fly midguts tested possessed glycoproteins with N-acetyl-galactosamine (GalNAc). The same group (Myšková et al., 2016) characterised an O-linked glycoprotein named LuloG from *Lu. longipalpis* found on the midgut epithelium, but were unable to completely block binding of *Leishmania infantum* to the midgut using anti-LuloG antibodies. The method of midgut attachment remains a complicated story with many interactions likely occurring in parallel.

Components of the host bloodmeal have a role in *Leishmania*-vector interaction. Sand flies can take multiple bloodmeals during the lifecycle of *Leishmania* within the vector and this affects parasite development (Elnaiem et al., 1994; Moraes et al., 2018; Serafim et al., 2018; Hall et al., 2021). These subsequent bloodmeals are suggested to be a trigger for reverse metacyclogenesis of metacyclic stages into retroleptomonads, extending the infectiousness of the vector (Serafim et al., 2018). More recently, dog IgM was hypothesised to lead to the formation of a *Leishmania* mating clump, allowing hybridisation and genetic exchange (Serafim et al., 2023). Bloodmeal components are likely to have important roles in the *Leishmania* lifecycle within the sand fly.

Leishmania are known to interact with the blood component C-reactive protein (CRP) (Pritchard et al., 1985; Raynes et al., 1993; Culley et al., 1996, 1997, 2000; Bee et al., 2001; Bodman-Smith et al., 2002). CRP is a pentraxin, that is part of an evolutionarily conserved family of plasma proteins involved in acute immunological responses. Almost all pentraxins have a pentameric structure and are calcium-dependent binders (Pepys, 2018). CRP was shown to bind *Leishmania donovani* promastigotes with metacyclics promastigotes having the highest avidity (Culley et al., 1996), act as an opsonin for parasite entry into macrophages (Culley et al., 1996, 1997; Bodman-Smith et al., 2002) and to bind *Leishmania* through the phosphorylated disaccharide repeats of LPG (Culley et al., 2000). CRP also triggers transformation of *L. donovani* (Mbuchi et al., 2006) and *Leishmania mexicana* metacyclics to amastigotes *in vitro* (Bee et al., 2001; Mbuchi et al., 2006). More recently, filamentous proteophosphoglycan (fPPG) and secreted acid phosphatase (ScAP) were identified as CRP ligands with Promastigote Secretory Gel (PSG)-CRP capable of binding C1q (Seow et al., 2023). Another pentraxin Serum Amyloid P (SAP), known to bind phosphoethanolamine (PEth) (Mikolajek et al., 2011), was found not to bind *Leishmania donovani* amastigotes or metacyclics (Raynes et al., 1993), however as not all promastigote forms were studied, there may be gaps in our understanding of this interaction. SAP did not have an effect on *L. mexicana* metacyclic to amastigote transformation (Bee et al., 2001).

In this work, we revisit the interaction of *Leishmania* promastigotes with SAP, to see if it has a role in the *L. mexicana* lifecycle within the permissive sand fly vector *Lu. longipalpis*. Specifically, we look to see if SAP could act as a cross-linker between the sand fly midgut and *L. mexicana* to facilitate attachment and resist defecation. We demonstrate by Western blot, ELISA and immunofluorescence that SAP binds to all lifecycle stages of *Leishmania* but not through LPG, with phosphoethanolamine (PEth)- containing surface molecules, such as glycoinositolphospholipids (GIPLs) potential ligand candidates. We use Surface Plasmon

Resonance (SPR), a novel method for studying parasite-midgut interactions. Initial immunoprecipitation experiments suggest SAP binds to midgut α-glucosidase and can survive protease degradation during bloodmeal digestion. Despite being able to bind to gut protein and *Leishmania*, SAP appears not to aid their interaction. Neither fly infection experiments or midgut parasite binding assays showed a role for SAP, with drugs and antibodies that target and block SAP function failing to alter the outcome.

Methods

Parasites and mice

All animal and sand fly infections in the UK were carried out in accordance with the UK Animal Scientific Procedure Act (ASPA) 1986, which transposes European Directive 2010/63/EU into UK national law. Animal studies are approved by the UK home office in granting Project licence 70/8427 under the Animal Scientific Procedure Act and all protocols had undergone appropriate local ethical review procedures by the Animal Welfare and Ethical Review Board (AWERB) of LSHTM.

Leishmania mexicana (MNYC/BZ/62/M379) amastigotes were obtained from cutaneous lesions on the backs of BALB/c mice 35-49 days post infection with 1×10^6 metacyclic promastigotes. Lesion amastigotes were used to infect sand flies for time course experiments and generate mid-logarithmic growth phase promastigotes that were cryo-preserved in 10% (v/v) dimethylsulphoxide (DMSO) in heat-inactivated (h.i.) foetal calf serum (FCS) and stored in liquid nitrogen until use. When needed, these first passage promastigotes were thawed and grown as promastigotes in M199 medium with Earle's salts, 20% (v/v) h.i. FCS (Gibco), 1 X Basal Medium Eagles' vitamins (Sigma), 1% (v/v) penicillin-streptomycin (Sigma), 30 mM sodium bicarbonate (Sigma), 2% (v/v) fresh filter-sterilised human urine, pH 7.2 at 26°C. Nectomonad promastigotes were harvested from 3 day promastigote cultures. Metacyclic promastigotes were obtained from 1×10^6/mL nectomonad promastigotes subpassaged into Grace's Insect medium supplemented with 20% (v/v) h.i. FCS (Gibco), 1 X Basal Medium Eagles' vitamins (Sigma), 1% (v/v) penicillin-streptomycin (Sigma), 30 mM sodium bicarbonate (Sigma), 2% (v/v) fresh filter-sterilised human urine, pH 5.5 and grown at 26°C for 5-7 days until 80%+ cells had differentiated into metacyclics, as determined by morphology of Giemsa-stained cells (Rogers et al., 2002). When required, thawed cells were grown overnight as promastigotes in this medium before transforming into axenic amastigotes by passaging them at 1×10^6/mL into an acidified version of the growth medium (pH 5.5) and incubated for four days at 34°C in an atmosphere of 5% CO_2. Axenic amastigotes were used in sand fly infections (Ismaeel et al., 1998).

SAP and CRP purification

Plasma was sourced from Dr Bramham (The Binding site) and converted to serum using 40 mL protamine sulphate per 1 L of plasma, leaving at 37°C for 1 hour and centrifuging for 1 hour at 2000 g, 10°C. Serum was first passed over phosphorylcholine Sepharose 4B beads (10 mL generated from CH Sepharose 4B and ρ-amino phenyl phosphorylcholine crosslinking) equilibrated in 10 mM Tris pH 8.0 with 0.15 M NaCl and 1 mM CaCl$_2$ and washed with the

same buffer before CRP fractions were eluted with 10 mM Tris pH 8.0 + 10 mM EDTA. The flow through containing SAP was passed over phosphoethanolamine Sepharose 4B beads (20 mL EAH Sepharose coupled to phosphorylethanolamine) and SAP fractions eluted with the same buffer systems. Protein concentrations of fractions were measured spectrophotometrically with optical densities over 0.2 being combined, diluted to 0.1 M NaCl and run on a DE-52 anion-exchange column (4057050, Whatman) and fractions eluted using a salt gradient (7.5 mM Tris + 0.1 M NaCl to 10 mM Tris + 1 M NaCl). The last stage of purification was similar to that described by Loveless et al. (1992). A zinc chelating Sepharose column (10 mL; 17-0575-01, Cytiva) was equilibrated in 20 mM Tris pH 8, 0.15 M NaCl, with fractions loaded in the same buffer and eluted with a gradient of 20 mM Tris pH 8, 0. 15 M NaCl containing 0 - 30 mM histidine. Purity of SAP and CRP fractions was confirmed by SDS-PAGE under reducing conditions and Coomassie staining. SAP was dialysed into 10 mM Tris pH 8.0 containing 0.15 M NaCl. CRP was dialysed into PBS pH 7.4 and stored at 4°C.

LPG and GIPL enrichment

LPG and GIPL fractionation was carried out according to McConville et al. (1990). Parasite pellets were first sonicated at 50-60 Hertz for 5 – 15 minutes in an ultrasonic bath (XB2, Grant) in 1:1 chloroform: methanol (v/v) and centrifuged at 2250 g for 10 minutes. The supernatant was collected and the step repeated. The pellet was then sonicated in 1:2:0.8 chloroform: methanol: water and centrifuged at 2950 g for 10 minutes. The supernatant at this stage contains glycoinositolphospholipids (GIPLs). The pellet was dried using a nitrogen flow speed vacuum, and the pellet resuspended in 9% butanol. The sample was sonicated and centrifuged at 16000 g for 40 minutes. The supernatant containing LPG was dried using the speed vacuum. LPG samples were resuspended in distilled water, and GIPL samples resuspended in 100-500 µL 0.1 M ammonium acetate pH 6.5 containing 5% (v/v) propan-1-ol.

Western and dot blots

Western blotting used 10% resolving gels with these being transferred to PVDF (Millipore) using semi-dry blotting. Membranes were blocked overnight at 4°C in 1 x PBS + 2% (v/v) Bovine Serum Albumin (BSA) + 0.05% (v/v) Tween-20. Membranes were washed with 1 x TBS + 0.05% (v/v) Tween-20 with either 0.5 mM $CaCl_2$ or 10 mM EDTA. Membranes were washed three times for 5 minutes between each incubation step. Incubations took place in 1 x TBS + 0.05% (v/v) Tween-20 + 1% (v/v) BSA with either 0.5 mM Ca^{2+} or 10 mM EDTA. Stained membranes were incubated with BCIP (BCIP A1117, Applichem)/NBT (17341, Cambridge BioScience) until bands appeared and immersed in wash buffer to halt the reaction. For Western blots, 3 µg of LPG-enriched material per lane were run under reducing conditions. For dot blots, 3 µL of

diluted LPG- or GIPL-enriched material was pipetted onto a nitrocellulose membrane (Amersham), left to airdry and blocked as described. For probing with CRP, 1 μg/mL CRP with or without 10 mM EDTA or no CRP was used, followed by 1:10,000 anti-CRP (235752, Calbiochem) and 1:5000 anti-rabbit-alkaline phosphatase (AP) (AI-48-150-AP, Seralab). For probing with SAP, 1 μg/mL SAP with or without 10 mM EDTA or no SAP was used, followed by 1:12 supernatant or 1:500 purified 5.4D (specific to SAP) (O'Sullivan et al., 1991) and 1:3000 anti-mouse-AP (AP124A, Millipore). For CA7AE, 1:1000 CA7AE (GTX39838, GeneTex) or no antibody was then followed by 1:30,000 anti-mouse IgM-AP (A-9688, Sigma). For LT6, 1:8 LT6 (provided by Dr T Ilg), specific to phosphorylated repeat domain of LPG [-6Galβ1,4Manα1-PO$_4$-]$_x$) or no antibody was then followed by 1:3000 anti-mouse-AP.

ELISA

PCh-BSA was generated using carbodiimide (EDC) coupling of BSA and ρ-amino phenyl phosphorylcholine (Ahmed et al., 2016). PEth-cellulose was produced by IPTG induction on YESCA plates from K-12 non-pathogenic with plasmid PMMB956 strain; AR-3110 csg form of *Escherichia coli* expression from vector provided by Dr L Cegelski and purified as described (Thongsomboon et al., 2018). Either 1 μg/mL LPG for LT6 competition or 2 μg/mL LPG/PC-BSA or 1:20 PEth-cellulose for SAP and CRP competition was immobilised onto a PVC plate (2595, Costar) overnight at 4°C. The plate was washed in 1 x HBS + 0.05% (v/v) Tween-20 + 0.5 mM Ca^{2+}, followed by blocking with 1 x PBS + 2% (v/v) BSA + 0.05% (v/v) Tween-20 and incubated for 2 hours at room temperature. All incubations from here were 1 hour. For LT6 competition, plates were probed with various concentrations (0.0027 – 2 μg/mL) of SAP or CRP with or without 1:10 LT6. For SAP and CRP competition, 0.5 μg/mL CRP or SAP + 0 - 20 μg/mL of the competing pentraxin was used. Material was diluted in 1 x HBS + 1% (v/v) BSA + 0.5 mM Ca^{2+}. For LT6 competition, wells incubated with SAP were then incubated with 1:1000 rabbit anti-SAP (Calbiochem), followed by 1:3000 anti-rabbit-horseradish peroxidase (HRP) (170-6515, Bio-Rad). For SAP and CRP competition, 1:1000 5.4D followed by 1:3000 anti-mouse HRP (170-6516, Bio-Rad) was used. CRP wells were incubated with anti-CRP, followed by anti-rabbit-HRP. Tetramethylbenzidine (TMB) substrate was added, with this reaction stopped using 2 M H$_2$SO$_4$ and the plate read at 450 nm (titertek multiscan). Conditions were run in triplicate.

Time course

L. mexicana lesion amastigotes were transformed and grown in M199 promastigote media (pH 7.2) at 26°C for 3 days, where cells were predominantly nectomonad promastigotes. At this point, parasites were subpassaged into supplemented Grace's Insect medium (pH 5.5) and sampled over the next 18 days, with 4x10^6 parasites recovered daily. They were washed once

in PBS + 20 mM EDTA, followed by two washes in PBS. For Western blotting, $2x10^6$ parasites were resuspended in 200 µL 1 x sample buffer and boiled for at least 5 minutes before storing at -20°C. Membranes were probed with SAP, CRP and LT6 as already described.

For immunofluorescence, $2x10^6$ parasites were resuspended in 1 mL 4% (w/v) paraformaldehyde and incubated at room temperature for 30 minutes. The parasites were then washed three times in PBS, resuspended in 200 µL, with 25 µL dried to wells of a multi-test slide. These were stored at 4°C for staining. Slides were incubated for 1 hour with 5 µg/mL SAP or CRP with or without 15 mM EDTA in M199 (no FCS), or M199 only (no FCS) in a humidity chamber. Slides were then washed three times in PBS for 5 minutes. Wells previously incubated with SAP were incubated with 1:100 5.4D and CRP wells were incubated with 1:100 anti-CRP. M199 wells were incubated with 1:10 LT6 or M199 only. Slides were washed again. SAP, LT6 and M199 wells were then incubated with anti-mouse-A660 (A21054, Invitrogen) and CRP with anti-rabbit-AF488 (A11008, Invitrogen) in the dark. Slides were washed again, left to airdry, with 3 µL Vectashield + DAPI (H-2000-2) and a coverslip then being added, and sealed with nail varnish. Images were collected using the Zeiss LSM880 confocal microscope and then analysed using ZEN Blue lite with brightness and contrast edited to maximise the signal from the images. Images were collected using an 100x objective. A 561 nm HeNe laser was used to excite TRITC (see *lpg1*$^{-/-}$ parasite experiment) and AF660, a 405 nm laser diode used to excite DAPI and a 488 argon laser to excite AF488. All images had a frame time of 21.92 seconds.

lpg1$^{-/-}$ L. mexicana *immunofluorescence*

A total of 10^6 *lpg1*$^{-/-}$ parasites were washed once with PBS containing 15 mM EDTA and then twice in PBS. Parasites were incubated in M199 (no FCS) media containing 10 µg/mL SAP, control media only or media with SAP and 15 mM EDTA for 1 hour at room temperature. Parasites were centrifuged and fixed in 4% (w/v) PFA, washed and $2.5x10^5$ parasites air dried per sample onto slides. Slides were rehydrated and stained with 1:100 5.4D followed by 1:500 anti-mouse IgG TRITC (T-5393, Sigma) both for 1 hour with washing between stages. The slides were dried and counterstained with Vectashield + DAPI and coverslips attached. Slides were visualised using the Zeiss LSM880 confocal microscope and a 63x objective. A frame time of 14.08 seconds was used for SAP and 13.47 seconds used for SAP + EDTA.

Time course for SAP in bloodmeal

Adult female *Lu. longipalpis* were fed (3-5 days post-emergence) fresh human blood. Midguts from 10 flies were dissected daily for 5 days and placed into 50 µL RIPA buffer lysis system (Santa Cruz, sc-24948). For dissections, flies were briefly washed in MilliQ water with detergent to remove setae. In PBS, the digestive tract of the fly was extracted, with the hindgut, malpighian tubules and crop removed. A separate group of fed flies were given a second blood feed 5 days after the first bloodmeal and dissected daily for 5 days. Midguts were homogenised in a 1.5 mL Eppendorf with a pestle and centrifuged at 16300 g for 10 minutes at 4°C (Serafim et al., 2023). The supernatant was recovered and stored at -20°C until needed. The equivalent of 2 midguts were run per lane on 10% SDS-PAGE under reducing conditions, transferred to PVDF, with membranes probed with or without 1:12 5.4D supernatant or with 1:8 LT6 and 1:3000 anti-mouse-AP. SAP was loaded alongside the samples.

SPR

A CM5 chip was activated in flow cell (Fc) 1 and 2 according to the Biacore protocol for amine coupling using a 7 minute activation period with fresh 0.4 M EDC and 0.1 M NHS. Midgut protein extract was diluted to 10 µg/mL in 20 mM sodium acetate buffer pH 4.0 and flowed over Fc 2 at 3 µL/min for a total of 30 minutes. Ethanolamine (1 M pH 8.0) was flowed over both surfaces for 7 minutes to deactivate remaining sites. A total of 850 RU midgut protein extract was immobilised in Fc 2.

Pentraxin (SAP and CRP at 1 or 10 µg/mL) and other protein binding was examined during an association phase for 3 minutes and dissociation for 5 minutes with a flow rate of 30 µL/min in 10 mM HEPES buffered saline with 0.5 mM $CaCl_2$. Between each run, bound pentraxin was eluted with 10 mM EDTA (10 µL). The data was analysed in BiaEval 4.1. and after subtracting the blank Fc 1 trace, was transferred to Prism for presentation. The curves were analysed using simple 1:1 Langmuir separate dissociation and association kinetic models, seen in Figure S3 for 1 µg/mL SAP (Figure 7B).

Microvillar-enriched midgut extract Western blots

Midguts were dissected from nonfed, 50% (w/v) sucrose fed or (human) blood fed *Lutzomyia longipalpis* as previously described, and microvillar-enriched protein extracted using the protocol of Dillon and Lane (1999). Though this protocol is enriching for microvillar proteins, non-protein material may also be present. Microvillar extracts were run on gels as previously

described under reducing and non-reducing conditions and probed with SAP and CRP as described previously.

Immunoprecipitation

Microvillar extracts from 1200 *Lu. longipalpis* unfed midguts was dialysed (Visking tubing, size 14-18 kDa) into TBS + 0.5 mM Ca^{2+} + 0.05% (v/v) Tween-20. Antibody-coupled beads were prepared using 100 μL Pierce NHS-activated magnetic beads (88826) and 50 μg anti-SAP antibody 5.4D following the protocol recommended for the beads. The exception was PBS + 0.5 M NaCl, pH 7 was used instead of the recommended 0.1 M glycine, pH 2 wash. An additional step of incubating SAP with the antibody-coupled beads was performed. First, 20 μL of 10 mg/mL antibody-coupled beads were washed in 400 μL TBS + 0.5 mM Ca^{2+} + 0.05% (v/v) Tween-20. Then, 30 μg SAP in TBS + 0.5 mM Ca^{2+} + 0.05% (v/v) Tween-20 was added and incubated on a rotator at room temperature for 2 hours. The sample was vortexed every 5 minutes for 15 seconds during the first 30 minutes, and every 15 minutes for the remaining time. The beads were washed again and resuspended in the same buffer. The *Lu. longipalpis* protein sample was precleared by incubating for 30 minutes at room temperature with 7.5 μL antibody-coupled beads. The sample was vortexed every 5 minutes for 15 seconds, followed by a wash step. For the immunoprecipitation, 7.5 μL SAP-antibody-coupled beads were incubated with 200 μL pre-cleared *Lu. longipalpis* protein and incubated on a rotator overnight at 4°C, followed by a wash. The whole sample was run on an 10% SDS-PAGE gel and stained with Coomassie followed by destaining. This was carried out in 40% methanol destaining solution (10% acetic acid, 50% MilliQ water) followed by 10% solution. Bands were cut and sequenced by the Metabolomics and Proteomics Laboratory at the University of York who provided the following; "following in-gel digestion, peptides were analysed over 10 minute acquisitions with elution from a 50 cm Micro Pillar C18 column (Pharma Fluidics) onto a Bruker maXis qTOF operated in a data dependent acquisition mode. Resulting peptide spectra were searched against the Uniprot protein database entries."

Midgut binding assays

Logarithmic phase *L. mexicana* culture parasites grown in M199 + 20% FCS were washed for 30 minutes on a shaker in 10 mL PBS + 20 mM EDTA, followed by washing twice in 10 mL PBS by resuspension and centrifugation at 2500 g. Parasites were resuspended in PBS + 1 mM $CaCl_2$, containing 40 μg/mL SAP or 40 μg/mL SAP + 20 mM EDTA. This SAP concentration is within the average physiological range (Du Clos, 2013). Previously sugar fed *Lu. longipalpis* midguts were dissected as previously described, followed by careful 'unzipping' to reveal the inner lumen. Midguts were incubated for 30 minutes at 26°C in $2x10^6$ parasites in 50 μL. The midguts were

washed individually in three successive drops of PBS with agitation applied, before being placed into a 1.5 mL Eppendorf containing 30 µL PBS. Midguts were homogenised using a disposable pestle and 10, 5 and 3 µL airdried to the well of a multitest slide (096041505, MP Biomedicals). Samples were fixed with methanol and stained using Giemsa. Entire wells were scanned using a microscope (Leitz, Laborlux K) and the number of parasites identified recorded.

Sand fly infections

Unfed flies (3-5 days old) were fed through a chicken skin membrane on heat-inactivated (h.i.) human blood in an artificial feeder (Hemotek). For control experiments, blood contained 5×10^5/mL *L. mexicana* axenic amastigotes and 25 µg/mL SAP. Test experiments contained either CPHPC – a drug against SAP or anti-SAP monoclonal antibodies dezamizumab or 5.4D.3B with amastigotes and blood. CPHPC (SML2571, Sigma-Aldrich) was prepared at 25 mg/mL by reconstituting in PBS + 10 mM Tris, 140 mM NaCl, 2 mM $CaCl_2$, pH 8 (Kolstoe et al., 2009) and diluted to 1 mg/mL with blood. The drug CPHPC has been shown to crosslink SAP pentamers forming decamers (Pepys et al., 2002) and reduces circulating SAP in human studies (Richards et al., 2015). Antibodies against human SAP, Dezamizumab (PX-TA1441-1MG, ProteoGenix) and 5.4D.3B (CBL305, Chemicon) were both diluted 1:50 giving concentrations in the blood of 67 µg/mL and 2 µg/mL, respectively. Dissected midguts (as previously described) were added to 30 µL PBS and homogenised with a disposable pestle. For each midgut sample, 10 µL with 2 µL 4% PFA was added to a disposable hemocytometer (BVS100H, Immune Systems) and 16 squares counted. If no parasites were observed, another 16 squares were counted. The number of parasites per midgut was then calculated.

Data and statistical analyses

GraphPad Prism software version 9.5.1 was used for all statistical analysis. Normality of data was determined using the Shapiro-Wilk test. The Kolmogorov-Smirnov test was used for non-normal unpaired data. For paired data, either the Wilcoxon matched-pair or paired t test were used depending on if the data was normally distributed. All statistical tests were two-tailed. A *P* value of <0.05 was deemed significant (*P < 0.05, **P<0.01, ***P<0.001). ImageJ was used to calculate the mean grey value of dot blots using an ImageJ protocol (ImageJ, 2023). An asymmetric sigmoidal, 5PL, standard curve was fit and dilution factors for each sample interpolated from a set mean grey area value of 25.

Results

SAP and CRP bind to all L. mexicana *lifecycle stages* in vitro

L. mexicana parasites from culture sampled daily were fixed, stained with SAP and CRP and imaged using immunofluorescence. Ubiquitous binding could be seen on the surface of every *Leishmania* morphological stage (amastigotes, procyclic promastigotes, nectomonad promastigotes, leptomonad promastigotes, haptomonad promastigotes, metacyclic promastigotes) for both pentraxins (Figure 1). The intensity of staining varied within stages, with some parasites exhibiting no staining, however no correlation was found between dead parasites and SAP staining (using L34983 Invitrogen, data not shown). LT6 (specific to repeating disaccharides of LPG) staining was also sporadic (Figure S1). Though LPG is downregulated in *L. mexicana* amastigotes, LT6 is likely binding amastigote proteophosphoglycans (aPPGs) that present similar structures to LPG (Bahr et al., 1993; Ilg et al., 1998). This variation may potentially be due to different levels of ligand shedding between parasites before fixing. No staining was observed when parasites were incubated with no pentraxins present or pentraxins + 15 mM EDTA.

Crude parasite extracts were produced daily from the same culture and used in immunoblotting. On day 3 the culture was subpassaged into Grace's + 20% FCS to initiate metacyclogenesis. SAP and CRP binding was detected for every day tested (Figure 2). Binding of SAP was unchanged in pattern or intensity across the differentiation stages whereas CRP showed stronger binding to metacyclic extracts. The increased binding of CRP suggests multiple CRP subunits can bind the longer metacyclic LPG (previously seen for *Leishmania donovani*, Culley et al., 2000).

SAP and CRP L. mexicana *binding sites differ, with SAP not binding LPG*

Immunoblotting of unfractionated *L. mexicana* extracts (Figure 2) show SAP binding to multiple discrete bands ranging from 72-250 kDa, with a lower band of ~15 kDa also seen. CRP and LT6 both bound LPG, with the characteristic smear of this molecule seen for CRP binding. Only lower molecular weight LPG was detected by LT6 for earlier time points, with the molecular weight detected increasing at later time points, reflecting the increase in the repeating disaccharide of LPG during metacyclogenesis (Sacks et al., 1990; Forestier et al., 2015). SAP + 10 mM EDTA and no LT6 controls showed no binding, with CRP binding significantly reduced when 10 mM EDTA was present. When LPG-enriched material was probed with SAP (Figure 3A), binding was seen but this was fainter than CRP. No binding was seen when pentraxins were absent. The smear seen with SAP binding to LPG extract (Figure 3A) and multiple bands in Figure 2A would be consistent with SAP binding to a glycolipid ligand.

To confirm SAP is not binding to LPG via the repeating disaccharide which is the ligand for CRP, we carried out an LT6 competition assay. Signal was low for SAP binding LPG-enriched material when using ELISA, with no significant reduction in binding seen to log phase LPG when LT6 was present (Figure 3B). This suggests SAP does not bind to LPG via the phosphorylated disaccharide repeats. In contrast the same LT6 did inhibit CRP (Figure 3C) as previously reported (Culley et al., 1996). LT6 was more efficient at inhibiting binding to the log phase LPG as this is a shorter and less avid ligand for CRP than the metacyclic LPG (Culley et al., 2000). Further confirmation was achieved by immunofluorescence with SAP binding retained to *lpg1*$^{-/-}$ parasites lacking repeating disaccharide and cap regions of LPG (Figure 4).

The different binding sites for CRP and SAP was also confirmed with a competition assay of pentraxin binding to LPG-enriched material. When increasing concentrations of SAP were incubated with CRP, there was very little change in CRP binding (Figure 3E). Detection of SAP was weak and likely only to non-LPG material in this enriched fraction. However, binding decreased to almost zero when high concentrations of CRP were incubated with SAP (Figure 3D).

The difference in binding pattern and binding intensity over developmental time to crude *L. mexicana* material extracts, the low level of detection by ELISA for SAP binding to LPG-enriched material, LT6 competition not affecting binding, as well as SAP lacking the ability to inhibit CRP binding suggests SAP does not bind to LPG.

One explanation for the ability of CRP to inhibit SAP binding is that CRP binding to the extended molecule LPG may sterically prevent access of SAP to binding sites close to the membrane anchor regions or on short glycan chains. Alternatively, CRP might compete with an SAP ligand such as phosphoethanolamine which is a ligand for both proteins.

SAP likely binds L. mexicana *GIPLs*

Binding of SAP and CRP was seen to dot blots of log phase LPG- and GIPL-enriched material from *L. mexicana* (Figure 5). Technical and theoretical issues of what parameter to use meant we did not measure absolute quantitation but compared the relative binding of pentraxins in limiting dilution assays, with relative binding between the samples reported. As expected, CRP bound strongly to the LPG-enriched material, but also to a lesser extend the GIPL-enriched fraction. The same mean grey value (sum of grey value pixels divided by number of pixels in the ImageJ selection) was reported for 1:915 dilution LPG-enriched material compared to 1:407 for GIPL-enriched material. CRP is likely binding delipidated LPG (Tolson et al., 1994), seen as a low molecular weight smear when blots of GIPL-enriched material were probed with CA7AE, LT6 and CRP (data not shown). SAP preferentially bound the GIPL-enriched fraction,

with a 1:20 GIPL dilution giving the same mean grey value as a 1:7 dilution of LPG-enriched material.

SAP is not degraded by the midgut environment but is lost during defecation

To further elucidate the role of SAP in the *Leishmania* lifecycle within the sand fly, the presence of SAP in the fly was tracked for five days after a bloodmeal was taken, with the results seen in Figure 6. SAP was detected by Western blotting until day 4 – when the majority of flies had defecated the bloodmeal remnants. Other blood proteins were also detected due to cross-reactivity of the anti-mouse IgG secondary used. SAP was also tracked in flies which had taken a second bloodmeal, with SAP detected until the majority of flies had defecated on day 10.

SAP binds to microvillar extracts from Lu. longipalpis

Midgut samples enriched for microvillar proteins were run under reducing and non-reducing conditions on an SDS-PAGE gel and PVDF blots probed for SAP and CRP binding (Figure 7A). When probed with SAP, two bands were present at ~130 kDa and ~80 kDa under non-reducing conditions and these were found in female and male adult sand flies. Midguts from flies fed on different diets were run under reducing conditions and this gave bands of size ~80 kDa and ~75 kDa. No difference in band intensity was seen between feeding conditions. SAP attachment to microvillar extracts was also detected by SPR, seen in Figure 7B. This interaction could be inhibited with the addition of *L. mexicana* LPG-enriched material in a concentration-dependent manner (Figure 7C), but log phase LPG-enriched material showed no significant binding to the microvillar extracts (Figure 7D). No CRP binding was seen to the microvillar extracts when using either Western blotting (Figure 7A) or SPR (Figure 7B).

Immunoprecipitation of the microvillar-enriched extracts using SAP bound to 5.4D-coupled magnetic beads was carried out, with the retrieved proteins ran on an SDS-PAGE gel and stained using Coomassie. Bands of the expected sizes were not seen, likely due to the low concentration of protein retrieved from 1200 flies (IP starting material ~150 µg total protein). Therefore, a region around the expected band size was cut and sent for sequencing. Tentative identification suggests this protein is an α-glucosidase, with the top two sequence peptides (TANVYQIYPR and LVGTDILAYE) matching different α-glucosidase protein sequences on UniProt (A0A7G3A834 and A0A1B0CTF6).

***SAP does not affect** L. mexicana **attachment to** Lu. longipalpis **midguts** ex vivo*

To see if SAP enhanced *L. mexicana* attachment to the *Lu. longipalpis* midgut, *ex vivo* midgut binding assays were carried out. Similar numbers of parasites per midgut were observed in the presence of SAP, no SAP or SAP + 20 mM EDTA (Figure 8). A significant difference was found in the number of parasites bound per midgut for *L. mexciana* between PBS + 1 mM CaCl$_2$ and the + 40 µg/mL SAP test, however no significant difference was found between the test and the 20 mM EDTA control.

***CPHPC and antibodies against SAP do not block** L. mexicana **binding to the** Lu. longipalpis midgut*

To test whether SAP has a role in *Leishmania* attachment to the sand fly midgut, *Lu. longipalpis* flies were infected with *L. mexicana* amastigotes and parasite numbers in the midgut tracked over the course of the infection (seen in Figure 8). Test groups contained either a binding site inhibitor against SAP called CPHPC, anti-SAP antibody dezamizumab or anti-SAP antibody 5.4D.3B. A significant difference was found in the number of parasites per midgut on all days tested between the control group and flies with CPHPC. However, when this experiment was repeated, only day 5 was statistically significant. There was no significant difference between parasite numbers between flies with and without dezamizumab. For 5.4D.3B, a significant difference was seen for days 3 and 7. However, though some days tested had a significant difference between control and test conditions, it is clear parasite numbers are still high in these flies. Furthermore, when both CPHPC and 5.4D.3B were used, there was no significant difference found between the test and the control on any days post infection. If SAP has a role in parasite-midgut attachment, it is additive at most.

Discussion

CRP is known to interact with *Leishmania* LPG via the phosphorylated disaccharide repeats (Culley et al., 2000), bind C1q and activate complement (Seow et al., 2023) and trigger transformation of metacyclics to amastigotes (Bee et al., 2001; Mbuchi et al., 2006). However, the only previous report on interaction of *Leishmania* and SAP examined metacyclic *L. donovani* parasites and showed no clear binding in comparison with CRP (Raynes et al., 1993). In this report however we show SAP binding to parasites of all development stages including amastigotes. The Raynes group have previously seen SAP binding to *Leishmania*, however, they were unable to repeat the result (personal communication). It is clear from Western blotting, competition assays and *lpg1*^{-/-} immunofluorescence that SAP does not share the same binding epitope as CRP.

Though the binding site of SAP to *L. mexicana* could not be confirmed, SAP was found to preferentially bind GIPL-enriched material. CRP binding was comparatively higher, but this may be due to differences in detection system. We speculate the SAP ligand is PEth, found on a range of *Leishmania* surface molecules including GIPLs (McConville et al., 1993) and GP63 (Naderer and McConville, 2002). SAP and CRP could both bind *L. mexicana* amastigotes, a stage with few LPG molecules (McConville and Blackwell, 1991) however this stage has around 2×10^7 ethanolamine containing GIPLs per *Leishmania* (Winter et al., 1994). CRP is also known to bind PEth (Mikolajek et al., 2011), with this pentraxin likely binding PEth-containing surface molecules along with binding LPG. The LPG-enriched, GIPL-enriched and crude parasite extract samples will all contain PEth, and banding patterns may relate to PEth-containing surface molecules but also PEth-glycolipids running with other material. Unfortunately, no antibodies are commercially available to probe for GIPLs. In the absence of mutants lacking PEth and specific reagents that selectively bind PEth, we were unable to provide evidence of direct binding.

Immunofluorescence showed a varied binding pattern of SAP to promastigotes as seen for *lpg1*^{-/-} parasites in Figure 4, with no staining seen, staining just at the flagellar pocket or staining over the entire surface of the cell. Variation in staining was also observed for the wild-type parasites. The washing of parasites before fixing may affect the amount of GPI-anchored surface molecules shed (Ilg et al., 1992), leading to varied staining intensity. Binding of SAP at the flagellar pocket may be capturing the emergence of PEth-containing surface molecules before they diffuse across the cell surface or capturing endocytosis (Weise et al., 2000). Intense regions of binding can also be observed away from the flagella pocket, potentially due to binding of SAP to lipid rafts, reported to contain GP63, LPG, some GIPLs, sphingolipids and sterols (Denny et al., 2001).

SAP is detected in the fly until the bloodmeal is defecated. This is not surprising as it was previously predicted that physiological concentrations of Ca^{2+} would at least partially protect SAP from proteolysis (Kinoshita et al., 1992) and SAP was found to protect amyloid deposits from proteolysis (Li and McAdam, 1984). It is therefore likely SAP encounters all *Leishmania* lifecycle stages within the sand fly. For *Leishmania* (*Leishmania*) species, like *L. mexicana*, amastigotes will be taken up alongside SAP when a sand fly bites an infected host and enter the midgut (Kamhawi, 2006). Both *Leishmania* and SAP will then be encapsulated by the peritrophic matrix (PM) (Kamhawi, 2006). When nectomonad stages escape the PM, SAP will be present in the midgut up until the sand fly defecates the bloodmeal remnants. It is likely the sand fly will then take a second bloodmeal, with leptomonad and metacyclic promastigote stages present in the thoracic midgut (Rogers et al., 2002; Kamhawi, 2006) interacting with components of the bloodmeal as it moves to the abdominal midgut. Haptomonads will likely be attached to the stomodeal valve (Volf et al., 2004) and the PSG will be present in the pharynx and the thoracic midgut (Rogers, 2012). PSG plug formation and stomodeal valve degradation by haptomonad chitinases (Volf et al., 2004) may mean parasites are found in the foregut. As PSG is soluble, it will mix with the new bloodmeal and SAP will come into contact with the *Leishmania* stages present (Rogers, 2012). As nutrients from a second bloodmeal are thought to lead to metacyclic transformation into retroleptomonads, SAP will also interact with this stage (Serafim et al., 2018).

Using SPR it was found LPG inhibits SAP binding to microvillar-enriched *Lu. longipalpis* midgut protein but LPG itself does not bind midgut protein. It was previously seen that SAP does not bind LPG (Figure 3), so it is unlikely LPG competes for either SAP or midgut protein binding. Instead, negatively charged LPG (Eggimann et al., 2015) may cause a change in environment which affects SAP binding to the midgut protein.

Preliminary immunoprecipitation results suggest SAP may bind to *Lu. longipalpis* α-glucosidases (UniProt: A0A7G3A834 and UniProt: A0A1B0CTF6), an enzyme that hydrolyses terminal α-1,4 bonds on a range of saccharides with varying efficiency (Terra and Ferriera, 1994; da Costa-Latgé et al. 2021). da Costa-Latgé et al. (2021) identified α-glucosidase A0A1B0CTF6, named in the study as L1Aglu2, as part of the GH13 family of glycoside hydrolases. Many sequences considered as part of the study were incomplete, and may suggest our two peptides are part of the same α-glucosidase. de Costa-Latgé et al., did find potential O- and N-glycosylation sites on L1Aglu2, that could display GalNAc, thought to be important in parasite binding for permissive vectors (Myšková et al., 2007). A similar size *Lu. longipalpis* midgut protein as that seen with SAP binding was previously detected when probing with HPA (Myšková et al., 2016; Rogers lab, unpublished).

As SAP binding is seen to both *L. mexicana* and to *Lu. longipalpis* microvillar-enriched midgut extract, we wanted to see if blocking SAP activity within the fly would reduce parasite numbers after defecation, indicating a role for SAP in attachment. It seemed likely that a component of the bloodmeal may be important for binding as it would be found in all infected permissive vectors. Commercially available antibodies and a drug for reducing SAP are also available and could be used as transmission-blocking therapy. However, the structure of pentraxins with the binding face of the pentamers all facing along the same axis (Pepys, 2018) does not lend itself to a cross-linking function. It is unlikely SAP is involved in midgut attachment as it is lost during defecation of the bloodmeal remnants and flies infected alongside anti-SAP drugs and antibodies could still sustain infections. Furthermore, the initial significant differences seen for fly infection intensities when CPHPC was present may have been an unrelated effect caused by the high concentration used. The antibodies provide a more selective inhibitor. As previously mentioned, sand flies take multiple bloodmeals during the course of an infection and so SAP could still be interacting with a range of lifecycle stages. Work is ongoing to see whether SAP acts as a trigger for amastigote transformation into procyclic stages, similarly seen for CRP being a trigger for metacyclic to amastigote transformation (Bee et al., 2001).

In conclusion, we demonstrate that SAP binds to a range of parasite stages in a sporadic manner through its calcium-dependent binding site. The preference of SAP for the GIPL-enriched fraction, suggests PEth-containing GIPLs are a major binding candidate. Though SAP also binds to *Lu. longipalpis* microvillar-enriched midgut extract, there does not seem to be a role for this pentraxin in parasite-midgut attachment. The data shown here suggests SAP interacts with a range of morphological stages within the vector during first and subsequent bloodmeals, with work ongoing to deduce the role of this interaction.

References

World Health Organisation. WHO | Leishmaniasis [Internet]. Leishmaniasis. 2023 [cited 2023 Apr 23]. Available from: Leishmaniasis (who.int)

Volf P, Myšková J. Sand flies and *Leishmania*: specific versus permissive vectors. Trends Parasitol. 2007;23(3):91-92.

Turco SJ. The leishmanial lipophosphoglycan: a multifunctional molecule. Exp Parasitol. 1990;70:241-245.

McConville MJ, Thomas-Oates JE, Ferguson MAJ, Homans SW. Structure of the lipophosphoglycan from *Leishmania major.* J Biol Chem. 1990;265(32):19611-19623.

Forestier CL, Gao Q, Boons GJ. *Leishmania* lipophosphoglycan: how to establish structure-activity relationships for this highly complex and multifunctional glycoconjugate? Front Cell Infect Microbiol. 2015;4:193.

Pimenta PFP, Turco SJ, McConville MJ, Lawyer PG, Perkins PV, Sacks DL. Stage-specific adhesions of *Leishmania* promastigotes to the sandfly midgut. Science. 1992;256:1812-1815.

Pimenta PFP, Saraiva EMB, Rowton E, Modi GB, Garraway LA, Beverley SM, Turco SJ, Sacks DL. Evidence that the vectorial competence of phlebotomine sand flies for different species of *Leishmania* is controlled by structural polymorphisms in the surface lipophosphoglycan. Proc Natl Acad Sci USA. 1994; 91:9155-9159.

Kamhawi S, Ramalho-Ortigao M, Pham VM, Kumar S, Lawyer PG, Turco SJ, Barillas-Mury C, Sacks DL, Valenzuela JG. A role for insect galectins in parasite survival. Cell. 2004;119:329-341.

Di-Blasi T, Lobo AR, Nascimento LM, Córdova-Rojas JL, Pestana K, Marín-Villa M, Tempone AJ, Telleria EL, Ramalho-Ortigão M, McMahon-Pratt D, Traub-Csekö YM. The flagellar protein FLAG1/SMP1 is a candidate for *Leishmania*-sand fly interaction. Vector Borne Zoonotic Dis. 2015;15(3):202-209.

Rogers ME, Ilg T, Nikolaev AV, Ferguson AJ, Bates PA. Transmission of cutaneous leishmaniasis by sand flies is enhanced by regurgitation of fPPG. Nature. 2004;430:463-467.

Myšková J, Svobodová M, Beverley SM, Volf P. A lipophosphoglycan independent development of *Leishmania* in permissive sand flies. Microbes Infect. 2007;9:317–24.

Svárovská A, Ant TH, Seblová V, Jecná L, Beverley SM, Volf P. *Leishmania major* glycosylation mutants require phosphoglycans (*lpg2⁻*) but not lipophosphoglycan (*lpg1⁻*) for survival in permissive sand fly vectors. PLoS Negl Trop Dis. 2010;4(1):e580.

Secundino N, Kimblin N, Peters NC, Lawyer P, Capul AA, Beverley SM, Turco SJ, Sacks D. Proteophosphoglycan confers resistance of *Leishmania major* to midgut digestive enzymes induced by blood feeding in vector sand flies. Cell Microbiol. 2010;12(7):906-918.

Jecna L, Dostalova A, Wilson R, Seblova V, Chang KP, Bates PA, Volf P. The role of surface glycoconjugates in *Leishmania* midgut attachment examined by competitive binding assays and experimental development in sand flies. Parasitology. 2013;140:1026-1032.

Dostálová A, Volf P. *Leishmania* development in sand flies: parasite-vector interactions overview. Parasit Vectors. 2012;5:276.

Sacks DL, Modi G, Rowton E, Späth G, Epstein L, Turco SJ, Beverley SM. The role of phosphoglycans in *Leishmania*-sand fly interactions. Proc Natl Acad Sci USA. 2000;97(1):406-411.

Coutinho-Abreu IV, Oristian J, de Castro W, Wilson TR, Meneses C, Soares RP, Borges VM, Descoteaux A, Kamhawi S, Valenzuela JG. Binding of *Leishmania infantum* lipophosphoglycan to the midgut is not sufficient to define vector competence in *Lutzomyia longipalpis* sand flies. mSphere. 2020;5:e00594-20.

Myšková J, Dostálová A, Pěničková L, Halada P, Bates PA, Volf P. Characterization of a midgut mucin-like glycoconjugate of *Lutzomyia longipalpis* with a potential role in *Leishmania* attachment. Parasit Vectors. 2016;9:413.

Elnaiem DA, Ward RD, Young PE. Development of *Leishmania chagasi* (Kinetoplastida: Trypanosomatidae) in the second blood-meal of its vector *Lutzomyia longipalpis* (Diptera: Psychodidae). Parasitol Res. 1994;80(5):414-419.

Moraes CS, Aguiar-Martins K, Costa SG, Bates PA, Dillon RJ, Genta FA. Second blood meal by female *Lutzomyia longipalpis*: enhancement by oviposition and its effects on digestion, longevity, and *Leishmania* infection. Hindawi. 2018:2472508.

Serafim TD, Coutinho-Abreu IV, Oliveira F, Meneses C, Kamhawi S, Valenzuela JG. Sequential blood meals promote *Leishmania* replication and reverse metacyclogenesis augmenting vector infectivity. Nat Microbiol. 2018;3:548-555.

Hall MJR, Ghosh D, Martín-Vega, Clark B, Clatworthy I, Cheke RA, Rogers ME. Micro-CT visualization of a promastigote secretory gel (PSG) and parasite plug in the digestive tract of the sand fly *Lutzomyia longipalpis* infected with *Leishmania mexicana*. PLoS Negl Trop Dis. 2021;15(8):e0009682.

Serafim TD, Iniquez E, Barletta ABF, Doehl JSP, Short M, Lack J, Cecilio P, Nair V, Distuar M, Wilson T, Coutinho-Abrey IV, Oliveira F, Meneses C, Barillas-Mury C, Andersen J, Ribeiro JMC, Beverley SM, Kamhawi S, Valenzuela JG. *Leishmania* genetic exchange is mediated by IgM natural antibodies. Nature. 2023;623(7985):149-156.

Pritchard DG, Volanakis JE, Slutsky GM, Greenblatt CL. C-reactive protein binds leishmanial excreted factors. Proc Soc Exp Biol Med. 1985;178(3):500-503.

Raynes JG, Curry A, Harris RA. Binding of C-reactive protein to *Leishmania*. Biochem. 1993;22:35.

Culley FJ, Harris RA, Kaye PM, McAdam KPWJ, Raynes JG. C-reactive protein binds to a novel ligand on *Leishmania donovani* and increases uptake into human macrophages. J Immunol. 1996;156(12):4691-4696.

Culley FJ, Thomson M, Raynes JG. C-reactive protein increases C3 deposition on *Leishmania donovani* promastigotes in human serum. Biochem Soc Trans. 1997;25(2):286S.

Culley FJ, Bodman-Smith KB, Ferguson MAJ, Nikolaev AV, Shantilal N, Raynes JG. C-reactive protein binds to phosphorylated carbohydrates. Glycobiology. 2000;10(1):59-65.

Bee A, Culley FJ, Alkhalife IS, Bodman-Smith KB, Raynes JG, Bates PA. Transformation of *Leishmania mexicana* metacyclic promastigotes to amastigotes-like forms mediated by binding of human C-reactive protein. Parasitology. 2001;122:521-529.

Bodman-Smith KB, Mbuchi M, Culley FJ, Bates PA, Raynes JG. C-reactive protein-mediated phagocytosis of *Leishmania donovani* promastigotes does not alter parasite survival or macrophage responses. Parasite Immunol. 2002;24:447-454.

Pepys MB. The pentraxins 1975–2018: serendipity, diagnostics and drugs. Front Immunol. 2018;9:2382.

Mbuchi M, Bates PA, Ilg T, Coe JE, Raynes JG. C-reactive initiates transformation of *Leishmania donovani* and *L. mexicana* through binding to lipophosphoglycan. Mol Biochem Parasitol. 2006;146(2):259-264.

Seow ES, Doran EC, Schroeder JH, Rogers ME, Raynes JG. C-reactive protein binds to short phosphoglycan repeats of *Leishmania* secreted proteophosphoglycans and activates complement. Front Immunol. 2023;14:1256205.

Mikolajek H, Kolstoe SE, Pye VE, Mangione P, Pepys MB, Wood SP. Structural basis of ligand specificity in the human pentraxins, C-reactive protein and serum amyloid P component. J Mol Recognit. 2011;24:371-377.

Rogers ME, Chance ML, Bates PA. The role of promastigote secretory gel in the origin and transmission of the infective stage of *Leishmania mexicana* by the sandfly *Lutzomyia longipalpis*. Parasitology. 2002;124(5):495-507.

Ismaeel AY, Garmson JC, Molyneux DH, Bates PA. Transformation, development, and transmission of axenically cultured amastigotes of *Leishmania mexicana in vitro* and in *Lutzomyia longipalpis*. Am J Trop Med Hyg. 1998;59(3):421-425.

Loveless RW, O'Sullivan FG, Raynes JG, Yuen CT, Feizi T. Human serum amyloid P is a multispecific adhesive protein whose ligands include 6-phosphorylated mannose and the 3-sulphated saccharides galactose, N-acetylgalactosamine and glucuronic acid. EMBO J. 1992;11(3):813-819.

McConville MJ, Thomas-Oates JE, Ferguson MAJ, Homans SW. Structure of the lipophosphoglycan from *Leishmania major*. J Biol Chem. 1990;265(32):19611-19623.

O'Sullivan G, McAdam KPWJ, Raynes JG. Amyloid and Amyloidosis 1990: Monoclonal antibodies to human serum amyloid P-component. Springer, Dordrecht;1991.

Ahmed UK, Maller NC, Iqbal AJ, Al-Riyami L, Harnett W, Raynes JG. The carbohydrate-linked phosphorylcholine of the parasitic nematode product ES-62 modulates complement activation. J Biol Chem. 2016;291(22):11939-11953.

Thongsomboon W, Serra DO, Possling A, Hadjineophytou C, Hengge R, Cegelski L. Phosphoethanolamine cellulose: a naturally produced chemically modified cellulose. Science. 2018;359(6373):334-338.

Dillon RJ, Lane RP. Detection of *Leishmania* lipophosphoglycan binding proteins in the gut of the sandfly vector. Parasitology. 1999;118(1):27-32.

Du Clos TW. Pentraxins: structure, function, and role in inflammation. ISRN Inflamm. 2013;379040.

Kolstoe SE, Ridha BH, Bellotti V, Wang N, Robinson CV, Crutch SJ, Keir G, Kukkastenvehmas R, Gallimore JR, Hutchinson WL, Hawkins PN, Wood SP, Rossor MN, Pepys MB. Molecular dissection of Alzheimer's disease neuropathology by depletion of serum amyloid P component. Proc Natl Acad Sci USA. 2009;106(18):7619-7623.

Pepys MB, Herbert J, Hutchinson WL, Tennent GA, Lachmann HJ, Gallimore JR, Lovat LB, Bartfai T, Alanine A, Hertel C, Hoffmann T, Jakob-Roetne R, Norcross RD, Kemp JA, Yamamura K, Suzuki M, Taylor GW, Thompson D, Purvis A, Kolstoe S, Wood SP, Hawkins PN. Targeted pharmacological depletion of serum amyloid P component for treatment of human amyloidosis. Nature. 2002;417:254-259.

Richards DB, Cookson LM, Berges AC, Barton SV, Lane T, Ritter JM, Fontana M, Moon JC, Pinzani M, Gillmore JD, Hawkins PN, Pepys MB. Therapeutic clearance of amyloid by antibodies to serum amyloid P component. N Engl J Med. 2015;373(12):1106-1114.

Bahr V, Stierhof YD, Ilg T, Demar M, Quinten M, Overath P. Expression of lipophosphoglycan, high molecular weight phosphoglycan and glycoprotein 63 in promastigotes and amastigotes of *Leishmania mexicana*. Mol Biochem Parasitol. 1993;58:107-122.

Ilg T, Craik D, Currie G, Multhaup G, Bacic A. Stage-specific proteophosphoglycan from *Leishmania mexicana* amastigotes. J Biol Chem. 1998;273(22):13509-13523.

ImageJ. Dot Blot Analysis [Internet]. [cited 2023 June 5] Available from: https://imagej.nih.gov/ij/docs/examples/dot-blot/

Sacks DL, Brodin TN, Turco SJ. Developmental modification of the lipophosphoglycan from *Leishmania major* promastigotes during metacyclogenesis. Mol Biochem Parasitol. 1990;42:225-234.

Tolson DL, Schnur LF, Jardim A, Pearson TW. Distribution of lipophosphoglycan-associated epitopes in different *Leishmania* species and in African trypanosomes. Parasitol Res. 1994;80(6):537-542.

McConville MJ, Collidge TA, Ferguson MA, Schneider P. The glycoinositol phospholipids of *Leishmania mexicana* promastigotes. Evidence for the presence of three distinct pathways of glycolipid biosynthesis. JBC. 1993;268(21):15595-15604.

Naderer T, McConville MJ. Characterization of a *Leishmania mexicana* mutant defective in synthesis of free and protein-linked GPI glycolipids. Mol Biochem Parasitol. 2002;125:147-161.

McConville MJ, Blackwell JM. Developmental changes in the glycosylated phosphatidylinositols of *Leishmania donovani*. J Biol Chem. 1991;266(23):15170-15179.

Winter G, Fuchs M, McConville MJ, Stierhof YD, Overath P. Surface antigens of *Leishmania mexicana* amastigotes: characterization of glycoinositol phospholipids and a macrophage-derived glycosphingolipid. J Cell Sci. 1994;107:2471-2482.

Ilg T, Etges R, Overath P, McConville MJ, Thomas-Oates J, Thomas J, Homans SW, Ferguson MA. Structure of *Leishmania mexicana* lipophosphoglycan. JBC. 1992;267(10):6834-6840.

Weise F, Stierhof YD, Kühn C, Wiese M, Overath P. Distribution of GPI-anchored proteins in the protozoan parasite *Leishmania*, based on an improved ultrastructural description using high-pressure frozen cells. J Cell Sci. 2000;113(24):4587-4603.

Denny PW, Field MC, Smith DF. GPI-anchored proteins and glycoconjugates segregate into lipid rafts in Kinetoplastida. FEBS Lett. 2001;491(1-2):148-153.

Kinoshita CM, Gewurz AT, Siegel JN, Ying SC, Hugli TE, Coe JE, Gupta RK, Huckman R, Gewurz H. A protease-sensitive site in the proposed Ca^{2+}-binding region of human serum amyloid P component and other pentraxins. Protein Sci. 1992;1:700-709.

Li JJ, McAdam WJ. Human amyloid P component: an elastase inhibitor. Scand J Immunol. 1984;20:219-226.

Kamhawi S. Phlebotomine sand flies and Leishmania parasites: friends or foes? Trends Parasitol. 2006;22(9):439-445.

Volf P, Hajmova M, Sadlova J, Votypka J. Blocked stomodeal valve of the insect vector: similar mechanism of transmission in two trypanosomatid models. Int J Parasitol. 2004;34(11):1221-1227.

Rogers ME. The role of Leishmania proteophosphoglycans in sand fly transmission and infection of the mammalian host. Front Microbiol. 2012;3(223).

Eggimann GA, Sweeney K, Bolt HL, Rozatian N, Cobb SL, Denny PW. The role of phosphoglycans in the susceptibility of *Leishmania mexicana* to the temporin family of anti-microbial peptides. Molecules. 2015;20(2):2775-2785.

Terra WR, Ferreira C. Insect digestive enzymes: properties, compartmentalization and function. Comp Biochem Physiol. 1994;109B(1):1-62.

da Costa-Latgé SG, Bates P, Dillon R, Genta FA. Characterization of glycoside hydrolase families 13 and 31 reveals expansion and diversification of α-amylase genes in the phlebotomine *Lutzomyia longipalpis* and modulation of sandfly glycosidase activities by *Leishmania* infection. Front Physiol. 2021;12:635633.

A
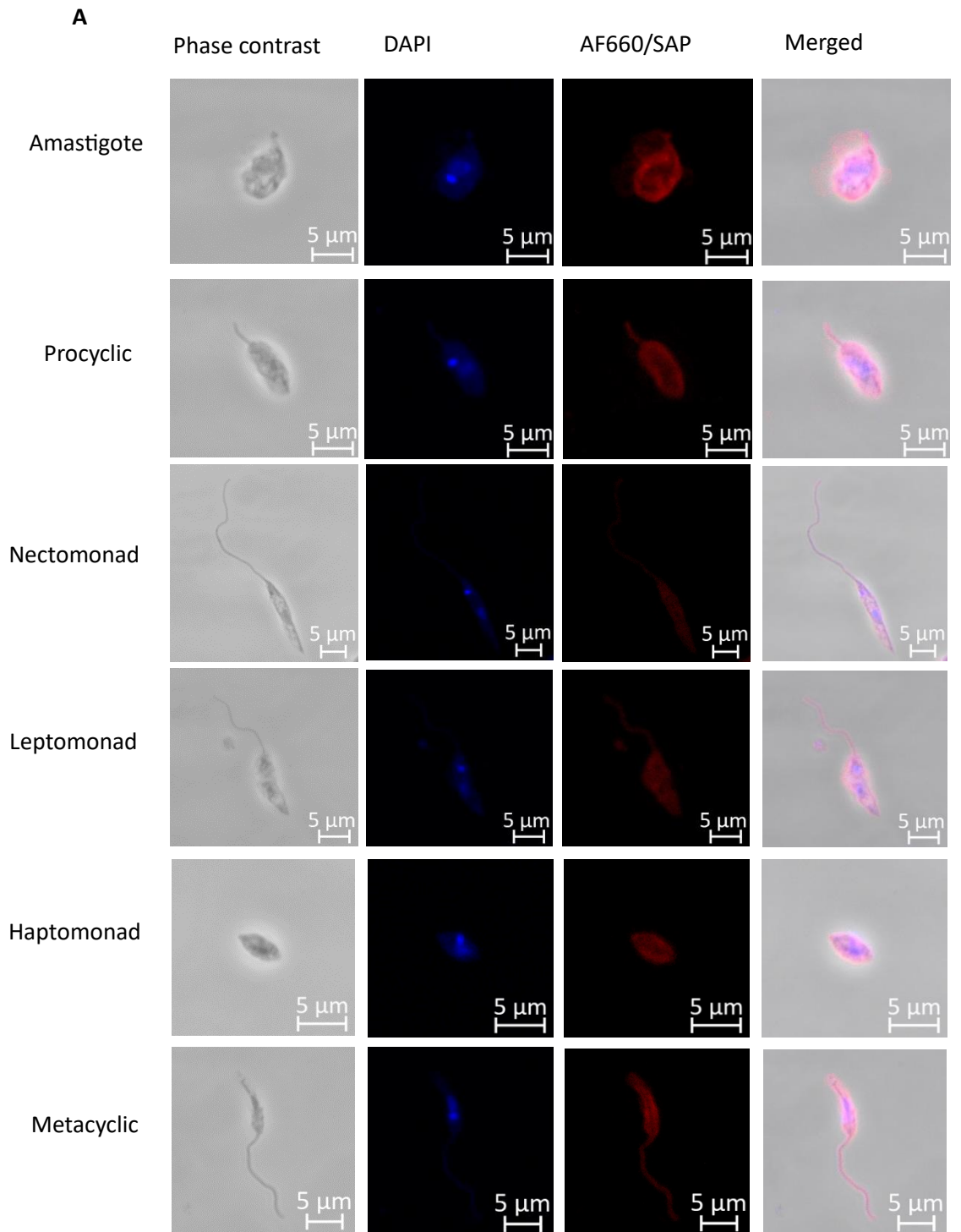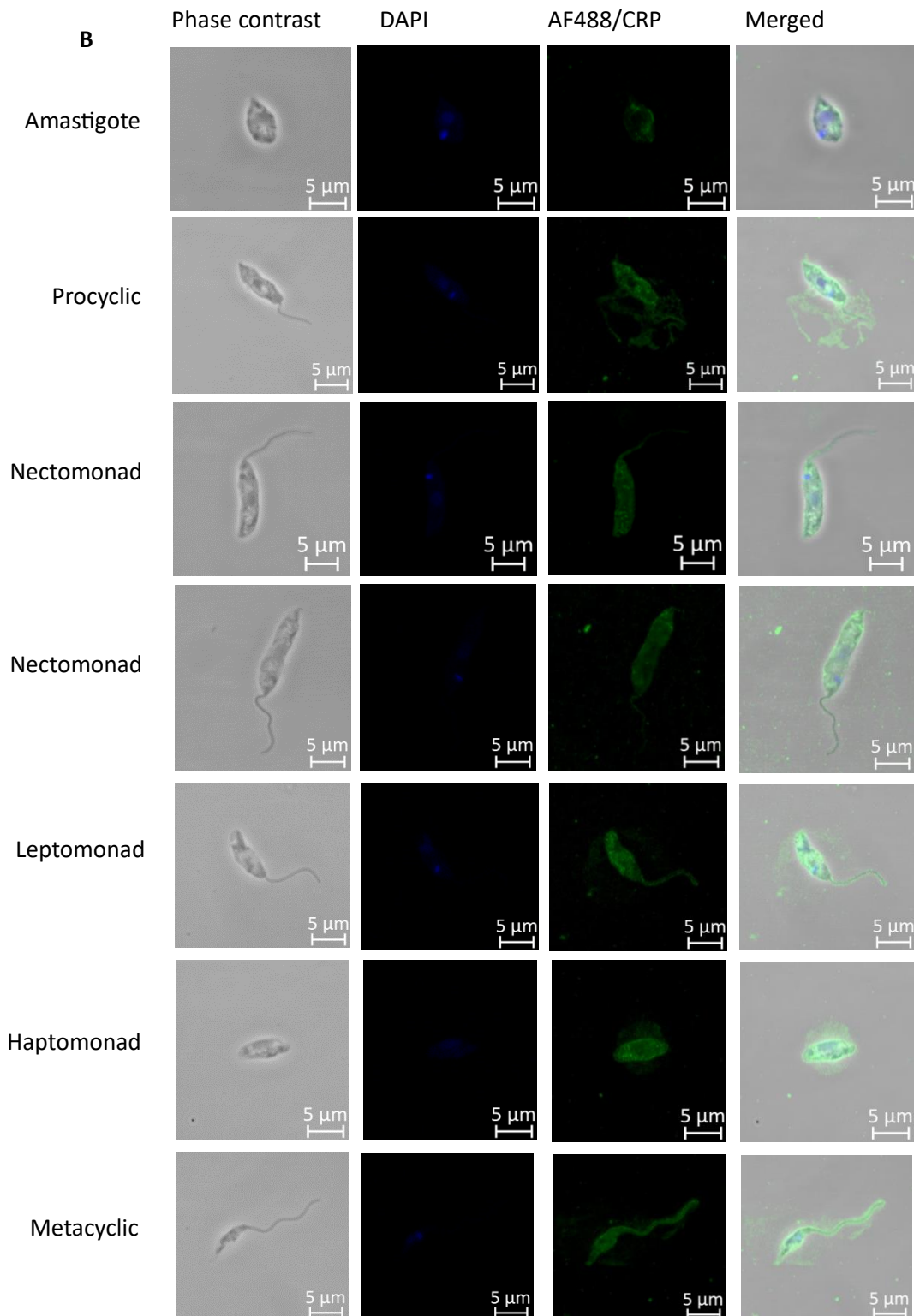
Figure 1. **SAP and CRP bind to all _Leishmania mexicana_ morphological stages**. However, binding varied between individual parasites. _L. mexicana_ culture was sampled daily, parasites were washed and resuspended in 4% paraformaldehyde. Parasites were then washed and airdried to a slide. The slides were incubated with SAP (**A**) or CRP (**B**) followed with primary and secondary antibodies and imaged using the Zeiss LSM880 confocal microscope. No staining was seen when parasites were incubated with pentraxin with 15 mM EDTA (seen in Figure S2) or when no pentraxin was present. Scale bars in white represent 5 μm.

161
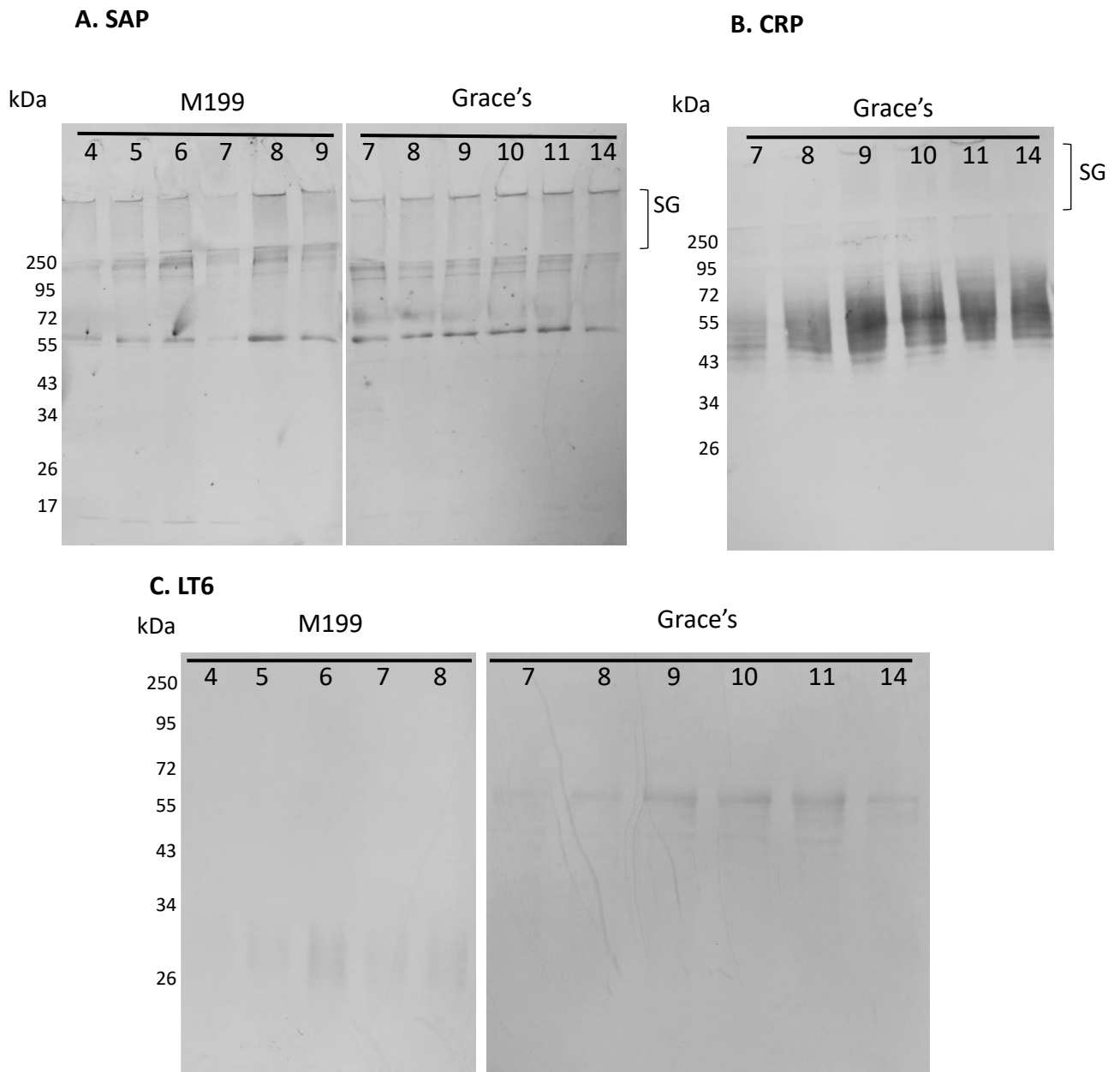
Figure 2. **SAP binds crude *Leishmania mexicana* extracts with binding similar for different days in culture (A). CRP binds LPG with this increasing during metacyclogenesis (B). The change in LPG molecular weight from log and stationary phase to metayclic stage was seen using LT6 (specific to [-6Galβ1,4Manα1-PO$_4$-]$_x$) (C).** *L. mexicana* parasites from a mouse lesion were put into culture with M199 + 20% FCS media. On day 3, the culture was subpassaged into Grace's + 20% FCS. Each day the parasites were washed and resuspended in 1 x sample buffer and boiled. Samples equivalent to 2x10^5 parasites were run per lane on an SDS-PAGE gel and transferred to PVDF. They were then probed with SAP (**A**), CRP (**B**) and LT6 (**C**). Control blots of pentraxins with 10 mM EDTA and a secondary only blot for LT6 were used with binding only seen in CRP + 10 mM EDTA but this was fainter than the test. SG = stacking gel.
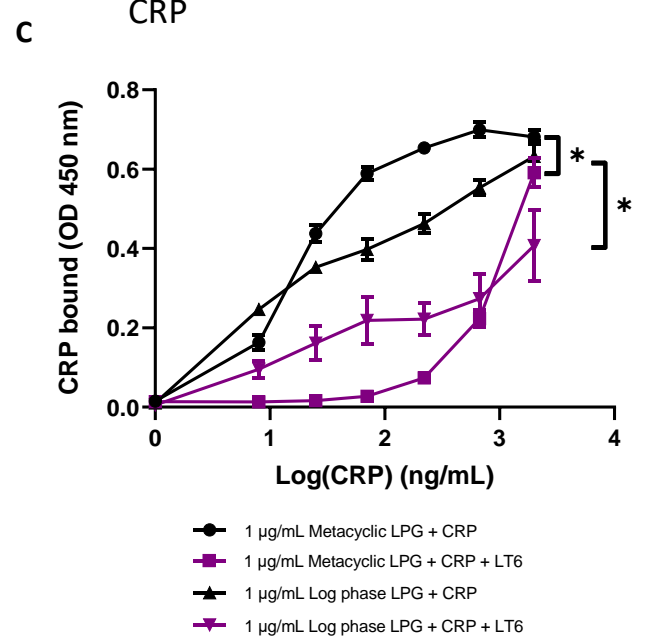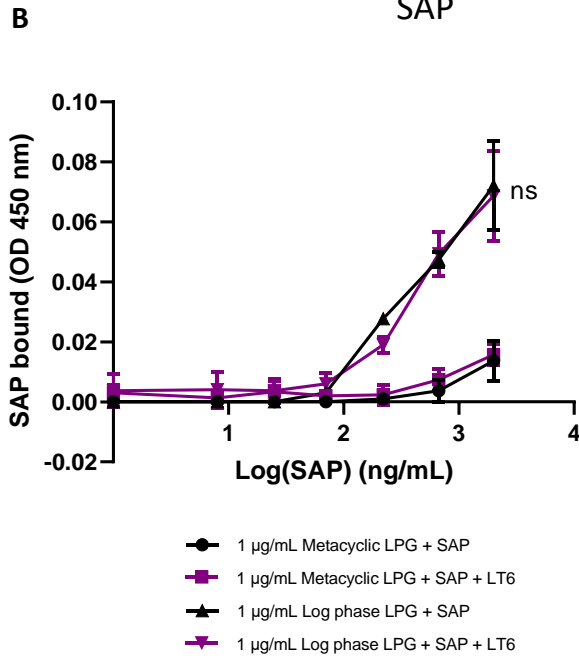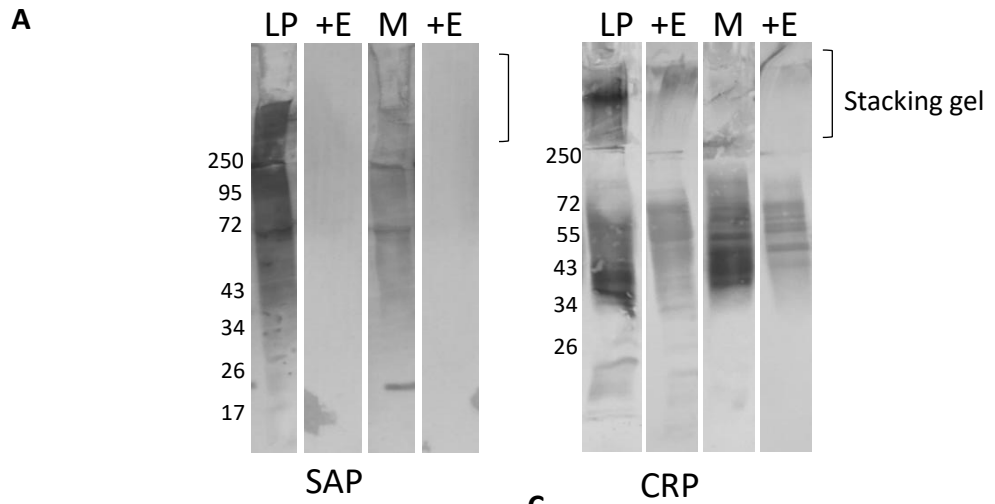
Figure 3. **SAP and CRP *Leishmania mexicana* binding sites differ, with SAP not binding LPG**. SAP and CRP bind log phase and metacyclic LPG-enriched material when using Western blotting (**A**). Attachment of CRP but not SAP to LPG can be reduced us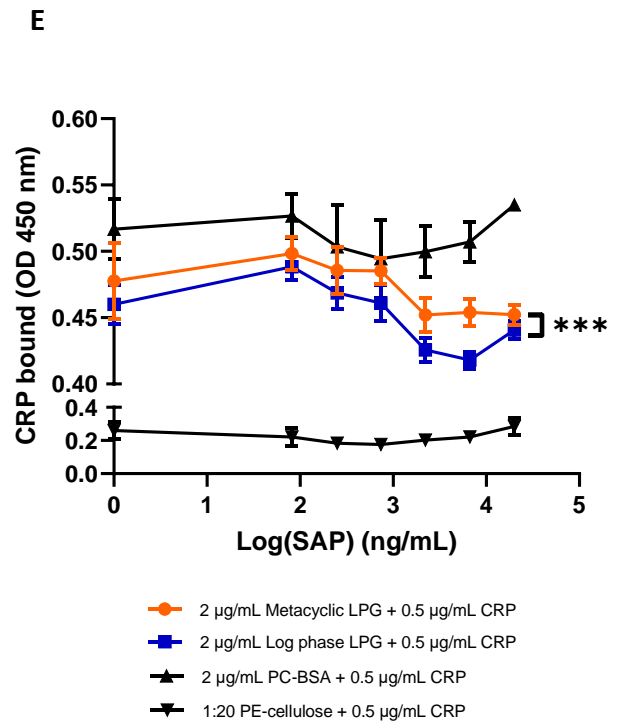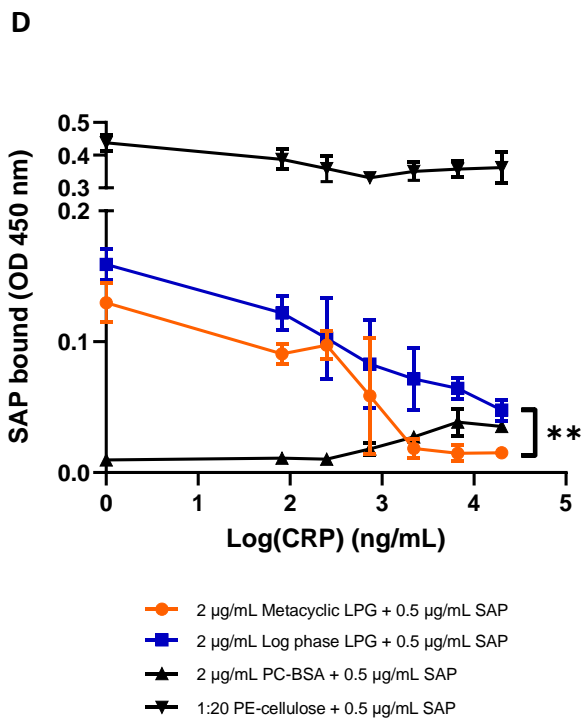ing LT6 (specific to [-6Galβ1,4Manα1-PO$_4$-]$_x$) (**B, C**). CRP competition reduces SAP bound to LPG in a concentration-dependent manner (**D**) but SAP does not compete for CRP binding (**E**). Detection of SAP binding to LPG using ELISA is very low. In **A**, 3 µg LPG-enriched material from *L. mexicana* were run on an SDS-PAGE gel and transferred to PVDF. The blots were probed with CRP, and SAP with or without 10 mM EDTA. Blots were also probed with no pentraxin with no binding seen in these experiments. LP = log phase *L. mexicana* material enriched for LPG; M = Metacyclic *L. mexicana* material enriched for LPG, + E = with 10 mM EDTA. In **B** and **C**, 1 µg/mL of LPG was immobilised to a plate and probed with 0.027- 2 µg/mL SAP or CRP in or out of the presence of LT6 – an antibody against the [-6Galβ1,4Manα1-PO$_4$-]$_x$ on LPG. In **D** and **E**, 2 µg/mL LPG, PC-BSA or 1:20 PEth-cellulose were immobilised to a plate and probed with 0.5 µg/mL SAP or CRP in the presence of increasing concentrations (0.027 – 20 µg/mL) of the other pentraxin. For all graphs, the mean is shown (n=3), with error bars representing SD. **B** and **C** statistics used Wilcoxon matched-pairs signed rank tests, **D** and **E** used Two-tailed paired t test, *$P<0.05$, **$P<0.01$, ***$P<0.001$.
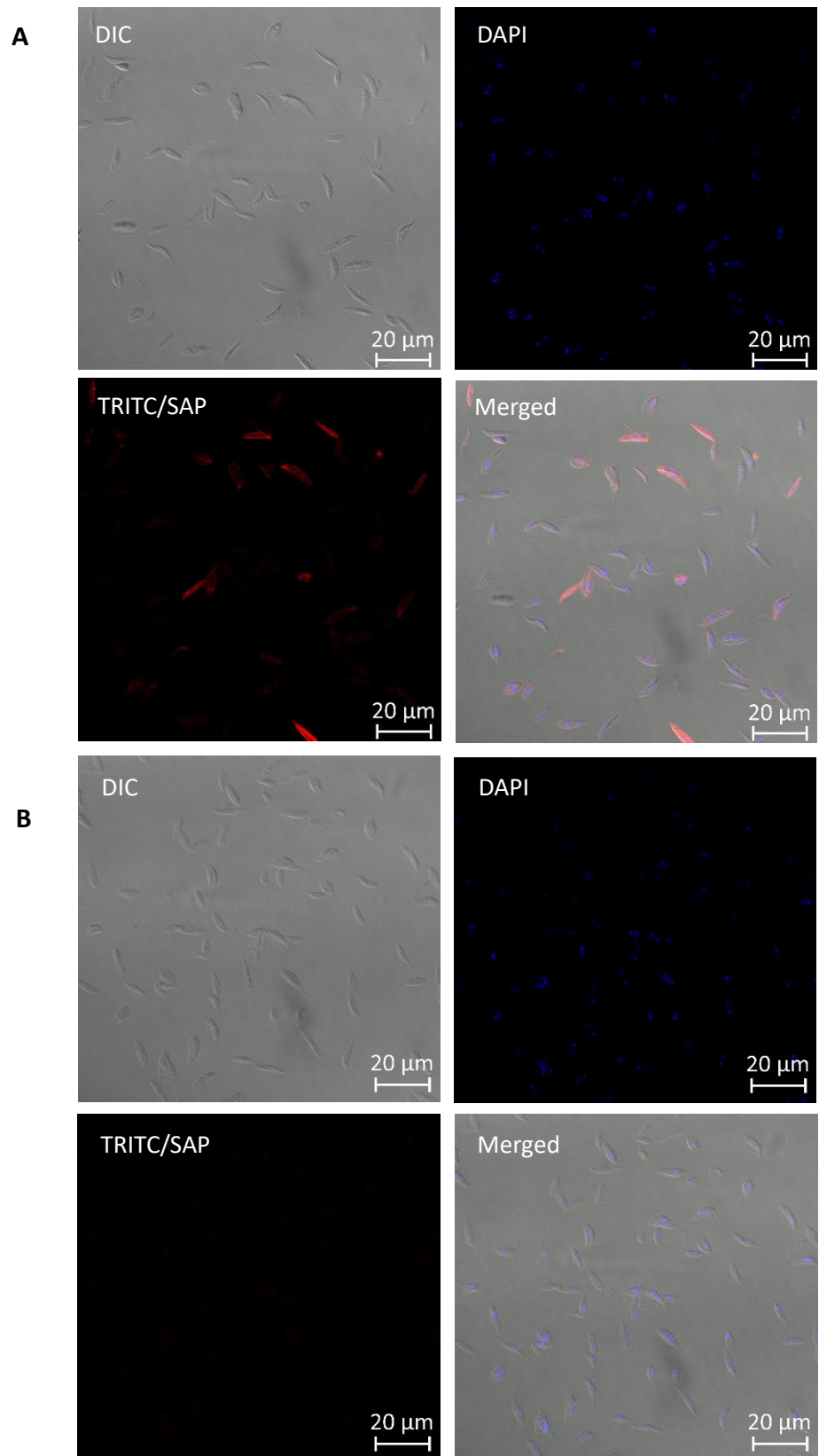
Figure 4. SAP can bind to LPG-deficient *Leishmania mexicana*. *L. mexicana lpg1*$^{-/-}$ parasites were washed, incubated with 10 μg/mL SAP, washed and resuspended in 4% paraformaldehyde. Parasites were washed and airdried to a slide followed by incubation with primary and secondary antibodies and imaged using the Zeiss LSM880 confocal microscope (**A**). No staining was seen when parasites were incubated with SAP with 15 mM EDTA (**B**) or when no SAP was present.

A

B
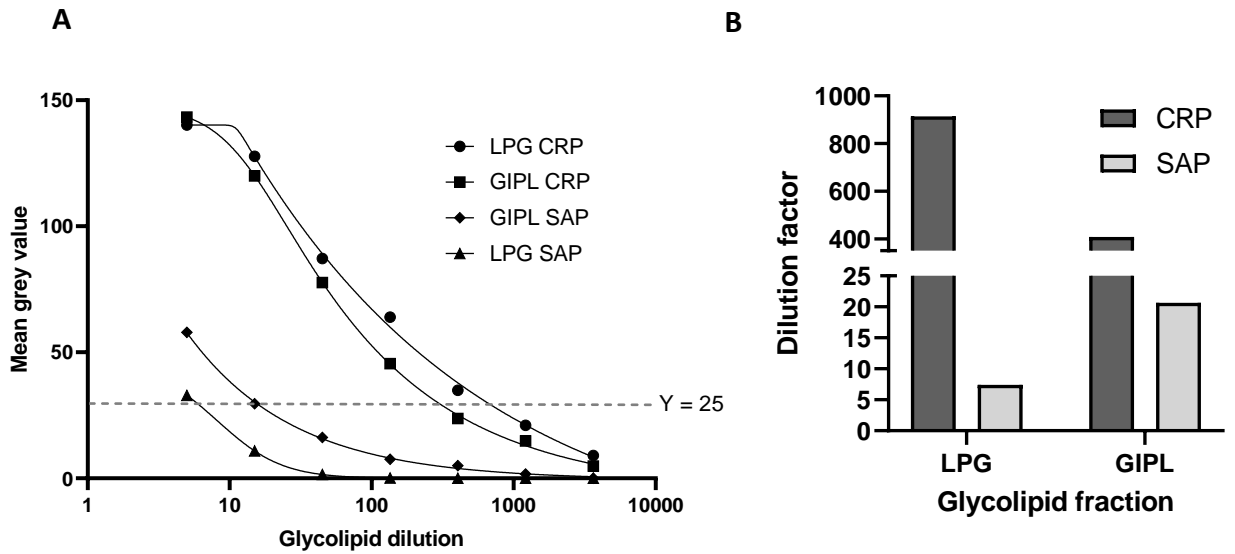
Figure 5. SAP preferentially binds *Leishmania mexicana* GIPL-enriched material, whereas CRP binds LPG-enriched material. Dots (3 µL) of serial diluted GIPL- and LPG-enriched material was probed with SAP and CRP. The mean grey value of each dot was calculated using ImageJ and plotted against the glycolipid dilution factor (**A**). Binding of the pentraxins to each glycolipid fraction was then compared at a set mean grey value (Y = 25) (**B**).
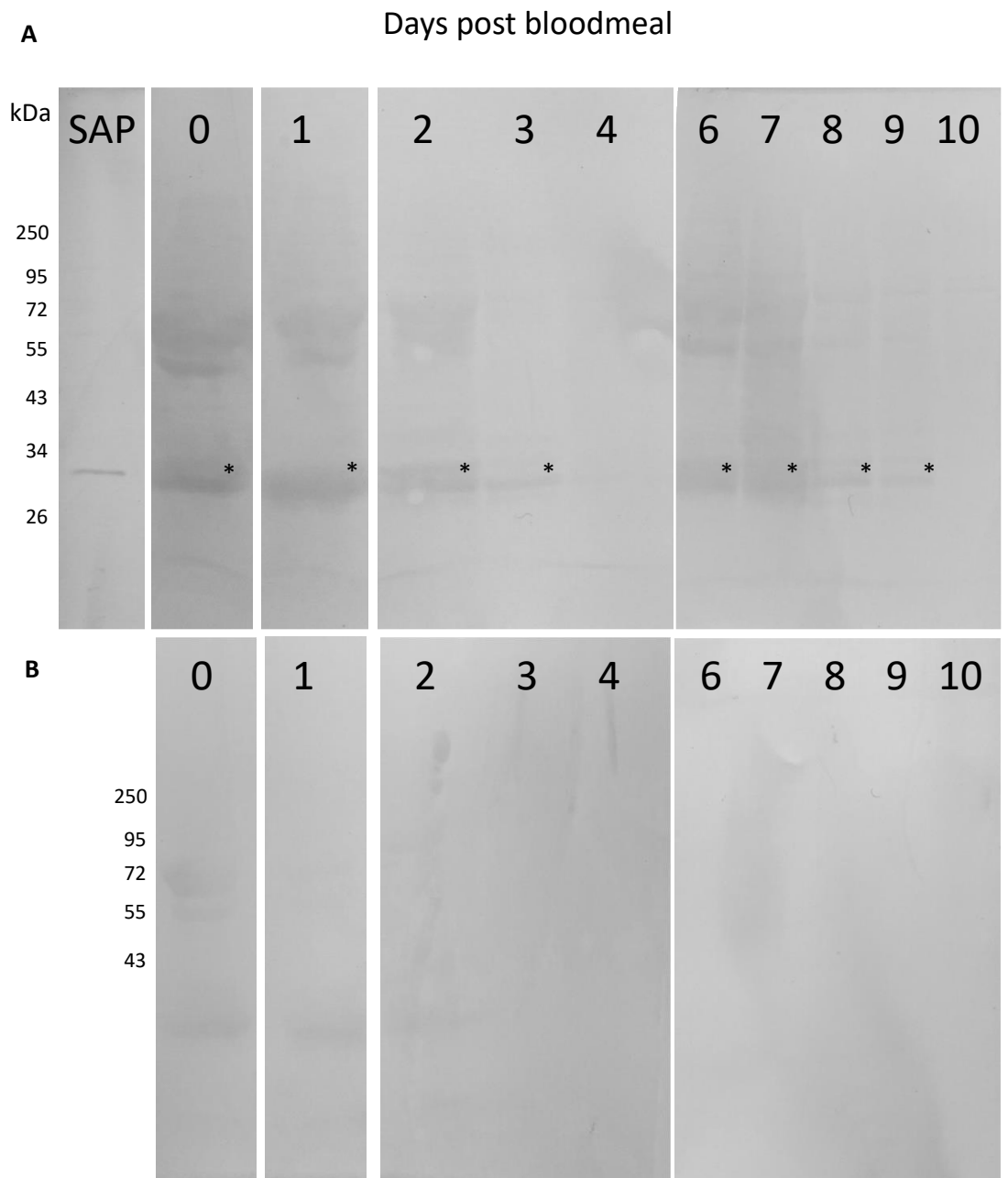
Figure 6. SAP in detected in the bloodmeal of a sand fly up until defecation of the bloodmeal remnants. Previously unfed flies were blood fed and dissected each day for 5 days, midgut proteins were extracted and the equivalent of 2 midguts per lane run on an SDS-PAGE gel. The proteins were transferred to a PVDF membrane and probed with anti-SAP and AP-conjugated secondary antibodies. For days 6-10, the same was done, but with flies given a second bloodmeal. SAP bands are indicated with an asterisk (**A**). The same was carried out but membranes were either probed with the secondary antibody only (days 0-4) or with an isotype control antibody, followed by the secondary (days 6-10) (**B**).
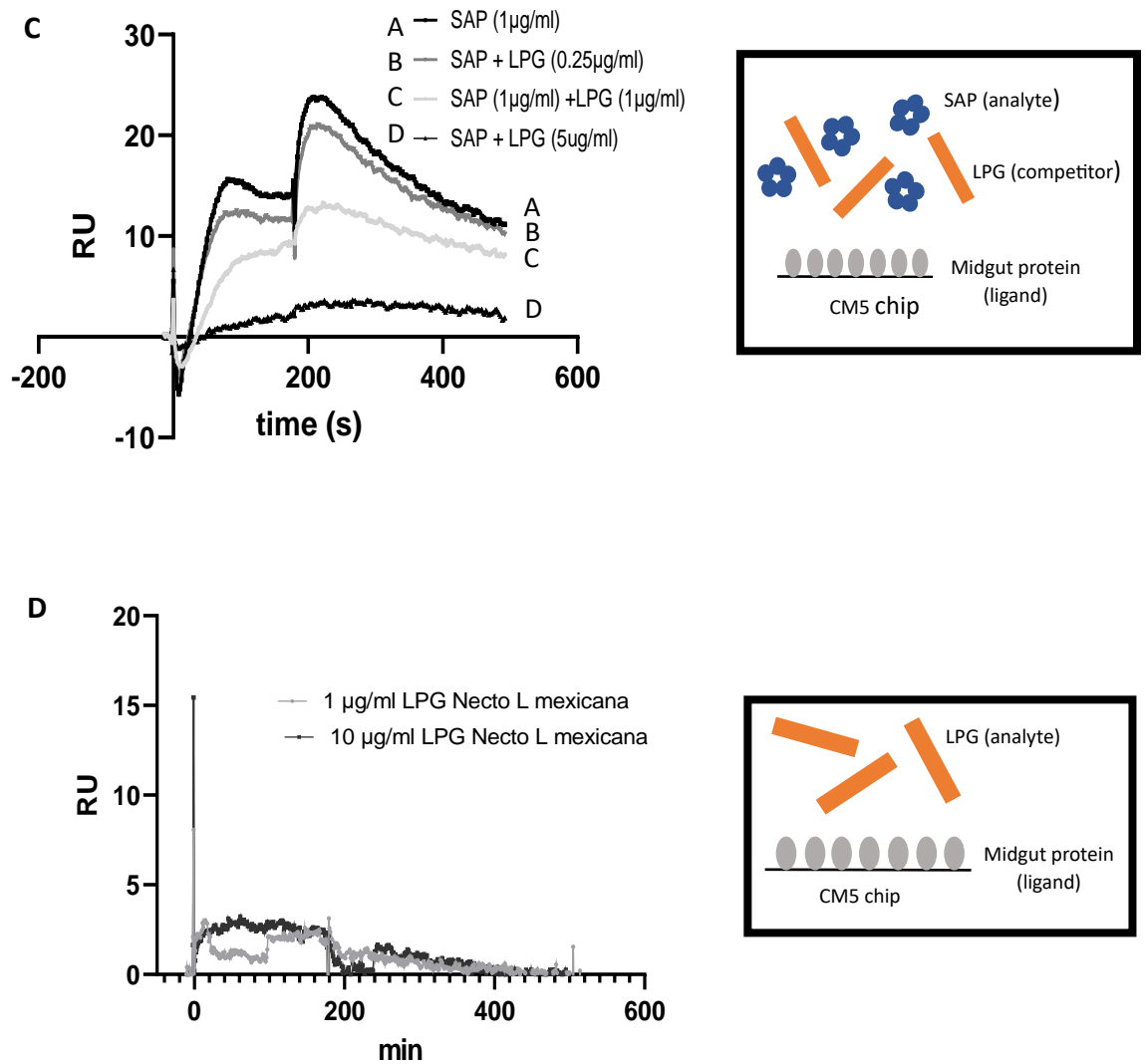
Figure 7. SAP, but not CRP, binds *Lutzomyia longipalpis* microvillar-enriched midgut extract. *Leishmania mexicana* **LPG can block SAP binding to the extract, but LPG does not bind the extract. A** *Lu. longipalpis* midgut proteins were extracted and enriched for microvillar proteins as previously described (Dillon and Lane, 1999). This was carried out using previously unfed adult males and females, with 1 μg of sample run under non-reducing conditions on an SDS-PAGE gel, transferred to PVDF and probed with 1 μg/mL SAP. 1 μg of sample from female flies fed on different diets was run per lane under reducing conditions, transferred and probed with SAP and CRP (**A**). SPR analysis of SAP binding to midgut protein extract coupled to a CM5 chip is seen in **B-D**. **B** Binding of SAP (1 and 10 μg/mL) passed over 850 RU of immobilised midgut protein. Association phase 3 minutes, dissociation 5 minutes and regenerated with 10 mM EDTA. 30 μL/mL flow rate. **C** Inhibition of binding of SAP by *L. mexicana* nectomonad (necto) LPG (0.25, 1.0 and 5 μg/mL) in association phase. **D** No significant binding of necto LPG (1 and 10 μg/mL) passed over 850 RU of immobilised midgut protein.
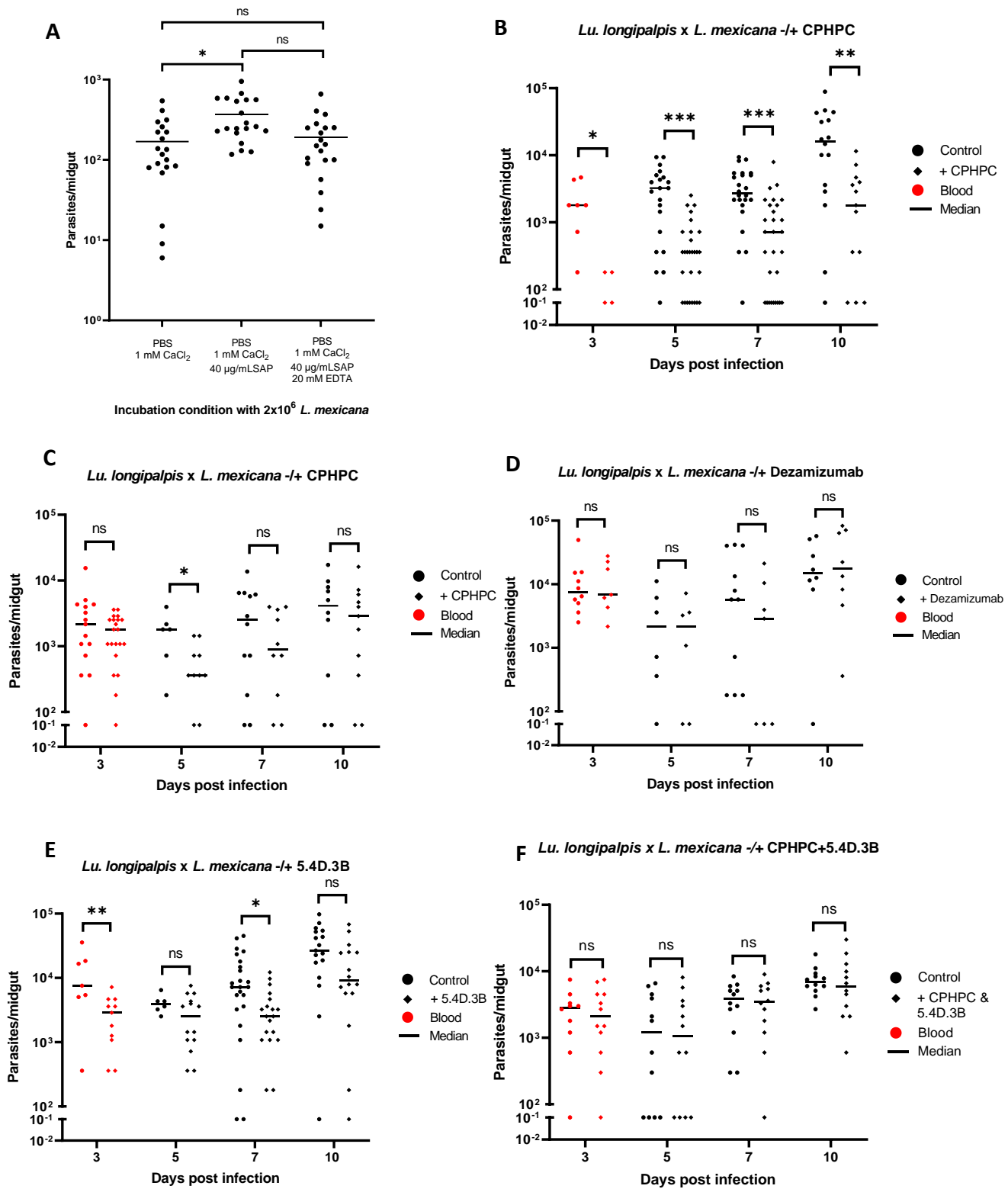
Figure 8. SAP and anti-SAP drug and antibodies do not seem to affect *Leishmania mexicana* attachment to the *Lutzomyia longipalpis* midgut. A *Ex vivo* midgut binding assays were carried out by incubating dissected and unzipped *Lu. longipalpis* midguts with 2×10^6 *L. mexicana.* Parasites were washed and resuspended in PBS containing 1 mM $CaCl_2$ only, + 40 µg/mL SAP or + 40 µg/mL SAP + 20 mM EDTA prior to incubation with midguts. **B-F** Unfed *Lu. longipalpis* were fed through a chicken skin membrane on heat-inactivated human blood, containing 25 µg/mL SAP and 5×10^5/mL axenic *L. mexicana* amastigotes (control). In **B** and **C**, the test sample also contained 1 mg/mL CPHPC, a competitive inhibitor of SAP (Pepys et al., 2002). The test in **D** contains 1:50 dezamizumab (67 µg/mL), and in **E** the test contains 1:50 5.4D.3B (2 µg/mL) which are both anti-SAP antibodies. In **F**, the test contained both 1 mg/mL CPHPC and 1:50 5.4D.3B (2 µg/mL). At day 3, only flies that still had their bloodmeal were included. After this, only parous flies which had defecated their bloodmeal were included. 0 results are plotted as 0.1 so a log scale could be used. The Kolmogorov-Smirnov test was used for statistical analysis, *$P<0.05$, **$P<0.01$, ***$P<0.001$.

	Phase contrast	DAPI	AF660/LT6	Merged
Amastigote				
Procyclic				
Nectomonad				
Leptomonad				
Haptomonad				
Metacyclic				

Phase contrast   DAPI   AF660/LT6   Merged
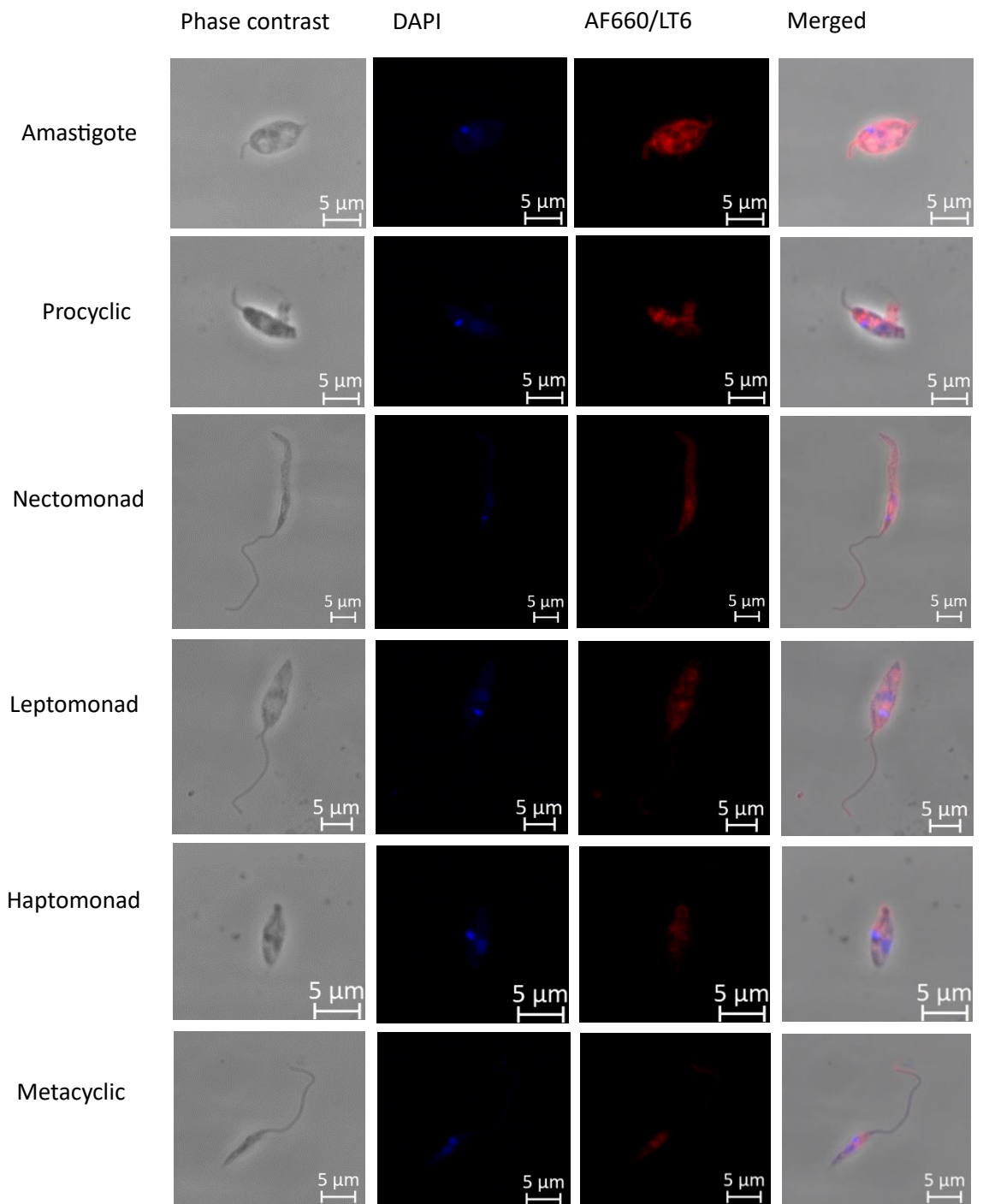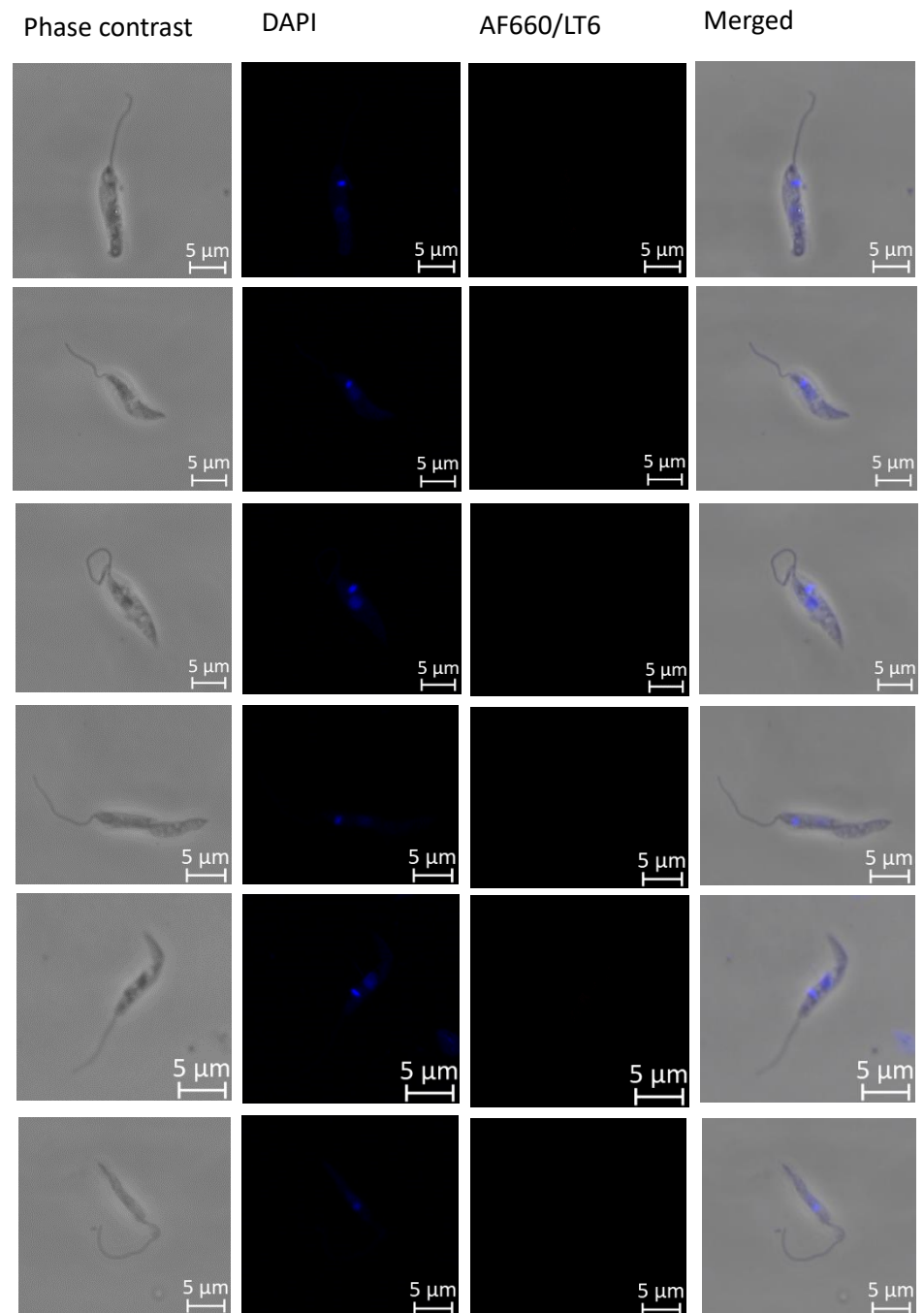
Figure S1. **LT6 binds to all *Leishmania mexicana* morphological stages.** However, binding varied between individual parasites. *L. mexicana* culture was sampled daily. Parasites were washed and resuspended in 4% paraformaldehyde. Parasites were then washed and airdried to a slide. The slides were incubated with LT6 followed with anti-mouse-AF660 antibody and imaged using the Zeiss LSM880 confocal microscope (**A**). No staining was seen when parasites were incubated without LT6 (**B**). Scale bars in white represent 5 µm.
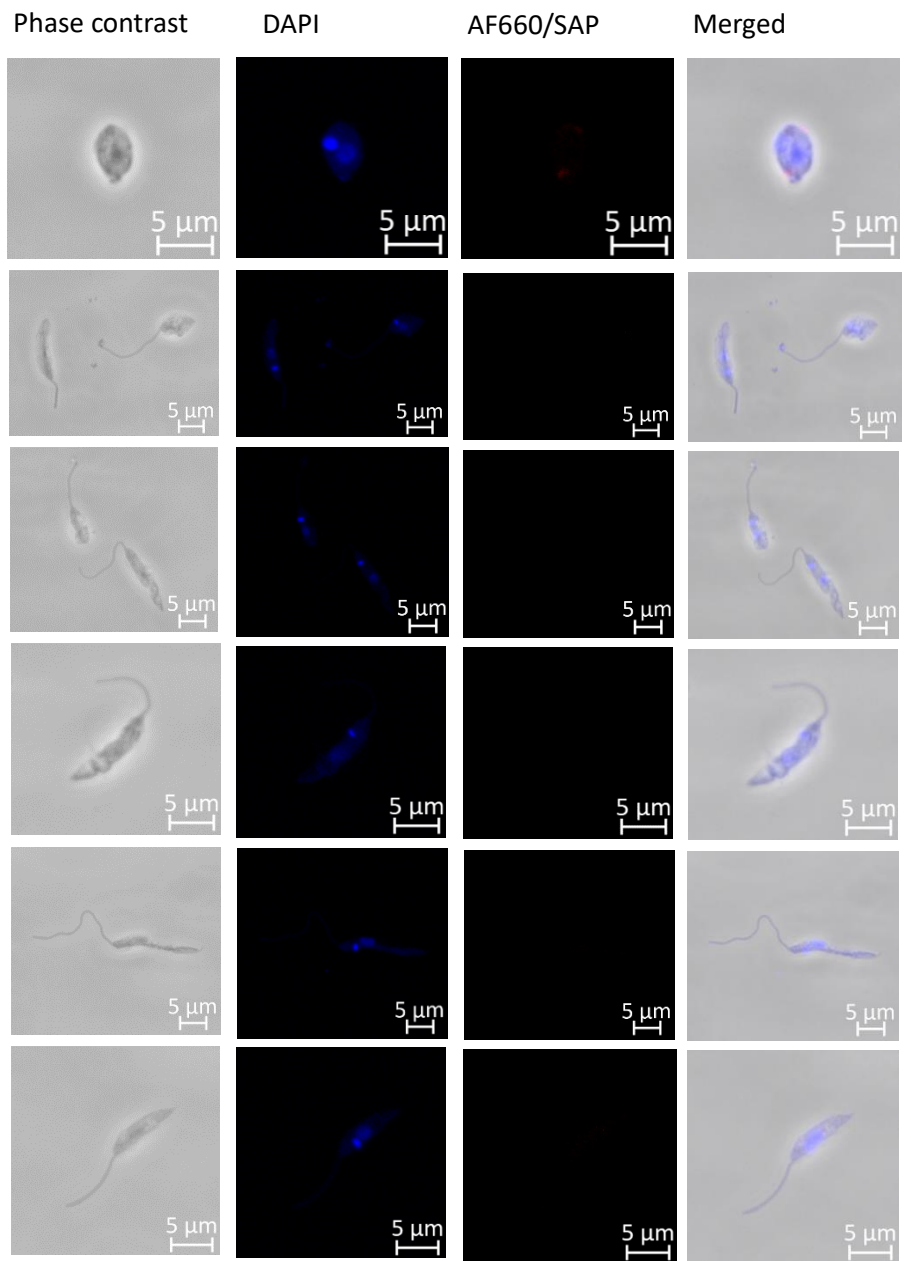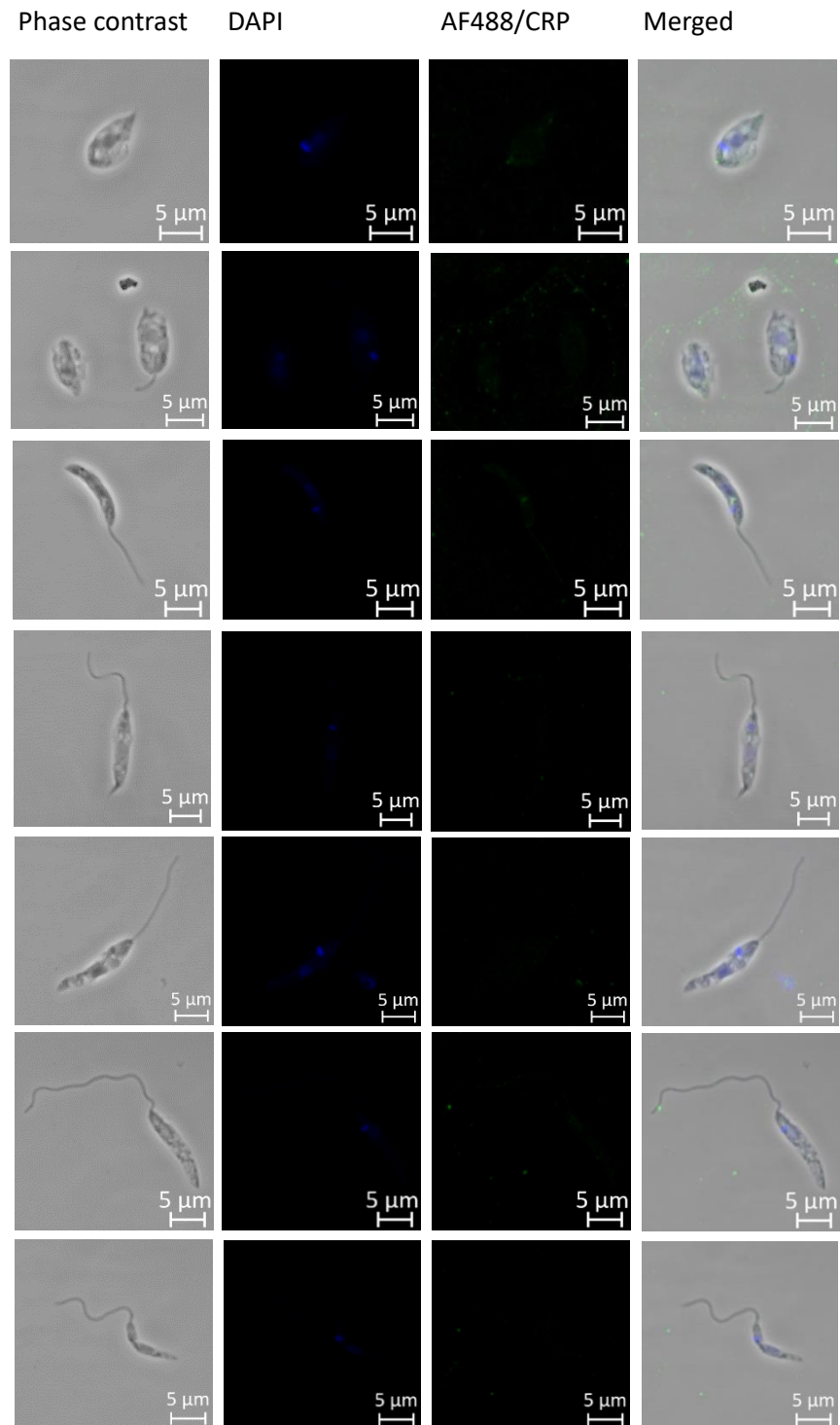
Figure S2. **No pentraxin binding to *Leishmania mexicana* is seen in the presence of EDTA.** Parasites were washed and resuspended in 4% paraformaldehyde. Parasites were then washed and airdried to a slide. The slides were incubated with SAP (A) or CRP (B) with EDTA, followed with primary and secondary antibodies and imaged using the Zeiss LSM880 confocal microscope. Scale bars in white represent 5 μm.
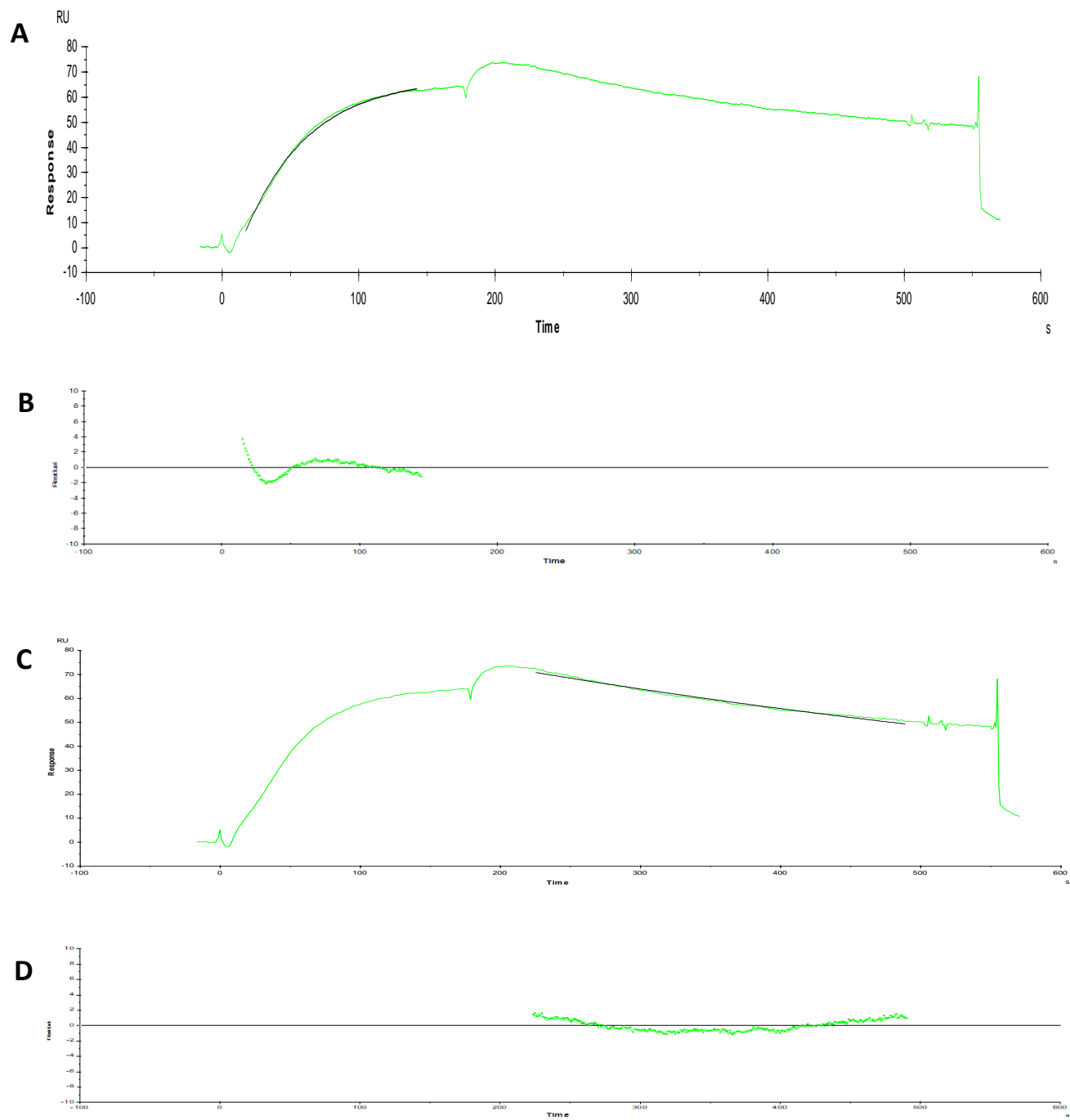
Figure S3. Example of SPR Langmuir 1:1 analysis. Separate on and off rate calculations for 1 µg/mL SAP seen in Figure 7B. Elution with 10 mM EDTA in flow buffer can be seen at 560 seconds. **A** shows association, with an association rate constant (K_a) of 2.51×10^6 (1/Ms), with the residuals of this analysis seen in **B. C** shows dissociation, with a dissociation constant (K_d) of 1.3×10^{-3} (1/s), with the residuals for this analysis seen in **D**.

6. C-reactive protein binds to short phosphoglycan repeats of *Leishmania* secreted proteophosphoglycans and activates complement

RESEARCH PAPER COVER SHEET

Please note that a cover sheet must be completed <u>for each</u> research paper included within a thesis.

SECTION A – Student Details

Student ID Number	1601303	Title	Miss
First Name(s)	Eve Christina		
Surname/Family Name	Doran		
Thesis Title	The role of human pentraxins for the *Leishmania*-vector interaction		
Primary Supervisor	Dr Matthew Rogers		

If the Research Paper has previously been published please complete Section B, if not please move to Section C.

SECTION B – Paper already published

Where was the work published?	Published (with edits to that shown here) in Frontiers in Immunology		
When was the work published?	31/08/23		
If the work was published prior to registration for your research degree, give a brief rationale for its inclusion			
Have you retained the copyright for the work?*	**Yes**	Was the work subject to academic peer review?	**Yes**

*If yes, please attach evidence of retention. If no, or if the work is being included in its published format, please attach evidence of permission from the copyright holder (publisher or other author) to include this work.

"The ownership of copyright in the text of individual articles (including research articles, opinion articles, book reviews, conference proceedings and abstracts) is not affected by its submission to or publication by Frontiers, whether for itself or for a Hosted Journal" (Frontiers, 2020).

Frontiers | Frontiers Copyright Statement [Internet]. 2020 [cited 2024 January 10] Available from: https://www.frontiersin.org/legal/copyright-statement

SECTION C – Prepared for publication, but not yet published

Where is the work intended to be published?	
Please list the paper's authors in the intended authorship order:	
Stage of publication	Choose an item.

SECTION D – Multi-authored work

For multi-authored work, give full details of your role in the research included in the paper and in the preparation of the paper. (Attach a further sheet if necessary)	I carried out the Western blot work seen in Figure 2 and Figure 5 as well as the immunofluorescence work seen in Figure 4. This paper was written by John Raynes.

SECTION E

Student Signature	EVE DORAN
Date	20/06/2023

Supervisor Signature	MATTHEW ROGERS
Date	04/07/2023

C-reactive protein binds to short phosphoglycan repeats of *Leishmania* secreted proteophosphoglycans and activates complement

Seow, Eu Shen., Doran Eve. C., Schroeder, Jan-Hendrik., Rogers, Matthew E., Raynes, John G*.

Dept. of Infection Biology, Faculty of Infectious and Tropical Diseases, London School of Hygiene and Tropical Medicine, Keppel St., London. WC1E 7HT.

*Corresponding author john.raynes@lshtm.ac.uk

Abstract

Human C-reactive protein (CRP) binds to lipophosphoglycan (LPG), a virulence factor of *Leishmania* spp*.,* through multiple repeats of the phosphodisaccharide region. We report here that both major components of promastigote secretory gel (PSG), the filamentous proteophosphoglycan (fPPG) and the secreted acid phosphatase (ScAP), are also ligands. CRP binding was mainly associated with the flagellar pocket when LPG-deficient *Leishmania mexicana* parasites were examined by fluorescent microscopy, consistent with binding to secreted material. ScAP is a major ligand in culture purified proteophosphoglycans (PPG) as demonstrated by much reduced binding to a ScAP-deficient mutant PPG in plate binding assays and ligand blotting. Previously we showed high avidity of CRP for LPG ligand that required multiple disaccharide repeats. Surface Plasmon Resonance (SPR) analysis showed that fPPG and ScAP also had high avidity for CRP despite having only short disaccharide repeat units due to the density of the carbohydrate ligands. The PPGs from many species such as *Leishmania donovani* and *L. mexicana* bound CRP strongly but *Leishmania tropica* and *Leishmania amazonensis* had low amounts of binding. The extent of side chain substitution of [$-PO_4$-6Galβ1-4Manα1-] disaccharides correlates inversely with binding of CRP. The ligand for the CRP on different species all had similar binding avidity as the half maximal binding concentration was similar. CRP bound strongly to the PSG from infected sand flies. Since the PSG is injected with the parasites into host blood pools and phosphoglycans (PG) are known to deplete complement, we showed that CRP makes a significant contribution to the activation of complement by PPG using serum from naive donors.

180

Introduction

Leishmaniasis is a zoonotic disease caused by the *Leishmania* genus of protozoan parasites and a major neglected tropical disease, with 1.5 to 2 million estimated cases and 50,000 fatalities per year. It affects diverse mammalian species and is transmitted by female *Phlebotominae* sand flies during bloodmeal feeding attempts.

During the insect stage and during the infection of mammalian hosts the parasites produce a variety of phosphoglycan structures that aid in their survival and virulence (Rogers, 2012). These include the relatively well studied membrane-associated lipophosphoglycan (LPG) ligand. However, parasites also produce proteophosphoglycans (PPG) including filamentous proteophosphoglycan (fPPG) and secreted acid phosphatase (ScAP) in the infected sand fly. The secreted PPGs are introduced into the feeding site as part of the promastigote secretory gel (PSG) alongside mammalian-infectious metacyclic promastigotes and sand fly saliva. Studies using knock outs of *LPG1* or *LPG2* have shown a complicated virulence phenotype varying for different parasites, for instance, LPG deficiency in *Leishmania major* (Spath et al., 2000) and *Leishmania infantum* (Jesus-Santos et al., 2020) show virulence in mammalian infection studies but *Leishmania mexicana* did not (Ilg et al., 2001).

Proteophosphoglycans share similar glycan moieties to LPG, as shown by the cross-reactivity of many antibodies between LPG and the PSG components fPPG and ScAP (Ilg et al., 1993). ScAP and fPPG have high carbohydrate contents, which form more than 70% of their molecular weight. While their exact function is currently unknown, PSG injected with or without saliva promotes cutaneous leishmaniasis infection in murine studies, suggesting that PSG may be a virulence factor (Rogers et al., 2004; Rogers et al., 2010). The main component of PSG is fPPG, a mucin-like molecule. The types and structures of the phosphoglycans show some similarities but also significant differences between species in terms of when expressed, glycan content and whether secreted or membrane bound. ScAP, is associated with fPPG and the subunits are hard to dissociate from the polymer structure (Ilg et al., 1994). The potential role of PSG in establishing human infection remains an underreported field of study, particularly in light of the likely importance of the early immune response to the determination of leishmaniasis outcome.

Among a number of possible innate recognition molecules, CRP has been shown to bind to *Leishmania* surface LPG (Culley et al., 1996). Classically CRP is known to bind in a calcium-dependent way to phosphorylcholine (PCh) which is a common component in a variety of fungal, bacterial and parasitic products. In this manner, CRP acts as an important innate immune activator of the classical complement pathway via CRP (Kaplan and Volanakis, 1974;

Haapasalo and Meri, 2019). In the case of *Leishmania*, CRP binds with high affinity in a calcium-dependent manner to the phosphorylated galactose mannose disaccharide repeat found in *Leishmania* lipophosphoglycan (Culley et al., 1996). High affinity interactions required between 3 and 10 repeats of [-PO$_4$-6Galβ1-4Manα1-] when provided as a chemically synthesised soluble form (Culley et al., 2000). This interaction with LPG has biological relevance for a number of reasons. It can lead to increased uptake into macrophages under physiological conditions, although this may not lead to increased killing but rather aid the parasite in establishing infection (Bodman-Smith et al., 2002). In addition, the binding of the CRP to the surface of the parasite has also been shown to help the parasite initiate transformation in *L. mexicana* (Bee et al., 2001) and *L. donovani* (Mbuchi et al., 2006). CRP interaction with LPG thus has importance in infection of the mammalian host from the sand fly.

This report now investigates the potential interaction of CRP with the PSG phosphoglycans. Whilst the longer LPG from metacyclic parasites shows greatly increased binding to CRP compared to 'non-infectious log phase promastigotes' both these have much greater length than that reported for the phosphoglycans of ScAP and proteophosphoglycans that have typically an average of 2-3 repeats (Ilg et al., 1994). Individual soluble synthetic structures were shown to have only very weak ability to interact with CRP (Culley et al., 2000). However, we demonstrate here that the interaction of CRP with the short repeats of [-PO$_4$-6Galβ1-4Manα1-] presented in multiple sites on a proteophosphoglycan can be high avidity.

One way in which the interaction of CRP might alter infection rates and/or survival of the parasite is through the complement pathway. CRP binding of a ligand does not inevitably lead to complement activation as seen recently for a phosphorylcholine substituted glycoprotein ES-62 (Ahmed at al., 2016). The LPG is a known activator of complement particularly to extended LPG in metacyclic forms causing deposition of C3b but without damaging the parasite (Sacks, 1992). This is in contrast to logarithmic phase parasites which are all rapidly killed by complement. It is already known that a potentially important role of secreted PPGs in PSG such as fPPG and ScAP is the activation and depletion of complement. PPG injected into a mouse could dramatically deplete complement by 90% within 30 minutes (Peters et al., 1997). The potential mechanisms of this could be classical or lectin pathway mediated as the activation was calcium-dependent but a role for CRP was not assessed. Here we show that using naïve donor sera CRP makes a significant contribution to the total complement activation by the proteophosphoglycan thereby implicating a role in complement depletion.

Methods

Purification of proteophosphoglycan

In this report, proteophosphoglycan (PPG) will be used to refer to fPPG and ScAP purified from parasite culture supernatant. PSG will only be used to refer to the material extracted from an infected fly.

Parasites of *Leishmania mexicana* (MNYC/BZ/62/M379); *Leishmania major* (LV39; (MRHO/SU/59/P); *Leishmania donovani* (MHOM/ET/67/HU3); *Leishmania panamenensis* (MHOM/PA/67/BOYNTON); *Leishmania infantum* (MHOM/BR/76/M4192); *Leishmania amazonensis* (LV79: MPRO/BR/72/M1841); *Leishmania aethiopica* (MHOM/ET/84/KH); *Leishmania tropica* (MHOM/AF/2015/HTD7) were cultured as described (Rogers et al., 2009). Lipophosphoglycan (LPG)- and phosphoglycan-deficient *L. mexicana* were a kind gift from Dr Thomas Ilg. The LPG-deficient mutant (*lpg1*$^{-/-}$) lacks the *LPG1* gene, which encodes a galactofuranosyltransferase required for synthesis of the LPG glycan core, rendering them deficient in LPG alone whilst *L. mexicana lpg2*$^{-/-}$ lacks all repeating phosphodisaccharides. Selection antibiotics hygromycin (20 µg/mL) and phleomycin (2.5 µg/mL) were added to the culture medium (Ilg, 2000; Ilg et al., 2001) for deficient *L. mexicana* mutants *lpg1*$^{-/-}$ and *lpg2*$^{-/-}$. *L. mexicana* Δ*lmScAP*1/2 and an add back of *ScAP2* were a kind gift of Dr Wiese (Wiese, 1998) which employed a similar selection antibiotic pressure but included G418 (10 µg/mL) in the add back.

Culture supernatants were clarified by centrifugation at low speed (800 g) and passed through an anion exchange column (DE-52) equilibrated in 20 mM Tris-HCl, 100 mM NaCl, pH 7.5 at a rate of 2 mL/min and eluted in 20 mM Tris-HCl, pH 7.5 containing 500 mM NaCl (Ilg et al., 1996). Following anion exchange, material was pelleted by ultracentrifugation at 100,000 g, 4°C for 4 hours in a Ti90 rotor and the pellet washed and resuspended in PBS.

A further step to remove more hydrophobic fractions such as LPG used hydrophobic interaction chromatography. Pelleted material was adjusted to 1 M ammonium sulphate via dilution with concentrated ammonium sulphate solution (10 M NH$_2$SO$_4$, 1:9 v/v ratio relative to material and added to a 5 mL column of octyl-Sepharose equilibrated in 20 mM Tris-HCl, 1 M NH$_2$SO$_4$, 5 mM EDTA, pH 7.5. This was followed by low ionic strength Tris-buffered saline (10 mL, 20 mM Tris-HCl, 100 mM NaCl, pH 7.5), Tris-buffered saline (20 mL, 20 mM Tris-HCl, pH 7.5) and then propan-1-ol (20%, 70% v/v) which eluted more hydrophobic glycans such as LPG. Quantification was based on A280 (Nanodrop) which correlated with the carbohydrate assay using the phenol-sulphuric acid method (Masuko et al., 2005). PPG material was dialysed and stored at -80°C in 20 µL aliquots.

The biotinylation of PPG was performed using a method with NHS-LC-biotin in pH 9.6 carbonate buffer as described previously (Ilg et al., 1996). Labelled material was repurified by anion exchange on DE-52 as used for purification with extensive washing to remove unreacted biotin. Plate assays showed biotin-PPG and PPG had similar CRP binding dose responses (data not shown).

Unfed *Lutzomyia longipalpis* flies (Jacobina colony, 3-5 days old) were fed through a chicken skin membrane on heat-inactivated (h.i.) human blood containing 2-3x10^6 *L. mexicana* axenic amastigotes/mL in an artificial feeder (Hemotek). Flies were maintained at 26°C and were fed 50% sucrose *ad libitum*. After day 7 post infection, flies were dissected in a drop of PBS with the digestive system removed and PSG carefully collected as previously described (Rogers et al., 2010).

CRP and biotinylated CRP

Human CRP and recombinant CRP were purified as described previously (Ahmed et al., 2016). Rat CRP was purified using phosphorylcholine Sepharose by the same protocol. CRP was biotinylated at a neutral pH as described for the reagent NHS-LC-biotin (Thermofisher) to prevent CRP denaturation. The CRP-biotin was repurified on PCh-Sepharose to remove non-binding protein with extensive washing to remove unreacted biotin.

PPG-pentraxin plate binding assays

Purified PPG (0-3 µg/mL) in PBS pH 7.4 was coated onto 96 well microtiter plates (Immulon™ 2 HB 96-Well Microtiter EIA Plate, ImmunoChemistry Technologies, LLC). Biotinylated and affinity purified CRP (0-3 µg/mL) in HBSC-BSA was added and the plates were incubated at room temperature for 1 hour. For inhibition assays, PCh chloride (Sigma-Aldrich) or EDTA (10 mM) or MgCl$_2$ (0.5 mM) and 10 mM EGTA or CRP depleted serum (5% v/v) was added at the CRP incubation stage. After washing with HBSC, the bound CRP was detected with streptavidin-HRP (Biosource diluted 1 in 15,000) and 3,3',5,5'-Tetramethylbenzidine (TMB, 0.1 mg/mL) in phosphate-citrate buffer (0.05 M, pH 5.0) with hydrogen peroxide (0.006% v/v) added following an HRP-conjugated antibody incubation stage. The subsequent colour change reaction was stopped with H$_2$SO$_4$ (2 M, 15 µL). The plate was read at wavelength 450 nm with subtraction of the reference wavelength at 405 nm (Titertek Multiskan MCC/340). Alternatively native pure CRP was used and detected with primary antibody rabbit anti-CRP (Dako: 1:800) followed by HRP-conjugated goat anti-rabbit IgG (Bio-Rad, 1:3000) in HBSC-BSA. Mouse CRP binding was examined using the same buffer system and plates but using mouse CRP and affinity purified goat anti-mouse CRP (both R and D).

Western/ligand blot and protein gel staining

SDS-PAGE was performed using an extended 4% stacking gel layer in combination with a 6% or 10% resolving gel layer with reducing conditions. The molecular weight standards used were prestained, broad range (10-250 kDa, New England Biolabs).

Gels were then stained with Coomassie blue or Stains-all (Ilg et al., 1993) or transferred by semi-dry blotting to PVDF membranes. Membranes were blocked with PBST containing 2% (w/v) BSA at 4°C o/n. Membranes were incubated with CRP-biotin (1 µg/mL) or CRP (as shown in Figures) in TBST containing 0.5 mM $CaCl_2$ and 1% (w/v) BSA for 1 hour at room temperature and after 3 washes in the same buffer, bands where CRP bound were visualised with streptavidin-alkaline phosphatase (AP) (1 in 500; SA5100 Vector labs) or anti-CRP-AP and colorimetric detection with substrate BCIP/NBT as described (Ahmed et al., 2016). Detection of phosphoglycan repeated disaccharide was performed using 1:1000 CA7AE (GTX39838, GeneTex) then followed by 1:30,000 anti-mouse IgM-AP (A-9688, Sigma). Fluorescent based detection was similar but used a combination of rabbit α-CRP (Dako, 1:1000) followed by IRDye® 800CW goat anti-rabbit IgG (Li-Cor) with false colour images captured and analysed on an Odyssey® CLx Imaging System (Li-Cor).

Surface plasmon resonance

Polycarboxylate chips with high charge density (Xantec, C30M) were washed and activated with EDC and NHS for 7 minutes. Aminodesthiobiotin at 0.5 mM in 10 mM sodium maleate buffer pH 6.8 was added at a flow rate of 2 µL/min for 40 minutes to give 150 RU attached. Reactive groups on both test and control surfaces were blocked with 1 M ethanolamine pH 8.0. Neutravidin (10 µg/mL) in calcium-containing HEPES buffer (HBSPC) was then immobilised on the desthiobiotin surface of both test and control surface to give a further 150 RU. Biotin labelled purified PPG was then added at 20 µg/mL till 220 RU was attached to the test well only. CRP was flowed over at 30 µL/min for 3 minutes at various concentrations in HBSPC buffer containing 0.5 mM $CaCl_2$ and dissociation assessed for 5 minutes before CRP was dissociated with HBS containing 10 mM EDTA. In other experiments, inhibitors were added with the CRP or other proteins. Between each addition, the chip was washed with HBS containing 10 mM EDTA.

Dextran-free C1 chips (Biacore) were directly immobilised with PPG purified by ultracentrifugation. The chip was activated with EDC and NHS and immobilisation was performed using amine coupling according to a standard protocol. PPG diluted to 100 µg/mL in 10 mM acetate buffer pH 4.5 was added to test Fc only at 5 µL/min till 420 RU was attached. Ethanolamine (1 M; pH 8.0) was used to block both control and test flow cells. Human or rat CRP binding was assessed using similar conditions and elution strategies as above.

Analysis was performed using BiaEval 4.1.1. Control flow cells were subtracted and traces overlain. Kinetic data was obtained using Langmuir analysis with separate analysis of on-rate and off-rate for each concentration.

Serum CRP depletion

Carboxylated magnetic beads (Mobitec-beads, 100 µL) were washed into PBS buffer. N-(3-Dimethylaminopropyl)-N'-ethylcarbodiimide (10 µL, 10 mg/mL) was added to the beads and left to incubate at room temperature on a rocker for 5 minutes. Chicken anti-CRP IgG antibody (1 mg/mL, 25 µL, Norwegian Antibodies) was added and left to incubate and cross-link overnight at room temperature. Blocking of remaining active cross-linking sites was achieved by incubation in 0.1 M glycine buffer (pH 8.3) for 1 hour at room temperature. Beads were washed into phosphate-buffered saline pH 7.4 with BSA (1% w/v) then washed into HEPES-buffered saline (20 mM HEPES, 150 mM NaCl, pH 7.4) with 0.5 mM $CaCl_2$ (HBSC) and stored at 4°C. Whole serum from normal, healthy donors collected under ethical approval (100 µL) was mixed with the anti-CRP beads and allowed to incubate on a rocker at 2°C for an hour immediately prior to experiments. Typical reduction in CRP concentrations were 50-95% determined using a sandwich ELISA for CRP (de Yong et al., 2016).

Complement assays:

C1q capture assay

An immune complex capture assay (Ahmed et al., 2016) was used to measure complex formation between CRP and different CRP ligands, including PPG or control PCh-BSA.

Purified C1q (Calbiochem, 10 µg/mL) was coated onto 96 well microtiter plates (Immulon 4 HBX, Thermo Fisher Scientific) at 4°C overnight. Plates were incubated with BSA (3% w/v) and Tween-20 (0.05% v/v) in PBS for non-specific site blocking at room temperature for 2 hours.

Serum was obtained from healthy donors under informed consent at London School of Hygiene and Tropical Medicine (ethical approval 10672/RR/3680). Serum was diluted (1:20 v/v) with CRP (1 µg/mL) and BSA (1% w/v) in veronal-buffered saline (VBS) with 0.15 mM $CaCl_2$ and 0.5 mM $MgCl_2$, with or without EDTA (10 mM). CRP ligand (PPG, PCBSA) was added at a range of concentrations (0-3 µg/mL), and the plate was incubated at room temperature for 1 hour. Detection step was performed with a sheep anti-CRP conjugated with horseradish peroxidase (1:2000).

C3d deposition assay

To assess C3 convertase formation, an existing protocol to detect the C3 convertase downstream product C3d was adapted (Ahmed et al., 2016). *L. infantum* or *L. mexicana* PPG (4 µg/mL) or PCh-BSA (0.4 µg/mL) was diluted in PBS and immobilised on 96 well microtiter plates (Immulon™ 2 HB 96-Well Microtiter EIA Plate, ImmunoChemistry Technologies, LLC). Ligand concentration was chosen to allow equivalent CRP binding as determined by previous CRP-ligand ELISA.

In order to prevent complement activation until the start of the experiment, all serum additions were carried out with the reagents, serum and microtiter plate on ice ($0^{o}C$). Donor serum was added to the wells (1:100 dilution) in GVBSCaMg (VBS with 0.2% v/v gelatin, 0.15 mM $CaCl_2$ and 0.5 mM $MgCl_2$), with or without additional purified CRP (0.4 µg/mL). C3d deposition with or without purified CRP was also analysed in the presence or absence of the non-specific ion chelator EDTA (10 mM), and the specific calcium chelator EGTA (10 mM) plus 0.5 mM $MgCl_2$.

Plates were brought up to a uniform temperature in a water bath ($37^{o}C$) and incubated for 20 minutes. For C3d detection, plates were incubated with primary biotinylated anti-C3d antibody (1:1000) followed by HRP conjugated streptavidin (1:15000) in HBSC-BSA.

iC3b deposition assay

For iC3b deposition, plates were washed and iC3b detected with 1 µg/mL biotinylated antibody to neoepitope of iC3b (Quidel) followed by streptavidin-HRP (Invitrogen).

Immunofluorescent (confocal) microscopy

A total of 10^6 *lpg1*$^{-/-}$ and WT *L. mexicana* parasites were washed with PBS and incubated in M199 medium containing 10 µg/mL CRP, control media only or media with CRP and 15 mM EDTA for 1 hour at room temperature. Parasites were centrifuged and fixed in 4% (w/v) PFA, washed and 2.5×10^5 parasites air dried onto slides. Slides were rehydrated and stained with rabbit anti human CRP (Calbiochem) followed by anti-rabbit IgG FITC (Dako) both for 1 hour with washing between stages. The slides were dried and counterstained with Vectorshield + DAPI and coverslips attached. Slides were visualised using the Zeiss LSM880 confocal microscope and 63x objective. Image analysis was carried out using ZEN Blue lite with brightness and contrast edited to maximise the signal from the images. A 405 nm laser diode was used to excite DAPI and a 488 argon laser to excite AF488. For *lpg1*$^{-/-}$ images, the frame time was 13.47 seconds and for wild-type, the frame time was 28.16 seconds.

Results

L. mexicana *PPG binds to CRP*

Purified PPG showed a heterogeneous but very high molecular weight as previously described and as shown by stains all of material above 100 kDa (Figure S1). Western blotting showed material in the stacking gel and above 200 kDa in the resolving gel that contained phosphoglycan as revealed by the monoclonal antibody CA7AE. This material was adsorbed onto a microtitre plate and CRP showed strong binding with a half maximal binding seen at 30 ng/mL (Figure 1A) with significant binding detected at less than 1 ng/mL CRP. This binding was not inhibited by the presence of 5% (v/v) CRP-depleted serum indicating a lack of competition by other serum proteins at any CRP concentration (Figure 1B). Although most LPG is removed at the hydrophobic interactions stage of purification, to confirm that CRP binding was not due to contamination by small quantities of LPG we also showed binding to PPG from a mutant lacking LPG (*lpg1*^{-/-}) (Figure 1C). In contrast, the same preparations from the *LPG2* mutant that lacks all addition of phosphoglycan to any protein or lipid showed no binding of CRP (Figure 1C). As expected for an interaction with the major ligand binding site on CRP, the relatively lower affinity ligand soluble monomer phosphorylcholine (PCh) significantly inhibits CRP-binding in a competitive manner (Figure 1D). The binding was inhibitable completely with either EDTA or EGTA Mg (Figure 1A and 1B) consistent with the calcium-dependent binding site seen previous for binding of CRP to LPG (Culley et al., 1996).

Kinetics of CRP-PPG interaction by SPR

Binding of CRP to immobilised *L. mexicana* PPG (Figure 1E) was examined over a range of CRP concentrations utilising the calcium dependency to allow complete elution of CRP between associations. As previously reported for other ligands, CRP shows complex interaction kinetics as expected for a pentamer binding to a ligand that is also potentially multimeric (Ahmed et al., 2016). The analysis used a low density of PPG on the surface to reduce the potential for multimeric interaction. We used an estimate based on the simplest analysis since no more complex analysis would lead to a more meaningful set of data for different binding states. The average off-rate (k_d) was approximately $1.2-1.7 \times 10^{-3}$ s^{-1} for *L. mexicana* in this orientation (Figure S2A and Table 1). The on-rate was approximately 5×10^5 M^{-1}s^{-1} for CRP at 2.5 and 5 µg/mL when the curve analysis was most accurate (Figure S2B). Overall avidity was estimated at 3×10^{-9} M consistent with the nanomolar CRP concentrations at which CRP binds in plate assays. PPG from *L. mexicana* LPG-deficient (*lpg1*^{-/-}) mutant also bound in SPR experiments (data not shown).

CRP of other mammalian species also binds to repeating disaccharide

CRP is present at high concentrations in the rat sera and easily purified on PCh Sepharose, therefore we tested binding and showed that rat CRP bound strongly to PPG in a calcium-dependent way (Figure S3). We saw little interaction with human SAP which was previously shown not to bind to LPG nor to hamster female protein an SAP homologue. A further control confirmed that these proteins purified on PCh were not binding to PCh as a monoclonal antibody to PCh did not bind to PPG (data not shown). Although CRP in mice is relatively low in concentration and sex dependent, the low concentrations required for binding are within physiological concentrations and we tested recombinant mouse CRP binding to PPG from different species. The order of binding was in broad agreement with that seen for human CRP (Figure S4). The only exceptions being *L. amazonensis* (moderate rather than weak) and *L. mexicana* (strong rather than moderate).

The major CRP binding component of the purified PPG is the ScAP component

CRP was also shown to bind to the PPG when separated by electrophoresis and transferred to membrane and the membrane was probed with CRP. Binding in the resolving gel was consistent with the molecular weight of ScAP. Binding to the material in the stacking gel could be to the filamentous proteophosphoglycan or to the acid phosphatase as this is strongly associated with the fPPG (Ilg et al., 1994).

Therefore we used a mutant of *L. mexicana* that lacks both secreted acid phosphatases (Δ*lmScAP*1/2) and an add back of *ScAP2* (Wiese, 1998). The filamentous phosphoglycan is also a ligand as the mutant still retained binding in the stacking gel by blotting which could only be the fPPG (Figure 2A). Quantitation of relative binding by microtitre plate binding assay confirmed the reduced CRP binding to the ScAP-deficient PPG (Figure 2B). Binding of CRP was partially restored in the add back as seen in both assays (Figure 2A and 2B). In the add back, the amount of restored CRP binding was low, consistent with the plate binding assays but clearly associated with the ScAP2 that generated a band in the region of 200 kDa (Figure 2B). This suggested that the ScAP was a major ligand for CRP binding PPG.

CRP binding to PPG from different Leishmania species shows similar high avidity but different ligand density.

We examined the binding to PPG derived from different *Leishmania* species. The species included were five from the Old World and three from the New World and these are shown in these groups in Figure 3A where binding was performed with a dose response of CRP to a constant PPG on the plate. In contrast, the panels in Figure 3B show the binding of a constant

CRP to a range of ligand coating concentrations. The dose response of CRP binding to all parasites (Figure 3A) suggests that the ligand is of a similar high avidity for most parasites since the half maximal binding concentration (1-20 ng/mL) was similar for most species. High amounts of CRP binding represented a greater density of sites and binding to different species varied considerably at constant CRP (Figure 3B), for example, *L. donovani* had approximately 2 orders of magnitude more than *L major*. There was no link between Old and New World species, nor did CRP binding appear different between species that cause different clinical presentation (visceral, cutaneous, or mucocutaneous). Previous studies by Thomas Ilg had characterised the proteophosphoglycan structures of different *Leishmania* species and correlated this with reactivity to monoclonal antibodies. A major factor in differences between species was side chain substitution, with strongest binding seen to those species that had little side chain substitution (discussed later).

The binding of CRP in plate assays was confirmed by the ligand blotting assays which showed a large amount of binding to material in the separating gel consistent with binding to ScAP (Figure 3C). *L. donovani* and *L. panamenensis* PPG had particularly high binding capacity. *L. tropica* as in the plate assays shown very little CRP binding activity.

CRP binding to PPG in lpg1$^{-/-}$ parasites is located to the flagellar pocket

In order to locate the CRP ligand in the LPG-deficient and wild-type parasites we performed immunofluorescent detection of ligand on live mutant and wild-type parasites. The wild-type showed strong and even binding across the surface of the parasite (Figure 4B) consistent with previous data for *L. donovani* (Culley et al., 1996). In contrast the *lpg1*$^{-/-}$ strain showed staining that was localised close to the flagellar pocket (Figure 4A). In order to observe this, the methodology was altered to reduce washing post CRP addition. If the parasites were centrifuged and resuspended in wash buffer then we observed numerous punctate staining particles separate from the parasites consistent with detached secreted PPG-CRP complex (data not shown).

CRP binding to native sand fly derived proteophosphoglycan (PSG) is mainly to fPPG

Although CRP binds to the purified cultured parasite PPG, it was important to determine the binding to the physiological native promastigote secretory gel (PSG) found in infected sand flies. Previously it was shown that in *L. mexicana* the sand fly PSG was mainly composed of fPPG and there was little ScAP (Stierhof et al., 1999). PSG is associated with the parasites in the sand fly but also introduced at sand fly bites, therefore PSG was generated by microdissection and tested for binding to the CRP. Consistent with the limited ScAP presence we saw little binding to 200 kDa but very strong binding to the stacking gel and fPPG (Figure 5). This

suggests that the main ligand in sand fly PSG was fPPG in contrast to the purified PPGs from cultured parasites. Since the PSG from infected sand flies also contains *Leishmania* parasites the presence of LPG is detected as a broad band at around 50 kDa.

CRP binding to PPG activates complement

It was previously shown that *L. infantum* PSG when injected with parasites caused an increased local survival of parasites (Rogers et al., 2010) and *L. infantum* phosphoglycan is implicated in parasite virulence (Jesus-Santos et al., 2020). fPPG and ScAP from *L. infantum* and *L. me*xicana bound CRP in a similar way (Figure 2 and 3). A proteophosphoglycan from *L. mexicana* amastigotes with similar carbohydrate structure to fPPG including repeating disaccharide was previously shown to deplete complement (Peters et al., 1997). Therefore, we chose PPG from both these parasites to explore the ability of bound CRP to activate complement.

Using a capture assay with C1q attached to the plate with serum containing CRP showed no binding of CRP to the C1q until PPG addition which then generated a complex with the C1q. This showed a dose response as expected (Figure 6A). *L. tropica* did not lead to binding (Figure 6A) consistent with the PPG from this species failing to interact with CRP previously (Figure 3A and B). This interaction would be expected to lead to complement activation. This was confirmed when *L. mexicana* PPG was used as a ligand coated onto the plate surface with deposition of C3bi or C3d demonstrated to be by the classical pathway (Figure 6B). Activation was increased by addition of CRP and reduced when CRP was partially depleted (Figure 6C). The depletion of CRP was about 50-95% but the strong binding of CRP to its ligand suggests that the CRP would still have some contribution to the overall complement activation in this depleted sera. Nevertheless, it was possible to demonstrate that a significant proportion of the activation of complement in serum was mediated by CRP. The lack of phosphoglycan and CRP ligand in *L. mexicana lpg2*$^{-/-}$ mutant resulted in a lack of CRP dependent complement activation (Figure S5).

When CRP was added to individual sera and C3d activation was assayed there was a clear and consistent increase in activation apparent across different individual sera (Figure 6D). Activation was similar or greater than that for a PCh-BSA positive control, a known strong ligand for CRP mediated complement activation. The background activation was however also variable suggesting a potential cross-reacting antibody was present in some sera.

Discussion

CRP binding to ScAP and fPPG

Previously we demonstrated CRP binding to the extended repeating disaccharide of LPG. Here we have demonstrated the CRP can also bind with high avidity to multiple short disaccharides expressed on a backbone of a high molecular weight glycoprotein. Although previously we observed weak binding of CRP to soluble short repeats of the disaccharide in solution (Culley et al., 2000), the binding to multiple such structures on fPPG or ScAP was able to generate affinities similar to those seen previously to LPG. Although serum did not inhibit binding to the repeating disaccharide suggesting that CRP is the only major serum protein interacting with this epitope, CRP is not the only serum protein that binds to fPPG and the glycan structures present. These include antibody and mannose-binding lectin (MBL) which have been detected by us using methods such as immunoprecipitation and others such as MBL which bound to amastigote PPG (aPPG) containing similar phosphoglycans to fPPG (Peters et al., 1997). The binding was consistent with the known binding properties of CRP in terms of calcium dependency and phosphorylcholine inhibition, in addition the kinetics showed that the avidity of binding was largely related to a slow off-rate (Figure 1E) perhaps not surprising given the multimeric nature of this interaction.

The observation that rat CRP binds *L. mexicana* PPG is interesting, showing the phenomena is not restricted to human CRP although this needs extending to further species. Rat CRP is present at high concentrations and is not an acute phase protein but also has interesting binding features in that it binds to PCh but does not require the amino regions of the choline. In contrast, the HFP which is a homologue of SAP but also binds to phosphocholine in addition to phosphoethanolamine (Coe et al., 1981) did not bind.

For purified PPG we observed that most of the binding was to the ScAP component, despite being a minor component in terms of amount produced (Wiese, 1998). fPPG having less binding for CRP is possible due to differences in the glycosylation of the PPG which has a shorter Gal-Man repeat compared with ScAP and more frequent end capping that could mask the availability of the short repeat structure (Klein et al., 1999). However, the purification involved column separations and it is quite plausible that this process has enriched the lower molecular species at the expense of fPPG rich complexes trapped due to size by affinity media. The major ligand in PSG from sand flies was fPPG as very little binding was seen in gels corresponding to ScAP. This does not rule out some binding in the stacker gel being due to ScAP but since fPPG is the major component this indicates that the major ligand in the gel is fPPG. The *fPPG1* gene is present in most *Leishmania* species and fPPG has been shown in *L.*

mexicana, *L. major*, *L. amazonensis*, *Leishmania braziliensis*, *L. tropica* and *L. aethiopica* (Ilg et al., 1991). The gel of PSG from infected sand flies also contains LPG as expected, revealed by CRP and CA7AE binding. We have focused on *L. mexicana* but conclusions about relative binding of CRP will not necessarily apply to other species since ultrastructural features such as not forming filament networks have been recorded for *L. donovani* (Stierhof et al., 1994). Differences in size of fPPG and developmental changes have been shown for *L. major, L. mexicana* and *L. donovani* (Montgomery et al., 2002). There was no evidence for binding to other phosphoglycans such as aPPG or pPPG2 (Göpfert et al., 1999) nor is aPPG a likely ligand since repeating disaccharide monoclonal LT6 does not bind (Klein et al., 1999).

Secretion of proteophosphoglycan

The secreted polymer PPG has previously been shown to be located and polymer proposed to assemble in the flagellar pocket (Stierhof et al., 1994) so we expected that PPGs would be localised here. This was demonstrated and shown to be quite different to the pattern for LPG-containing parasites where the LPG ligand is located over the whole parasite surface. The secreted PPG was more localised to the flagellar pocket than previously suggested when *L. donovani* was analysed (Samant et al., 2007). In this study using an antibody generated to a protein part of fPPG, the whole surface was also found to be labelled but there is little evidence elsewhere for the presence of fPPG bound to the surface. However, alternative carbohydrate substituted variants may be possible and there was heterogeneity in fPPG observed in our studies and elsewhere. Membrane PPGs (mPPG2) have been reported but do not appear to be a major feature in *L. mexicana* in terms of CRP binding as seen in the lack of CRP binding to the membrane in fluorescent micrographs of *lpg1*$^{-/-}$ parasites and consistent with structure discussed earlier.

Inverse correlation of binding and side chain substitution

Previous analysis of CRP binding to different *Leishmania* species LPG showed a high density of binding sites to certain species including *L. donovani*, whilst others only showed very weak or lack of binding to LPG. The binding was correlated inversely with the presence of LPG side chain substitution on the repeating disaccharide regions which hindered access to the disaccharide (Raynes et al., 1994). Monoclonals generated against phosphoglycan structures show strong similarity in their ability to bind proteophosphoglycan and LPG from the same parasite (Ilg et al., 1993; Bates et al., 1990). In addition, comparison of the LPG and PPG side chains characterised by anion exchange HPLC show essentially the same pattern of structure for LPG and PPG but for *L. mexicana* the PPG contained much less side chain (Ilg et al., 1996). Therefore, we predicted that CRP binding to PPG from different *Leishmania* would show the

same pattern of binding as seen for LPG. *L. donovani* LPG is classified as type I with no side chain substitution and therefore we predicted that *L. donovani* PPG would be a strong binder as was found. Also in the *Viannia* subgenus, *L. braziliensis* and *L. panamenensis* have little side chain substitution (Muskus et al., 1997) and *L. panamenensis* was found to be a good binder of CRP. In other reports *L. braziliensis* procyclic forms have variable side chain substitution but the metacyclic forms do not (Soares et al., 2005). The binding to *L. donovani* was also interesting because it had much longer repeat units (up to 32) on the ScAP analogous to that seen in LPG (Lippert et al., 1999). *L. infantum* is devoid of side chain in the procyclic LPG form but has some in the metacyclic stage (Soares et al., 2002) and most strains of *L. infantum* are type I but variability is seen in certain strains (Coelho-Finamore et al., 2011).

L. tropica LPG (classified as type 2) has been shown to be highly substituted with almost all repeating units substituted at the C-3 position of the galactose with structures that are longer and often terminated with arabinopyranose (McConville et al., 1995). *L. amazonensis* has a high proportion of C-3 Gal positions substituted with chains of 2-3 sugars (Noguiera et al., 2017) and notably does not have significant binding to the CA7AE antibody that binds to repeating disaccharide repeats. Both these would suggest that CRP would have poor binding as indeed was demonstrated. Another LPG type 2 is *L. major* but this parasite shows considerable variation between strains for side chain substitution (McConville et al., 1995). It was observed that the side chain substitution of the *L. major* fPPG was less than that observed for the LPG from the same parasite, perhaps leading to significant CRP binding in these studies compared to *L. tropica* which did not bind.

L. aethiopica is known to be a type 3 LPG with substitution of a single mannose on the C-2 of mannose of the LPG repeats (McConville et al., 1995). It was previously suggested that this substitution site would have considerable effects on the conformation of LPG and its backbone which was supported by the failure of monoclonals to the repeating disaccharide to bind to this parasite LPG (Schnur et al., 1972). CRP bound strongly to the PPG, suggesting the different conformation of the repeating disaccharide allows CRP binding.

Phosphoglycans including the repeating disaccharide appear to be a feature across the *Leishmania* spectrum and most recently were confirmed in *Leishmania (Mundinia) enriettii* (Paranaíba et al., 2015). However, there is no information about *Leishmania (Sauroleishmania) tarentolae*. The good correlation between low side chain substitution of *Leishmania* PPGs and strong CRP binding is consistent with the presence of the genes responsible for phosphoglycan synthesis, particularly those responsible for repeating disaccharide and side chain substitution (SCGs and SCGR families) in different species (Azevedo et al., 2020).

Complement activation by PPG

It was important to know if CRP activated complement at and beyond the C3 stage when binding to a phosphoglycan. Previously we showed that binding of CRP to another glycan structure terminating in a phosphorylcholine substituted onto an N glycan of filaria parasites effectively bound C1q and was able to generate C4b. However, this did not efficiently activate C2 and thus did not lead to an active C3 convertase but did deplete complement (Ahmed et al., 2016). This was related to the mobility of the glycan. For filaria, the lack of complement activation was important since any inflammatory response is damaging to survival, however infectious *Leishmania* is largely resistant to complement attack. It is not surprising therefore that the parasite generates material capable of strong activation of complement. PPG injected into a mouse could dramatically deplete complement by 90% within 30 minutes (Peters et al., 1997) and lasted for 24 hours. The potential mechanisms of this could be classical or lectin pathway mediated as the activation was calcium-dependent and MBL was able to bind to the PPG but CRP was not assessed. The mouse is unusual in that CRP is present at low levels even during inflammation. PPG as a component in sand fly bites is however more relevant to early infection in mammals.

The role for different complement pathways in activation of complement by *Leishmania* at the site of infection through surface and secreted components which are mainly phosphoglycan dominated is poorly defined. Whilst many studies have shown a role of the alternative pathway for killing of promastigotes by human serum (Hoover et al., 1984; Mosser et al., 1986), this evidence came from parasites being killed in serum depleted of different components and lysed in Mg-EGTA but not EDTA buffers. Whilst there is little evidence for CRP or other innate proteins such as MBL or innate antibody having a role in killing metacyclic infectious promastigotes, these experimental systems may be too simplistic and do not rule out other roles for such activation in terms of altering survival *in vivo.*

It was previously shown that early stage infections with *L. amazonensis* promastigotes caused a reduction in complement in mice. Complement-depleted mice showed an increased parasite burden and lacked the C3 deposition seen in non-depleted mice at the site of infection and also showed a rescued inflammatory response. This suggests that complement activation in the site of infection was increasing uptake and survival (Laurenti et al., 1996).

CRP makes a significant contribution to the activation of complement seen to PPG. Although significant data was generated with addition and depletion, our methodology for CRP depletion and addition was only partially effective with residual CRP in depleted sera and normal non supplemented sera still able to provide some activation. Thus, the relative contribution of CRP

may be underestimated. Whilst normal CRP concentrations (less than 10 µg/mL) are sufficient to cause strong binding to PPG, concentrations are usually high in *Leishmania* patients (Wasunna et al., 1995). A recent paper reported that *L. infantum* promastigotes activated both the classical and alternative pathways to different extents in different sera (dog, cat, and human). Each however caused functional depletion of both pathways (Tirado et al., 2021).

PPG has been reported to be involved in a number of cell responses in the infected host (Rogers, 2012), thus CRP may also have influence on responses other than complement or other responses indirectly through the complement effect.

These data demonstrate CRP-PPG interactions can have a role in parasite infection in sand flies when CRP is ingested as part of the bloodmeal. Effects of the bloodmeal are complex and have significant effects on parasite differentiation and infectivity (Serafim et al., 2018). This may be further complicated because insects have complement-inactivation mechanisms to protect their own epithelium which will affect the parasite susceptibility to bloodmeal derived complement (Mendes-Sousa et al., 2013). CRP may alter the physiological state of the phosphoglycan and/or the interaction with the parasite.

In conclusion, we found CRP is able to bind both ScAP and fPPG that make up PSG. CRP binding to PPGs from different *Leishmania* species is inversely correlated with side chain substitution, similar to previously seen for CRP binding to LPG. The CRP-PPG interaction is able to activate and deplete complement. Though the current study focuses on the role of CRP within the human host, these interactions may also be applicable to the sand fly vector.

References

Rogers ME. The role of *Leishmania* proteophosphoglycans in sand fly transmission and infection of the mammalian host. Front Microbiol. 2012;3:223. doi: 10.3389/fmicb.2012.00223.

Spath GF, Epstein L, Leader B, Singer SM, Avila HA, Turco SJ, Beverley SM. Lipophosphoglycan is a virulence factor distinct from related glycoconjugates in the protozoan parasite *Leishmania major*. Proc Natl Acad Sci USA. 2000;97(16):9258–9263. doi: 10.1073/pnas.160257897.

Jesus-Santos FH, Lobo-Silva J, Ramos PIP, Descoteaux A, Lima JB, Borges VM and Farias LP. LPG2 gene duplication in *Leishmania infantum*: a case for CRISPR-Cas9 gene editing. Front Cell Infect Microbiol. 2020;10:408. doi: 10.3389/fcimb.2020.00408.

Ilg T, Demar M, Harbecke D. Phosphoglycan repeat-deficient *Leishmania mexicana* parasites remain infectious to macrophages and mice. J Biol Chem. 2001;276(7):4988-4997. doi: 10.1074/jbc.M008030200.

Ilg T, Harbecke D, Wiese MA, Overath P. Monoclonal antibodies directed against *Leishmania* secreted acid phosphatase and lipophosphoglycan. Eur J Biochem. 1993;217:603-615.

Rogers ME, Ilg T, Nikolaev AV, Ferguson MA, Bates PA. Transmission of cutaneous leishmaniasis by sand flies is enhanced by regurgitation of fPPG. Nature. 2004;430:463-467. doi: 10.1038/nature02675.

Rogers ME, Corware K, Müller I, Bates PA. *Leishmania infantum* proteophosphoglycans regurgitated by the bite of its natural sand fly vector, *Lutzomyia longipalpis*, promote parasite establishment in mouse skin and skin-distant tissues. Microbes Infect. 2010;12(11):875-879. doi: 10.1016/j.micinf.2010.05.014.

Ilg T, Overath P, Ferguson MA, Rutherford T, Campbell DG, McConville MJ. O- and N-glycosylation of the *Leishmania mexicana*-secreted acid phosphatase. Characterization of a new class of phosphoserine-linked glycans. J Biol Chem. 1994;269(39):24073-24081.

Culley FJ, Harris RA, Kaye PM, McAdam KPWJ, Raynes JG. C-reactive protein binds to a novel ligand on *Leishmania donovani* and increases uptake into human macrophages. J Immunol. 1996;156:4691-4696.

Kaplan MH, Volanakis JE. Interaction of C-reactive protein complexes with the complement system. I. Consumption of human complement associated with the reaction of C-reactive protein with pneumococcal C-polysaccharide and with the choline phosphatides, lecithin and sphingomyelin. J Immunol. 1974;112:2135–47.

Haapasalo K, Meri S. Regulation of the complement system by pentraxins. Front Immunol. 2019;10:1750. doi: 10.3389/fimmu.2019.01750.

Culley FJ, Bodman-Smith KB, Ferguson MAJ, Nikolaev AV, Shantilal N, Raynes JG. C-reactive protein binds to phosphorylated carbohydrates. Glycobiology. 2000;10:59-65.

Bodman-Smith KB, Mbuchi M, Culley FJ, Bates PA, Raynes JG. C-reactive protein mediated phagocytosis of *Leishmania donovani* promastigotes does not alter parasite survival or macrophage responses. Parasite Immunol. 2002;24:447-454.

Bee A, Culley FJ, Alkhalife IS, Bodman Smith K, Pratdesaba RA, Raynes JG, Bates PA. *Leishmania mexicana*; differentiation and signal transduction in metacyclic promastigotes mediated by C-reactive protein. Parasitology. 2001;122:521-529.

Mbuchi M, Bates PA, Ilg T, Coe JE, Raynes JG. C-reactive protein initiates transformation of *Leishmania donovani* and *L. mexicana* through binding to lipophosphoglycan. Mol Biochem Parasitol. 2006;146(2):259-64.

Ahmed UK, Maller NC, Iqbal AJ, Al-Riyami L, Harnett W, Raynes JG. The carbohydrate-linked phosphorylcholine of the Parasitic Nematode product ES-62 modulates complement activation. J Biol Chem. 2016;291(22):11939-53.

Sacks DL. The structure and function of the surface lipophosphoglycan on different developmental stages of *Leishmania* promastigotes. Infect Agents Dis. 1992;1(4):200-206.

Peters C, Kawakami M, Kaul M, Ilg T, Overath P, Aebischer T. Secreted proteophosphoglycan of *Leishmania mexicana* amastigotes activates complement by triggering the mannan binding lectin pathway. Eur J Immunol. 1997;27(10):2666-2672.

Rogers M, Kropf P, Choi BS, Dillon R, Podinovskaia M, Bates P, Müller I. Proteophosophoglycans regurgitated by *Leishmania*-infected sand flies target the L-arginine metabolism of host macrophages to promote parasite survival. PLoS Pathog. 2009;5(8):e1000555. doi: 10.1371/journal.ppat.1000555.

Ilg T. Lipophosphoglycan is not required for infection of macrophages or mice by *Leishmania mexicana*. EMBO J. 2000;19(9):1953-1962. doi: 10.1093/emboj/19.9.1953.

Wiese M. A mitogen-activated protein (MAP) kinase homologue of *Leishmania mexicana* is essential for parasite survival in the infected host. EMBO J. 1998;17(9):2619-2628. doi: 10.1093/emboj/ 17.9.2619.

Ilg T, Stierhof YD, Craik D, Simpson R, Handman E, Bacic AJ. Purification and structural characterization of a filamentous, mucin-like proteophosphoglycan secreted by *Leishmania* parasites. J Biol Chem. 1996;271(35):21583-96.

Masuko T, Minami A, Iwasaki N, Majima T, Nishimura S-I, Lee YC. Carbohydrate analysis by a phenol-sulfuric acid method in microplate format. Anal Biochem, 2005;339(1):69-72.

de Jong SE, Selman MHJ, Adegnika AA, Amoah AS, van Riet E, Kruize YCM, Raynes JG, Rodriguez A, Boakye D, von Mutius E, Knulst AC, Genuneit J, Cooper PJ, Hokke CH, Wuhrer M, Yazdanbakhsh M. IgG1 Fc N-glycan galactosylation as a biomarker for immune activation. Sci Rep. 2016;6:28207. doi: 10.1038/srep28207.

Stierhof YD, Bates PA, Jacobson RL, Rogers ME, Schlein Y, Handman E, Ilg T. Filamentous proteophosphoglycan secreted by *Leishmania* promastigotes form gel-like three-dimensional networks that obstruct the digestive tract of infected sandfly vectors. Eur J Cell Biol. 1999;78(10):675-689.

Coe JE, Margossian SS, Slayter HS, Sogn JA. Hamster female protein. A new pentraxin structurally and functionally similar to C-reactive protein and amyloid P component. J Exp Med. 1981;153(4):977-991. doi: 10.1084/jem.153.4.977.

Klein C, Gopfert U, Goehring N, Stierhof Y-D, Ilg Y. Proteophosphoglycans of *Leishmania mexicana*. Biochem J. 1999;344,775–786.

Ilg T, Stierhof Y-D, Etges R, Adrian M, Harbecke D, Overath P. Secreted acid phosphatase of *Leishmania mexicana*: a filamentous phosphoglycoprotein polymer. Proc Natl Acad Sci USA. 1991;88:8774-8778.

Stierhof YD, Ilg T, Russel DG, Hohenberg H, Overath P. Characterization of polymer release from the flagellar pocket of *Leishmania mexicana* promastigotes. J Cell Biol. 1994;125(2):321-331.

Montgomery J, Curtis J, Handman E. Genetic and structural heterogeneity of proteophosphoglycans in *Leishmania*. Mol Biochem Parasitol. 2002;121(1):75-85.

Göpfert U, Goehring N, Klein C, Ilg T. Proteophosphoglycans of *Leishmania mexicana*. Molecular cloning and characterization of the *Leishmania mexicana* ppg2 gene encoding the

proteophosphoglycans aPPG and pPPG2 that are secreted by amastigotes and promastigotes. Biochem J. 1999;344(Pt 3):787-795.

Samant M, Sahasrabuddhe AA, Singh N, Gupta SK, Sundar S, Dube A. Proteophosphoglycan is differentially expressed in sodium stibogluconate-sensitive and resistant Indian clinical isolates of *Leishmania donovani*. Parasitology. 2007;134:1175-1784. doi: 10.1017/S0031182007002569.

Raynes JG, Curry A, Harris RA. Binding of C-reactive protein to *Leishmania*. Biochem Soc Trans. 1994;22(1):3S. doi: 10.1042/bst022003s.

Bates PA, Hermes I, Dwyer DM. Golgi-mediated post-translational processing of secretory acid phosphatase by *Leishmania donovani* promastigotes. Mol Biochem Parasitol. 1990;39(2):247-55. doi: 10.1016/0166-6851(90)90063-r.

Muskus C, Segura I, Oddone R, Turco SJ, Leiby DA, Toro L, Robledo S, Saravia NG. Carbohydrate and LPG expression in *Leishmania viannia* subgenus. J Parasitol. 1997;83(4):671-678.

Soares RP, Cardoso TL, Barron T, Araujo MS, Pimenta PF, Turco SJ. *Leishmania braziliensis*: a novel mechanism in the lipophosphoglycan regulation during metacyclogenesis. Int J Parasitol. 2005;35(3):245–253. doi: 10.1016/j.ijpara.2004.12.008.

Lippert DN, Dwyer DW, Li F, Olafson RW. Phosphoglycosylation of a secreted acid phosphatase from *Leishmania donovani*. Glycobiology. 1999;9(6):627-636.

Soares RRP, Macedo ME, Ropert C, Gontijo NF, Almeida IC, Gazzinelli RT, Pimenta PFP, Turco SJ. *Leishmania chagasi*: lipophosphoglycan characterization and binding to the midgut of the sand fly vector *Lutzomyia longipalpis*. Mol Biochem Parasitol. 2002;121(2):213–224. doi: 10.1016/S0166-6851(02)00033-6.

Coelho-Finamore JM, Freitas VC, Assis RR, Melo MN, Novozhilova N, Secundino NF, Pimenta PF, Turco SJ, Soares RP. *Leishmania infantum*: lipophosphoglycan intraspecific variation and interaction with vertebrate and invertebrate hosts. Int J Parasitol. 2011;41(3-4):333-342.

McConville MJ, Schnur LF, Jaffe C, Schneider P. Structure of *Leishmania* lipophosphoglycan: inter- and intra-specific polymorphism in Old World species. Biochem J. 1995;310(Pt 3):807-818. doi: 10.1042/bj3100807.

Nogueira PM, Guimarães AC, Assis RR, Sadlova J, Myšková J, Pruzinova K, Hlavackova J, Turco SJ, Torrecilhas AC, Volf P, Soares RP. Lipophosphoglycan polymorphisms do not affect *Leishmania amazonensis* development in the permissive vectors *Lutzomyia migonei* and *Lutzomyia longipalpis*.   Parasit Vectors. 2017;10(1):608. doi: 10.1186/s13071-017-2568-8.

Schnur LF, Zuckerman A, Greenblatt CL. Leishmanial serotypes as distinguished by the gel diffusion of factors excreted *in vitro* and *in vivo*. Isr J Med Sci. 1972;8(7):932-942.

Paranaíba LF, de Assis RR, Nogueira PM, Torrecilhas AC, Campos JH, Silveira AC, Martins-Filho OA, Pessoa NL, Campos MA, Parreiras PM, Melo MN, Gontijo NF, Soares RP. *Leishmania enriettii*: biochemical characterisations of lipophosphoglycans (LPGs) and glycoinositolphospholipids (GIPLs) and infectivity to *Cavia porcellus*. Parasit Vectors. 2015;8(31).

Azevedo, L.G., de Queiroz, A.T.L., Barral, A. Santos LA, Ramos PIP. Proteins involved in the biosynthesis of lipophosphoglycan in *Leishmania*: a comparative genomic and evolutionary analysis. Parasit Vectors. 2020;13:44. https://doi.org/10.1186/s13071-020-3914-9.

Hoover DL, Berger M, Nacy CA, Hockmeyer WT, Meltzer MS. Killing of *Leishmania tropica* amastigotes by factors in normal serum. J Immunol. 1984;132(2):893-897.

Mosser DM, Burke SK, Coutavas EE, Wedgewood JF, Edelson PJ. *Leishmania* species: mechanisms of complement activation by five strains of promastigotes. Exp Parasitol. 1986;62(3):394-404.

Laurenti MD, Corbett CE, Sotto MN, Sinhorini IL, Goto H. The role of complement in the acute inflammatory process in the skin and in host-parasite interaction in hamsters inoculated with *Leishmania (Leishmania) chagasi.* Int J Exp Pathol. 1996;77(1):15-24. doi: 10.1046/j.1365-2613.1996.958096.x.

Wasunna KM, Raynes JG, Were JBO, Muigai R, Sherwood J., Gachihi G, Carpenter L, McAdam KPWJ. Acute phase protein concentrations predict clearance rate during therapy for visceral leishmaniasis. Trans R Soc Trop Med Hyg. 1995;89(6):678-681.

Tirado TC, Bavia L, Ambrosio AR, Campos MP, de Almeida Santiago M, Messias-Reason IJ, Figueiredo FB. A comparative approach on the activation of the three complement system pathways in different hosts of visceral Leishmaniasis after stimulation with *Leishmania infantum*. Dev Comp Immunol. 2021;120:104061. doi: 10.1016/j.dci.2021.104061.

Serafim TD, Coutinho-Abreu IV, Oliveira F, Meneses C, Kamhawi S, Valenzuela JG. Sequential blood meals promote *Leishmania* replication and reverse metacyclogenesis augmenting vector infectivity. Nat Microbiol. 2018;3(5):548-555. doi: 10.1038/s41564-018-0125-7.

Mendes-Sousa AF, Nascimento AAS, Queiroz DC, Vale VF, Fujiwara RT, Araújo RN, Pereira MH, Gontijo NF. Different host complement systems and their interactions with saliva from *Lutzomyia longipalpis* (Diptera, Psychodidae) and *Leishmania infantum* promastigotes. PLoS One. 2013;8(11):e79787. doi: 10.1371/journal.pone.0079787.
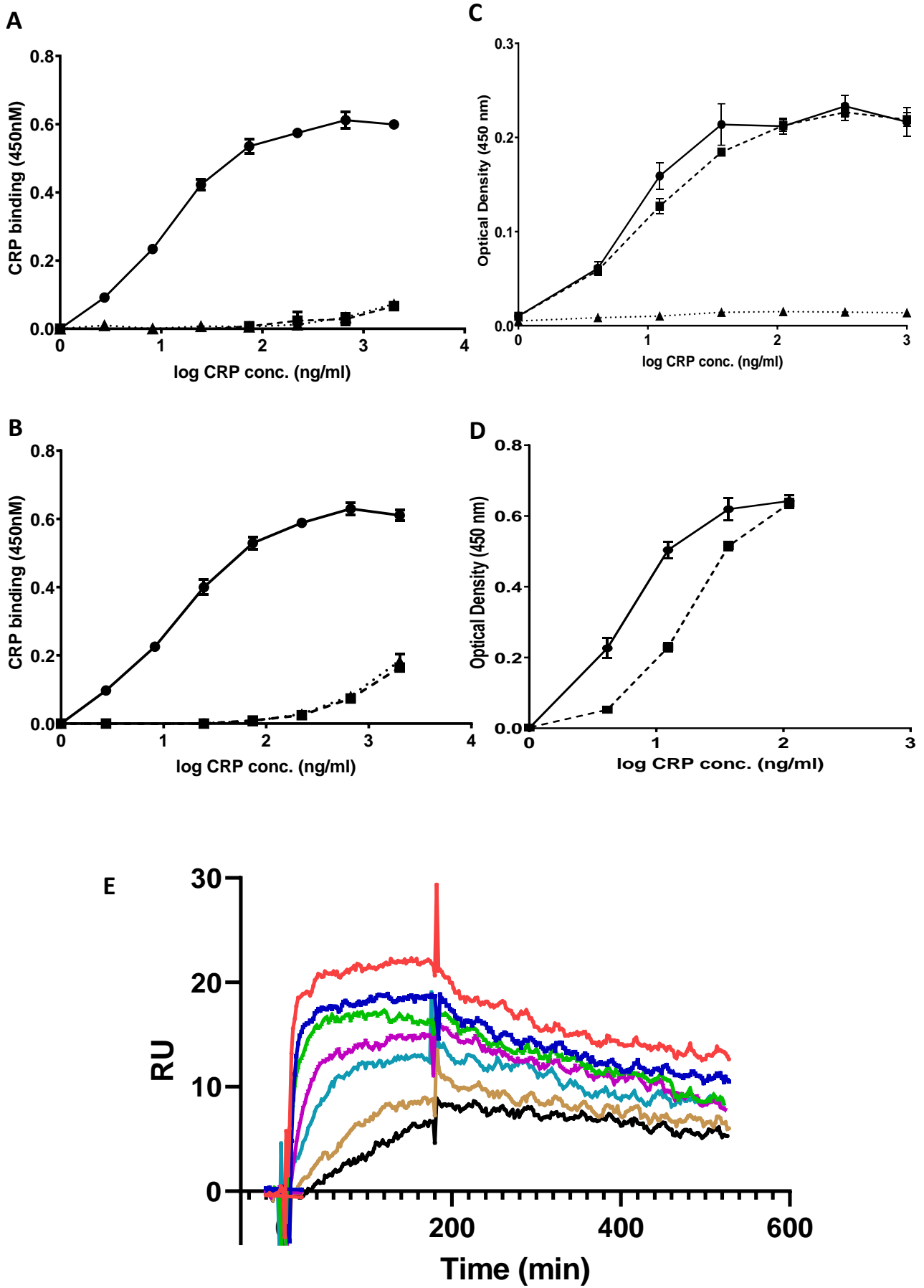
201

Figure 1. A-D CRP binds to *L. mexicana* PPG. A. **CRP binds to PPG in a calcium- but not magnesium-dependent manner**. *L. mexicana* wild-type PPG (1 µg/mL) was immobilised on microtitre plates and biotin-conjugated CRP (0 - 2.0 µg/mL) was added in the presence of Ca^{2+} (0.5 mM) (●); EDTA (10 mM) (▲) or Mg^{2+} (0.5 mM) EGTA (10 mM) (■). CRP binding was detected using HRP-conjugated Streptavidin (1:15000) and TMB substrate (OD 450 nm). **B. Serum components do not compete with CRP binding.** As in **A** but 5% (v/v) CRP-depleted serum was added. **C. CRP binding to PPG is independent of LPG.** Biotinylated CRP (0 - 1.0 µg/mL) binds to immobilised *L. mexicana* PPG coated at 0.3 µg/mL from WT (●) and *lpg1*$^{-/-}$ mutant (■) but not *lpg2*$^{-/-}$ mutant (▲). **D. PCh competition inhibits CRP binding to PPG.** As in **A** but in the presence (■) or absence (●) of added PCh (10 mM). n=3. Error bars represent standard deviation. **E. Biosensor analysis of CRP binding to *L. mexicana* PPG-biotin immobilised onto neutravidin surface.** Neutravidin (185 RU) captured 340 RU of biotinylated PPG. CRP (0.6-40 µg/mL) was added for 3 minutes followed by 5 minutes dissociation. Traces show dose response of binding at two-fold dilutions after control flow cell subtraction.

Table 1. Kinetic parameters and K_D for CRP binding to PPG.

CRP concentration	Off rate (s^{-1})	On rate ($M^{-1}s^{-1}$)	K_D
1.6×10^{-7} M	$1.4 +/- 0.3 \times 10^{-3}$	nd	nd
8×10^{-8} M	$1.7 +/- 0.3 \times 10^{-3}$	nd	nd
4×10^{-8} M	$1.56 +/- 0.3 \times 10^{-3}$	$4.8 +/- 0.1 \times 10^{5}$	2.91×10^{-9} M
2×10^{-8} M	$1.51 +/- 0.3 \times 10^{-3}$	$5.1 +/- 0.2 \times 10^{5}$	2.77×10^{-9} M
1×10^{-8} M	$1.35 +/- 0.4 \times 10^{-3}$	$3.5 +/- 0.4 \times 10^{5}$	4.05×10^{-9} M
0.8×10^{-8} M	$1.23 +/- 0.4 \times 10^{-3}$	nd	nd

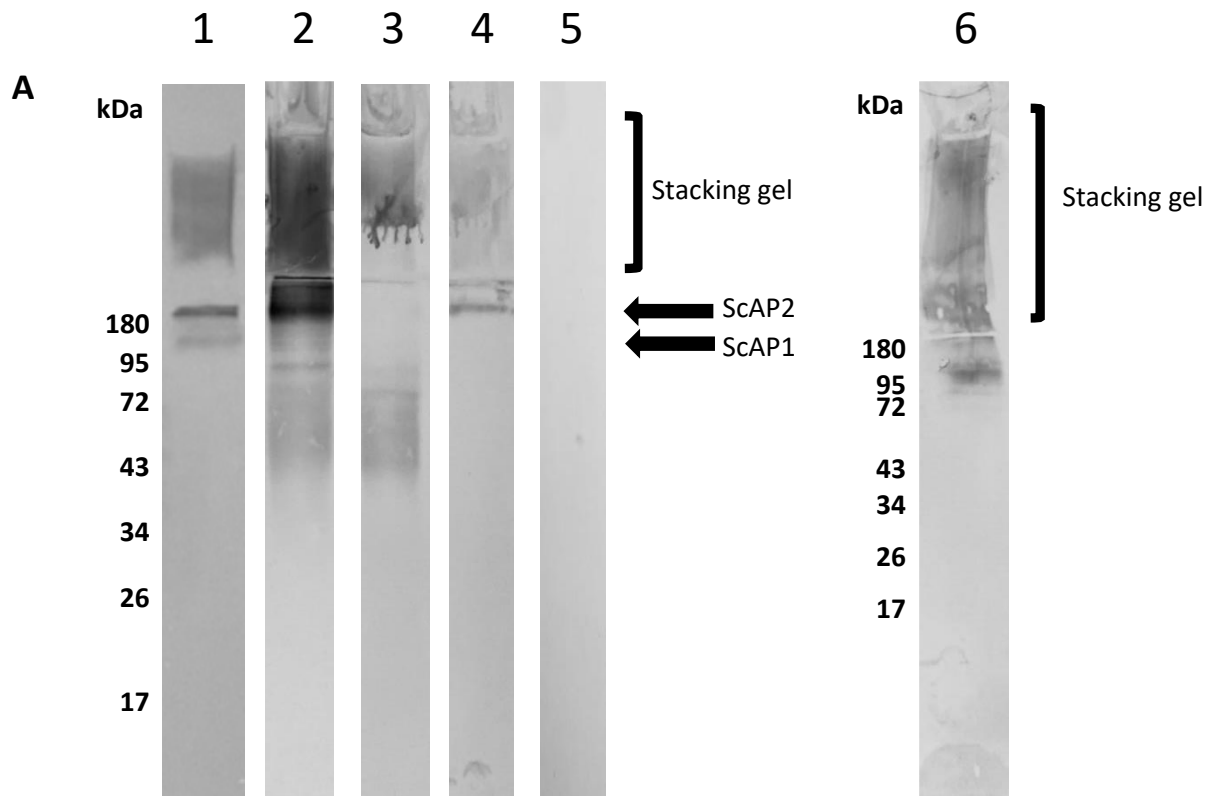**Figure 2. CRP binding to ScAP and fPPG from *L infantum* and *L. mexicana* WT; Δ*lmScAP*1/2 and Δ*lmScAP*1/2 + *ScAP2*. A.** PPG (3 μg) was separated on 10% gels with stacking gel and transferred to PVDF membranes. Lane 1 membranes were probed with CA7AE and anti-mouse IgM to detect repeating disaccharide. Lanes 2 – 6 were probed with CRP and anti-CRP except Lane 5 which was a no CRP control. *L. mexicana* WT (Lanes 1, 2 and 5), Δ*lmScAP*1/2 (Lane 3), Δ*lmScAP*1/2 + *ScAP2* (Lane 4), *L. infantum* WT probed with CRP (Lane 6). **B. ScAP provides the majority of CRP binding capacity in purified phosphoglycan.** Dose-Response of binding of purified CRP (0 - 1.0 μg/mL) to immobilised *L. mexicana* PPG (WT) (●), Δ*lmScAP*1/2 (■) Δ*lmScAP*1/2 + *ScAP2* (▲). In both **A and B**, CRP binding was detected using rabbit anti-CRP antibody, HRP-conjugated goat anti rabbit antibody and TMB substrate (OD 450 nm). n=4. Error bars represent standard deviation. Statistical comparison was performed for ScAP deficient versus add-back (Δ*lmScAP*1/2 vs Δ*lmScAP*1/2 + *ScAP2*). * P<0.01 ** P <0.001.
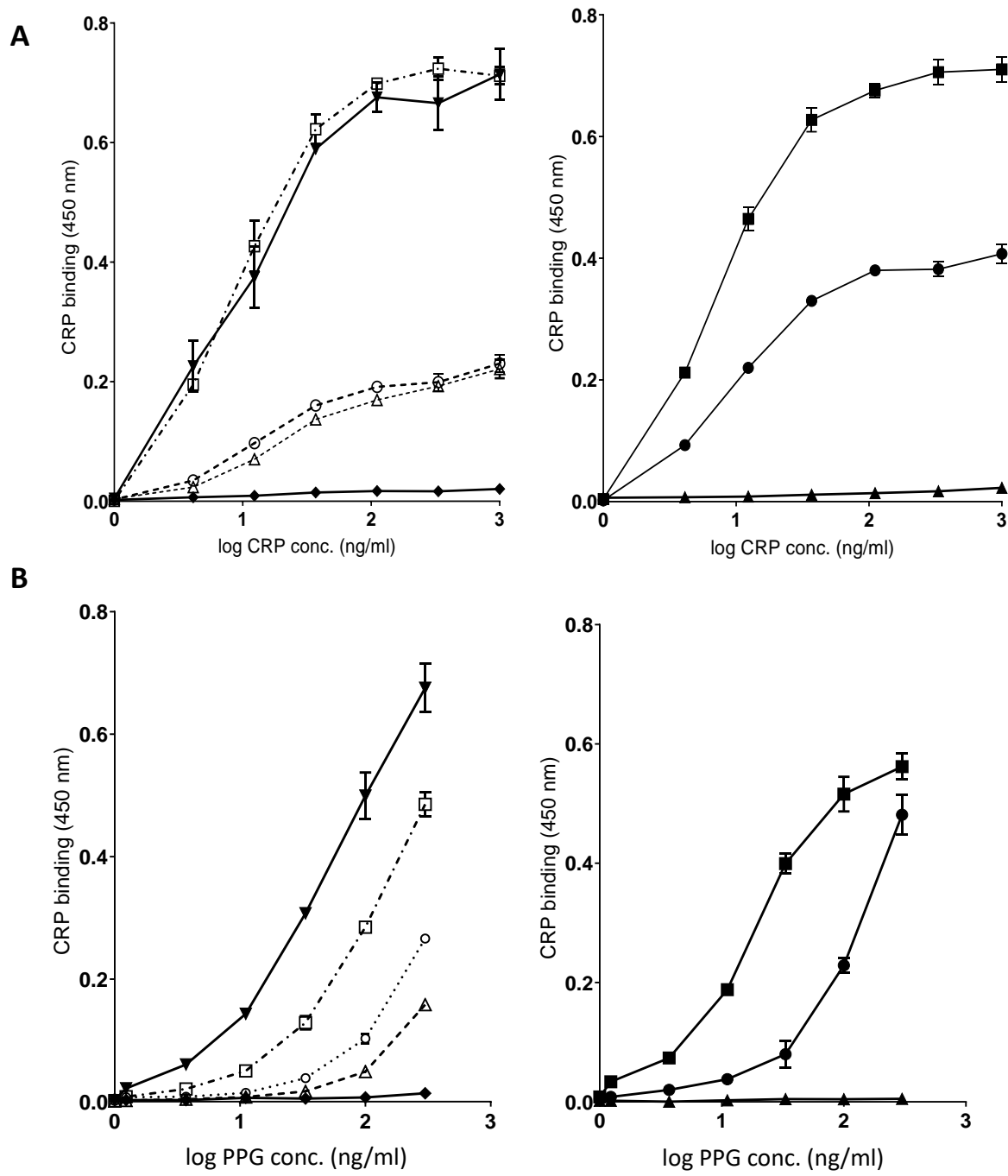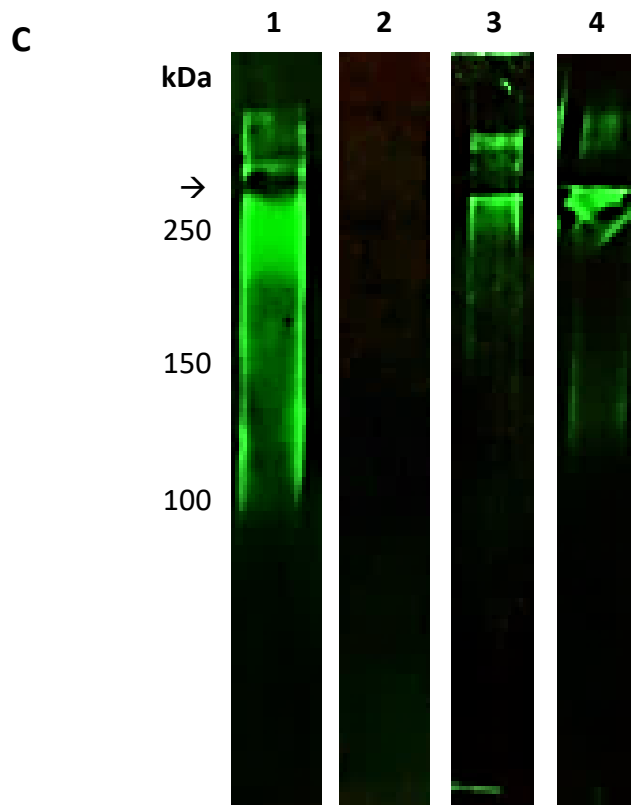
Figure 3. **PPG from different *Leishmania* species exhibit widely varying CRP binding capacities. A.** Dose response of binding of purified CRP (0 - 1.0 µg/mL) to PPG (0.3 µg/mL) from different *Leishmania* species immobilised on microtitre plates. Bound CRP was detected using anti-CRP HRP. **B**. CRP binding to varied PPG coating concentrations with a constant CRP concentration. Left hand panel Old World species: *L. tropica* (♦); *L. major* (Δ); *L. infantum* (○); *L. donovani* (▼)*; L. aethiopica* (□)*.* Right hand panel New World Species: *L. amazonensis* (▲)*; L. mexicana* (●)*; L. panamenensis* (■)*.* Error bars represent standard deviation n=3. **C.** CRP binding to 3 µg purified PPG *L. panamensis* (Lane 1), *L. aethiopica* (Lane 3), *L. donovani* (Lane 4) but not *L. tropica* (Lane 2). PPG was run on SDS with stacker and 10% resolving gel and transferred to PVDF and probed with CRP, rabbit anti-CRP and IR800 anti-rabbit IgG. Images obtained from Storm are depicted in false colour.

A. *lpg1*^{-/-}

DIC DAPI 488/CRP Merged
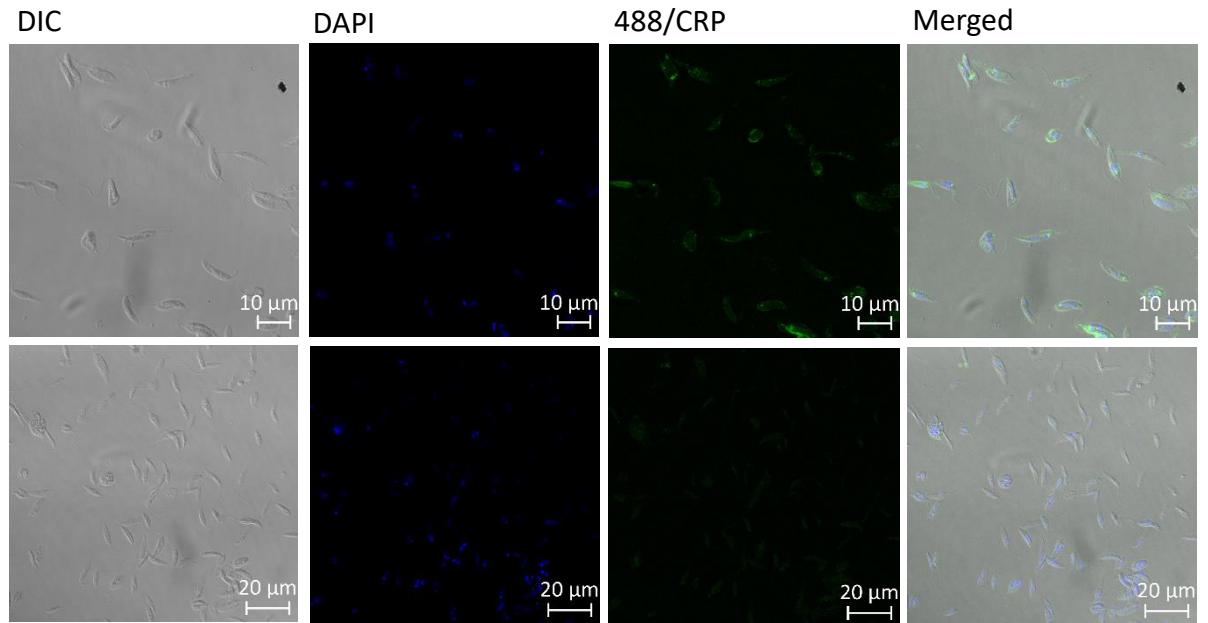
B. Wild-type
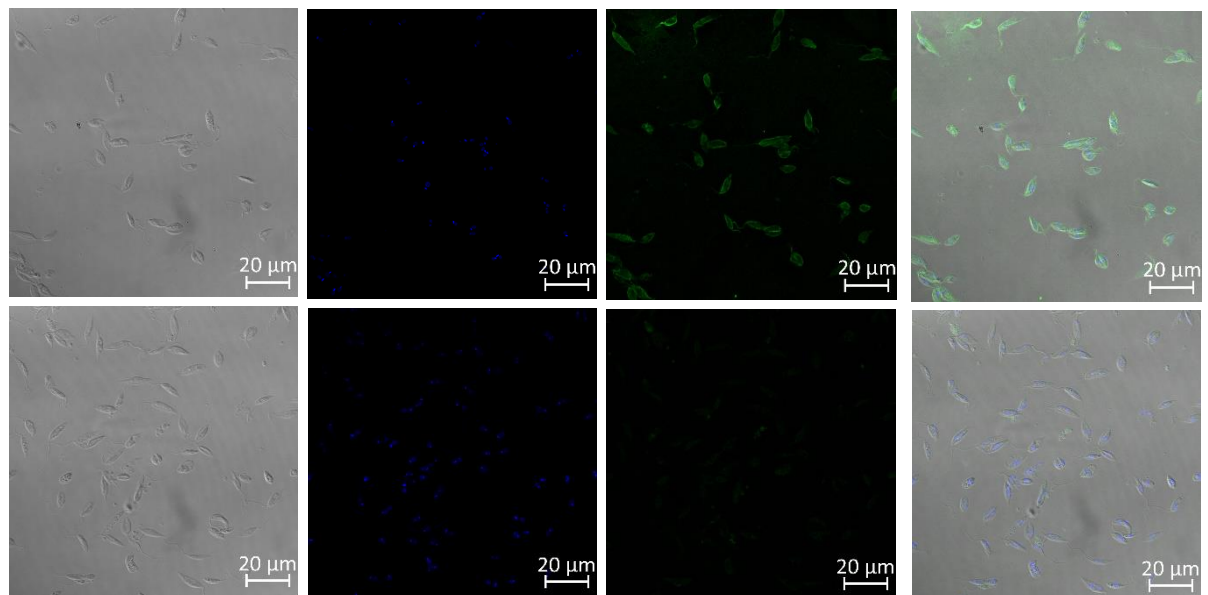
Figure 4. *L. mexicana* WT binds CRP all over surface in contrast to *lpg1*^{-/-} mutant binding at flagellar pocket. A *L. mexicana lpg1*^{-/-} and **B** *L. mexicana* WT parasites were incubated with CRP and gently washed before fixing and CRP detected using rabbit anti-human CRP followed by anti-rabbit IgG FITC. DAPI was used as a counterstain. Images from left to right; DIC, DAPI, CRP immunofluorescence; merged. Lower panels as above but without CRP.

207

Figure 5. Native sandfly derived PSG is a strong ligand for CRP. Sand fly PSG (0.5 μg/mL Lane 1) and purified PPG (0.5 μg/mL Lane 2) from pa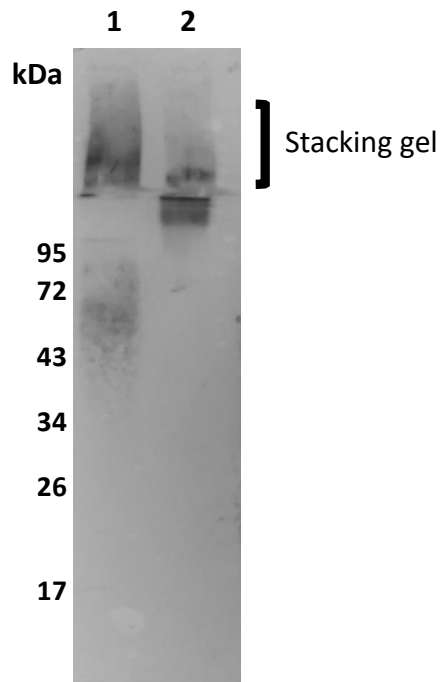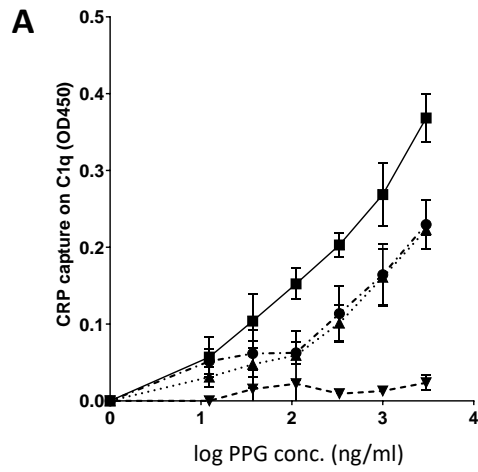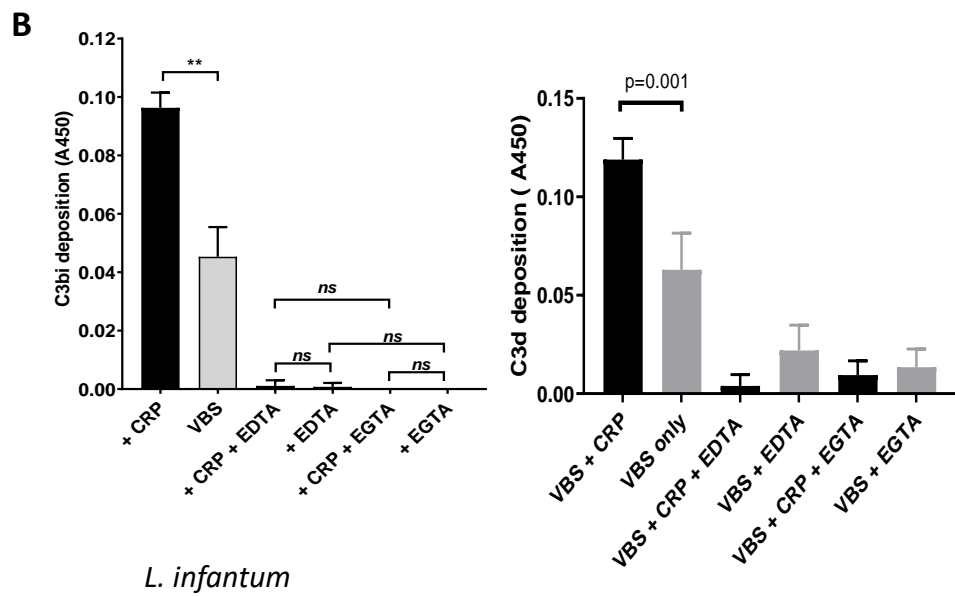rasites were run on a 10% resolving gel with an extended stacking gel and transferred to PVDF membrane and probed with CRP-biotin (1 μg/mL) and streptavidin-AP (1/500).
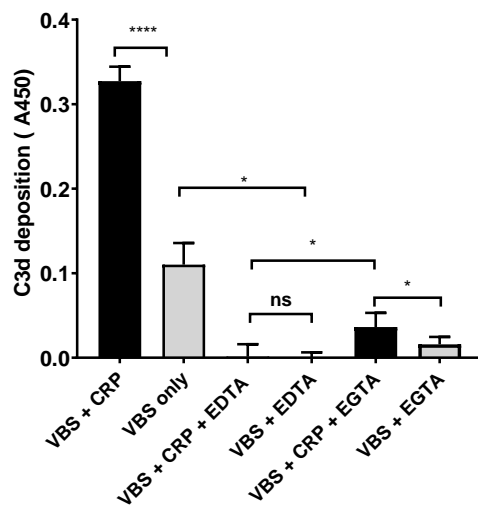
A

L. mexicana **L. mexicana**
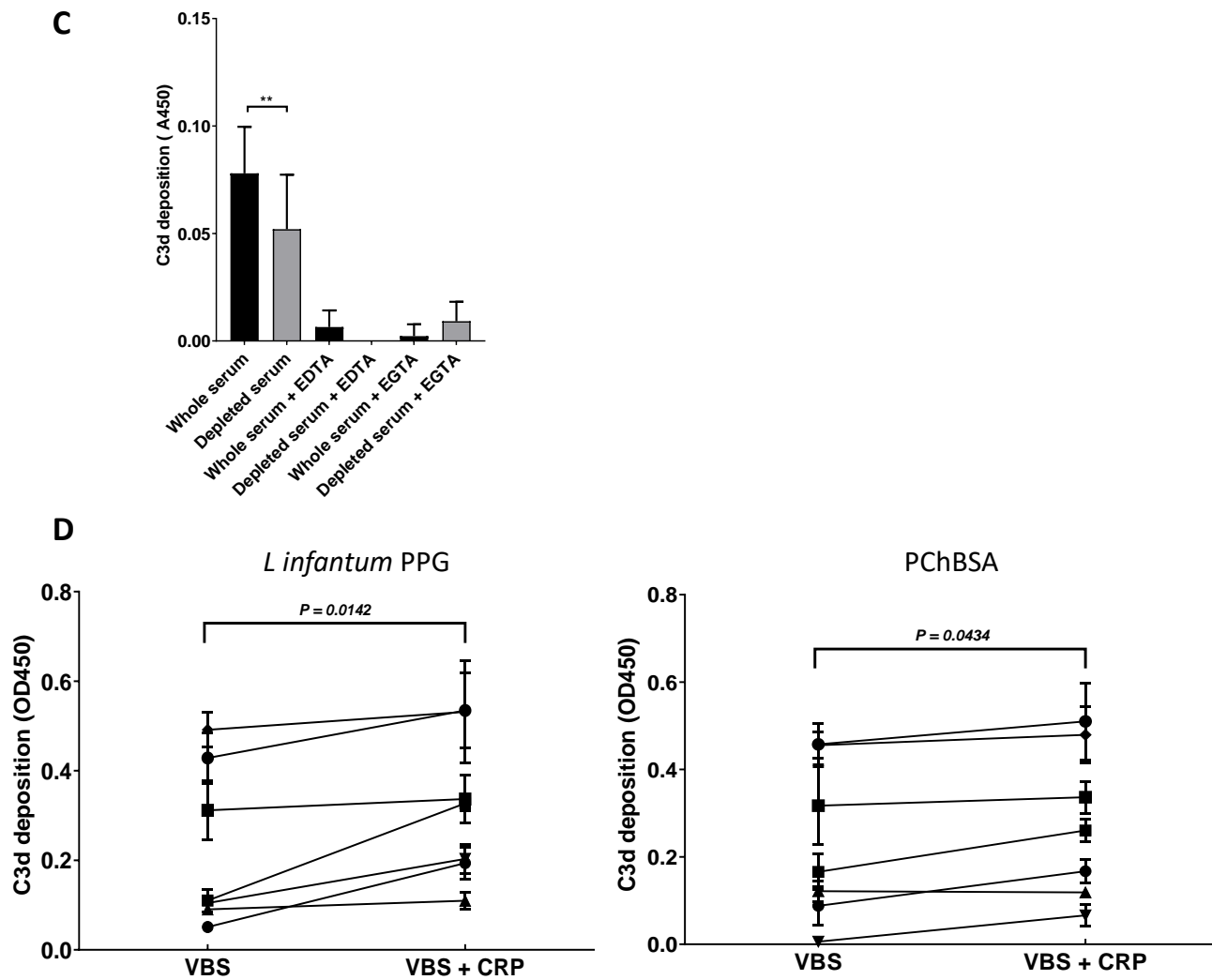
B

L. infantum

Figure 6. CRP contributes to PPG mediated complement activation. A. CRP that has bound to PPG in fluid phase can be captured on C1q coated plates. Plates were coated with C1q. CRP (1 μg/mL) was added with various different amounts of PPG (0-3 μg/mL) and complex binding to the surface was detected with anti-CRP. Error bars represent standard deviation (n= 3) *L. aethiopica* (●) *L. infantum* (■) *L. donovani* (▲) *L. tropica* (▼). **B. PPG from *L. mexicana* or *L. infantum* activates complement through the classical pathway and CRP**. Microtitre plate assays of complement activation by PPG from *L. mexicana or L. infantum* coated at 2 μg/mL. Wells with immobilised PPG were incubated with serum (1:100 dilution) for 20 minutes at 37°C in the presence (filled bars) or absence (shaded bars) of additional purified CRP (0.4 μg/mL) in VBS Mg Ca buffer, EDTA (5mM) or Mg EGTA. Deposited C3bi or C3d was detected with biotinylated antibody followed by streptavidin HRP. C3bi mean and s.d, n=6. C3d mean and s.d, n=4. **C. Depletion of CRP in serum decreases the classical complement activation in response to PPG from *L. mexicana*.** Methods used the same as in **B**, but with whole serum and partially CRP diluted serum compared at the same dilution. **D. Variation in CRP mediated PPG classical complement pathway activation in multiple donors.** Added CRP (0.4 μg/mL) increases complement activation measured through C3d deposition as in **A** in response to PPG coated at 0.4 μg/mL and PChBSA (0.1 μg/mL) and PChBSA in the presence and absence of additional purified CRP. Paired t test on 7 donors.
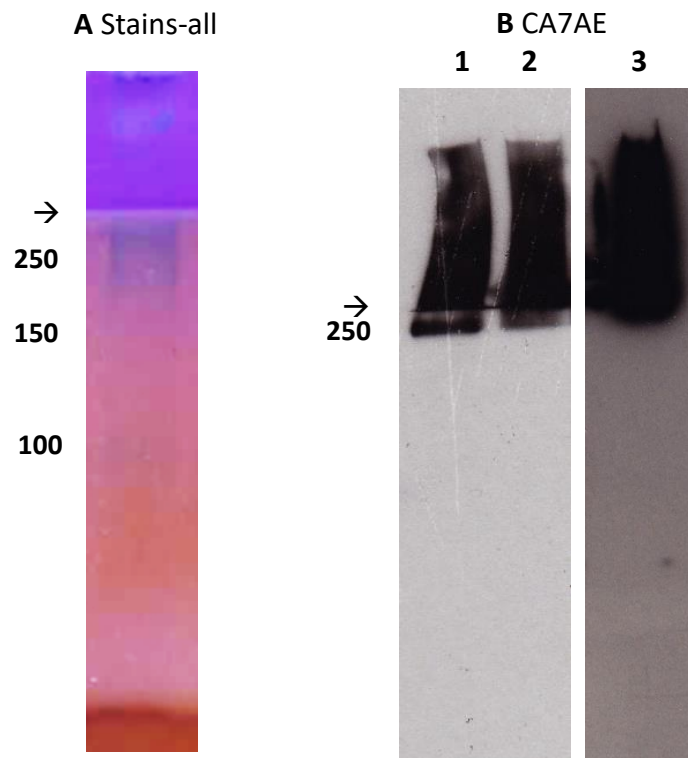
Figure S1. SDS-PAGE shows high molecular weight phosphoglycan of cell culture purified PPGs. **A.** Gel incubated with stains-all. **B.** Western blot of DE-52 purified *L. mexicana* (Lanes 1 and 2) and *L. infantum* (Lane 3) PPG probed with CA7AE (specific for the phosphorylated repeats). Arrow shows where resolving and stacking gels meet.

A

B
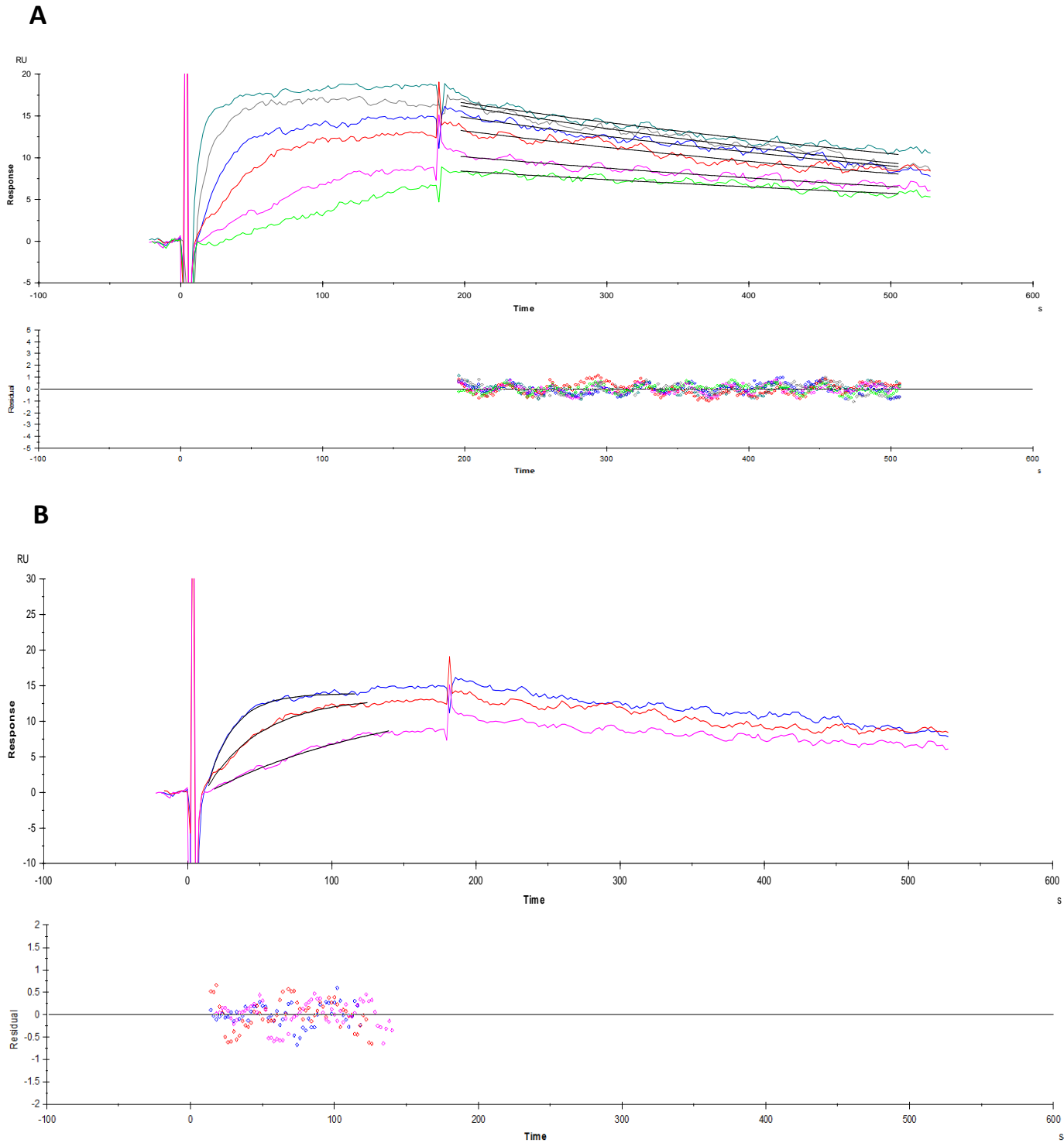
Figure S2. Biosensor analysis of CRP binding to *L. mexicana* PPG-biotin immobilised onto neutravidin surface. Neutravidin (185 RU) captured 340 RU of biotinylated PPG and CRP at (1-20 µg/mL) was added for 3 minutes followed by 5 minutes dissociation. **A.** Off-rate analysis (1.5 e^{-3} s^{-1}) was performed using BiaEval. **B**. Association fit for CRP binding to *L. mexicana* PPG.
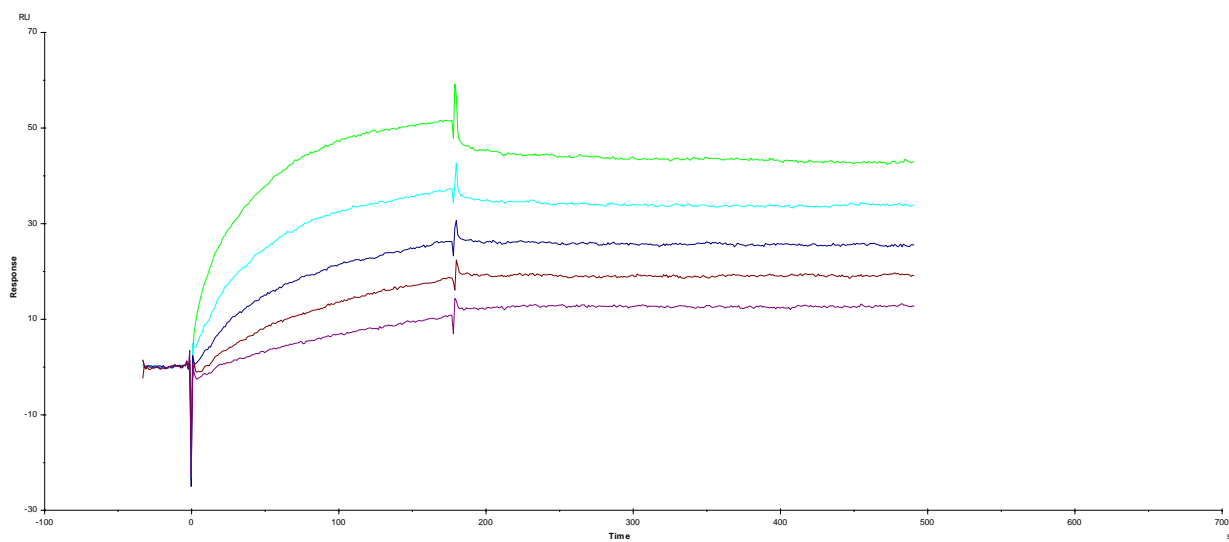
Figure S3. Rat CRP binding to *L. mexicana* PPG. The surface was prepared using amine coupling to a C1 chip and rat CRP flowed over the surface at a range of concentrations for 3 minutes and dissociation followed for 5 minutes before elution with EDTA. On-rates were approximately 10^5 $M^{-1}s^{-1}$ and off-rates 5×10^{-5} s^{-1}.
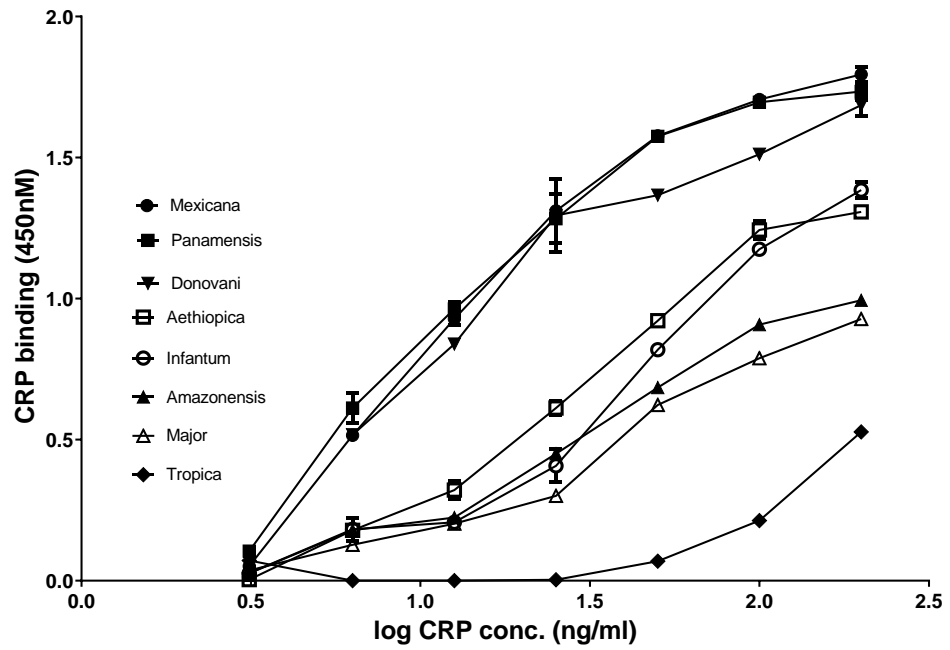
Figure S4. Mouse CRP binding to PPG from different species. *L. tropica* (♦)*; L. major* (Δ)*; L. infantum* (○)*; L. donovani* (▼)*; L. aethiopica* (□)*; L. amazonensis* (▲)*; L. mexicana* (●)*; L. panamenensis* (■)*.* Error bars represent standard deviation n=3.
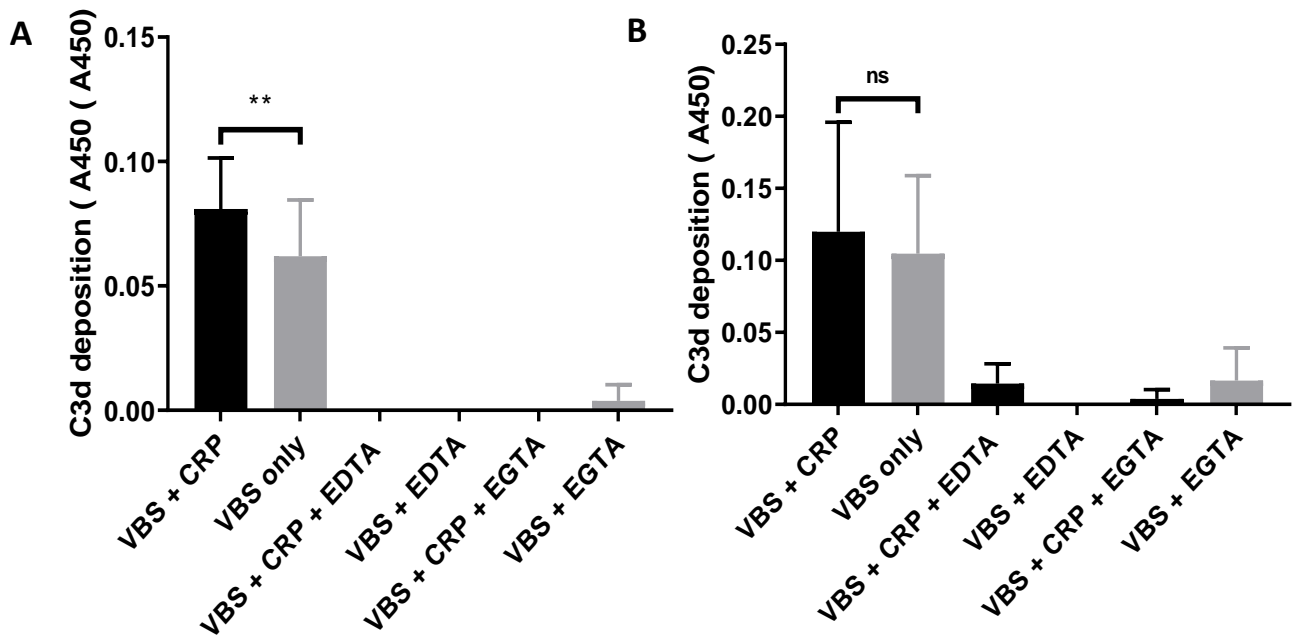
Figure S5. PPG from *L. mexicana lpg1$^{-/-}$* (A) but not *lpg2$^{-/-}$* (B) shows CRP mediated complement activation. Data generated as in Figure 6. Mean +/- s.d. n =6 ** p<0.01.

7. **The binding interactions of _Leishmania (Mundinia)_ with midge midguts**

As previously discussed in Chapter 1, there has been a growing field of research over the past 20 years into midges being vectors for *Leishmania*. Heavy late stage *Leishmania (Mundinia)* infections have previously be observed experimentally in the colony midge species *Culicoides sonorensis* (Becvar et al., 2021). However, the mechanism of attachment of *Leishmania (Mundinia)* species to the midge midgut has yet to be established. The aim of this work was to see if interactions of *Leishmania* and pentraxins are similar in midges to those seen in Chapter 5 for *Lu. longipalpis*. This chapter will discuss the preliminary results of this work. The methods used for the results in this chapter can be seen in Chapter 3, sections: 3.6 and 3.7. Dr Matthew Rogers helped with midge and sand fly dissections.

7.1 Results

7.1.1 CA7AE binds to *Leishmania (Mundinia) chancei*

The structure of *Leishmania (Mundinia) enriettii* has previously been reported (Paranaíba et al., 2015). To our knowledge, the structure of LPG from *Leishmania (Mundinia) chancei* has not been reported. LPG-enriched material purified from *L. (M.) chancei* log phase promastigotes and metacyclics were run on an SDS-PAGE gel, transferred to a PVDF membrane and probed with anti-LPG antibody CA7AE, with results seen in Figure 7.1. CA7AE binding to *L. (M). chancei* parasites was also observed using immunofluorescence, seen in Figure 7.2 and 7.3.
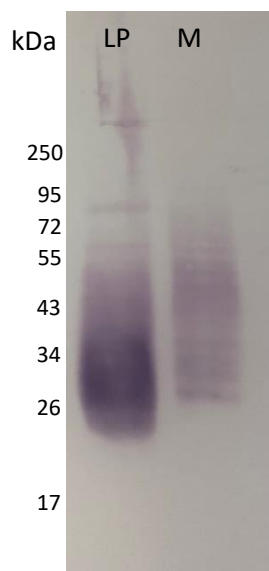
Figure 7.1. CA7AE binds *Leishmania (Mundinia) chancei* LPG by Western blot. 10 μL LPG-enriched material from *L. (M.) chancei* log phase (LP) and metacyclic (M) promastigotes were run on an SDS-PAGE gel, transferred to PVDF and probed with CA7AE followed by anti-IgM-AP.
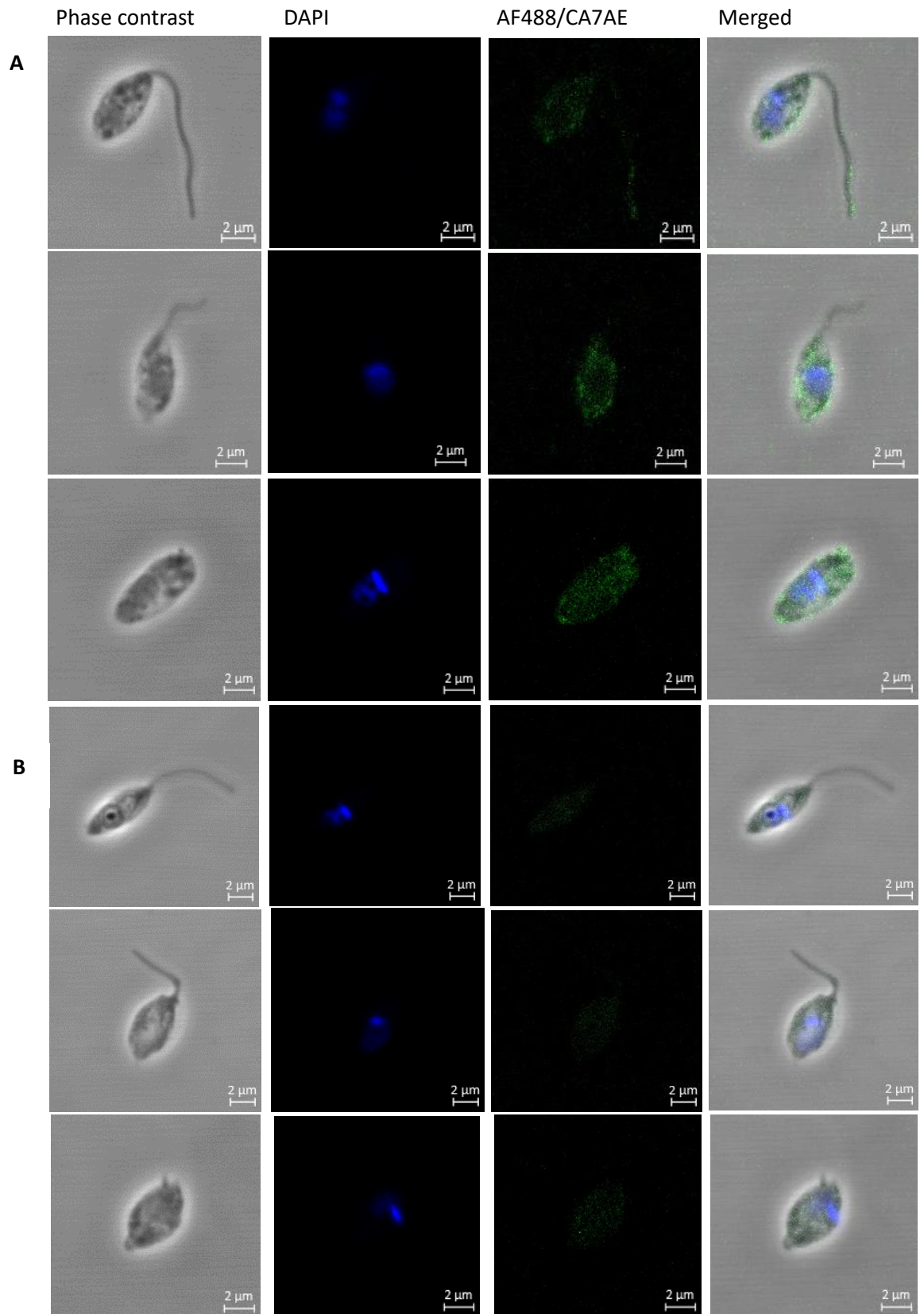
Figure 7.2. CA7AE binds to the surface of *Leishmania (Mundinia) chancei* log phase promastigotes when using immunofluorescence. Culture parasites were washed and resuspended in 4% paraformaldehyde. Parasites were then washed and airdried to a slide. The slides were incubated with CA7AE followed by anti-IgM-AF448 and imaged using the Zeiss LSM880 confocal microscope (**A**). In the presence of just anti-IgM-AF448, no staining was observed (**B**). White scale bars represent 2 μm.
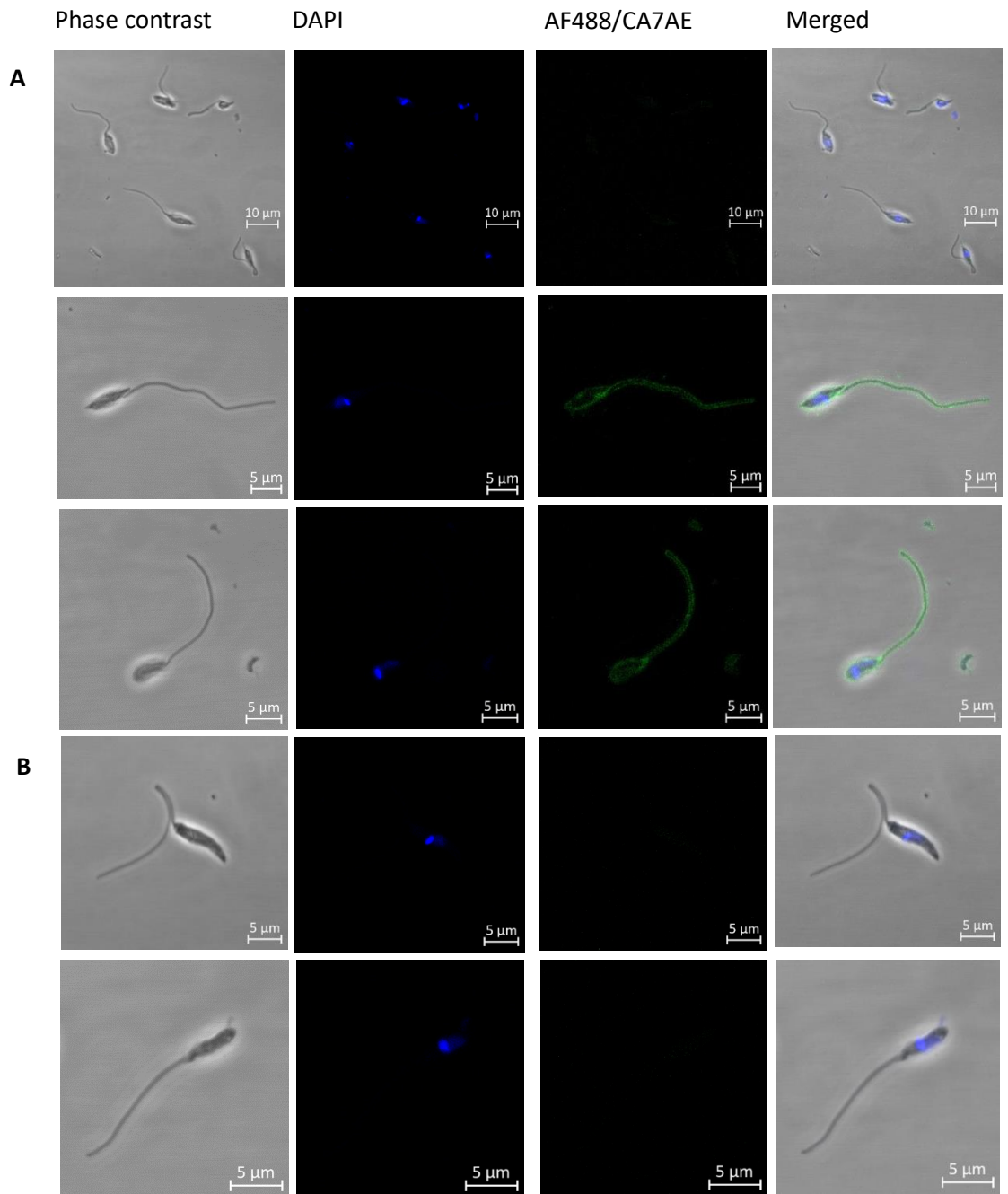
Figure 7.3. CA7AE binds to the surface of *Leishmania (Mundinia) chancei* metacyclic promastigotes when using immunofluorescence. Culture parasites were washed and resuspended in 4% paraformaldehyde. Parasites were then washed and airdried to a slide. The slides were incubated with CA7AE followed by anti-IgM-AF448 and imaged using the Zeiss LSM880 confocal microscope (**A**). In the presence of just anti-IgM-AF448, no staining was observed (**B**). White scale bars represent 10 µm (panels on first row) or 5 µm.

L. (M.) chancei metacyclic LPG has a higher molecular weight than that of log phase LPG, suggesting *L. (M.) chancei* also exhibits an increase in LPG length during metacyclogenesis (Sacks et al., 1990; McConville et al., 1992). *L. (M.) chancei* has previously been reported to have a characteristic morphology for the *Leishmania* genus (Kwakye-Nuako et al., 2023), which was seen here again by immunofluorescence. Immunofluorescence results showed binding to the whole surface of some *Leishmania* parasites but not to others. As discussed in Chapter 3, this variation in CA7AE binding may be due to movement of LPG across the surface which may be affected by wash steps and other parts of the protocol. There may be variation in internalisation or shedding rates with staining captured for some but not other parasites. Edge effects may be the cause for lack of CA7AE binding to some parasites, but multiple areas of the slide were imaged.

7.1.2 *L. (M.) chancei* LPG does not bind to *C. sonorensis* microvillar-enriched midgut extract by ligand blotting

One of the initial hypotheses of this project was that SAP acted as a cross-linker between *Leishmania (Leishmania)* LPG and the sand fly midgut. 3 µg *Lu. longipalpis* microvillar-enriched midgut extract was run on an SDS-PAGE gel and transferred to a PVDF membrane. This was then probed with or without SAP followed by LPG and CA7AE. However, no clear LPG binding was observed with or without SAP present, seen in Figure 7.4. Very faint bands between 72 and 85 kDa can be seen when the blot is probed with just LPG. This may mean LPG and midgut extract compete for SAP binding.

We extended this hypothesis to *Leishmania (Mundinia)* and microvillar-enriched midge midgut extracts. However we had previously seen no binding of SAP to *C. sonorensis* midgut extract and so we only looked at LPG binding to the midge. Microvillar-enriched midgut extract was run in a reduced state on a gel and transferred to a PVDF membrane. No binding of LPG to the microvillar-enriched midge midgut extract was seen, however detection of the *L. (M.) chancei* LPG log phase control was weak and varied between blots, seen in Figure 7.5. Therefore, there may be issues with the method that need to be considered.
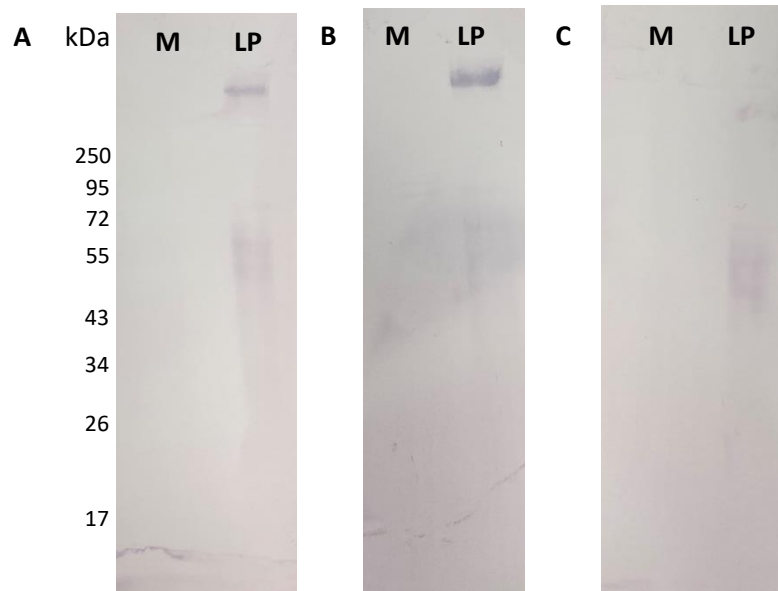
Figure 7.4. SAP does not cross-link *Leishmania mexicana* LPG to *Lutzomyia longipalpis* microvillar-enriched midgut extract. 3 µg *Lu. longipalpis* microvillar-enriched midgut extract (M) and 1 µg *L. (L.) mexicana* log phase LPG (LP) were run on an SDS-PAGE gel and transferred to PVDF. The blots were probed with 1 µg/mL SAP followed by 1 µg/mL *L. (L.) mexicana* log phase LPG and CA7AE (**A**). **B** was probed with 1 µg/mL *L. (L.) mexicana* log phase LPG and CA7AE and **C** with CA7AE only. All were visualised using anti-IgM-alkaline phosphatase, with no staining seen when just this antibody was used (data not shown).
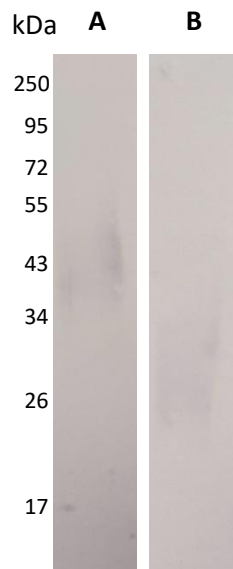
Figure 7.5. *Leishmania (Mundinia) chancei* LPG detection with CA7AE was inconsistent. 5 µL *L. (M.) chancei* log phase LPG was used as a control for an experiment looking at LPG attachment to *Culicoides sonorensis*, *Culicoides nubeculosus* and *Lutzomyia longipalpis* microvillar-enriched midgut extract. Midgut extract and LPG were run on SDS-PAGE gels and transferred to PVDF. The blots were probed with either 1 µg/mL *L. (M.) chancei* log phase LPG, followed by CA7AE and anti-IgM-AP (**A**) or 1 µg/mL *L. (M.) chancei* log phase LPG + 250 mM GalNAc, followed by CA7AE and anti-IgM-AP (**B**). Blots were also probed with CA7AE and anti-IgM-AP only but no binding to the control was seen.

7.1.3 GalNAc displaying glycoconjugates are present in the *C. sonorensis* and *C. nubeculosus* midgut

Myšková et al. (2007; 2016) found all midgut homogenates from permissive but not restrictive vectors tested had N-acetyl-galactosoamine (GalNAc)-displaying glycoconjugates. This pattern suggested *Leishmania* parasites in permissive vectors may attach to the midgut via GalNAc. As we did not find a clear role for SAP in the attachment of *Leishmania (Leishmania)* to *Lu. longipalpis*, and we have not seen a role so far for SAP in *Leishmania (Mundinia)*-midge interactions, we looked to see if midge midguts displayed GalNAc.

C. sonorensis, *C. nubeculosus* and *Lu. longipalpis* microvillar-enriched midgut extract were run in a reduced state on an SDS-PAGE gel, transferred to a nitrocellulose membrane and probed with *Helix pomatia* agglutinin (HPA)-biotin, followed by streptavidin-alkaline phosphatase, seen in Figure 7.6. For *Lu. longipalpis*, a range of bands were observed: 35 kDa, 40 kDa smear of multiple bands and a faint band at 80 kDa. Both midge species shared a strong band at ~80 kDa. Interestingly, another band was observed at ~40 kDa for *C. sonorensis* that was not seen in *C. nubeculosus*. This band also aligns with one seen in *Lu. longipalpis*. However, when repeating this blot, not all bands were present for every experiment, and background binding varied.
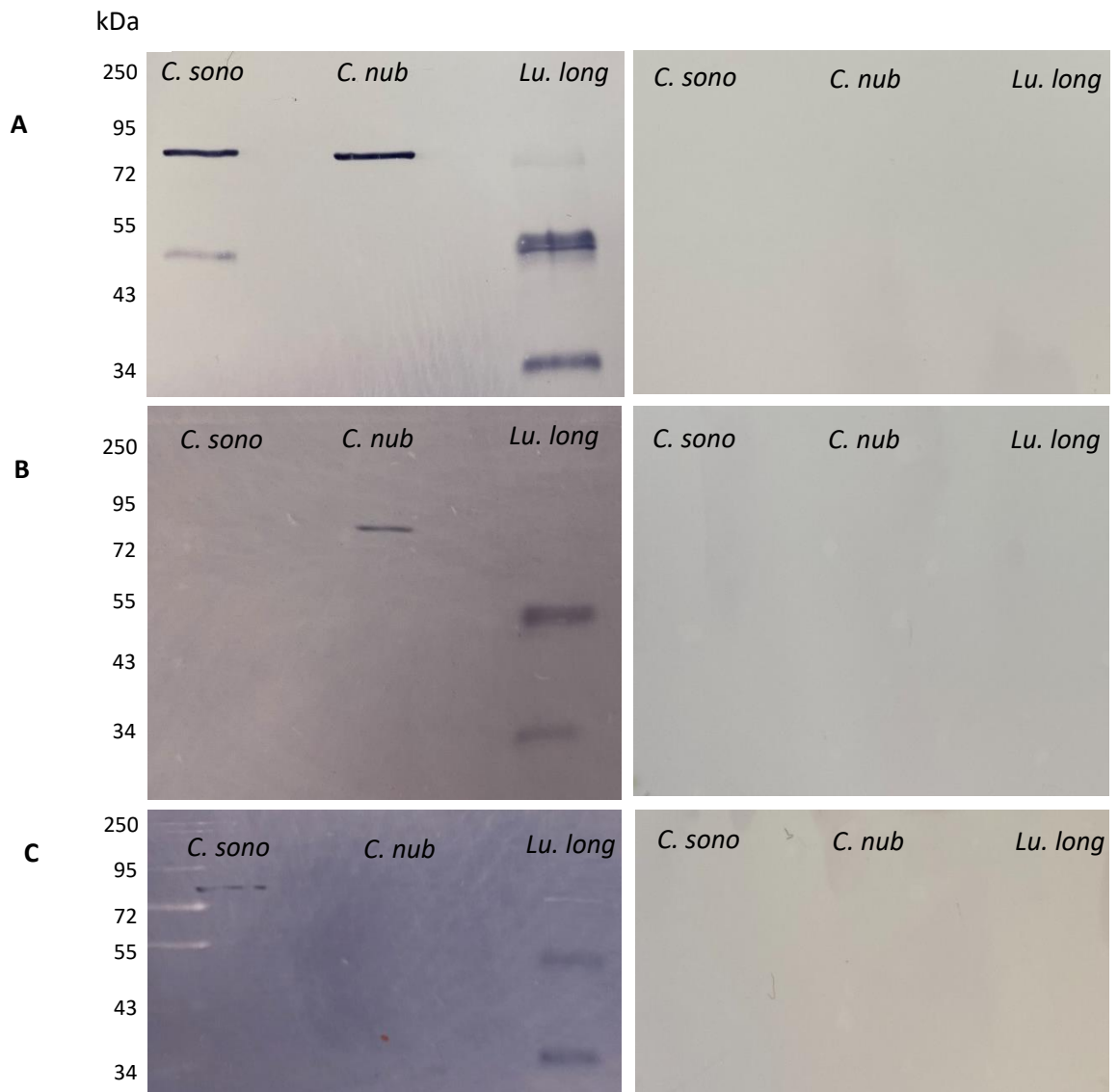
Figure 7.6. The midge midgut microvillar display GalNAc. 1 µg *Culicoides sonorensis* (*C. sono*), *Culicoides nubeculosus* (*C. nub*) and *Lutzomyia longipalpis* (*Lu. long*) microvillar-enriched midgut extract was run on an SDS-PAGE gel, transferred to a nitrocellulose membrane and probed with HPA-biotin followed by streptavidin-alkaline phosphatase. **A**, **B** and **C** show three experimental repeats. Blots probed with streptavidin-alkaline phosphatase only (control for **A**) or when HPA was incubated with 250 mM GalNAc (**B** and **C**) showed no binding.

7.2 Discussion

Research into midges as vectors for *Leishmania (Mundinia)* species has accelerated in recent years. When trying to understand the interactions of *Leishmania* with their vectors, it is important to now look at both sand flies and midges. *Mundinia* is thought to be the oldest subgenus of *Leishmania* (Jariyapan et al., 2018), with midges therefore potentially the first vector, and so they may offer a simplified model of interaction.

Dillon and Lane (1999) have previously shown *L. major* LPG attachment to *P. papatasi* microvillar-enriched midgut extract by Western blot. Here, we carried out similar experiments with *Lu. longipalpis* midgut samples probing with *L. (L.) mexicana* log phase LPG, as well as with *Lu. longipalpis*, *C. sonorensis* and *C. nubeculosus* probing with *L. (M.) chancei* log phase LPG. In these initial experiments, we have been unable to show LPG attachment to the midgut extract samples. For the later experiment, transfer of proteins to a nitrocellulose membrane, as done by Dillon and Lane (1999) also led to no binding of LPG to the midgut proteins and LPG controls failed. The highest amount of protein sample loaded on a gel by Dillon and Lane is 24 µL – equivalent to 0.96 µg of protein, therefore the difference in results is not due to the amount of protein loaded. The lack of detection may have been due to our use of 1 µg/mL LPG for probing compared to Dillon and Lane's 6 µg/mL. As previously mentioned in Chapter 3, our LPG samples are only enriched for LPG and so may have been further diluted with other contaminating molecules. The most likely cause for the differences seen is the use of reduced protein samples in our experiments, compared to Dillon and Lane using non-reduced, stating they saw an increase in binding when using this type of sample. However, with this being said, we would still expect to see some binding rather than none at all. The differences may be due to Dillon and Lane using a restrictive *Leishmania*-vector system. It is currently unknown if midges can be divided into restrictive and permissive, but for *Lu. longipalpis*, we may be seeing no attachment of LPG to the midgut protein as this interaction may not be as strong in a permissive vector. Multiple interactions are likely taking place with these being both LPG-dependent and -independent (Rogers et al., 2004; Hall et al., 2020).

Previous work found all permissive sand fly midgut homogenates tested had GalNAc-displaying glycoconjugates (Myšková et al., 2007). We expanded this work to look at whether GalNAc is also displayed on *C. sonorensis* and *C. nubeculosus* midguts. There were fewer HPA reactive bands to our *Lu. longipalpis* microvillar-enriched midgut extract compared to Myšková et al. (2016). However, the midgut homogenate used by Myšková et al. was produced by mechanical freezing and thawing of the midgut sample, and did not enrich for microvillar proteins, so we would expect fewer proteins to be present in our sample. Three repeats of this experiment lead to varying banding patterns which are likely caused by heterogeneity in the microvillar-

enriched sample. This may be due to different researchers carrying out the extractions, or slight differences in the midges used for each extraction such as age. There seems to be GalNAc-displaying midgut material that is expressed at a higher level in the midges tested compared to *Lu. longipalpis* (band seen at ~80 kDa) as well as a *Lu. longipalpis* specific band seen at 35 kDa. Interestingly, there is also a band shared between the midge *C. sonorensis* and *Lu. longipalpis*, (seen at ~50 kDa) that is not seen in *C. nubeculosus*. In *Lu. longipalpis*, there is staining to a range of bands at this size, potentially suggesting varied glycosylation or an expansion of this gene. This shared band of *C. sonorensis* and *Lu. longipalpis* may suggest this midge species is a permissive *Leishmania* vector like *Lu. longipalpis*, whereas *C. nubeculosus* is a restrictive *Leishmania* vector. This theory is supported by laboratory infections carried out by Seblova et al. (2012) where *L. (L.) infantum* and *L. (L.) major* were unable to survive in *C. nubeculosus* after defecation, however, no *in vivo* experiments with *Mundinia* species have been carried out. In comparison late stage infections have been seen for *L. (M.) enriettii*, *Leishmania (Mundinia) macropodum*, *L. (M.) chancei*, *Leishmania (Mundinia) orientalis* and *Leishmania (Mundinia) martiniquensis* in *C. sonorensis* (Seblova et al., 2015; Chanmol et al., 2019; Becvar et al., 2021). *Ex vivo* midgut binding assays carried out by a Masters student, William Paine, found significantly more *L. (M.) chancei* parasites attached to the midguts of *C. sonorensis* compared to *C. nubeculosus* (data not shown).

7.3 Conclusion

Initial experiments suggest SAP does not act as a cross-linker between *L. (M.) chancei* and *C. sonorensis* midguts. We have also been unable to show LPG attachment to both midge species and *Lu. longipalpis*. However, there are GalNAc displaying molecules within the microvillar-enriched midgut extract, with different patterns seen for the two midge species. The similarity of *Lu. longipalpis* and *C. sonorensis* having a band at ~50 kDa that is absent in *C. nubeculosus* may suggest midges also divide into permissive and restrictive vectors.

8. <u>Discussion</u>

The overarching aim of this thesis was to further our understanding of the *Leishmania* parasite interaction with the sand fly midgut, focusing predominantly on the role of human pentraxins Serum Amyloid P (SAP) and C-reactive protein (CRP). We hoped to deduce the binding sites of SAP on both the *Leishmania* surface and the sand fly midgut luminal surface. For CRP, we wanted to explore if there are other *Leishmania* surface or excreted products this pentraxin interacts with, other than LPG. Though previous work has investigated CRP and its interactions with *Leishmania*, only one had previously looked at SAP and *Leishmania*. As midges are emerging as likely vectors of *Mundinia* species of *Leishmania*, it seemed necessary to extend our work to include the midge species available to us. Up until this thesis, no studies have explored the mechanism of *Leishmania (Mundinia)* attachment to midge midguts. We also aimed to carry out a systematic review and meta-analysis of *in vivo* fly infections and *ex vivo* midgut binding assays – methods which are crucial to understanding *Leishmania*-vector interactions. This provided an opportunity to study these methods in detail and contribute to or ask further biological questions about the *Leishmania*-sand fly interaction.

8.1 Chapter 4

Takeaway conclusions from Chapter 4:

- The majority of *in vivo* fly infection studies use *in situ* grading to quantitate *Leishmania* intensities of infected flies, but this data is hard to compare between studies
- Parasite infection densities over 10^6/mL (but likely even lower) seem to be superfluous and do not lead to higher infection intensities
- *Ex vivo* attachment of *L. mexicana* to the gut of the permissive sand fly *Lu. longipalpis* increases with the density of co-incubated parasites but reaches saturation between 1-2x10^6 promastigotes/mL

8.1.1 *Leishmania* number limit in sand flies

In Chapter 4, we proposed there is a cap in the number of parasites a sand fly can sustain and suggested various factors that may be limiting this e.g. access to nutrients, midgut binding sites and space due to PSG production. For the first bloodmeal, it seems likely that nutrients are the limiting factor, as upon a second bloodmeal, parasites are able to replicate (Serafim et al., 2018; Hall et al., 2021), increasing the original number of *Leishmania* within the fly. However, though potentially minor, other factors still need to be considered in this interaction. There will be parasites transmitted during the second bloodmeal, along with deposition of PSG when the sand fly bites. The second bloodmeal will also only be partial due to the accumulation of PSG

and blockage of the anterior midgut (Rogers et al., 2012), generating a smaller window for parasite replication before nutrients are exhausted. Though currently unknown, it is thought retroleptomonads will have characteristics of leptomonads such as the production of PSG (Bates, 2018). Confirmation of this will be crucial in fully understanding the limitations of parasite numbers within the fly. Though lower infection intensities are usually seen in nature (Serafim et al., 2018), the high infection intensities seen in experimental infections will be advantageous in finding the maximum number of parasites a sand fly can sustain. As suggested by Serafim et al. (2018), flies with high parasite numbers are likely to cause more cases of disease, due to more frequent high-dose bites. Understanding the maximum number of parasites within a sand fly after first and second bloodmeals will inform *Leishmania* epidemiology.

8.1.2 Issues with *in situ* grading quantitation

We had to exclude many papers from our meta-analysis due to data being recorded categorically and then presented as relative frequencies. This shed a light on the comparability of this *in situ* grading method between studies. There are many advantages to this method which have already been discussed. A small change could be made in the future by clearly reporting the number of flies in each category. Studies currently report the total number of flies used per time point post infection, however the number of flies in each parasite per midgut category (usually <100, 100-1000, >1000) then needs to be calculated using ImageJ, leading to fractions of flies. However, even this will cause problems when trying to carry out statistics. A number would have to be picked to represent each group, with statistics carried out on only these three numbers. Using a hemocytometer still offers many of the advantages of *in situ* grading (all except the location of parasites within the gut) as well as allowing comparison between studies.

8.2 Chapter 5

Takeaway conclusions from Chapter 5:

- SAP binds to the surface of all *L. mexicana* morphological stages

- SAP and CRP binding sites differ, with SAP likely binding PEth on GIPLs

- SAP is present in the *Lu. longipalpis* midgut until defecation

- SAP binds microvillar-enriched midgut extracts, with α-glucosidase identified as a potential binding site or ligand

- SAP and anti-SAP antibodies and drug do not affect parasite attachment to the midgut

---

8.2.1 PEth binding sites on *Leishmania*

Our intention for studying SAP and CRP from the bloodmeal was to identify interactions that may be applicable to all *Leishmania* and sand fly species pairings.

GIPL structures vary between species, with *L. mexicana* amastigotes having a particularly high ratio (60%) of the GIPL EPiM3 which contains ethanolamine-phosphate. Promastigotes from *L. mexicana* still contain the EPiM3 form, but other forms not containing ethanolamine are more dominant (Winter et al., 1994). Ethanolamine-phosphate containing GIPLs were not found in any other *Leishmania* species GIPLs tested (McConville et al., 1990; McConville and Blackwell, 1991; Schneider et al., 1994; Zawadzki et al., 1998; Assis et al., 2012). Though it seems likely the binding site on *L. mexicana* GIPLs would be PEth, SAP is also known to bind carbohydrates (Loveless et al., 1992; Du Clos, 2013) which may allow for this same binding interaction in other species.

Leishmania species LPG side chain variation will likely impact the accessibility of SAP to the PEth ligand found close to the membrane. This may be further impacted if CRP is already bound. Along with GIPLs, GPI anchors also contain phosphatidylethanolamine (Azevedo et al., 2020), however we assume as these are so close to the *Leishmania* surface, they would be inaccessible for binding.

Ethanolamine is found in GP63 of *L. major* (Schneider et al., 1990) and *L. mexicana* (Ralton and McConville, 1998). This may offer a more universal *Leishmania* source of PEth for SAP attachment. GP63 has previously been suggested as important for *L. mexicana* attachment to *Lu. longipalpis* with GPI8 null mutants which displays GPI-anchored molecules like LPG and GIPLs but not GPI-anchored proteins such as GP63 being heavily outcompeted by wild-type parasites for midgut binding (Jecna et al., 2013).

8.2.2 Alternative roles for SAP in the vector midgut

SAP was found not to be a cross-linker of *Leishmania* parasites to the sand fly midgut, however, interactions of SAP with both *Leishmania* and the sand fly midgut were found. Therefore, it seems likely SAP does have a role within the *Leishmania* lifecycle within the vector midgut.

An alternative hypothesis is SAP and *Leishmania* are in competition for midgut binding. In Chapter 5, we found binding of SAP to microvillar-enriched midgut extract, with α-glucosidase identified as a possible binding site in preliminary immunoprecipitation experiments. da Costa-Latgé et al. (2021) found potential O- and N-glycosylation sites on α-glucosidases from *Lu. longipalpis* and suggested these could be sites of *L. mexicana* attachment to the midgut. However, further work is needed to confirm SAP does bind α-glucosidase. When the

microvillar-enriched midgut extract from *Lu. longipalpis* was probed with HPA (see Chapter 7), a very faint band or potentially two bands were seen at ~80 kDa, matching the size of the SAP bound bands under reducing conditions. The ~80 kDa band is also found in midges where the binding is much stronger. As *Leishmania* is thought to bind GalNAc in permissive vectors (Myšková et al., 2007; 2016), this may suggest SAP and *Leishmania* share GalNAc displaying binding sites.

A reason for SAP and *Leishmania* competing for binding to the midgut microvillar wall can currently only be speculative. It may allow for stage-specific binding of nectomonads to the midgut if SAP outcompetes procyclics for attachment but not nectomonads. SAP could be involved in detachment of parasites if it outcompetes nectomonad stages for midgut binding, however this would likely rely on a second bloodmeal, as we found SAP is defecated along with the bloodmeal remnants. SAP binding to the midgut could be a cue for sand flies to initiate blood fed specific mechanisms.

SAP attachment to *Leishmania* parasites may also be a trigger for morphological transitions as previously seen for CRP. CRP was found to transform *L. mexicana* (Bee et al., 2001) and *L. donovani* (Mbuchi et al., 2006) metacyclics to amastigote forms, with activation of cAMP suggested as the mechanism behind this (Bee et al., 2001). SAP was found to have no effect in these experiments. However, SAP may carry out a similar function at a different part of the lifecycle, specifically the transition of amastigotes to procyclic promastigotes when they first enter the sand fly midgut.

In contrast to CRP, SAP has been seen to inhibit bacterial classical complement pathway activation, with the cause of this suggested to be competition between SAP and C1q for bacterial LPS (de Haas et al., 2000). LPS is somewhat analogous to *Leishmania* glycolipid, with some bacterial species LPS displaying PEth (Caroff and Karibian, 2003). Therefore another potential role for SAP may be to provide protection to *Leishmania* against complement within the bloodmeal. A similar role has previously been studied and discussed for Factor H (Filho et al., 2021).

8.2.3 Explanation of differing SAP-*Leishmania* interaction results in Raynes et al., 1993

Raynes et al. (1993) previously saw no interaction of SAP with a range of *Leishmania* species. As discussed in Chapter 3 and mentioned in Chapter 5, we saw sporadic binding of SAP to the *Leishmania* surface using immunofluorescence. We think it is likely that GPI-anchored molecules are transient on the *Leishmania* surface, as seen for trypanosomes (Engstler et al.,

2007), with the methods used, such as fixing parasite prior to staining, crucial to observing binding.

8.3 Chapter 6

Takeaway conclusions from Chapter 6:

- CRP binds to ScAP and to fPPG, the components of PSG
- CRP binding inversely correlates with the amount of side chain substitution of the phosphorylated disaccharide repeats
- CRP-PPG activates complement

The focus of Chapter 6 was how CRP-PSG interacted in the host after being deposited during a sand fly bloodmeal. However, this interaction is likely also occurring in the vector. PSG is known to influence promastigote motility (Stierhof et al., 1999; Rogers et al., 2002), but this does not occur for metacyclics of *L. major* in *P. duboscqi* (Lawyer et al., 1990). A previous PhD student of the Rogers lab, Oihane Martin, focused on the interaction of PSG with *L. mexicana*. She found a statistically significant amount of nectomonad stage parasites attached to PSG compared to the other stages tested (procyclics, leptomonads and metacyclics) *in vitro*. It was also found that movement of wild-type *L. mexicana* but not *lpg1*$^{-/-}$ mutant nectomonads or wild-type metacyclics was impaired by PSG (Martin, 2013). Martin (2013) suggested PSG acts as a 'sieve' with only mature infectious metacyclics able to escape and therefore migrate forward in the digestive tract for transmission. The mechanism behind this has not been identified, except for LPG likely playing a role. CRP may also play a role in this interaction of parasites with PSG, potentially by changing the PSG environment, affecting the physiological state of the phosphoglycans or as a cross-linker between PSG and *Leishmania* LPG. This is a current focus for the Rogers lab.

8.4 Chapter 7

Takeaway conclusions from Chapter 7:

- CA7AE binds *L. (M.) chancei*
- SAP does not bind *C. sonorensis* microvillar-enriched midgut extract in preliminary experiments
- *C. sonorensis* and *C. nubeculosus* have GalNAc displaying bands. A band is shared between these midges and *Lu. longipalpis*. A band is also shared just between *C. sonorensis* and *Lu. longipalpis*

The finding that *C. sonorensis* and *C. nubeculosus* have HPA reactive bands but these both match and differ from each other and *Lu. longipalpis* sparks some interesting questions. As GalNAc is suspected to be a binding site for *Leishmania* on permissive sand fly midguts (Myšková et al., 2007; 2016; Hall et al., 2020) and *Mundinia* is thought to be the earliest branching *Leishmania* subgenus (Jariyapan et al., 2018), it may suggest the *Leishmania*-GalNAc interaction is the original mechanism of *Leishmania* attachment. As multiple interactions are thought to be occurring in attachment, further *Leishmania*-sand fly mechanisms may have evolved. This could in part be supported by Becvar et al. (2021) finding that some *Leishmania (Mundinia)* species could survive to late stage infections in *P. argentipes*, with binding potentially to the GalNAc presenting molecule seen in the midges and sand fly tested (Figure 7.6).

A previous study by Paranaíba et al. (2015) characterised the structure of *L. (M.) enriettii* LPG and GIPLs. They found the LPG of strains L88 and Cobaia to be devoid of side chain substitutions. The Western blot of strain L88 showed high molecular weights, differing from the usual characteristic smear and differing from our blots of *L. (M). chancei* (Figure 7.1). It was suggested this was due to *L. (M.) enriettii* L88 having more phosphorylated disaccharide repeats. More phosphorylated disaccharide repeats than usually seen for LPG and no side chain substitutions would suggest this LPG would have high avidity for CRP (Culley et al., 1996). *L. (M.) enriettii* Cobaia had a smear within the range of *L. infantum* BH46 LPG. The carbohydrate composition of the GIPLs were determined, with L88 suggested to be type II GIPLs and the Cobaia strain contained glucose – not previously seen in a *Leishmania* GIPL. However, characterisation was not taken further than this, so we cannot comment on possible SAP interaction.

8.5 Future opportunities

Though not a focus of this thesis, it would be interesting to further understand the movement of GPI-anchored surface molecules over the *Leishmania* surface. As discussed in Chapter 3, our attempts to capture LPG movement over the *Leishmania* surface using pulse-chase experiments were unsuccessful. As this was not the focus of the project, it was not pursued further, but future work using a protocol similar to Engstler et al. (2007) may confirm this movement.

A lot of data was collated as part of the systematic review and meta-analysis discussed in Chapter 4. The main barrier to this work has been how to usefully present and interpret the data we have from *in situ* grading studies. However, data that is comparable from all quantitation methods is the percentage of flies infected. Collation of this data may confirm previous conclusions that higher infection concentrations lead to a higher percentage of flies infected with late stage infections (Seblova et al., 2013; Pruzinova et al., 2015). Before submission of this study, relevant papers we had difficulty accessing need to be included into the analysis. A bias analysis also needs to be included.

To confirm the SAP binding site on *Leishmania*, a pure GIPL fraction or an anti-GIPL antibody is required. The method for GIPL purification used in Chapter 5 is similar to that described and used by others in the field (Schneider et al., 1994; Zawadzki et al., 1998). However, the surface components of *Leishmania* have similar properties which makes separating them difficult. As discussed in Chapter 3, we had difficulty with further GIPL purification using an Octyl Sepharose column and a propan-1-ol gradient (Assis et al., 2012). We suggested our issues with slow movement and pullback of the liquid through the column system may have been caused by larger material purified alongside the GIPLs clogging the top of the column. An additional low centrifugation step may remove any larger structure that may be present in this fraction. In house or commercial production of an anti-GIPL antibody would also allow us to confirm the presence of GIPL in our GIPL-enriched fraction and to show SAP and anti-GIPL have similar binding patterns. Another potential binding site as discussed above is GP63. Commercial antibodies are available to GP63, though they are expensive.

With CRP found to bind different *Leishmania* species phosphoglycans (Raynes et al., 1993; Culley et al., 1996; Chapter 6) to varying degrees and speculation here that SAP binding to the potential ligand of PEth would vary between *Leishmania* species, it would be interesting to compare SAP and CRP binding to the surface of different *Leishmania* species using immunofluorescence. Competition assays using both pentraxins may improve our understanding of how these pentraxins affect the others binding to the *Leishmania* surface.

These results may differ from the competition assays carried out in Chapter 5 using purified material.

As discussed above, SAP may be a trigger for transition between amastigote to procyclic promastigotes. Preliminary experiments have been carried out following *L. mexicana* in culture over subsequent days. Axenic amastigotes were washed and put in to M199 media alone, or with physiological concentrations of SAP and CRP, both separately and together. The experiment was also set up over a range of days to increase the chances of capturing the increase in parasite numbers as the culture entered logarithmic phase growth. So far results have been mixed, with further optimisation and repeats needed.

We found SAP is defecated along with the bloodmeal remnants, therefore understanding the interactions of SAP in an already infected fly when taking a second bloodmeal may provide more information on the function of SAP in the midgut. At this point, SAP will be interacting with a range of *Leishmania* stages. It is unlikely SAP will act as a trigger for morphological transformation at later time points, as the *Leishmania* lifecycle is commonly completed in once fed sand fly colonies. However, it would be interesting to see if like CRP, SAP also binds PSG. Western blots of LPG-enriched material suggest some contaminating fPPG is present, with SAP binding seen (Chapter 5). Furthermore, it would be interesting to expand research of CRP-PSG interaction, discussed in Chapter 6, into the sand fly environment by first carrying out a time course of CRP in the sand fly (like seen in Chapter 5, Figure 6 for SAP).

Our understanding of the role of SAP in the vector midgut will be enhanced by repeating experiments in other *Leishmania*-sand fly pairings. *Lu. longipalpis* with *L. mexicana* is an unnatural pairing, however it has been used in many vital studies looking at *Leishmania*-sand fly interaction (Stierhof et al., 1999; Rogers et al., 2002; Moraes et al., 2018; Hall et al., 2020). However, repeating experiments seen in Chapter 5 with a natural pairing such as *Lu. longipalpis* with *L. infantum*, will allow comparisons between a natural and unnatural system. This will also provide further information on if the interaction of SAP occurs in multiple *Leishmania*-sand fly pairings.

Furthermore, only preliminary experiments have been carried out looking at the interaction of SAP with midges. We have only carried out a few experiments looking at SAP binding to the *C. sonorensis* midgut. We are yet to investigate SAP binding to *L. (M). chancei*, which will provide information to see if this interaction of SAP spans *Leishmania* subgenera.

There is a range of future work to delve further into the interaction of *Mundinia* species with midges. Both *in vivo* infections and *ex vivo* midgut binding assays could be carried out with and without HPA to see if binding of *Mundinia* species to midges can be blocked. Furthermore,

immunofluorescence microscopy could be used to visualise HPA interactions with midge midguts and to *Mundinia* parasites. It would also be interesting to see if when using the microvillar-enrichment protocol used in this study (Dillon and Lane, 1999), whether any GalNAc staining is seen for restrictive sand fly species. It may be that binding of HPA to these species was not previously observed as the molecules were at too low a concentration for the sensitivity of Western blotting. This may add to our understanding of what makes a vector restrictive or permissive.

Though not discussed in the results of this thesis, some preliminary experiments were carried out as part of this project to investigate whether sand flies themselves have pentraxins or pentraxin-like proteins. We identified a gene region in *Lu. longipalpis* with over 30% identity to human SAP and CRP. This region was part of a larger gene containing many domains, previously identified in humans called polydom or SVEP1 (for sushi, von Willebrand factor type A, EGF, pentraxin domain-containing protein 1) (Schwarz et al., 2008; Jung et al., 2021). In *P. papatasi*, all other domains of the polydom were found except for the one similar to pentraxins. A small amount of further bioinformatics was carried out as well as qPCR experiments amplifying and confirming the pentraxin domain sequence. However, this was taken no further as other experiments were prioritised. It would be interesting to expand this work to other sand fly and midge species, to see if the pentraxin-like domain is only present in permissive vectors. Expression of this domain could also be compared between different feeding and infection stages.

8.6 Overall conclusions of this thesis

Studying the *Leishmania*-vector lifecycle is crucial for identifying *Leishmania*-midgut attachment mechanisms that can be disrupted, allowing development of transmission-blocking strategies. An overlooked component of this interaction is the host bloodmeal. For the first time, we show human SAP can bind both *Leishmania* and the sand fly midgut, with CRP found to bind PSG. We were unable to find a role for SAP in attachment as a cross-linker between the parasite and the midgut. However, the ability of SAP to bind to both could suggest competition for SAP binding, with the effect of this on the *Leishmania* lifecycle a topic for future research. For the first time, GalNAc displaying molecules were identified in midge midgut extracts, suggesting this may be important for *Leishmania*-midge interaction as found for permissive sand flies. A pan permissive vector binding interaction would allow one transmission-blocking strategy for a range of *Leishmania*-vector pairs. Our suggestion of a limit in the number of parasites a sand fly can sustain will help inform leishmaniasis epidemiology, and implementation of transmission-blocking strategies. With current drugs having severe side effects and no vaccine available to treat human leishmaniasis, continued research into transmission-blocking vaccines could mean this disease was no longer a consideration for millions of individuals living in endemic areas.

References for Chapters 1, 3, 7 and 8

Abdellahi L, Iraji F, Mahmoudabadi A, Hejazi SH. Vaccination in Leishmaniasis: a review article. Iran Biomed J. 2022;26(1):1-35.

Abernethy TJ, Avery OT. The occurrence during acute infections of a protein not normally present in the blood. I. Distribution of the reactive protein in patients' sera and the effect of calcium on the flocculation reaction with c polysaccharide of Pneumococcus. J Exp Med. 1941;73(2):173-182.

Agrawal A, Xu Y, Ansardi D, Macon KJ, Volanakis JE. Probing the phosphocholine-binding site of human C-reactive protein by site-directed mutagenesis. 1992;257(35):25352-25358.

Ahmed UK, Maller NC, Iqbal AJ, Al-Riyami L, Harnett W, Raynes JG. The carbohydrate-linked phosphorylcholine of the parasitic nematode product ES-62 modulates complement activation. J Biol Chem. 2016;291(22):11939-11953.

Akhoundi M, Kuhls K, Cannet A, Votýpka J, Marty P, Delaunay P, Sereno D. A historical overview of the classification, evolution, and dispersion of *Leishmania* parasites and sandflies. PLoS Negl Trop Dis. 2016;10(3):e0004349.

Alsford Lab. Sandfly dissection [Internet]. 2022 [cited 2023 June 5] Available from: https://blogs.lshtm.ac.uk/alsfordlab/2022/07/21/y11-12-research-experience-lshtm/sandfly-dissection/

Alvar J, Yactayo S, Bern C. Leishmaniasis and poverty. Trends Parasitol. 2006;22(12):552-557.

Alzheimer Europe. Clinical Trials: DESPIAD [Internet]. 2019 [cited 2023 June 5] Available from: https://www.alzheimer-europe.org/research/clinical-trials/despiad

Assis RR, Ibraim IC, Noronha FS, Turco SJ, Soares RP. Glycoinositolphospholipids from *Leishmania braziliensis* and *L. infantum*: modulation of innate immune system and variations in carbohydrate structure. PLoS Negl Trop Dis. 2012;6(2):e1543.

Azevedo LG, de Queiroz ATL, Barral A, Santos LA, Ramos PIP. Proteins involved in the biosynthesis of lipophosphoglycan in *Leishmania*: a comparative genomic and evolutionary analysis. Parasit Vectors. 2020;13(44).

Baltz ML, De Beer FC, Feinstein A, Pepys MB. Calcium-dependent aggregation of human serum amyloid P component. Biochim Biophys Acta. 1982;701:229-236.

Barratt J, Kaufer A, Peters B, Craig D, Lawrence A, Roberts T, Lee R, McAuliffe G, Stark D, Ellis J. Isolation of novel trypanosomatid, *Zelonia australiensis* sp. nov. (Kinetoplastida: Trypanosomatidae) provides support for a Gondwanan origin of dixenous parasitism in the Leishmaniinae. PLoS Negl Trop Dis. 2017;11(1):e0005215.

Bates PA. Transmission of *Leishmania* metacyclic promastigotes by phlebotomine sand flies. Parasitol. Int. 2007;37:1097-1106.

Bates PA. *Leishmania* sand fly interaction: progress and challenges. Curr Opin Microbiol. 2008:11(4):340-344.

Bates PA, Depaquit J, Galati EAB, Kamhawi S, Maroli M, McDowell MA, Picado A, Ready PD, Salomón OD, Shaw JJ, Traub-Csekö YM, Warburg A. Recent advances in phlebotomine sand fly research related to leishmaniasis control. Parasit Vectors. 2015;8:131.

Bates PA. Revising *Leishmania*'s life cycle. Nat Microbiol. 2018:3(5);529-530.

Becvar T, Vojtkova B, Siriyasatien P, Votypka J, Modry D, Jahn P, Bates P, Carpenter S, Volf P, Sadlova J. Experimental transmission of *Leishmania (Mundinia)* parasites by biting midges (Diptera: Ceratopogonidae). PLoS Pathog. 2021;17(6):e1009654.

Bee A, Culley FJ, Alkhalife IS, Bodman-Smith KB, Raynes JG, Bates PA. Transformation of *Leishmania mexicana* metacyclic promastigotes to amastigotes-like forms mediated by binding of human C-reactive protein. Parasitology. 2001;122:521-529.

Bodin K, Ellmerich S, Kahan MC, Tennent GA, Loesch A, Gilbertson JA, Hutchinson WL, Mangione PP, Gallimore JR, Millar DJ, Minogue S, Dhillon AP, Taylor GW, Bradwell AR, Petrie A, Gillmore JD, Bellotti V, Botto M, Hawkins PN, Pepys MB. Antibodies to human serum amyloid P component eliminate visceral amyloid deposits. Nature. 2010;468:93-97.

Bodman-Smith KB, Mbuchi M, Culley FJ, Bates PA, Raynes JG. C-reactive protein-mediated phagocytosis of *Leishmania donovani* promastigotes does not alter parasite survival or macrophage responses. Parasite Immunol. 2002;24:447-454.

Boisseau-Garsaud AM, Cales-Quist D, Desbois N, Jouannelle J, Jouannelle A, Pratlong F, Dedet JP. A new case of cutaneous infection by a presumed monoxenous trypanosomatid in the island of Martinique (French West Indies). Trans R Soc Trop Med Hyg. 2000;94(1):51-52.

Bongiorno G, Muccio TD, Bianchi R, Gramiccia M, Gradoni L. Laboratory transmission of an Asian strain of *Leishmania tropica* by the bite of the southern European sand fly *Phlebotomus perniciosus*. Int J Parasitol. 2019;49:417-421.

Borja-Cabrera GP, Correia Pontes NN, da Silva VO, Paraguai de Souza E, Santos WR, Gomes EM, Luz KG, Palatnik M, Palatnik de Sousa CB. Long lasting protection against canine kala-azar using the FML-QuilA saponin vaccine in an endemic area of Brazil (São Gonçalo do Amarante, RN). Vaccine. 2002;20(27-28):3277-3284.

Borovsky D, Schlein Y. Trypsin and chymotrypsin-like enzymes of the sandfly *Phlebotomus papatasi* infected with *Leishmania* and their possible role in vector competence. Med Vet Entomol. 1987;1(3):235-242.

Boulanger N, Lowenberger C, Volf P, Ursic R, Sigutova L, Sabatier L, Svobodova M, Beverley SM, Späth G, Brun R, Pesson B, Bulet P. Characterisation of a defensin from the sand fly *Phlebotomus duboscqi* induced by challenge with bacteria or the protozoan parasite *Leishmania major*. Infect Immun. 2004;72(12):7140-7146.

Butcher BA, Turco SJ, Hilty BA, Pimenta PF, Panunzio M, Sacks DL. Deficiency in β1,3-galactosyltransferase of a *Leishmania major* lipophosphoglycan mutant adversely influences the *Leishmania*-sand fly interaction. J Biol Chem. 1996;271(34):20573-20579.

Butenko A, Kostygov AY, Sádlova J, Kleschenko Y. Bečvár T, Podešvová L, Macedo DH, Žihala D, Lukes J, Bates PA, Volf P, Opperdoes FR, Yurchenko V. Comparative genomics of *Leishmania* (*Mundinia*). BMC Genomics. 2019;20:726.

Butler PJG, Tennent GA, Pepys MB. Pentraxin-chromatin interactions: serum amyloid P component specifically displaces H1-type histones and solubilizes native long chromatin. J Exp Med. 1990;172:13-18.

Caroff M, Karibian D. Structure of bacterial lipopolysaccharides. Carbohydr Res. 2003;338(23):2431-2447.

Cecílio P, Cordeiro-da-Silva A, Oliveira F. Sand flies: basic information on the vectors of leishmaniasis and their interactions with *Leishmania* parasites. Commun Biol. 2022;5:305.

Centers for Disease Control and Prevention. CDC | Leishmaniasis [Internet]. 2020 [cited 2023 June 4] Available from: https://www.cdc.gov/parasites/leishmaniasis/

Chanmol W, Jariyapan N, Somboon P, Bates MD, Bates PA. Development of *Leishmania orientalis* in the sand fly *Lutzomyia longipalpis* (Diptera: Psychodidae) and the biting midge *Culicoides soronensis* (Diptera: Ceratopogonidae). Acta Trop. 2019;199:105157.

Coelho-Finamore JM, Freitas VC, Assis RR, Melo MN, Novozhilova N, Secundino NF, Pimenta PF, Turco SJ, Soares RP. *Leishmania infantum*: lipophosphoglycan intraspecific variation and interaction with vertebrate and invertebrate hosts. Int J Parasitol. 2011;41(3-4):333-342.

Colacicco-Mayhugh MG, Grieco JP, Putnam JL, Burkett DA, Coleman RE. Impact of phlebotomine sand flies on United States military operations at Tallil air base, Iraq: 5. Impact of weather on sand fly activity. J Med Entomol. 2011;48(3):538-545.

Coutinho-Abreu IV, Sharma NK, Robles-Murguia M, Ramalho-Ortigao M. Targeting the midgut secreted PpChit1 reduces *Leishmania major* development in its natural vector, the sand fly *Phlebotomus papatasi*. PLoS Negl Trop Dis. 2010;4(11):e901.

Coutinho-Abreu IV, Oristian J, de Castro W, Wilson TR, Meneses C, Soares RP, Borges VM, Descoteaux A, Kamhawi S, Valenzuela JG. Binding of *Leishmania infantum* lipophosphoglycan to the midgut is not sufficient to define vector competence in *Lutzomyia longipalpis* sand flies. mSphere. 2020;5:e00594-20.

Culley FJ, Harris RA, Kaye PM, McAdam KPWJ, Raynes JG. C-reactive protein binds to a novel ligand on *Leishmania donovani* and increases uptake into human macrophages. J Immunol. 1996;156(12):4691-4696.

Culley FJ, Thomson M, Raynes JG. C-reactive protein increases C3 deposition on *Leishmania donovani* promastigotes in human serum. Biochem Soc Trans. 1997;25(2):286S.

Culley, Fiona; (1997) Ligand specificity and functional implications of C-reactive protein binding to *Leishmania* promastigotes. PhD thesis, London School of Hygiene & Tropical Medicine.

Culley FJ, Bodman-Smith KB, Ferguson MAJ, Nikolaev AV, Shantilal N, Raynes JG. C-reactive protein binds to phosphorylated carbohydrates. Glycobiology. 2000;10(1):59-65.

da Costa-Latgé SG, Bates P, Dillon R, Genta FA. Characterization of glycoside hydrolase families 13 and 31 reveals expansion and diversification of α-amylase genes in the phlebotomine *Lutzomyia longipalpis* and modulation of sandfly glycosidase activities by *Leishmania* infection. Front Physiol. 2021;12:635633.

de Haas CJC, van Leeuwen EMM, van Bommel T, Verhoef J, van Kessel KPM, van Strijp JAG. Serum amyloid P component bound to gram-negative bacteria prevents lipopolysaccharide-mediated classical pathway complement activation. Infect Immun. 2000;68(4):1753-1759.

Desbois N, Pratlong F, Quist D, Dedet JP. *Leishmania (Leishmania) martiniquensis* n. sp. (Kinetoplastida : Trypanosomatidae), description of the parasite responsible for cutaneous leishmaniasis in Martinique island (French West Indies). Parasite. 2014;21(12).

Di-Blasi T, Lobo AR, Nascimento LM, Córdova-Rojas JL, Pestana K, Marín-Villa M, Tempone AJ, Telleria EL, Ramalho-Ortigão M, McMahon-Pratt D, Traub-Csekö YM. The flagellar protein

FLAG1/SMP1 is a candidate for *Leishmania*-sand fly interaction. Vector Borne Zoonotic Dis. 2015;15(3): 202-209.

Dillon RJ, Lane RP. Detection of *Leishmania* lipophosphoglycan binding proteins in the gut of the sandfly vector. Parasitology. 1999;118(1):27-32.

do Vale VF, Pereira MH, Gontijo NF. Midgut pH profile and protein digestion in the larvae of *Lutzomyia longipalpis* (Diptera: Psychodidae). J Insect Physiol. 2007;53(11):1151-1159.

Doni A, Parente R, Laface I, Magrini E, Cunha C, Colombo FS, Lacerda JF, Campos Jr A, Mapelli SN, Petroni F, Maertens J, Lambris JD, Bottazzi B, Garlanda C, Botto M, Carvalho A, Mantovani A. Serum amyloid P component is an essential element of resistance against *Aspergillus fumigatus*. Nat Commun. 2021;12:3739.

Dostálová A, Volf P. *Leishmania* development in sand flies: parasite-vector interactions overview. Parasit Vectors. 2012;5:276.

Dougall A, Shilton C, Low Choy J, Alexander B, Walton S. New reports of Australian cutaneous leishmaniasis in Northern Australian macropods. Epidemiol Infect. 2009;137:1516-1520.

Dougall AM, Alexander B, Holt DC, Harris T, Sultan AH, Bates PA, Rose K, Walton SF. Evidence incriminating midges (Diptera : Ceratopogonidae) as potential vectors of *Leishmania* in Australia. Int J Parasitol. 2011;4:571-579.

Du Clos TW, Mold C, Paterson PY, Alroy J, Gewurz H. Localisation of C-reactive protein in inflammatory lesions of experimental allergic encephalomyelitis. Clin Exp Immunol. 1981;43(3):565-573.

Du Clos TW, Zlock LT, Rubin RL. Analysis of the binding of C-reactive protein to histones and chromatin. J Immunol. 1988;141(12):4266-4270.

Du Clos TW. C-reactive protein reacts with the U1 small nuclear ribonucleoprotein. J Immunol. 1989;143(8):2553-2559.

Du Clos TW. Pentraxins: structure, function, and role in inflammation. ISRN Inflamm. 2013;379040.

Du R, Hotez PJ, Al-Salem WS, Acosta-Serrano A. Old world cutaneous leishmaniasis and refugee crises in the Middle East and North Africa. PLoS Negl Trop Dis. 2016;10(5):e0004545.

Engstler M, Pfohl T, Herminghaus S, Boshart M, Wiegertjes, Heddergott N, Overath P. Hydrodynamic flow-mediated protein sorting on the cell surface of trypanosomes. Cell. 2007;131(3):505-515.

Espinosa OA, Serrano MG, Camargo EP, Teixeira MMG, Shaw JJ. An appraisal of the taxonomy and nomenclature of trypanosomatids presently classified as *Leishmania* and *Endotrypanum*. Parasitology. 2018;145:430-442.

European Centre for Disease Prevention and Control. ECDC | Phlebotomine sand flies – Factsheet for experts [Internet]. 2020 [cited 2023 June 4] Available from: https://www.ecdc.europa.eu/en/disease-vectors/facts/phlebotomine-sand-flies

Fernandes ACS, Soares DC, Saraiva EM, Meyer-Fernandes JR, Souto-Padrón T. Different secreted phosphatase activities in *Leishmania amazonensis*. FEMS Microbiol Lett. 2013;340:117-128.

Fernández Cotrina J, Iniesta V, Monroy I, Baz V, Hugnet C, Marañon F, Fabra M, Gómez-Nieto LC, Alonso C. A large-scale field randomised trial demonstrates safety and efficacy of the vaccine LetiFend® against canine leishmaniosis. Vaccine. 2018;36(15):1972-1982.

Ferreira TN, Pita-Pereira D, Costa SG, Brazil RP, Moraes CS, Díaz-Albiter HM, Genta FA. Transmission blocking sugar baits for the control of *Leishmania* development inside sand flies using environmentally friendly beta-glycosides and their aglycones. Parasit Vectors. 2018;11:614.

Field MC, Carrington M. Intracellular membrane transport systems in *Trypanosome brucei*. Traffic. 2004;5:905-913.

Filho AAP, Nascimento AAS, Saab NAA, Fugiwara RT, Pessoa GCD, Koerich LB, Pereira MH, Araújo RN, Sant'Anna MRV, Gontijo NF. Evasion of the complement system by *Leishmania* through the uptake of factor H, a complement regulatory protein. Acta Trop. 2021;224:106152.

Forestier CL, Gao Q, Boons GJ. *Leishmania* lipophosphoglycan: how to establish structure-activity relationships for this highly complex and multifunctional glycoconjugate? Front Cell Infect Microbiol. 2015;4:193.

Ganguly S, Das NK, Barbhuiya JN, Chatterjee M. Post-kala-azar dermal leishmaniasis – an overview. Int J Dermatol. 2010;49:921-931.

Giraud E, Martin O, Yakob L, Rogers M. Quantifying *Leishmania* metacyclic promastigotes from individual sandfly bites reveals the efficiency of vector transmission. Commun Biol. 2019;2:84.

González E, Molina R, Iriso A, Ruiz S, Aldea I, Tello A, Fernández D, Jiménez M. Opportunistic feeding behaviour and *Leishmania infantum* detection in *Phlebotomus perniciosus* females collected in the human leishmaniasis focus of Madrid, Spain (2012-2018). PLoS Negl Trop Dis. 2021;15(3):e0009240.

Grimaldi Jr G, Teva A, dos-Santos CB, Santos FN, Pinto Id-S, Fux B, Leite GR, Falqueto A. Field trial of efficacy of the Leish-tec® vaccine against canine leishmaniasis caused by *Leishmania infantum* in an endemic area with high transmission rates. PLoS ONE. 2017;12(9):e0185438.

Guimarães AC, Nogueira PM, Silva SdO, Sadlova J, Pruzinova K, Hlavacova J, Melo MN, Soares RP. Lower galactosylation levels of the lipophosphoglycan from *Leishmania (Leishmania) major*-like strains affect interaction with *Phlebotomus papatasi* and *Lutzomyia longipalpis*. Mem Inst Oswaldo Cruz. 2018;113(5):e170333.

Hall AR, Blakeman JT, Eissa AM, Chapman P, Morales-García AL, Stennett L, Martin O, Giraud E, Dockrell DH, Cameron NR, Wiese M, Yakob L, Rogers ME, Geoghegan M. Glycan-glycan interactions determine *Leishmania* attachment to the midgut of permissive sand fly vectors. Chem Sci. 2020;11:10973.

Hall MJR, Ghosh D, Martín-Vega D, Clark B, Clatworthy I, Cheke RA, Rogers ME. Micro-CT visualization of a promastigote secretory gel (PSG) and parasite plug in the digestive tract of the sand fly *Lutzomyia longipalpis* infected with *Leishmania mexicana*. PLoS Negl Trop Dis. 2021;15(8):e0009682.

Hind CRK, Collins PM, Baltz ML, Pepys MB. Human serum amyloid P component, a circulating lectin with specificity for the cyclic 4,6-pyruvate acetal of galactose. Interactions with various bacteria. Biochem J. 1985;225:107-111.

Ilg T, Stierhof YD, Craik D, Simpson R, Handman E, Bacic A. Purification and structural characterization of a filamentous, mucin-like proteophosphoglycan secreted by *Leishmania* parasites. J Biochem. 1996;271(35):21583-21596.

Ilg T. Lipophosphoglycan is not required for infection of macrophages or mice by *Leishmania mexicana*. EMBO J. 2000;19(9):1953-1962.

Ilg T, Demar M, Harbecke D. Phosphoglycan repeat-deficient *Leishmania mexicana* parasites remain infectious to macrophages and mice. J Biol Chem. 2001;276(7):4998-4997.

ImageJ. Dot Blot Analysis [Internet]. [cited 2023 June 5] Available from: https://imagej.nih.gov/ij/docs/examples/dot-blot/

Isnard A, Shio MT, Olivier M. Impact of *Leishmania* metalloprotease GP63 on macrophage signaling. Front Cell Infect Microbiol. 2012;2:72.

Ives A, Ronet C, Prevel F, Ruzzante G, Fuertes-Marraco S, Schutz F, Zangger H, Revaz-Breton M, Lye LF, Hickerson SM, Beverley SM, Acha-Orbea H, Launois P, Fasel N, Masina S. *Leishmania* RNA virus controls the severity of mucocutaneous leishmaniasis. Science. 2011;331(6018):775-778.

Jariyapan N, Daroontum T, Jaiwong K, Chanmol W, Intakhan N, Sor-suwan S, Siriyasatien P, Somboon P, Bates MD, Bates PA. *Leishmania (Mundinia) orientalis* n. sp. (Trypanosomatidae), a parasite from Thailand responsible for localised cutaneous leishmaniasis. Parasit Vectors. 2018;11:351.

Jecna L, Dostalova A, Wilson R, Seblova V, Chang KP, Bates PA, Volf P. The role of surface glycoconjugates in *Leishmania* midgut attachment examined by competitive binding assays and experimental development in sand flies. Parasitology. 2013;140:1026-1032.

Jung I-H, Elenbaas JS, Alisio A, Santana K, Young EP, Kang CJ, Kachroo P, Lavine KJ, Razani B, Mecham RP, Stitziel NO. SVEP1 is a human coronary artery disease locus that promotes atherosclerosis. Sci Transl Med. 2021;13(586):eabe0357.

Kamhawi S. The biological and immunomodulatory properties of sand fly saliva and its role in the establishment of *Leishmania* infections. Microbes Infect. 2000;2:1765-1773.

Kamhawi S, Ramalho-Ortigao M, Pham VM, Kumar S, Lawyer PG, Turco SJ, Barillas-Mury C, Sacks DL, Valenzuela JG. A role for insect galectins in parasite survival. Cell. 2004;119(3):329-341.

Kamhawi S. Phlebotomine sand flies and *Leishmania* parasites: friends or foes? Trends Parasitol. 2006;22(9):439-445.

Kantzanou M, Karalexi MA, Theodoridou K, Kostares E, Kostare G, Loka T, Vrioni G, Tsakris A. Prevalence of visceral leishmaniasis among people with HIV: a systematic review and meta-analysis. Eur J Clin Microbiol Infect Dis. 2023;42(1):1-12.

Kaye P, Scott P. Leishmaniasis: complexity at the host-pathogen interface. Nat Rev Microbiol. 2011;9:604-615.

Killick-Kendrick R, Molyneux DH, Ashford RW. *Leishmania* in phlebotomid sandflies I. modifications of the flagellum associated with attachment to the mid-gut and oesophageal valve of the sandfly. Proc R Soc Lond. 1974;186:409-419.

Killick-Kendrick R, Wilkes TJ, Bailly M, Bailly I, Righton LA. Preliminary field observations on the flight speed of a phlebotomine sandfly. Trans R Soc Trop Med Hyg. 1986;80:138-142.

Killick-Kendrick R. Phlebotomine vectors of the leishmaniases: a review. Med Vet Entomol. 1990;4:1-24.

Killick-Kendrick R. The biology and control of Phlebotomine sand flies. Clin Dermatol. 1999;17:279-289.

King DL, Chang YD, Turco SJ. Cell surface lipophosphoglycan of *Leishmania donovani*. Mol Biochem Parasitol. 1987;24:47-53.

Kinoshita CM, Gewurz AT, Siegel JN, Ying SC, Hugli TE, Coe JE, Gupta RK, Huckman R, Gewurz H. A protease-sensitive site in the proposed Ca2+ -binding region of human serum amyloid P component and other pentraxins. Protein Sci. 1992;1:700-709.

Koch LK, Kochmann J, Klimpel S, Cunze S. Modeling the climatic suitability of leishmaniasis vector species in Europe. Sci Rep. 2017;7(1):13325.

Kolstoe SE, Ridha BH, Bellotti V, Wang N, Robinson CV, Crutch SJ, Keir G, Kukkastenvehmas R, Gallimore JR, Hutchinson WL, Hawkins PN, Wood SP, Rossor MN, Pepys MB. Molecular dissection of Alzheimer's disease neuropathology by depletion of serum amyloid P component. Proc Natl Acad Sci USA. 2009;106(18):7619-7623.

Kumar R, Nylén S. Immunology of visceral leishmaniasis. Front Immunol. 2012;3:251.

Kwakye-Nuako G, Mosore MT, Duplessis C, Bates MD, Puplampu N, Mensah-Attipoe I, Desewu K, Afegbe G, Asmah RH, Jamjoom MB, Ayeh-Kumi PF, Boakye DA, Bates PA. First isolation of a new species of *Leishmania* responsible for human cutaneous leishmaniasis in Ghana and classification in the *Leishmania enriettii* complex. Int J Parasitol. 2015;45:679-684.

Kwakye-Nuako G, Mosore MT, Boakye D, Bates PA. Description, biology, and medical significance of *Leishmania (Mundinia) chancei* n. sp. (Kinetoplastea: Trypanosomatidae) from Ghana and *Leishmania (Mundinia) procaviensis* n. sp. (Kinetoplastea: Trypanosomatidae) from Namibia. J Parasitol. 2023;109(1) :43-50.

Laboratory Imaging |NIS-Elements Viewer User's Guide [Internet]. 2020 [cited 2023 October 27] Available from:https://downloads.microscope.healthcare.nikon.com/phase4/literature/Manuals/NIS-Elements_Viewer-en-5.21.00.pdf

Lainson R, Shaw JJ. Evolution, classification and geographical distribution. London: Academic Press;1987.

Lane RP. Medical Insects and Arachnids: Sandflies (Phlebotominae). Springer, Dordrecht;1993.

Lawyer PG, Ngumbi PM, Anjili CO, Odongo SO, Mebrahtu YB, Githure JI, Koech DK, Roberts CR. Development of *Leishmania major* in *Phlebotomus duboscqi* and *Sergentomyia schwetzi* (Diptera: Pyschodidae). Am J Trop Med Hyg. 1990;43(1):31-43.

Li JJ, McAdam PWJ. Human amyloid P component: an elastase inhibitor. Scand J Immunol. 1984;20:219-226.

Li YP, Mold C, Du Clos TW. Sublytic complement attack exposes C-reactive protein binding sites on cell membranes. J Immunol. 1994;152(6):2995-3005.

Lobsiger L, Müller N, Schweizer T, Frey CF, Wiederkehr D, Zumkehr B, Gottstein B. An autochthonous case of cutaneous bovine leishmaniasis in Switzerland. Vet Parasitol. 2010;169(3-4):408-414.

Louradour I, Ghosh K, Inbar E, Sacks DL. CRISPR/Cas9 mutagenesis in *Phlebotomus papatasi*: the immune deficiency pathway impacts vector competence for *Leishmania major*. mBio. 2019;10:e01941-19.

Loveless RW, Floyd-O'Sullivan G, Raynes JG, Yuen CT, Feizi T. Human serum amyloid P is a multispecific adhesive protein whose ligands include 6-phosphorylated mannose and the 3-sulphated saccharides galactose, N-acetylgalactosamine and glucuronic acid. EMBO J. 1992;11(3):813-819.

Lu J, Mold C, Du Clos TW, Sun PD. Pentraxins and Fc receptor-mediated immune responses. Front. Immunol. 2018;9:2607.

Machado MI, Milder RV, Pacheco RS, Silva M, Braga RR, Lainson R. Naturally acquired infections with *Leishmania enriettii* Muniz and Medina 1948 in guinea-pigs from São Paulo, Brazil. Parasitology. 1994;109:135-138.

Mann S, Frasca K, Scherrer S, Henao-Martínez AF, Newman S, Ramanan P, Suarez JA. A review of leishmaniasis: current knowledge and future directions. Curr Trop Med Rep. 2021;8:121-132.

Maroli M, Gramiccia M, Gradoni L, Ready PD, Smith DF, Aguino. Natural infections of phlebotomine sandflies with Trypanosomatidae in central and south Italy. Trans R Soc Trop Med Hyg. 1988;82(2):227-228.

Martin, Oihane; (2013) Leishmaniasis transmission biology: role of promastigote secretory gel as a transmission determinant. PhD thesis, London School of Hygiene & Tropical Medicine.

Mbuchi M, Bates PA, Ilg T, Coe JE, Raynes JG. C-reactive initiates transformation of *Leishmania donovani* and *L. mexicana* through binding to lipophosphoglycan. Mol Biochem Parasitol. 2006;146(2):259-264.

McConville MJ, Bacic A. A family of glycoinositol phospholipids from *Leishmania major.* J Biol Chem. 1989;264(2):757-766.

McConville MJ, Homans SW, Thomas-Oates JE, Dell A, Bacic A. Structure of the glycoinositolphospholipids from *Leishmania major*, a family of novel galactofuranose-containing glycolipids. J Biol Chem. 1990;265(13):7385-7394.

McConville MJ, Blackwell JM. Developmental changes in the glycosylated phosphatidylinositols of *Leishmania donovani*. J Biol Chem. 1991;266(23):15170-15179.

McConville MJ, Turco SJ, Ferguson MAJ, Sacks DL. Developmental modification of lipophosphoglycan during the differentiation of *Leishmania major* promastigotes to an infectious stage. EMBO J. 1992;11(10):3593-3600.

Meira CdS, Gedamu L. Protective or detrimental? Understanding the role of host immunity in Leishmaniasis. Microorganisms. 2019;7:695.

Mellor PS, Boorman J, Baylis M. Culicoides biting midges: their role as arbovirus vectors. Annu Rev Entomol. 2000;45:307-340.

Mikolajek H, Kolstoe SE, Pye VE, Mangione P, Pepys MB, Wood SP. Structural basis of ligand specificity in the human pentraxins, C-reactive protein and serum amyloid P component. J Mol Recognit. 2011;24:371-377.

Modi GB, Tesh RB. A simple technique for mass rearing *Lutzomyia longipalpis* and *Phlebotomus papatasi* (Diptera: Psychodidae) in the laboratory. J Med Entomol. 1983; 20(5):568-569.

Mold C, Baca R, Du Clos TW. Serum amyloid P component and C-reactive protein opsonize apoptotic cells for phagocytosis through Fcγ receptors. J Autoimmun. 2002;19:147-154.

Mold C, Gresham HD, Du Clos TW. Serum amyloid P component and C-reactive protein mediate phagocytosis through murine FcγRs. J Immunol. 2001;166(2):1200-1205.

Moraes CS, Aguiar-Martins K, Costa SG, Bates PA, Dillon RJ, Genta FA. Second blood meal by female *Lutzomyia longipalpis*: enhancement by oviposition and its effects on digestion, longevity, and *Leishmania* infection. Hindawi. 2018:2472508.

Moreno J, Vouldoukis I, Schreiber P, Martin V, McGahie D, Gueguen S, Cuisinier AM. Primary vaccination with the LiESP/QA-21 vaccine (CaniLeish®) produces a cell-mediated immune response which is still present 1 year later. Vet Immunol Immunopathol. 2014;158(3-4):199-207.

Mortz E, Krogh TN, Vorum H, Görg A. Improved silver staining protocols for high sensitivity protein identification using matrix-assisted laser desorption/ionization – time of flight analysis. Proteomics. 2001;1(11):1359-1363.

Mukhopadhyay D, Dalton JE, Kaye PM, Chatterjee M. Post kala-azar dermal leishmaniasis: an unresolved mystery. Trends Parasitol. 2014;30(2):65-74.

Mullen GR. Biting midges (Ceratopogonidae). In: Mullen GR, Durden LA, 2nd ed. Medical and veterinary entomology. Academic Press;2009:169-172.

Müller N, Welle M, Lobsiger L, Stoffel MH, Boghenbor KK, Hilbe M, Gottstein B, Frey CF, Geyer C, von Bomhard W. Occurrence of *Leishmania* sp. in cutaneous lesions of horses in Central Europe. Vet Parasitol. 2009;166:346-351.

Myšková J, Svobodová M, Beverley SM, Volf P. A lipophosphoglycan independent development of *Leishmania* in permissive sand flies. Microbes Infect. 2007;9:317–24.

Myšková J, Dostálová A, Pěničková L, Halada P, Bates PA, Volf P. Characterization of a midgut mucin-like glycoconjugate of *Lutzomyia longipalpis* with a potential role in *Leishmania* attachment. Parasit Vectors. 2016;9:413.

Nogueira PM, Guimarães AC, Assis RR, Sadlova J, Myšková J, Pruzinova K, Hlavackova J, Turco SJ, Torrecilhas AC, Volf P, Soares RP. Lipophosphoglycan polymorphisms do not affect *Leishmania amazonensis* development in the permissive vectors *Lutzomyia migonei* and *Lutzomyia longipalpis*. Parasit Vectors. 2017;10:608.

Noursadeghi M, Bickerstaff MCM, Gallimore JR, Herbert J. Cohen J, Pepys MB. Role of serum amyloid P component in bacterial infection: protection of the host or protection of the pathogen. Proc Natl Acad Sci USA. 2000;97(26):14584-14589.

Oggioni M, Mercurio D, Minuta D, Fumagalli S, Popiolek-Barczyk K, Sironi M, Ciechanowska A, Ippati S, De Blasio D, Perego C, Mika J, Garlanda C, De Simoni MG. Long pentraxin PTX3 is upregulated systemically and centrally after experimental neurotrauma, but its depletion leaves unaltered sensorimotor deficits or histopathology. Sci Rep. 2021;11:9616.

Paranaíba LF, de Assis RR, Nogueira PM, Torrecilhas AC, Campos JH, Silveira AC, Martins-Filho OA, Pessoa NL, Campos MA, Parreiras PM, Melo MN, Gontijo NF, Soares RP. *Leishmania enriettii*: biochemical characterisations of lipophosphoglycans (LPGs) and

glycoinositolphospholipids (GIPLs) and infectivity to *Cavia porcellus*. Parasit Vectors. 2015;8(31).

Pepys MB, Dash AC, Munn EA, Feinstein A, Skinner M, Cohen AS, Gewurz H, Osmand AP, Painter RH. Isolation of amyloid P component (protein AP) from normal serum as a calcium-dependent binding protein. Lancet. 1977;309(8020);1029-1031.

Pepys MB, Dash AC, Markham RE, Thomas HC, Williams BD, Petrie A. Comparative clinical study of protein SAP (amyloid P component) and C-reactive protein in serum. Clin Exp Immunol. 1978;32(1):119-124.

Pepys MB, Baltz M, Gomer K, Davies AJS, Doenhoff M. Serum amyloid P-component is an acute-phase reactant in the mouse. Nature. 1979;278:259-261.

Pepys MB, Rademacher TW, Amatayakul-Chantler S, Williams P, Noble GE, Hutchinson WL, Hawkins PN, Nelson SR, Gallimore JR, Herbert J, Hutton T, Dwek RA. Human serum amyloid P component is an invariant constituent of amyloid deposits and has a uniquely homogeneous glycostructure. Proc Natl Acad Sci USA. 1994;91:5602-5606.

Pepys MB, Herbert J, Hutchinson WL, Tennent GA, Lachmann HJ, Gallimore JR, Lovat LB, Bartfai T, Alanine A, Hertel C, Hoffman T, Jakob-Roetne R, Norcross RD, Kemp JA, Yamamura K, Suzuki M, Taylor GW, Murray S, Thompson D, Purvis A, Kolstoe S, Wood SP, Hawkins RN. Targeted pharmacological depletion of serum amyloid P component for treatment of human amyloidosis. Nature. 2002;417:254-259.

Pepys MB. The pentraxins 1975-2018: Serendipity, diagnostics and drugs. Front Immunol. 2018;9:2382.

Pimenta PFP, Turco SJ, McConville MJ, Lawyer PG, Perkins PV, Sacks DL. Stage-specific adhesions of *Leishmania* promastigotes to the sandfly midgut. Science. 1992;256:1812-1815.

Pimenta PFP, Saraiva EMB, Rowton E, Modi GB, Garraway LA, Beverley SM, Turco SJ, Sacks DL. Evidence that the vectorial competence of phlebotomine sand flies for different species of *Leishmania* is controlled by structural polymorphisms in the surface lipophosphoglycan. Proc Natl Acad Sci. 1994; 91:9155-9159.

Pimenta PFP, Modi GB, Pereira ST, Shahabuddin M, Sacks DL. A novel role for the peritrophic matrix in protecting *Leishmania* from the hydrolytic activities of the sand fly midgut. Parasitology. 1997;115:359-369.

Poché RM, Garlapati R, Elnaiem DEA, Perry D, Poché D. The role of Palmyra palm trees (*Borassus flabellifer*) and sand fly distribution in northeastern India. J Vector Ecol. 2012;37(1):148-153.

Pritchard DG, Volanakis JE, Slutsky GM, Greenblatt CL. C-reactive protein binds leishmanial excreted factors. Proc Soc Exp Biol Med. 1985;178(3):500-503.

Pruzinova K, Sadlova J, Seblova V, Homola M, Votypka J, Volf P. Comparison of bloodmeal digestion and the peritrophic matrix in four sand fly species differing in susceptibility to *Leishmania donovani*. PLoS ONE. 2015:10(6):e0128203.

Pruzinova K, Sadlova J, Myšková J, Lestinova T, Janda J, Volf P. *Leishmania* mortality in sand fly blood meal is not species-specific and does not result from direct effect of proteinases. Parasit Vectors. 2018;11(1):37.

Ralton JE, McConville MJ. Delineation of three pathways of glycosylphosphatidylinositol biosynthesis in *Leishmania mexicana*. Precursors from different pathways are assembled on distinct pools of phosphatidylinositol and undergo fatty acid remodeling. J Biol Chem. 1998;273(7):4245-4257.

Raynes JG, Curry A, Harris RA. Binding of C-reactive protein to *Leishmania*. Biochem Soc Trans. 1993;22:35.

Ready PD. Biology of Phlebotomine sand flies as vectors of disease agents. Annu Rev Entomol. 2013;58:227-250

Ready PD. Factors affecting egg production of laboratory-bred *Lutzomyia longipalpis* (Diptera: Psychodidae). J Med Entomol. 1979;16(5):413-423.

Ready PD. Leishmaniasis emergence and climate change. Rev Sci Tech. 2008;27(2):399-412.

Reuss SM, Dunbar MD, Calderwood Mays MB, Owen JL, Mallicote MF, Archer LL, Wellenhan. Jr. JFX. Autochthonous *Leishmania siamensis* in horse, Florida, USA. Emerg Infect Dis. 2012;18(9):1545-1547.

Richards D, Millns H, Cookson L, Lukas MA. An observational, non-interventional study for the follow-up of patients with amyloidosis who received miridesap followed by dezamizumab in a phase I study. Orphanet J Rare Dis. 2022;17:259.

Rogers ME, Chance ML, Bates PA. The role of promastigote secretory gel in the origin and transmission of the infective stage of *Leishmania mexicana* by the sandfly *Lutzomyia longipalpis*. Parasitology. 2002;124:495-507.

Roger ME, Ilg T, Nikolaev AV, Ferguson MAJ, Bates PA. Transmission of cutaneous leishmaniasis by sand flies is enhanced by regurgitation of fPPG. Nature. 2004;430(6998):463-467.

Rogers ME, Hajmová M, Joshi MB, Sadlova J, Dwyer DM, Volf P, Bates PA. *Leishmania* chitinase facilitates colonization of sand fly vectors and enhances transmission to mice. Cell Microbiol. 2008;10(6):1363-1372.

Rogers ME. The role of *Leishmania* proteophosphoglycans in sand fly transmission and infection of the mammalian host. Front Microbiol. 2012;3(223).

Rose K, Curtis J, Baldwin T, Mathis A, Kumar B, Sakthianandeswaren A, Spurck T, Choy JL, Handman E. Cutaneous leishmaniasis in red kangaroos: isolation and characterisation of the causative organisms. Int J Parasitol. 2004;34 :655-664.

Rossi E, Bongiorno G, Ciolli E, Di Muccio T, Scalone A, Gramiccia M, Gradoni L, Maroli M. Seasonal phenology, host-blood feeding preferences and natural *Leishmania* infection of *Phlebotomus perniciosus* (Diptera, Psychodidae) in a high-endemic focus of canine leishmaniasis in Rome province, Italy. Acta Trop. 2008;105(2):158-65.

Sacks DL. Metacyclogenesis in *Leishmania* promastigotes. Exp Parasitol. 1989;69:100-103.

Sacks DL, Brodin TN, Turco SJ. Developmental modification of the lipophosphoglycan from *Leishmania major* promastigotes during metacyclogenesis. Mol Biochem Parasitol. 1990;42:225-234.

Sacks DL, Pimenta PFP, McConville MJ, Schneider P, Turco SJ. Stage-specific binding of *Leishmania donovani* to the sand fly vector midgut is regulated by conformational changes in the abundant surface lipophosphoglycan. J Exp Med. 1995;181:685-697.

Sacks DL, Modi G, Rowton E, Beverley SM. The role of phosphoglycans in *Leishmania*-sand fly interactions. Proc Natl Acad Sci USA. 2000;97(1):406-411.

Sacks D, Kamhawi S. Molecular aspects of parasite-vector and vector-host interactions in leishmaniasis. Annu Rev Microbiol. 2001;55:453-483.

Sadlova J, Dvorak V, Seblova V, Warburg A, Votypka J, Volf P. *Sergentomyia schwetzi* is not a competent vector for *Leishmania donovani* and other *Leishmania* species pathogenic to humans. Parasit Vectors. 2013;6:186.

Sadlova J, Homola M, Myšková J, Jancarova M, Volf P. Refractoriness of *Sergentomyia schwetzi* to *Leishmania* spp. Is mediated by the peritrophic matrix. PLoS Negl Trop Dis. 2018;12(4):e0006382.

Schlein Y, Romano H. *Leishmania major* and *L. donovani*: effects on proteolytic enzymes of *Phlebotomus papatasi* (Diptera, Psychodidae). Exp Parasitol. 1986;62:376-380.

Schlein Y, Jacobson RL, Shlomai J. Chitinase secreted by *Leishmania* functions in the sandfly vector. Proc R Soc Lond B. 1991;245:121-126.

Schneider P, Ferguson MAJ, McConville MJ, Mehlert A, Homans SW, Bordier C. Structure of the glycosyl-phosphatidylinositol membrane anchor of the *Leishmania major* promastigote surface protease. J Biol Chem. 1990;265(28):16955-16964.

Schneider P, Schnur LF, Jaffe CL, Ferguson MAJ, McConville MJ, Glycoinositol-phospholipid profiles of four serotypically distinct Old World *Leishmania* strains. Biochem J. 1994;304:603-609.

Schwarz RS, Bosch TCG, Cadavid LF. Evolution of polydom-like molecules: identification and characterization of cnidarian polydom (Cnpolydom) in the basal metazoan Hydractinia. Dev Comp Immunol. 2008;32(10):1192-1210.

Seblova V, Sadlova J, Carpenter S, Volf P. Development of *Leishmania* parasites in *Culicoides nubeculosus* (Diptera: Ceratopogonidae) and implications for screening vector competence. J Med Entomol. 2012; 49(5):967-970.

Seblova V, Volfova V, Dvorak V, Pruzinova K, Votypka J, Kassahun A, Gebre-Michael T, Hailu A, Warburg A, Volf P. *Phlebotomus orientalis* sand flies from two geographically distant Ethiopian localities: biology, genetic analyses and susceptibility to *Leishmania donovani.* PLoS Negl Trop Dis. 2013;7(4):e2187.

Seblova V, Sadlova J, Vojtkova B, Votypka J, Carpenter S, Bates PA, Volf P. The biting midge *Culicoides sonorensis* (Diptera: Ceratopogonidae) is capable of developing late stage infections of *Leishmania enriettii.* PLoS Negl Trop Dis. 2015;9(9):e0004060.

Senghor MW, Niang AA, Depaquit J, Ferté H, Faye MN, Elguero E, Gaye O, Alten B, Perktas U, Cassan C, Faye B, Bañuls AL. Transmission of *Leishmania infantum* in the canine leishmaniasis focus of Mon-Rolland, Senegal: ecological, parasitological and molecular evidence for a possible role of *Sergentomyia* sand flies. PLoS Negl Trop Dis. 2016;10(11):e0004940.

Serafim TD, Coutinho-Abreu IV, Oliveira F, Meneses C, Kamhawi S, Valenzuela JG. Sequential blood meals promote *Leishmania* replication and reverse metacyclogenesis augmenting vector infectivity. Nat Microbiol. 2018;3:548-555.

Serafim TD, Iniquez E, Barletta ABF, Doehl JSP, Short M, Lack J, Cecilio P, Nair V, Distuar M, Wilson T, Coutinho-Abrey IV, Oliveira F, Meneses C, Barillas-Mury C, Andersen J, Ribeiro JMC,

Beverley SM, Kamhawi S, Valenzuela JG. *Leishmania* genetic exchange is mediated by IgM natural antibodies. Nature. 2023;623(7985):149-156.

Service M. Medical entomology for students. Cambridge University Press, Cambridge; 2012.

Shaw J. The leishmaniases – survival and expansion in a changing world. A mini-review. Mem Inst Oswaldo Cruz. 2007;102(5):541-547.

Soares RP, Altoé ECF, Ennes-Vidal V, da Costa SM, Rangel EF, de Souza NA, da Silva VC, Volf P, d'Avila-Levy CM. *In vitro* inhibition of *Leishmania* attachment to sandfly midguts and LL-5 cells by divalent metal chelators, anti-gp63 and phosphoglycans. Protist. 2017;168:326-334.

Späth GF, Epstein L, Leader B, Singer SM, Avila HA, Turco SJ, Beverley SM. Lipophosphoglycan is a virulence factor distinct from related glycoconjugates in the protozoan parasite *Leishmania major*. Proc Natl Acad Sci USA. 2000;97(16):9258-9263.

Späth GF, Beverley SM. A lipophosphoglycan-independent method for isolation of infective *Leishmania* metacyclic promastigotes by density gradient centrifugation. Exp Parasitol. 2001;99(2);97-103.

Stamper LW, Patrick RL, Fay MP, Lawyer PG, Elnaiem DEA, Secundino N, Debrabant A, Sacks DL, Peters NC. Infection parameters in the sand fly vector that predict transmission of *Leishmania major*. PLoS Negl Trop Dis. 2011;5(8):e1288.

Stierhof YD, Ilg T, Russell DG, Hohenberg H, Overath P. Characterisation of polymer release from the flagellar pocket of *Leishmania mexicana* promastigotes. J Cell Biol. 1994;125(2):321-331.

Stierhof YD, Wiese M, Ilg T, Overath P, Häner M, Aebi U. Structure of a filamentous phosphoglycoprotein polymer: the secreted acid phosphatase of *Leishmania mexicana*. J Mol Biol. 1998;282:137-148.

Stierhof YD, Bates PA, Jacobson RL, Rogers ME, Schlein Y, Handman E, Ilg T. Filamentous proteophosphoglycan secreted by *Leishmania* promastigotes forms gel-like three-dimensional networks that obstruct the digestive tract of infected sandfly vectors. Eur J Cell Biol. 1999;78:675-689.

Sunter J, Gull K. Shape, form, function and *Leishmania* pathogenicity: from textbook descriptions to biological understanding. Open Biol. 2017;7:170165.

Svárovská A, Ant TH, Seblová V, Jecná L, Beverley SM, Volf P. *Leishmania major* glycosylation mutants require phosphoglycans *(lpg2⁻)* but not lipophosphoglycan *(lpg1⁻)* for survival in permissive sand fly vectors. PLoS Negl Trop Dis. 2010;4(1):e580.

Taki T, Gonzalez TV, Goto-Inoue N, Hayasaka T, Setou M. Protein blotting and detection. Methods in molecular biology: TLC blot (far-eastern blot) and its applications. Humana Press;2009.

Telleria EL, Sant'Anna MRV, Ortigão-Farias JR, Pitaluga AN, Dillon VM, Bates PA, Traub-Csekö YM, Dillon RJ. Caspar-like gene depletion reduces *Leishmania* infection in sand fly host *Lutzomyia longipalpis*. J Biol Chem. 2012;287(16):12985-12993.

Telleria EL, Sant'Anna MRV, Alkurbi MO, Pitaluga AN, Dillon RJ, Traub-Csekö YM. Bacterial feeding, *Leishmania* infection and distinct infection routes induce differential defensin expression in *Lutzomyia longipalpis*. Parasit Vectors. 2013;6(12).

Telleria EL, Martins-da-Silva A, Tempone AJ, Traub-Csekö YM. *Leishmania*, microbiota and sand fly immunity. Parasitology. 2018;145:1336-1353.

Thompson D, Pepys MB, Wood SP. The physiological structure of human C-reactive protein and its complex with phosphocholine. Structure. 1999;7(2):169-177.

Thongsomboon W, Serra DO, Possling A, Hadjineophytou C, Hengge R, Cegelski L. Phosphoethanolamine cellulose: a naturally produced chemically modified cellulose. Science. 2018;359(6373):334-338.

Ticha L, Sadlova J, Bates P, Volf P. Experimental infections of sand flies and geckos with *Leishmania (Sauroleishmania) adleri* and *Leishmania (S.) hoogstraali*. Parasit Vectors. 2022;15(289).

Tonelli GB, Binder C, Margonari C, Dilermando J, Filho JDA. Sand fly behaviour: much more than weak-flying. Mem Inst Oswaldo Cruz. 2021;116:e210230.

Turco SJ, Descoteaux A. The lipophosphoglycan of *Leishmania* parasites. Annu Rev Microbiol. 1992;46:65-94.

Volanakis JE, Kaplan MH. Specificity of C-reactive protein for choline phosphate residues of Pneumococcal C-polysaccharide. Proc Soc Exp Biol Med. 1971;136(2):612-614.

Volanakis JE, Wirtz KW. Interaction of C-reactive protein with artificial phosphatidylcholine bilayers. Nature. 1979;281:155-157.

Volf P, Hajmova M, Sadlova J, Votypka J. Blocked stomodeal valve of the insect vector: similar mechanism of transmission in two trypanosomatid models. Int J Parasitol. 2004;34(11):1221-1227.

Volf P, Myšková J. Sand flies and *Leishmania*: specific versus permissive vectors. Trends Parasitol. 2007;23(3):91-92.

Volf P, Volfova V. Establishment and maintenance of sand fly colonies. J Vector Ecol. 2011; Suppl 1:S1-9.

Velez R, Gállego M. Commerically approved vaccines for canine leishmaniosis: a review of available data on their safety and efficacy. Trop Med Int Health. 2020;25(5):540-557.

Wilson R, Bates MD, Dostalova A, Jecna L, Dillon RJ, Volf P, Bates PA. Stage-specific adhesion of *Leishmania* promastigotes to sand fly midguts assessed using an improved comparative binding assay. PLoS Negl Dis. 2010;4(9):e816.

Winter G, Fuchs M, McConville MJ, Stierhof YD, Overath P. Surface antigens of *Leishmania mexicana* amastigotes: characterization of glycoinositol phospholipids and a macrophage-derived glycosphingolipid. J Cell Sci. 1994;107:2471-2482.

World Health Organisation. WHO | Control of the leishmaniases: WHO TRS N°949. 2010 [cited 2023 June 4] Available from: https://www.who.int/publications/i/item/WHO-TRS-949

World Health Organisation. WHO | Leishmaniasis [Internet]. 2023a [cited 2023 June 4] Available from: https://www.who.int/news-room/fact-sheets/detail/leishmaniasis

World Health Organisation. WHO | Map Gallery [Internet]. 2023b [cited 2023 June 4] Available from: https://www.who.int/data/gho/map-gallery-search-results?&maptopics=910b5dfc-ce2e-4440-8b43-8d83f4a85485&term=leishmaniasis

Yanase R, Moreira-Leite F, Rea E, Wilburn L, Sádlová J, Vojtkova B, Pružinová K, Taniguchi A, Nonaka S, Volf P, Sunter JD. Formation and three-dimensional architecture of *Leishmania* adhesion in the sand fly vector. Elife. 2023;12:e84552.

Yoneyama KAG. Tanaka AK, Silveira TGV, Takahashi HK, Straus AH. Characterization of *Leishmania (Viannia) braziliensis* membrane microdomains, and their role in macrophage infectivity. J Lipid Res. 2006;47:2171-2178.

Yuste J, Botto M, Bottoms SE, Brown JS. Serum amyloid P aids complement-mediated immunity to *Streptococcus pneumoniae*. PLoS Pathog. 2007;3(9):e120.

Zawadzki J, Scholz C, Currie G, Coombs GH, McConville MJ. The glycoinositolphospholipids from *Leishmania panamensis* contain unusual glycan and lipid moieties. J Mol Biol. 1998;282(2):287-299.

Zeiss | Ten quick tips for starting with ZEN Blue [Internet]. 2020 [cited 2023 October 27] Available from: https://www.zeiss.com/content/dam/Microscopy/us/download/pdf/zen-software-education-center/ten-quick-tips-for-starting-in-zen-blue.pdf